Phenotypic characterization of pathogenic mutations in GPIBDs

Inaugural-Dissertations
to obtain the academic degree

Doctor rerum naturalium
(Dr. rer. nat.)

submitted to the

Department of Biology, Chemistry and Pharmacy

of

Freie Universität Berlin

by

Alexej Knaus

from Kiev / Ukraine

2019

The thesis was completed at the

Institute for Medical Genetics and Human Genetics
Charité – Universitätsmedizin Berlin

from February 2015 to March 2019

First referee: Prof. Dr. Uwe Kornak

Institute for Medical Genetics and Human Genetics,

Charité – Universitätsmedizin Berlin

Augustenburger Platz 1

13353 Berlin

eMail: uwe.kornak@charite.de

Second referee: Prof. Dr. Sigmar Stricker

Department of Biology, Chemistry and Pharmacy,

Institute of Chemistry and Biochemistry

Freie Universität Berlin

Thielallee 63

14195 Berlin

eMail: sigmar.stricker@fu-berlin.de

Submitted on 31st of March 2019

Date of defense: 21st of August 2019

Declaration

I hereby declare that this thesis entitled “Phenotypic characterization of pathogenic mutations in GPIBDs” has been composed solely by myself, independently and with no other sources or aids than those cited or acknowledged. I testify that this thesis has not been previously submitted, in whole or in part, for a degree or any other qualification.

Berlin, Friday, August 30, 19

_____

Alexej Knaus

Acknowledgement

Firstly, I would like to express my sincerest gratitude Anja Ludwig for her unconditional love, her every day support, and for the endless scientific discussions.

Furthermore, I am especially grateful to Prof. Dr. med. Dipl. Phys. Peter Krawitz for his guidance and supervision, mind-opening discussions, and long-lasting motivation to complete this thesis.

Prof. Dr. med. Stefan Mundlos deserves my acknowledgment for giving me the opportunity to accomplish my thesis in the Institute for Medical Genetics and Human Genetics at the Charité University Hospital Berlin and the Max Planck Institute for Molecular Genetics Berlin.

Gratitude is owed to Prof. Dr. med. Uwe Kornak and Prof. Dr. Sigmar Striker who supervised my work and were always available for discussion, Prof. Dr. Denise Horn who motivated me in my studies and helped in the publication of my work.

I would like to express my sincere appreciation to Floriane Hennig for the endless support in the laboratory.

Explicitly, I would like to thank Björn Fischer for the guidance in the lab, Miguel Rodriguez de los Santos for his inspiration, Ulrike Krüger and Jochen Hecht for their expertise in next generation sequencing, Mohsen Karbasiyan, as well as Susanne Rothe, Gabriele Hildebrand, Anja Lekaj, and Patrick Sauer for their continuous assistance.

All members of the AG Kornak group not explicitly named deserve thankfulness for their daily support in the lab and discussions.

I would like to thank all members of the Institute for Medical Genetics and Human Genetics and the Max Planck Institute for Molecular Genetics for their scientific input and support.

I would like to express my gratitude to all coauthors of the publication for outstanding collaboration and enormous contribution.
Special thanks are owed to Harald Stachelscheid for using the stem cell core facility.
I owe gratitude to the Berlin School for Regenerative Therapies Berlin (BSRT), in particular to Dr. Sabine Bartosch for the opportunity to develop social competencies in various courses and programs. For the financial support I would like to thank the BSRT and the association “Freunde und Förderer der Berliner Charité”.
Furthermore, I would like to thank the members of the Institute for Genomic Statistics and Bioinformatics who support me in my daily work.
I would also like to thank my parents and my family who believed in me and provided me with the necessary support to achieve this level of education and maturity. Special thanks goes to my son Leonard Ludwig who cheered me up every day after work.
Finally, I would like to thank all patients and their parents for their trust in my work and their contribution to greater scientific development.

Table of content

1 Abstract

The glycosylphosphatidylinositol (GPI) anchor is a glycolipid with one function: tethering proteins to the cell surface. Synthesis and remodeling of the GPI anchor and linkage of proteins are highly conserved processes in a magnitude of species. About 10% of all surface proteins are anchored via the GPI moiety on all cells of the human body. GPI-APs (GPI anchored proteins) play important roles in a high variety of vital processes from embryogenesis over immune system regulation to neuronal function. Consequently, deficiencies in the pathway of GPI anchor biosynthesis have essential implications in life, as more than 200 individuals with disease-causing mutations in 21 of the genes of the GPI anchor biosynthesis pathway have been described in the literature.

Despite the advances in next generation sequencing (NGS) technology, the assessment of exome or genome data of individuals with suspected biosynthesis defects of the GPI anchor (GPIBDs) remains challenging due to the broad phenotypic spectrum. During my thesis I contributed to the publication of over 29 cases that were diagnosed with advanced phenotyping approaches for GPIBDs in NGS, flow cytometry, and computer-assisted facial image analysis.

The narrative of the three articles about congenital GPIBDs follows an improvement of diagnostic methods: First, the development of NGS based techniques that enabled the identification of non-coding mutations in *PGAP3* in clinically well characterized cases of HPMRS4. Second, I used a standardized flow cytometry analysis on fibroblasts, permitting functional validation of inherited pathogenic mutations in *PIGG*. Third, the application of automated facial analysis as proof of principle for a disorder specific facial gestalt in congenital GPIBDs as a pathway disorder. In the fourth article, I present results of a novel disease entity in an acquired GPIBD and methods for its clinical diagnostics.

Conclusively, the completion of this thesis returned advanced methods that improved the diagnostic yield of GPIBDs and can also be transferred to other rare monogenic disorders.

2 Introduction

2.1 The GPI anchor

All eukaryotic cells harbor a highly conserved sugar moiety whose purpose it is to link proteins in a specific manner to the cell surface: the glycosylphosphatidylinositol anchor (GPI-anchor). Synthesis of the GPI anchor and loading of GPI anchored proteins (GPI-APs) occurs in the endoplasmatic reticulum (ER). The glycosylation of proteins to the GPI anchor is part of post-translational modification. GPI-APs play a crucial role in embryonal development, cell adhesion, cell-cell communication and signal transduction, as well as antigen presentation (Ikezawa, 2002; Kinoshita & Fujita, 2015; Kinoshita, Fujita, & Maeda, 2008; Orlean & Menon, 2007).

2.1.1 Glycosylphosphatidylinositol anchor

The core structure of the GPI anchor is EtNP-6Manα1-2Manα1-6Manα1-4GlcNα1-6*myo*Inositol-phospholipid (where EtNP is phosphoethanolamine, Man is mannose, and GlcN is glucosamine). GPI-APs are linked with the C-terminus via an amide-bond to the EtNP of Man3. Some GPIs carry side branches on the mannose residues. The core GPI anchor may be extended by a fourth mannose that is α1-2-linked to Man3. GPI precursors during synthesis in the ER carry an EtNP on Man2, while the EtNP at Man1 is an obligate side branch. Another side branch β1,4-linked to Man1 (R in Figure 1) is N-acetylgalactosamine (GalNAc), that itself may be modified by galactose and sialic acid (Baldwin, 2006). The phosphatidylinositol (PI) is alkylated and acylated on the first and second position, respectively with saturated fatty acids (Kinoshita, 2014).

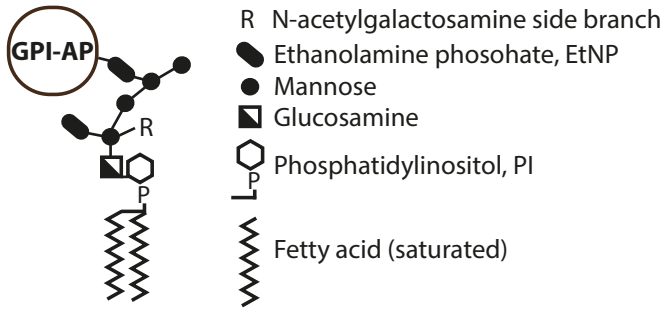

Figure 1. Structure of the mamalian GPI anchor.

2.1.2 GPI anchor biosynthesis pathway

To date, 29 genes are known to be involved in the biosynthesis and modification of the GPI anchor in humans. Five gene products contribute to the transamidase complex that attaches proteins to the GPI anchor in the ER. Another six genes are known to be involved in remodeling of the GPI anchor in the ER, Golgi, and on the cell surface (Table 1).

Table 1 – Genes involved in GPI anchor synthesis, GPI-AP loading, and GPI anchor remodeling

Gene	Chr	Protein / Protein complex	Function
PIGA	X	GPI-GlcNAc transferase, subunit	Synthesis of N-acetylglucosaminyl phosphatidylinositol (GlcNAc-PI)
PIGC	1	GPI-GlcNAc transferase, subunit	Synthesis of N-acetylglucosaminyl phosphatidylinositol (GlcNAc-PI)
PIGH	14	GPI-GlcNAc transferase, subunit	Synthesis of N-acetylglucosaminyl phosphatidylinositol (GlcNAc-PI)
PIGP	21	GPI-GlcNAc transferase, subunit	Synthesis of N-acetylglucosaminyl phosphatidylinositol (GlcNAc-PI)
PIGQ	16	GPI-GlcNAc transferase, subunit	Synthesis of N-acetylglucosaminyl phosphatidylinositol (GlcNAc-PI)
PIGY	4	GPI-GlcNAc transferase, subunit	Synthesis of N-acetylglucosaminyl phosphatidylinositol (GlcNAc-PI)
DPM2	9	Dolichyl-phosphate mannosyltransferase, subunit	Regulates and associates with the GPI GlcNAc transferase complex
PIGL	17	GlcNAc-PI de-N-acetylase	De-N-acetylation of GlcNAc-PI
PIGW	17	Inositol acyltransferase	Acrylates the inositol ring of phosphatidylinositol
PIGM	1	Mannosyltransferase I, subunit	Transfers Man1 to GlcNAc-PI
PIGX	3	Mannosyltransferase I, subunit	Transfers Man1 to GlcNAc-PI
PIGV	1	Mannosyltransferase II	Transfers Man2 to Man1
PIGN	18	EtNP transferase I	Transfers EtNP to Man1
PIGB	15	Mannosyltransferase III	Transfers Man3 to Man2
PIGO	9	EtNP transferase III, subunit	Transfers EtNP to Man3
PIGF	2	EtNP transferase II and III, subunit	Stabilizes EtNP transferase II and III
PIGG	4	EtNP transferase II, subunit	Transfers EtNP to Man2
PIGZ	3	Mannosyltransferase IV	Transfers Man4 to Man3
PIGK	1	GPI transamidase, subunit	Catalyzes transamidation of proteins to facilitate attachment to GPI
PIGS	12	GPI transamidase, subunit	Catalyzes transamidation of proteins to facilitate attachment to GPI
PIGU	20	GPI transamidase, subunit	Catalyzes transamidation of proteins to facilitate attachment to GPI
PIGT	20	GPI transamidase, subunit	Catalyzes transamidation of proteins to facilitate attachment to GPI

Gene	Chr	Protein / Protein complex	Function
GPAA1	8	GPI transamidase subunit	Catalyzes transamidation of proteins to facilitate attachment to GPI
PGAP1	2	Inositol deacylase	Catalyzes deacylation of inositol
PGAP2	11	Lyso-acyltransferase	Transfers saturated fatty acid to PI
PGAP3	17	GPI-Phospholipase A2	Removes unsaturated fatty acids from the sn-2 position of GPI (in the Golgi)
PGAP4	9	GPI-GalNAc transferase	Transfers GalNAc on the first mannose as side branch of GPI
PGAP5	18	Metallophosphoesterase I	Removes EtNP from the second mannose
PGAP6	16	GPI-Phospholipase A2	Removes an acyl-chain at the sn-2 position of GPI-anchor (on the plasma membrane)

In the first step of the GPI anchor biosynthesis pathway, a heptameric complex (encoded by *PIGA*, *PIGC*, *PIGH*, *PIGP*, *PIGQ*, *PIGY*, and *DPM2*) catalyzes the transfer of GlcNAc to a phospholipid (Murakami et al., 2005) After de-N-acetylation of GlcNAc-PI by *PIGL* (Watanabe, Ohishi, Maeda, Nakamura, & Kinoshita, 1999) the precursor of the GPI anchor is transferred by a postulated flippase to the luminal side of the ER where the gene product of *PIGW* acetylates a fatty acid to the second position of the inositol ring, generating GlcN-(acyl)-PI (Murakami et al., 2003). A complex encoded by *PIGM* and *PIGX* comprises the mannosyltransferase I that adds the first mannose (Man1) to the PI (Ashida et al., 2005). Subsequently the mannosyltransferase II (encoded by *PIGV*) adds the second mannose (Man2) (Kang et al., 2005). Thereafter the first EtNP is attached by the EtNP transferase I (encoded by *PIGN*) to the Man1 (Hong et al., 1999). The third mannose (Man3) is transferred (Mannosyltransferase III, ecoded by *PIGB*) onto the mannose core structure of the GPI anchor (Takahashi et al., 1996). The PIGF protein stabilizes the EtNP transferase III (encoded by *PIGO*) that links the third EtNP to Man3 (Hong et al., 2000), before EtNP transferase II (encoded by *PIGG* and associated with *PIGF*) adds the second EtNP on Man2 (Shishioh et al., 2005). The fully synthesized GPI anchor is attached to the GPI transamidase, a pentameric transmembrane protein complex (encoded by *PIGK*, *PIGU*, *PIGS*, *PIGT*, *GPAA1*) in the ER (Hong et al., 2003). Due to the N-terminal signal peptide GPI anchored protein precursors are synthesized through the ER membrane into the lumen. After removal of the ER signal peptide, GPI-AP precursors are linked to the luminal side of the ER membrane via the C-terminus. The C-terminal GPI attachment signal is recognized and cleaved by a cysteine protease motif of *PIGK* and covalently esterified to the transamidase, generating a substrate-enzyme complex. The trans-

amidation is completed after substitution of the thioester by an amide-bond of the third EtNP of the GPI anchor (Kinoshita, 2014; Yi et al., 2017).

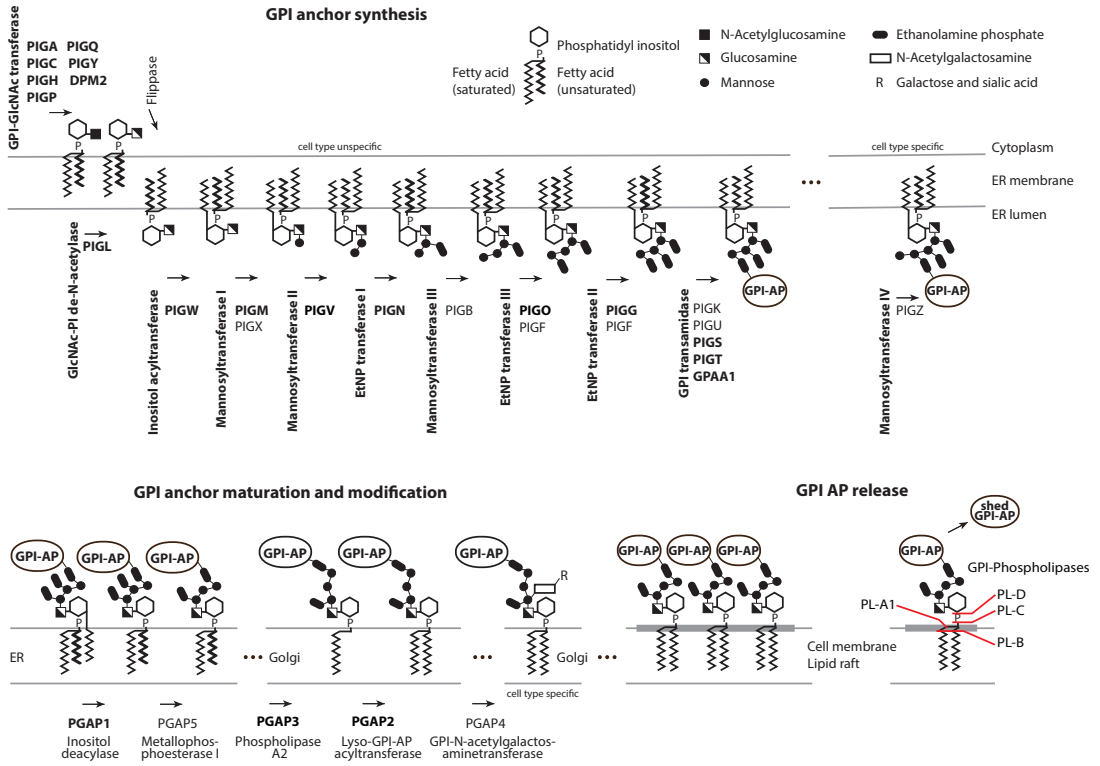

Figure 2. GPI anchor biosynthesis pathway.
Syndromic phenotypes have been linked to causal pathogenic mutations in 19 genes of the GPI anchor biosynthesis pathway (bold). Adapted from Krawitz (2016).

2.1.3 Remodeling and transport of GPI from ER to cell surface

The biosynthesis of the GPI anchor and its loading is carried out in the ER. In order to reach the plasma membrane GPI-APs are transported from ER through the Golgi apparatus. In the ER the inositol-deacylase (encoded by *PGAP1*) removes the acetylated fatty acid from the inositol ring (that was added by *PIGW*). This process occurs in almost all cells, with some exceptions: Complement factors in erythrocytes (Walter, Roberts, Rosenberry, Ratnoff, & Medof, 1990) and alkaline phosphatase in some cancer cells (Wong & Low, 1994). Dysfunction of *PGAP1* leads to a delayed transport of GPI-APs from ER (Tanaka, Maeda, Tashima, & Kinoshita, 2004). The removal of the EtNP from the second mannose of the glycan structure is facilitated by the metallophosphoesterase I (encoded by *PGAP5*). This step is important for the correct binding of GPI-APs to cargo receptors of the p24 family that in turn facilitates packaging of GPI-APs into COPII vesicles at ER exit sites and transfer from ER to Golgi (Bonnon,

Wendeler, Paccaud, & Hauri, 2010; Fujita et al., 2009, 2011). Due to a lower pH the p24 and COPII proteins dissociate from GPI-APs in the Golgi (Bonnon et al., 2010). The sequential remodeling of unsaturated to saturated fatty acid is promoted by the gene products of *PGAP3* and *PGAP2* in the Golgi: the phospholipase first removes unsaturated fatty acid from the PI moiety and the acyltransferase reacetylates the PI by a stearic acid (Maeda et al., 2007; Tashima et al., 2006). Thereafter, remodeled GPI-APs pass the trans-Golgi network (TGN) through the secretory pathway to the plasma membrane. Depending on the cell type and the cargo, GPI-APs are sorted differently in polarized cells (such as epithelial cells: apical domain, neurons: axon) and nonpolarized cells (fibroblasts: undirected distribution) (Muñiz & Riezman, 2015; Muñiz & Zurzolo, 2014; Zurzolo & Simons, 2016). Only correct remodeling of the fatty acids of the PI enables organization of GPI-APs with sphingolipids and cholesterol into specialized lipid-ordered domains that facilitate budding at the TGN (Zurzolo & Simons, 2016). On the cell surface GPI-APs are organized in lipid rafts where they can fulfill their function (Fujita & Kinoshita, 2012; Kinoshita & Fujita, 2015; Maeda et al., 2007). Various GPI-APs have been identified with modification of the core GPI anchor structure in yeast and mammals (Paulick & Bertozzi, 2008).

The third mannose can carry an additional mannose residue which is attached by the mannosyltransferase IV (encoded by *PIGZ*) that is mostly found in the brain and colon (Grimme, Westfall, Wiedman, Taron, & Orlean, 2001; Taron, Colussi, Wiedman, Orlean, & Taron, 2004). The addition of a fourth side branch to the first mannose is facilitated by the GPI-galactose-N-acetyl transferase (encoded by *PGAP4,* Hirata et al. 2018). The attached N-acetyl-galactoseamine (GalNAc) may be even further extended by galactose and sialic acid (Baldwin, 2006). The function of these modifications is, as yet, still for the most part not fully understood. However, a specific antibody (T5 4E10, Striepen *et al.*, 1992; Azzouz *et al.*, 2006) raised against the GalNAc epitope of the GPI anchor can be used to detect free GPI anchor molecules (Hirata et al., 2018).

2.1.4 GPI anchor breakdown

In the late maturation steps of the GPI anchor biosynthesis pathway the fatty acids that link the anchor to the cell surface are modified (Figure 2, lower panel). The re-

modeling does not only take place in the ER (*PGAP1*, inositoldeacylase) and the Golgi (*PGAP3*, phospholipase A2, Maeda *et al.*, 2007), but phospholipases are also found on the plasma membrane (*PGAP6*, phospholipase A2, Lee *et al.*, 2016) and in the extracellular space, such as blood serum (phospholipase D, Metz, Schenkman and Davitz, 1991) or neuromuscular junctions (phospholipase A, Su *et al.*, 1983). The lipase activity is important for triggering various signaling cascades (Fujihara & Ikawa, 2015; Suzuki, Fujiwara, Edidin, & Kusumi, 2007). GPI phospholipases (*GPI-PLA1*, *GPI-PLA2*, *GPI-PLB*, *GPI-PLC*, *GPI-PLD*) cleave the GPI anchor at different sites (Figure 2) and specific to the GPI-AP, thereby releasing the anchored protein from the membrane and providing specialized functions to GPI-APs (reviewed by Fujihara and Ikawa, 2015). However, only GPI anchors that were processed by the inositol deacylase (*PGAP1*) are prone to cleavage by phospholipases (Tanaka et al., 2004). On erythrocytes a lack of *PGAP1* activity leads to resistance of GPI-APs to phospholipase cleavage and GPI-APs remain attached to the cell surface by the inositol acyl chain. The GPI anchor synthesis, maturation and release of GPI-APs is illustrated in Figure 2 and reviewed by Ikezawa (2002), Orlean and Menon (2007), and Kinoshita (2014).

2.1.5 GPI anchored proteins

Many substrates of the transamidase are integral membrane proteins in the ER, prior to their attachment to the GPI anchor. As described in section 2.1.2, all these proteins undergo a similar process of posttranslational modification. As propeptides they share similar structural features such as an N-terminal signal peptide (for translation of the propeptide into the ER), a highly hydrophobic C-terminal tail (to interact with the GPI transamidase complex), and a ω-site (the cleavage site in the C-terminal tail, that is later covalently linked to the GPI anchor) (F. Eisenhaber et al., 2003). Hence, the bioinformatics prediction of GPI-APs is mainly based on the amino acid sequence and secondary structure of the signal peptide. Further features that frequently occur, are: a linker of about 11 residues before the ω-1 position; a region with small side chain residues around the cleavage site from ω-1 to ω+2; a spacer region between the positions ω+3 and ω+9 (Pierleoni, Martelli, & Casadio, 2008).
PredGPI, a tool developed by Pierleoni, Martelli and Casadio in 2008 predicted from the release 53 of SwissProt 485 proteins that are experimentally validated as GPI-

APs, and 26 proteins with an experimentally annotated ω-sites. Methods for functional validation of identified ω-sites were reviewed by Masuishi et al., (2018).

The function of GPI anchored proteins is manifold and includes catalytically active enzymes, membrane receptors, surface antigens, cell signaling, and more (Fujihara & Ikawa, 2015; Fujita & Kinoshita, 2012; Kinoshita, 2014; Kinoshita et al., 2008).

GPI-APs are found on the cell surface of all cells; hence, many GPI-APs were first described by the CD (cluster of differentiation) nomenclature. Exemplary important GPI-APs are listed in Table 2.

Table 2 – GPI anchored proteins

GPI-AP	Function	Cell type
AChE	Acetylcholinesterase	Erythrocytes, neurons
ALP	Alkaline phosphatase	Different isoforms on various cell types
CD14	Co-receptor with the Toll-like receptor TLR 4 and MD-2 for the detection of bacterial lipopolysaccharides	Macrophages, neutrophils, monocytes
CD16b	Fc portion of immunoglobulin G (encoded by *FCGR3B*)	NK-cells, granulocytes
CD24	Activation and differentiation of B lymphocytes	Granulocytes, B-cells, neuroblasts
CD55	Inhibitor of complement system (decay-accelerating factor, DAF)	All hematopoietic cells, fibroblasts
CD56	NCAM1, mediates adhesion between cells, e.g. pre- and postsynaptic membrane in neurons	Granulocytes, neurons
CD59	MAC-inhibitory protein, membrane inhibitor of reactive lysis (MIRL)	All hematopoietic cells, heart, fibroblasts
CD66b	Functions in cell adhesion, cell migration, and pathogen binding	Granulocytes, epithelial cells
CD66c	Functions in Cell adhesion, cellular migration, pathogen binding, and activation of signaling pathways	Activated neutrophils
CD73	Ecto-5'-nucleotidae, converts AMP to adenosine	B-cells, lung, heart, fibroblasts
CD87	Urokinase receptor, uPAR	Leukocytes, monocytes, heart,
CD90 (Thy1)	Regulate cell adhesion, migration, apoptosis, axon growth, cell-cell and cell-matrix interactions, T-cell activation, and fibrosis	Thymocytes, mesenchymal stem cells, hematopoietic stem cells, neurons, endothelial cells, and fibroblasts
CD109	May play a role in hematopoiesis and in cell-mediated immunity and in hemostasis	T-cells, platelets, stem cell progenitors, epithelial cells
RECK	Regulates WNT pathway signaling in the CNS, angiogenesis	Neuron, neuronal stem cells

2.2 GPI anchor deficiency

GPI anchor deficiencies are categorized based on when and where the pathogenic mutations in genes of the GPI anchor pathway occurred. Somatic mutations that are acquired in hematopoietic stem cells lead to paroxysmal nocturnal hemoglobinuria (PNH), a hemolytic disorder with variable manifestations. Congenitally inherited GPI biosynthesis defects (GPIBDs) can cause various syndromes, with intellectual disability, seizures, and other congenital malformations, or dysmorphic facial features as cardinal features, and are further classified on the basis of the underlying gene mutation.

2.2.1 Paroxysmal nocturnal hemoglobinuria (PNH)

The first reports of patients with symptoms of PNH date back to 1882 by Strübing. Enneking (1928) introduced the eponymous term paroxysmal nocturnal hemoglobinuria that describes the recurrent hemolysis at night and renal excretion of free hemoglobin. To date two forms of PNH were identified: PNH1 (also referred to as *PIGA*-PNH, MIM #300818) and PNH2 (also termed *PIGT*-PNH, MIM #615399).

Commonly, PNH1 is caused by somatic mutations in the X chromosomal gene *PIGA* (Takeda et al., 1993), whereas, loss of function (lof) mutations are acquired in a hematopoietic stem cell (HSCs) (Nafa et al., 1998). Clonal selection in combination with clonal expansion of the mutated stem cell and differentiation thereof leads to production of GPI deficient blood cells and thus to clinical manifestation of PNH (reviewed by Hill et al. 2017). The acquired PIGA deficiency leads to a complete loss of the GPI anchor and consequently a loss of GPI-APs on the surface of cells that arise from the hematopoietic clone. Erythrocytes lacking GPI-APs such as CD55 and CD59 are susceptible to complement mediated lysis by the membrane attack complex (MAC), as these proteins are main regulators of the complement cascade (Bessler et al., 1994; Rotoli, Bessler, Alfinito, & del Vecchio, 1993). The intravascular hemolysis results in anemia and thrombosis (Hill, Kelly, & Hillmen, 2013) as cardinal clinical features. Bone marrow failure is often associated with PNH and can emerge independently. The anti C5 antibody eculizumab and its derivates inhibits terminal activa-

tion of the complement cascade (Rother et al., 2007) and is therefore used to treat PNH (McKeage, 2019; Socié et al., 2019).

PNH2 or *PIGT*-PNH is caused by a combination of two mutation events: The identified patients carried a congenitally inherited heterozygous missense mutations in *PIGT* that affected protein function and was described in patients with inherited *PIGT* deficiency. Atypical PNH developed in patients after an acquisition of a large deletion encompassing the healthy *PIGT* allele in a HSC (Kawamoto, Murakami, Kinoshita, & Kohara, 2018; Krawitz et al., 2013; Murakami, Inoue, Kawamoto, Kohara, & Kinoshita, 2016). PNH2 manifested in the patients after clonal expansion and of the *PIGT* deficient HSC and production of GPI-AP deficient blood cells. Notably, treatment of the patients with eculizumab reverted the symptoms.

2.2.1.1 Clinical diagnosis of PNH

Apart from laboratory tests of the blood, that include complete blood count and differential with reticulocyte count, the diagnostic work up of PNH includes characterization of the GPI anchor and GPI-APs by flow cytometry of a freshly drawn blood sample. In 1992, Hillmen, Hows, and Luzzatto demonstrated that cell surface levels of CD55 and CD59 on erythrocytes of PNH patients were reduced compared to healthy controls. Later, improved flow cytometry panels that included a mutated and fluorescently labeled form of aerolysin (FLAER) were used for detection and characterization of PNH (Brodsky et al., 2000; Fletcher, Whitby, Whitby, & Barnett, 2016; Marinov, Illingworth, Benko, & Sutherland, 2016).

Molecular genetic analyses are used to reveal the underlying pathogenic mutation in PNH patients. Therefore, DNA extracted from blood (that contains a high proportion of GPI deficient cells) is sequenced. To determine the somatic origin of the pathogenic mutation sequencing data from blood derived DNA can be compared against DNA from saliva or buccal swabs.

2.2.2 Congenital GPI biosynthesis defects (GPIBDs)

Before the molecular basis was known, Mabry et al. (1970) described the first individuals from one family based on their clinical features characterized by mental retardation, seizures and high serum alkaline phosphatase (ALP) levels. Later Kruse et

al. (1988) presented nine patients that shared typical features for hyperphosphatasia with mental retardation syndrome (HPMRS) or Mabry syndrome: a characteristic facial gestalt, seizures, muscular hypotonia, and global developmental delay.

In 2006, Almeida et al. reported two cases with mutations in *PIGM* in patients with thrombosis, global developmental delay and seizures. Thrombosis and reduced GPI marker expression were considered shared features between PNH patients and the individuals described by Almeida, which led the genetic investigations. Homozygosity mapping reduced the search space to only one GPI gene – *PIGM*. This report was a hallmark of a rapidly expanding group of metabolic disorders that result from abnormal protein or lipid glycosylation, termed congenital disorders of glycosylation (CDG).

40 years after the first report by Mabry et al., Krawitz et al. (2010) identified the disease causing mutation in *PIGV* by whole exome sequencing as the cause of hyperphosphatasia with mental retardation syndrome (HPMRS1, MIM #239300). Subsequently, molecular diagnosis of novel patients expanded, the clinical and phenotypic spectrum of HPMRS1 (Horn, Krawitz, Mannhardt, Korenke, & Meinecke, 2011; Horn, Schottmann, & Meinecke, 2010; Reynolds, Juusola, Rice, & Giampietro, 2017; M. D. Thompson et al., 2012; M. Thompson et al., 2010; Xue, Li, Zhang, & Yang, 2016) and other GPI biosynthesis defects (GPIBDs, see Table 3). Over the recent years novel syndromic descriptions such as multiple congenital anomalies-hypotonia-seizures syndrome (MCAHS) were derived from phenotypic features of reported individuals that shared clinical features to Mabry patients, but were lacking hyperphosphatasia (Johnston et al., 2012; Kvarnung et al., 2013; Maydan et al., 2011).

Table 3 – GPIBDs and OMIM entries, sorted by year of publication

Abbreviation	Gene	Syndrome	MIM #	References with reported cases
GPIBD1	*PIGM*	Glycosylphosphatidylinositol deficiency	610293	Almeida et al. 2006
GPIBD2	*PIGV*	Hyperphosphatasia with mental retardation syndrome 1	239300	Krawitz et al. 2012; Nakamura et al. 2014; Xue et al. 2016; Morren et al. 2017; Tanigawa et al. 2017; Zehavi et al. 2017; Knaus et al. 2018

Abbreviation	Gene	Syndrome	MIM #	References with reported cases
GPIBD3	*PIGN*	Multiple congenital anomalies-hypotonia-seizures syndrome 1	614080	Maydan et al. 2011; Ohba et al. 2014; Brady et al. 2014; Fleming et al. 2016; Jezela-Stanek et al. 2016; Khayat et al. 2016; McInerney-Leo et al. 2016; Nakagawa et al. 2016; Ihara et al. 2017
GPIBD4	*PIGA*	Multiple congenital anomalies-hypotonia-seizures syndrome 2	300868	Johnston et al. 2012; Belet et al. 2014; van der Crabben et al. 2014; Swoboda et al. 2014; Kato et al. 2014; Tarailo-Graovac et al. 2015; Fauth et al. 2016; Kim et al. 2016; Low et al. 2018; Xie et al. 2018; Lin et al. 2018; Knaus et al. 2018
GPIBD5	*PIGL*	CHIME syndrome, HPMRS-7	280000	Ng et al. 2012; Fujiwara et al. 2015; Ceroni et al. 2018; Altassan et al. 2018
GPIBD6	*PIGO*	Hyperphosphatasia with mental retardation syndrome 2	614749	Krawitz et al. 2012; Nakamura et al. 2014; Xue et al. 2016; Pagnamenta et al. 2017
GPIBD7	*PIGT*	Multiple congenital anomalies-hypotonia-seizures syndrome 3	615398	Kvarnung et al. 2013; Nakashima et al. 2014; Lam et al. 2015; Skauli et al. 2016; Pagnamenta et al. 2017; Knaus et al. 2018
GPIBD8	*PGAP2*	Hyperphosphatasia with mental retardation syndrome 3	614207	Hansen et al. 2013; Jezela-Stanek et al. 2016; Naseer et al. 2016; Perez et al. 2017
GPIBD9	*PGAP1*	Mental retardation, autosomal recessive 42	615802	Murakami et al. 2014; Williams et al. 2015; Bosch et al. 2015; Kettwig et al. 2016
EEEI1	*PIGQ*	Epileptic encephalopathy, early infantile, 1	308350	Martin et al., 2014
GPIBD10	*PGAP3*	Hyperphosphatasia with mental retardation syndrome 4	615716	Abdel-hamid et al., 2017; Akgün Doğan et al., 2018; Balobaid et al., 2018; Howard et al., 2014; Knaus et al., 2016, 2018; Nampoothiri et al., 2017; Pagnamenta et al., 2017
GPIBD11	*PIGW*	Hyperphosphatasia with mental retardation syndrome 5	616025	Chiyonobu et al., 2014; Fu et al., 2019; Hogrebe et al., 2016

Abbreviation	Gene	Syndrome	MIM #	References with reported cases
GPIBD12	*PIGY*	Hyperphosphatasia with mental retardation syndrome 6	616809	Ilkovski et al. 2015
GPIBD13	*PIGG*	Mental retardation, autosomal recessive 53	616917	Makrythanasis et al. 2015; Zhao et al. 2017
GPIBD14	*PIGP*	Epileptic encephalopathy, early infantile, 55	617599	Johnstone et al. 2017
GPIBD15	*GPAA1*	Glycosylphosphatidylinositol biosynthesis defect 15	617810	Nguyen et al. 2017
GPIBD16	*PIGC*	Glycosylphosphatidylinositol biosynthesis defect 16	617816	Edvardson et al. 2017
GPIBD17	*PIGH*	Glycosylphosphatidylinositol biosynthesis defect 17	618010	Nguyen et al. 2018; Pagnamenta et al. 2018
GPIBD18	*PIGS*	Glycosylphosphatidylinositol biosynthesis defect 18	618143	Nguyen et al., 2018
CDG-Iu	*DPM2*	Congenital disorder of glycosylation, type Iu	615042	(Barone et al., 2012)

In a recent study, we provided a review of the main clinical features of the most prevalent forms of MCAHS (caused by mutations in *PIGN*, *PIGA*, and *PIGT*) and HPMRS (caused by mutations in *PIGV* and *PGAP3*), noting that affected individuals showed distinct facial patterns that can be detected by computer-assisted image analysis. The variable increases of ALP in serum as well as high variability of GPI-AP expression that can be detected by flow cytometry showed no correlation between the degree of neurologic involvement, mutation class, or gene involved. We concluded that a gene-centered classification should be preferred and grouped under the more encompassing term of GPI biosynthesis defects (GPIBDs).

2.2.3 Functional characterization of variants in congenital GPIBDs

The validation of underlying mutations that cause GPIBDs can be performed *in vitro* in model cell lines or *ex vivo* of patient samples. Depending on the genes mutated in the GPI anchor biosynthesis pathway the effect on the GPI anchor can be manifold: partial or total loss of the GPI anchor (mutations in *PIGA*, *PIGC*, *PIGH*, *PIGP*, *PIGQ*, *PIGY*, *PIGL* and *DPM2*), incomplete synthesis of the GPI anchor (mutations in *PIGV*, *PIGN*, *PIGB*, *PIGO*, and *PIGF*), missing or reduced linkage of GPI-APs to the anchor (mutations in *PIGK*, *PIGU*, *PIGS*, *PIGT*, and *GPAA1*), and partial or total lack of modification of fatty acids of the GPI anchor (mutations in *PGAP1*, *PGAP2*, *PGAP3*, *PGAP4*,

and *PGAP5*). The full structure of the GPI anchor can be analyzed by NMR (Nuclear Magnetic Resonance; B Striepen et al., 1992). Loss of function mutations are generally confirmed on RNA level (by qPCR or transcript sequencing) or protein level by western blotting. In the past studies, knock out and rescue experiments in Chinese Ovary Hamster (CHO) cell lines in combination with flow cytometry were used to elucidate genes of the GPI anchor pathway and to demonstrate pathogenicity of identified variants (Maeda, Ashida, & Kinoshita, 2006). Although, these methods allow assessment of gene function and validation of potentially pathogenic variants, they are also cumbersome, time consuming, and difficult to apply in a diagnostic setting. However, similar to diagnosis of PNH, flow cytometric analysis of GPI-APs on blood samples can also be carried out to diagnose congenital GPIBDs.

2.2.3.1 Flow cytometric analysis of GPI-APs

Blood samples of the patient and healthy controls are prepared for staining with antibodies directed against GPI-APs and markers characteristic for specific blood cell populations. Due to shedding of GPI-APs during shipping, blood samples are processed within 24 hours or collected in tubes containing preservatives (e.g. BCT Cyto-Chex tubes; containing para-formaldehyde and urea), shipped under refrigerated conditions, and processed in less than 96 hours (Middelhoven, Ager, Roos, & Verhoeven, 1997; Müller, Klöppel, Smith-Valentine, Van Houten, & Simon, 2012).

Expression of GPI-APs is conventionally measured on CD15 positive granulocytes. However, lymphocytes such as T and B cells can carry specific GPI-APs (such as CD16, CD56) and may serve well for analysis. The relative change of GPI-AP expression is determined by a ratio of the staining index (SI) of a patient to healthy control (parents or unrelated individuals): $relative\ marker\ expression = \frac{SI_{patient}}{SI_{control}}$

The SI is calculated as the ratio of median fluorescent intensity (MFI) of a stained cell population (MFI_{pos}) minus the MFI of unstained (or antibody isotype control stained) cell population (MFI_{neg}) to twice the standard deviation (SD) of MFI_{neg}:

$$SI = \frac{(MFI_{pos} - MFI_{neg})}{2\ SD\ MFI_{neg}}$$

Expression of FLAER, CD55, and CD59 are conventionally measured, as these markers are present on all cell types in blood. However, CD24 and CD16 / CD16b were shown to be very sensitive to pathogenic mutations in the GPI pathway. Other markers such

as CD56, CD66b and CD66c have been also used in other studies (Hogrebe et al., 2016; Kvarnung et al., 2013).

In cases where fast delivery of blood samples to a laboratory is not possible, immortalized B lymphoblastoid cell lines (LCLs) generated from B lymphocytes by Eppstein-Barr virus infection (Bosch et al., 2015; Murakami et al., 2014) or patient derived fibroblasts from skin biopsies have been also used for flow cytometric analysis of GPI-APs (Knaus et al., 2018; Thi Tuyet Mai Nguyen et al., 2017; Zhao et al., 2017). Marker expression analysis on fibroblasts is commonly performed on CD55, CD59, CD73, CD90, and CD109.

Despite of the growing number of known pathogenic variants (Figure 3), interpretation of novel variants with unknown clinical significance remains challenging. Due to mutation specific (hypomorphic variants) and patient specific variability of GPI marker expression, analysis of flow cytometry data may remain inconclusive. Henceforth, molecular genetic analysis is inevitable for clinical diagnostics of GPIBDs.

2.3 Next Generation Sequencing

The technical advancement in DNA sequencing introduced a fundamental change in clinical genetics. The emergence of next-generation sequencing (NGS) technologies gained enormous importance in this field. Since the beginning of this millennium the costs of sequencing DNA have continuously declined (Figure 3). With affordable sequencing, especially whole exome (WES) has become a routine test in the diagnostic workup of many suspected disorders (Neveling et al., 2013; Vissers et al., 2017). The new applications, however, entail novel challenges regarding data generation, data processing and variant detection, filtering and variant prediction, and finally functional characterization of pathogenic variants.

In the following section, the crucial steps from sequence generation to functional characterization of variants will be described.

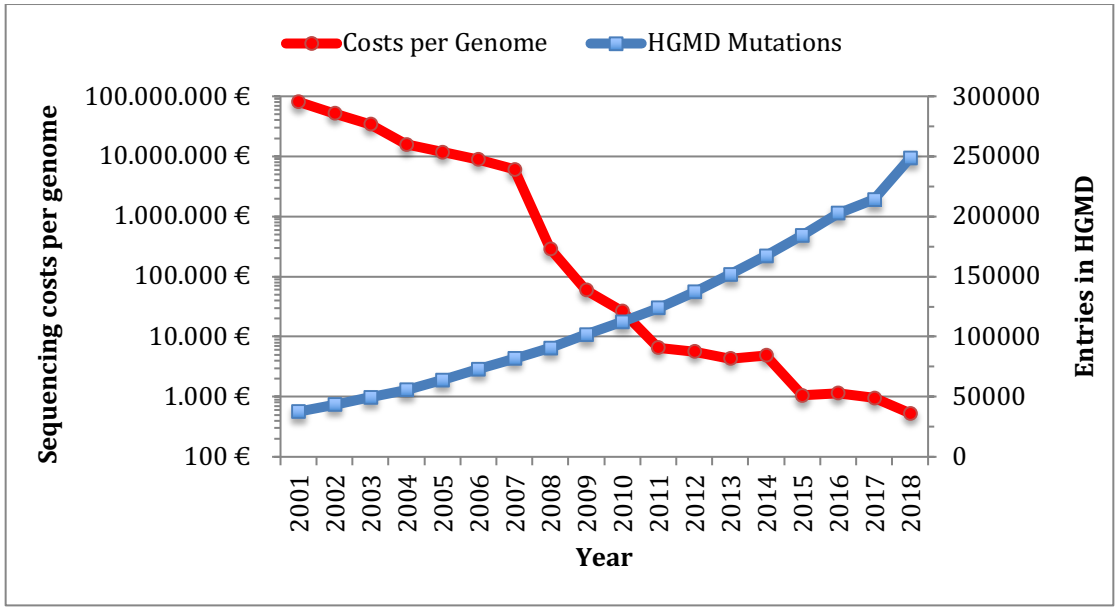

Figure 3. The falling costs for whole genome sequencing and increasing entries in HGMD over time.
The fall of costs for whole genome sequencing (red graph, log scale) is plotted against the surge of known pathogenic mutations in the HGMD.

The NGS technologies comprise of different procedures for sequencing fragments of DNA or RNA molecules and generating giga-bases of raw data. Currently Illumina® platforms are most commonly used and the technology is referred to as sequencing by synthesis (SBS).

2.3.1 Illumina – short read sequencing by synthesis

Before millions of small DNA molecules can be sequenced in parallel on Illumina's platforms (MiSeq, NextSeq, HiSeq, and NovaSeq), a library of genomic DNA has to be prepared. The DNA is first fragmented and adapter sequences are added to the fragments (Figure 4). In WES and other protocols that aim for a certain target region desired sequences are captured and enriched (Bentley et al., 2008; Bronner, Quail, Turner, & Swerdlow, 2009; Van Dijk, Jaszczyszyn, & Thermes, 2014).

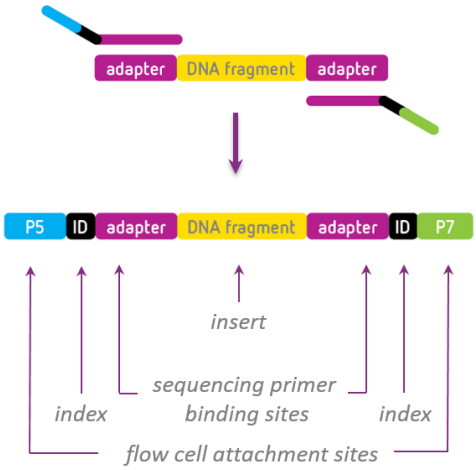

Figure 4. Schematic representation of a DNA fragment after library preparation.

Library preparation:

1. Fragmentation: DNA or RNA molecules are fragmented in an ultrasonic bath or by mechanical shearing into fragments of 75 – 150 bp.
    a. A complementary first and second strand of fragmented RNA molecules is generated by rtPCR using random hexamer primers.
2. End-Repair and phosphorylation: double stranded DNA (dsDNA) with 5' or 3' overhanging ends is repaired using a T4 DNA polymerase coupled with Klenow fragment. A T4 polynucleotide kinase transfers phosphate groups to the 5'-dephospho-DNA of dsDNA fragments in the same reaction.
3. A-Tailing: A taq-polymerase adds an overhanging adenosine to the blunt ended dsDNA fragments at the 3' end.
4. Adapter ligation: Adapters containing sequencing primer binding sites are added to the A-tailed dsDNA fragments.

5. Size selection: DNA fragments with a total size of around 75 – 300 bp are selected.
6. Amplification: DNA library is PCR amplified for quality control.

(7.) Target enrichment: Biotinylated baits with a complementary sequence to the target region are hybridized to the DNA fragments of particular interest (coding region). Streptavidin-linked magnetic beads are used to capture biotinylated bait-DNA-fragment complexes.

(8.) Amplification and indexing of enriched DNA library: The enriched DNA library is PCR amplified using indexing primers for multiplex sequencing containing P5 and P7 sequences that bind to the oligos on the surface of the flow cell.

Sequencing by synthesis (SBS):

1. Cluster generation: The DNA library is washed onto the flow cell and the DNA fragments bind with the P5 or P7 adaptors to the immobilized complementary sequence on the flow cell. Thereafter, the DNA fragments are bridge amplified on the flow cell to generate small clusters of the same fragment.
2. Sequencing: The stepwise sequencing is performed in a sequential PCR based manner.
    1.1. Dehybridization: The dsDNA clusters are dehybridized to form ssDNA (forward strand) clusters and unlinked DNA fragments (reverse strand) are washed from the flow cell.
    1.2. Priming: Primers complementary to the adaptor are annealed to the DNA fragments.
    1.3. Amplification: DNA polymerase and reversible fluorescent terminator deoxyribonucleotides are washed onto the flow cell and the primer is elongated for only one complementary nucleotide.
    1.4. Imaging and deblocking: The high-resolution fluorescence camera captures an image of the cluster that incorporated the fluorescent nucleotide. The chemical group at the 3’ end that is blocking the

addition of the next nucleotide and the fluorophores are removed by chemical cleavage.

The sequencing length of the fragments is limited to just several hundred base pairs; however, miniaturization and parallelization enables sequencing of millions of fragments at the same time. Thus, the output generated comprises mega to giga bases of target region sequenced. Depending on the scientific question under consideration, sequencing of a whole genome (WGS), only the protein coding part (exome), a targeted set of genes (gene panel), or even all transcripts of a gene panel (transcript panel) is possible. For the latter three, an enrichment step – either amplicon based (Multiplicon, RainDance) or hybridization with onligonucleotides (SureSelect, described in library preparation step 7.) is needed.

2.3.2 Bioinformatics processing of sequencing data

In most NGS protocols, the origin of sequence reads is quasi-random with respect to the target region (shotgun sequencing). Therefore, bioinformatics processing is necessary to realign the reads onto a known reference sequence (Figure 5).

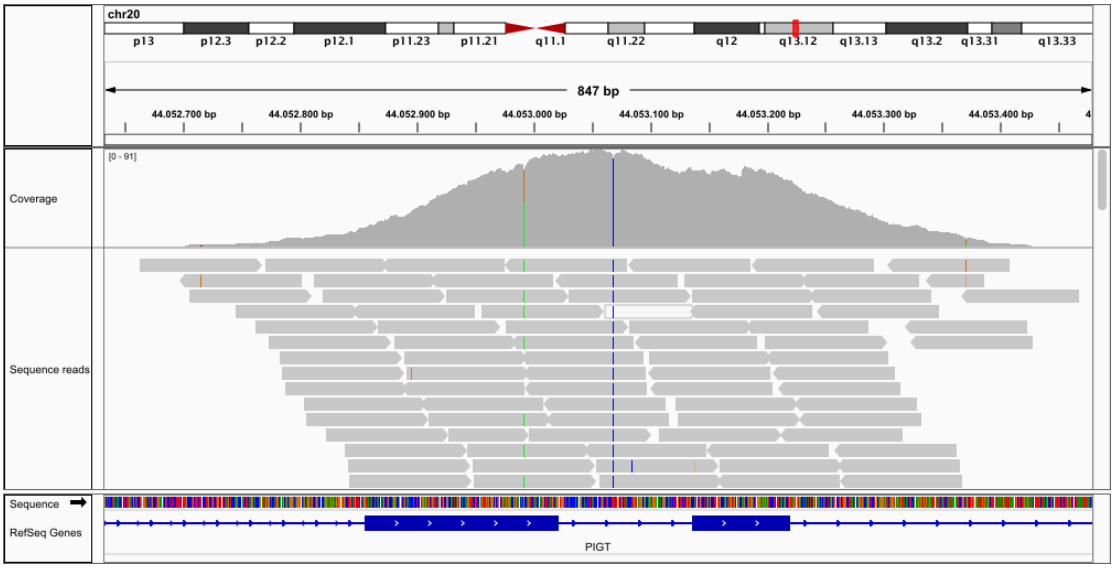

Figure 5. Sequence alignment from enriched sequencing of gDNA viewed in IGV browser. The coverage is depicted in the top panel as a distribution of the reads that are spanning over the exons. Fewer reads span over the intron-exon boundaries. A heterozygous (dashed green line) and a homozygous variant (vertical blue line) are illustrated

So called gapped short read mappers (BWA-MEM (H. Li & Durbin, 2009), Bowtie 2 (Langmead, Trapnell, Pop, & Salzberg, 2009), RNASequel (Wilson & Stein, 2015), and NovoAlign (Novoalign, 2017) and many more) use sophisticated heuristics to realign

the reads to a reference sequence, e.g. the 38th build from the *Genome Reference Consortium Human* (GRCh38). The quality of the aligned sequence reads can be visually inspected using the Integrative Genomics Viewer (Thorvaldsdóttir, Robinson, & Mesirov, 2013). After alignment, variant callers, such as Genome Analysis Tool Kit HaplotypeCaller – GATK (McKenna et al., 2010), Samtools (H. Li et al., 2009), Freebayes (Garrison & Marth, 2012)), can be used to detect deviations from the reference sequence. The results are reported in variant call format (VCF) files (Danecek et al., 2011). Further information on each variant can be added by tools such as Annovar (K. Wang, Li, & Hakonarson, 2010), Jannovar (Jäger et al., 2014), and the Ensembl Variant Effect Predictor (McLaren et al., 2016), which is retrieved from public databases: genomAD for allele frequency (Lek et al., 2016), Ensembl (Zerbino et al., 2017), RefSeq for gene name and variant effect prediction (Pruitt, Katz, Sicotte, & Maglott, 2017), and the dbSNP for a dbSNP ID (Sherry et al., 2001). Besides chromosomal position and the reference and alternative allele (genotype), a VCF can contain the dbSNP ID, gene name, quality of the variant (QUAL), coverage (reads that cover a particular variant), allele balance (reads carrying the reference allele divided by reads of the alternative allele), predicted effect of variant on RNA and protein level, and allele frequency (Figure 6). Finally, curated disease-specific databases (such as GeneTalk (Kamphans & Krawitz, 2012), LOVD (Fokkema et al., 2011), ClinVar (Landrum et al., 2014), RegulomeDB (Boyle et al., 2012), and HGMD (Stenson et al., 2012)) may provide additional information and annotation on a variant and its clinical significance.

Chrom	Pos	dbSNP ID	Gene	Ref	Genotype	Cov	AB		Effect/HGVS	Population Frequency	Annotations Click to show	
chr9	35094296	.	PIGO	G	A/A	241	1.00		missense	0 / 61434		Annotate
chr11	3832575	.	PGAP2	G	A/A	243	1.00		missense	-		Annotate
chr12	124229208	.	ATP6V0A2	C	C/G	247	0.43		missense	44 / 61478		Annotate
chr17	37829778	.	PGAP3	T	G/T	250	0.46		missense	5 / 66771		Annotate

Figure 6. VCF file viewed in GeneTalk.
Chromosome (Chrom), genomic position on the chromosome (Pos), reference allele (Ref), coverage (Cov), and allelic ballance (AB) are abbreviated. Clinical significance is represented by a star rating.

2.4 Interpretation of genetic variants

A major challenge in clinical genetics lies no longer in the identification of variants in sequence data, but in the interpretation thereof. The amount of identified sequence variants is dependent on the size of the sequenced region. Within the 3.2 billion bases of the human genome between 4 and 5 million variants (between 15,000 and 40,000 of those are in the coding region) per individual are expected, that implies a mean variant rate of about 1 per 1kb against a reference genome (T. 1000 G. P. Consortium, 2015). Many of these variants have been detected in the large sequencing projects (1kGP (T. 1000 G. P. Consortium, 2015), UK10K (T. U. Consortium, 2015), gnomeAD (Lek et al., 2016), and the Human Longevity Study (Telenti et al., 2016)). It is estimated that between 50 – 100 variants are personal and arise *de novo* in each individual (Besenbacher et al., 2015). Most of these variants are single nucleotide variants (SNVs) and small insertions and deletions (indels), copy number variants (CNVs) are less frequent (T. 1000 G. P. Consortium, 2015).

However, individuals with a single monogenetic disorder, carry only one or two disease-causing variants, while the remainder is part of normal genetic variation. If no known pathogenic variants are identified, further measures have to be undertaken, such as filtering out of non-pathogenic variants, prioritization and prediction of the remaining in order to pinpoint the disease-causing mutation.

2.4.1 Variant filtering

For variant analysis of rare disorders such as GPIBDs the allele frequency, estimated from large scale sequencing projects of healthy individuals, is highly valuable. In rare monogenic disorders with high penetrance variants with a high allele frequency (defined as an allele frequency >0.5%) can be excluded as disease-causing mutations.

SNVs can have different effects on RNA or protein level. Synonymous SNVs without splice site effect are commonly removed, while non-synonymous (missense, nonsense, and stop loss) variants and short indels (frameshift and non-frameshift) are retained.

The interpretation of splice site affecting variants – apart from constitutive splice sites – is often challenging, as these variants may be synonymous or non-

synonymous in the coding region, or deeply intronic (resulting in cryptic or alternative splice sites). Various tools with different algorithms predict the effect of SNVs on the splicing process (reviewed by Ohno et al. 2017). Therefore, a less conservative consideration of splice site affecting SNVs (± 20bp of the splice site) is recommended but yields a higher amount of putative splice site affecting variants. Further filtering and prioritization may reduce that number (Figure 7).

Information from parents is inevitable for the interpretation of disease-causing mutations. In dominant conditions only one copy of the gene is carrying the disease-causing mutation, that is absent in healthy parents or was inherited by the affected parent. Sometimes dominant disorders may have reduced penetrance, where not all individuals carrying the mutation are affected by the disorder (Posey et al., 2019). Furthermore, deep sequencing may reveal mosaicism in one parent (reviewed by Acuna-Hidalgo, Veltman and Hoischen, 2016). While individuals affected by a recessively inherited disorder, carry homozygous or compound heterozygous variants inherited from their parents (Kamphans et al., 2013).

In large families with multiple individuals affected by a recessive disorder the probability is very high that the disease causing variant lies within regions that are identical by descent (Krawitz et al., 2010), here linkage analysis can be performed. Furthermore, a linkage analysis can be useful for the identification of variants on gonosomes in individuals with suspected sex-linked disorders or sex-linked inheritance. Alternatively, after performance of linkage analysis, variants can be excluded that cannot be explained by Mendelian inheritance (Lohmann & Klein, 2014).

The analysis of variants from WES or WGS can be restricted by *in silico* gene panels to a smaller search space of certain molecular pathways that are related to the suspected disorder.

Finally, exclusion of sequencing artifacts is achieved by application of quality filters that take information form the QUAL column of the VCF file into account or are based on the read coverage of the variant. The quality of a called variant in the QUAL column is denoted as the negative logarithm to the base 10 of the probability that the variant call is wrong. As a rule of thumb, sequencing artifacts often show a value below 30. The read coverage of a variant in a VCF file is either denoted in the DP (sequencing depth), AD (number of sequence reads with the reference allele and the

alternative allele), or DP4 (number of reads with the reference or the alternative allele that have been aligned forward or reverse, separately listed) flags. To identify homozygous variants a sequencing depth of at least five reads and for heterozygous at least ten reads might be sufficient.

The functional implication of the remaining VOUCS (variants of unknown clinical significance) can be predicted on the basis of evolutionary conservation of nucleotide or amino acid exchange and the effect on the protein structure (Cooper & Shendure, 2011). Therefore, various tools have been developed in the past, of which the most common used are: Polyphen (Adzhubei, Jordan, & Sunyaev, 2015), MutationTaster (Schwarz, Cooper, Schuelke, & Seelow, 2014; Schwarz, Rödelsperger, Schuelke, & Seelow, 2010), Combined Annotation-Dependent Depletion (CADD, Kircher *et al.*, 2014), SIFT (Kumar, Henikoff, & Ng, 2009), and Functional Analysis Through Hidden Markov Models multiple kernel learning (FATHMM-MKL, Shihab *et al.*, 2015). Since there are no particular rules that dictate which combination of tools to apply, various filtering strategies and refiltering processes of variant data are possible (MacArthur et al., 2014).

2.4.2 Non-coding variants

Variants that are deeply intronic, up- or down-stream of the coding region of genes, in the 3’ or 5’ untranslated region (UTR), or between genes (intergenic) are summarized as non-coding variants. Although protein sequence is not altered, such variants can have disease-causing implications. It has been shown that non-coding variants affect the expression of genes when found in promotor, enhancer or silencer regions, or have an effect on chromatin architecture. Stability on mRNA can be altered by non-coding variants when found in the UTR or in non-coding RNAs (such as miRNas, lncRNAs, (reviewed by Meola et al. 2009; Lee & Young 2013; Zhang & Lupski 2015; Felekkis et al. 2010; Scacheri & Scacheri 2015). However, the interpretation and evaluation of pathogenicity of non-coding variants is more challenging than for coding variants. The effect of known non-coding variants can be annotated from RegulomeDB (Boyle et al., 2012) and scored by Genomiser (Smedley et al., 2015). Both tools rely on data from various studies that relate to chromatin structure, transcription factor prediction, consequences of histone modification, expression quanti-

tative trait loci (eQTL) and gene expression. Genotype-Tissue Expression (GTEx) is another vital resource containing information from variants with tissue-specific and shared regulatory eQTLs (GTEx Consortium, 2015). Further excellent scores for coding and non-coding variant analysis are hyperSMURF, developed by Schubach *et al.*, (2017), DeepSea (Zhou and Troyanskaya, 2015), DANN (Quang, Chen, & Xie, 2015) or Genome Wide Annotation of Variants (GWAWA, Ritchie *et al.*, 2014). They predict the effect of variants and score them by analysis of data form various resources using imbalance-aware machine learning.

2.4.3 Prioritization of variants

An increase of the diagnostic yield can be achieved by prioritization of annotated and scored variant data by tools such as Exomiser (Robinson et al., 2014; Smedley et al., 2015) and Genomiser (Smedley et al., 2016). Exomiser is a framework of tools that uses cross-species phenotype comparison (provided in HPO terms; Human Phenotype Ontology, Robinson et al. 2008; Köhler et al. 2017), information from protein interaction networks, allele frequency, and predicted pathogenicity in combination with computational filters and pedigree analysis to score and rank disease causing variants. Genomiser extends the filtering and scoring approach from Exomiser and combines these with regulatory sequences, chromosomal topological domains, and phenotypic relevance to rank coding and non-coding variants in Mendelian disorders. In a recent study, aiming to prioritize the disease-causing gene from exome data, facial image, and HPO features, a machine learning algorithm was developed. Three different scores from 1. the bioinformatically processed facial data (gestalt score from DeepGestalt (Gurovich et al., 2018)), 2. the deleteriousness score of variants (CADD score (Smedley et al., 2016), from exome data), and 3. feature scores (from Phenomizer (Köhler et al., 2009), BOQA (Bauer et al., 2012) and feature score from face2gene) were combined to the PEDIA (Proritization of Exome Data by Image Analysis) score. The tool achieved a high top 10 accuracy of above 90% for prioritization of the disease causing gene in a set of 105 syndromes in 679 molecularly diagnosed patients (Hsieh et al., 2018).

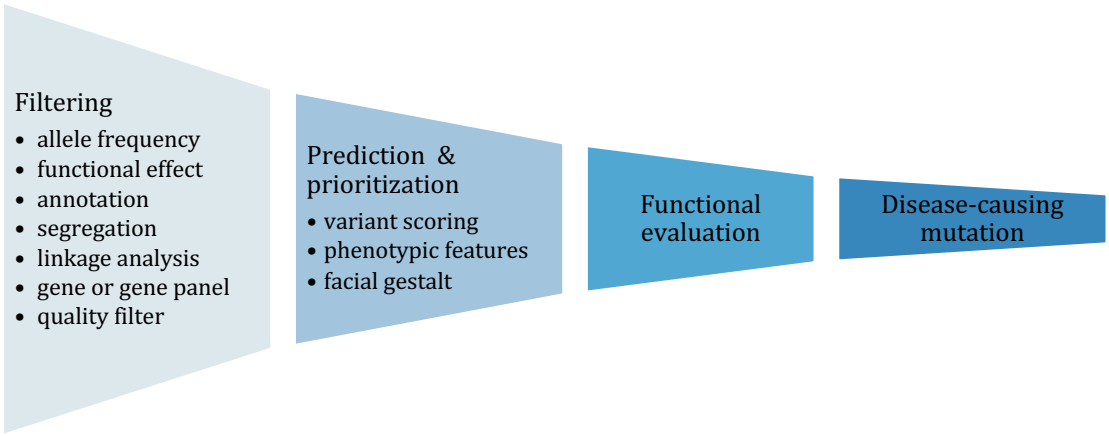

Figure 7. Schematic workflow for disease causing mutation identification.
Filtering of variants may be carried out in different order. Less stringent filtering criteria should be applied when no variants remain for functional evaluation.

2.4.4 Next generation phenotyping

Hennekam and Biesecker (2012) predicted that NGS in clinical application will increase the demand of deep phenotyping of patients in order to correctly interpret identified variants in a timely manner. Besides phenotypic descriptions in HPO terms (Köhler et al., 2017; Robinson et al., 2008) another pivotal source of information is found in the facial gestalt of individuals affected by monogenic disorders (Brunt, 1988). Recent developments in computer vision and machine learning were used to diagnose rare genetic diseases with craniofacial characteristics (Ferry et al., 2014; Kuru et al., 2014; Loos et al., 2003). Assuming that a recognizable facial gestalt is present in individuals affected by monogenic disorders, a classifier for facial pattern recognition can be trained to infer possible differential diagnoses. Loos and colleagues developed a program that compared the feature vectors at 32 facial nodes of 55 photographs from five different monogenic disorders (Loos et al., 2003). The program performed slightly better (recognition rate 76%), than well trained clinical geneticists. Ferry et al. (2014) used 36 feature points over an ordinary facial photograph to construct a Clinical Face Phenotype Space. By applying similarity learning, principal component analysis (PCA), and leave-one-out validation the authors were able to train an algorithm that reduced the diagnostic search space for eight different rare genetic disorders. Furthermore, the method allows clustering of affected individuals by facial gestalt aiding novel disease identification.

To date Face2Gene – a platform from Facial Dysmorphology Novel Analysis (FDNA Inc., Boston, MA) – provides the largest source of facial information on hundreds of monogenic disorders. The CLINIC application in Face2Gene allows the upload of a facial photo and description of the phenotypic features in HPO terms.

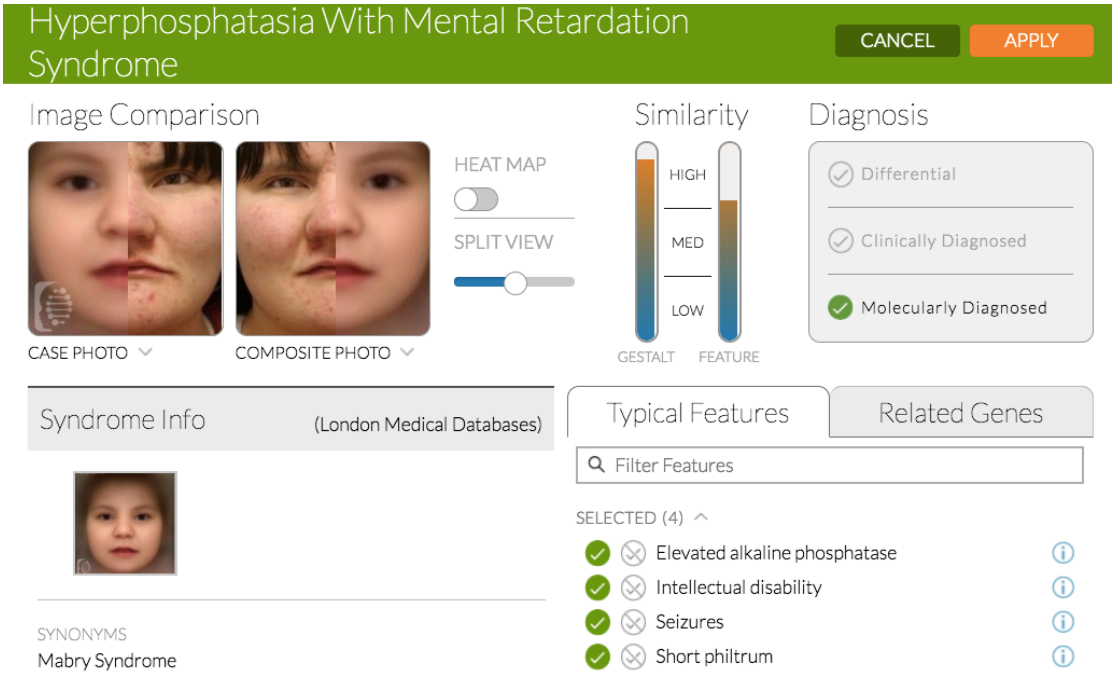

Figure 8. Image comparison of a HPMRS case and composite mask in Face2Gene. Split view image, gestalt and feature score of a patient with mutations *PGAP3* from Knaus et al. 2016.

The facial image is analyzed by Face2Gene's deep learning neural network (DeepGestalt) to generate the gestalt score (Gurovich et al., 2018). A feature score is calculated on the HPO terms that are provided by a clinician (Figure 8). A list of syndromes for differential diagnosis is then provided on the basis of both scores. Gripp et al. were the first to show in 2016 that facial image data can be used to guide WES data interpretation.

The RESEARCH application in Face2Gene facilitates comparison of different patient cohorts to each other. In recent proof of principle studies, FDNAs automated facial recognition technology was able to form clusters from photos of affected individuals of the same molecular subgroup (lysosomal storage disease: ML, MPS-I, and MPS-II, Pantel et al. 2017) or with disease-causing mutations in genes of a pathway (GPI, Knaus et al. 2018), thereby, indicating that the facial gestalt can be gene specific to a certain extent.

3 Publications

3.1 Knaus *et al.* Rare Noncoding Mutations Extend the Mutational Spectrum in the PGAP3 Subtype of HPMRS, 2016

***Alexej Knaus**, Tomonari Awaya, Ingo Helbig, Zaid Afawi, Manuela Pendziwiat, Jubran Abu-Rachma, Miles D. Thompson, David E. Cole, Steve Skinner, Fran Annese, Natalie Canham, Michal R. Schweiger, Peter N. Robinson, Stefan Mundlos, Taroh Kinoshita, Arnold Munnich, Yoshiko Murakami, Denise Horn, and Peter M. Krawitz;*

Published in *Human Mutation*, 2016 August;37(8):737-44,
doi: https://doi.org/10.1002/humu.23006

Hyperphosphatasia with mental retardation syndrome (HPMRS) or Mabry syndrome is a congenital disorder of glycosylation (CDG) that is caused by impairment of synthesis or maturation of the GPI anchor. In about half of the affected individuals with the clinical diagnosis of HPMRS pathogenic mutations were identified in *PGAP3*.
In this work, we describe a screening approach with sequence specific baits for transcripts of genes of the GPI pathway, thereby, facilitating the detection of pathogenic mutations in the 3' UTR and intronic variants affecting splicing. The identification of non-coding pathogenic mutations increases the diagnostic yield for HPMRS on the basis of intellectual disability and elevated serum alkaline phosphatase. In six families from different ethnicities we found seven novel pathogenic mutations in PGAP3. Besides five missense mutations we identified an intronic mutation, c.558-10G>A, that causes an aberrant splice product and a mutation in the 3'UTR (c.*559C>T) that is associated with substantially lower mRNA levels probably due to the formation of a new miRNA binding site.
Functional evaluation of pathogenicity was confirmed by real time PCR and flow cytometry of patient derived fibroblasts and blood samples. Here, the application of NGS based cDNA panel sequencing in combination with flow cytometry allowed the cost effective and precise analyses of pathogenic coding and non-coding variants.

Rare non-coding mutations extend the mutational spectrum in the *PGAP3* subtype of Hyperphosphatasia with Mental Retardation Syndrome.

Alexej Knaus[1,2,3,†], Tomonari Awaya[4,†], Ingo Helbig[5,7], Zaid Afawi[6], Manuela Pendziwiat[7], Jubran Abu-Rachma[6], Miles D. Thompson[8], David E. Cole[8], Steve Skinner[9], Fran Annese[9], Natalie Canham[10], Michal R. Schweiger[11], Peter N. Robinson[1,2], Stefan Mundlos[1,2], Taroh Kinoshita[12,13], Arnold Munnich[14], Yoshiko Murakami[12,13,*], Denise Horn[1,††, *], Peter M. Krawitz[1,2,††,*]

[1]Institute for Medical and Human Genetics, Charité-Universitätsmedizin Berlin, Augustenburger Platz 1, 13353 Berlin, Germany

[2]Max Planck Institute for Molecular Genetics, Ihnestr. 63–73, 14195 Berlin, Germany

[3]Berlin-Brandenburg School for Regenerative Therapies (BSRT), Charité Campus Virchow Klinikum, Augustenburger Platz 1, 13353 Berlin, Germany

[4]Department of Pediatrics, Kyoto University Graduate School of Medicine, 54 Shogoinkawaharacho, Sakyo, Kyoto, 6068507, Japan

[5]Division of Child Neurology, The Children's Hospital of Philadelphia, 34th St. and Civic Center Blvd., Philadelphia, PA 19104-4399, USA

[6]Sackler Faculty of Medicine, Tel Aviv University, Tel Aviv, Israel

[7]Department of Neuropediatrics, University Medical Center Schleswig-Holstein, Arnold-Heller-Str. 3, Building 9, 24105 Kiel, Germany

[8]Department of Laboratory Medicine and Pathobiology, University of Toronto, Toronto, ON, Canada

[9]Greenwood Genetic Center, Greenwood, USA

[10]North West Thames Regional Genetics Service, Northwick Park Hospital, Harrow HA1 3UJ, UK

[11]Epigenomics and Tumor Genetics, CCG, University of Cologne, Weyertal 115b, 50931 Cologne, Germany

[12]Department of Immunoregulation, Research Institute for Microbial Diseases, Osaka University, 3-1Yamada- oka, suita, Osaka 565, Japan

[13]World Premier International Immunology Frontier Research Center, Osaka University, 3-1Yamada- oka, suita, Osaka 565, Japan

[14]Hôpital Necker – Enfants Malades, Unité INSERM 781, Laboratoire de génétique moléculaire Tour Lavoisier – 2ème étage, 149 rue de Sèvres, 75743, Paris Cedex 15, France

†Equal contribution, ††Equal contribution ,

*Correspondence: peter.krawitz@charite.de, denise.horn@charite.de, yoshiko@biken.osaka-u.ac.jp

Grant sponsor: This work was supported by a grant of the German Research Foundation, P.M. K (KR3985/6-1), M.R.S. was supported by the Volkswagenstiftung (Lichtenberg program).

Abstract

HPMRS or Mabry syndrome is a heterogeneous glycosylphosphatidylinositol (GPI) anchor deficiency that is caused by an impairment of synthesis or maturation of the GPI-anchor. The expressivity of the clinical features in HPMRS varies from severe syndromic forms with multiple organ malformations to mild non-syndromic intellectual disability. In about half of the patients with the clinical diagnosis of HPMRS pathogenic mutations can be identified in the coding region in one of the six genes, among them *PGAP3*.

In this work we describe a screening approach with sequence specific baits for transcripts of genes of the GPI pathway that allows the detection of functionally relevant mutations also including introns and the 5' and 3' UTR. By this means we also identified pathogenic non-coding mutations which increases the diagnostic yield for HPMRS on the basis of intellectual disability and elevated serum alkaline phosphatase. In eight affected individuals from different ethnicities we found seven novel pathogenic mutations in *PGAP3*. Besides five missense mutations we identified an intronic mutation, c.558-10G>A, that causes an aberrant splice product and a mutation in the 3'UTR, c.*559C>T, that is associated with substantially lower mRNA levels. We show that our novel screening approach is a useful rapid detection tool for alterations in genes coding for key components of the GPI pathway.

Keywords: Intellectual disability, Hyperphosphatasia with Mental Retardation, Mabry syndrome, non-coding mutations, *PGAP3*

Introduction

Glycosylphosphatidylinositol (GPI) anchor deficiencies are a new class of congenital disorders of glycosylation that present with a broad phenotypic spectrum that is incompletely understood. The GPI is a glycolipid that anchors more than 150 proteins to the cell surface. At least 27 genes are involved in the biosynthesis and transport of GPI anchored proteins and disease-causing mutations have been described for 13 of these genes (Freeze, et al., 2014; Kinoshita, et al., 2008). Among the most common features in GPI-anchor deficiencies are intellectual disability, and epilepsies. For Mabry syndrome, a well characterized subtype of GPI-anchor deficiencies, an elevated serum activity of the alkaline phosphatase is an additional characteristic diagnostic marker that initially prompted Mabry and collaborators to postulate a separate syndrome that is now referred to as Hyperphosphatasia with Mental Retardation Syndrome (Horn, et al., 2010; Mabry, et al., 1970; Thompson, et al., 2010). As of 2016, six subtypes of HPMRS are known (OMIM Phenotypic Series, PS239300) and pathogenic mutations in the genes of the GPI anchor synthesis, *PIGV*, *PIGW, PIGY, PIGO*, as well as of the anchor maturation, *PGAP2* and *PGAP3* (OMIM Gene IDs *614207 and *615716), have been identified (Chiyonobu, et al., 2014; Hansen, et al., 2013; Howard, et al., 2014; Ilkovski, et al., 2015; Krawitz, et al., 2012; Krawitz, et al., 2013; Krawitz, et al., 2010). For GPI biosynthesis genes, most of the reported pathogenic variants are missense mutations, but loss of function mutations have also been identified. However, bi-allelic nonsense or frameshift mutations have not been observed in humans so far, but have only been found in compound heterozygous combinations with missense mutations. It is therefore assumed that all inherited forms of GPI-anchor deficiencies, IGDs, have a residual activity of GPI-anchored proteins. This assumption is supported by studies of animal models, as mice incapable of forming GPI-anchors are not viable (Nozaki, et al., 1999; Tarutani, et al., 1997).

Besides mutations that affect the protein function directly, hypomorphic mutations in the promoters for *PIGM* as well as *PIGY* have recently been reported (Almeida, et al., 2006; Ilkovski, et al., 2015). We therefore hypothesize that some of the unsolved cases with Mabry syndrome might also be due to a substantial reduction in the expression of wild type transcripts of the known genes. As a result, we refined our GPI-gene panel screening approach to detect affected individuals on the RNA rather than DNA level. In the current manuscript we present eight previously unreported patients with Mabry syndrome carrying novel mutations in *PGAP3*, a gene of the GPI-anchor maturation. The expressivity of the phenotype varies considerably for this cohort.

Material and Methods

Mutation Analysis

Genomic DNA (gDNA) was isolated from fibroblasts or blood of all participants of this study. The Charité University Medicine ethics board approved this study, and we obtained informed consent from the responsible persons (parents) on behalf of all study participants. The DNA was fragmented and a library for high-throughput sequencing was prepared according to standard procedures. RNA was obtained from fibroblast cultures, fragmented and reversely transcribed into a cDNA library. gDNA and cDNA libraries were enriched with exon specific oligonucleotide baits as previously described (Krawitz, et al., 2013) and high-throughput sequencing was performed on the MiSeq platform. All sequence reads were mapped to the genomic reference GRCh37 and processed with a splice junction mapper in case of cDNA. Most reads of the correctly spliced mRNAs were exon-spanning and fragments mapping to intronic sequences were rare. The coverage of coding exons of all known GPI-synthesis related genes was above twenty fold in all analyzed samples. Sequence variants in gDNA alignments were detected according to GATK's best practice guidelines. All variant calls from gDNA that are discussed in this manuscript were validated by ABI Sanger sequencing. Differences in transcript-specific expression were confirmed by quantitative PCR on RNA isolated from fibroblast cultures. qPCR measurements were performed in triplicates from two biological duplicates. dCt values were normalized agains GAPDH . Primer pair sequences and qPCR settings are available upon request. All sequence variants described in the manuscript have also been submitted to ClinVar and GeneTalk.de.

Characterization of non-coding Mutations

Short read fragments from high-throughput sequencing were first mapped to the human reference genome GRCh37 with bwa-mem and cDNA alignments were further refined with splice junction mapper TopHat. More than 95% of the coding positions of all known genes of

the GPI-anchor synthesis pathway were covered by more than 100 independent sequences. The allele specific ratios for RNA-seq experiments were assessed by considering only high-quality reads (phred>30, less than 3 mismatches).

Cell Culture and Flow Cytometry

Fibroblasts were obtained from deep skin biopsies, treated with collagenase and grown in a Dulbecco's Modified Eagles Media (DMEM) supplemented with 10% fetal bovine serum (FBS), 1% glutamine, 1% Penicillin/Streptomycin and grown in a 5% CO2 incubator.

For investigation of GPI-anchored proteins, cultured skin fibroblasts derived from patient A-II-1, patient B-II-2, patient C-II-2, and controls were removed from the dish with cold EDTA and a cell scraper, pipetted several times to get a single cell suspension, counted, washed and stained with FLAER (Fluorescent labeled aerolysin (AF-488)) and antibodies against GPI-linked proteins (CD55-PE, CD59-PE, CD87-APC, CD73-PE-Cy7) in phosphate buffered saline (PBS) without calcium or magnesium and supplemented with 2% FBS for 1 hour at room temperature. Cells were then centrifuged at 300 g for 3 minutes and washed twice in the above solution. Labelled cells were analyzed using a CantoII flow cytometer (BD Biosciences) and FlowJo™ v. 9.8.2 software.

Results

In all individuals with the minimal diagnostic criteria developmental delay, intellectual disability and elevated serum alkaline phosphatase, we first analyzed the gDNA of GPI-anchor pathway genes for coding mutations as previously described (Howard, et al., 2014). At the time of writing we have 37 individuals who meet these criteria in our ongoing study and were genetically confirmed. In this work we focus on the molecular findings in patients from six unrelated families, who showed mutations in *PGAP3*. In three of these families the results from gDNA sequencing were inconclusive as only one heterozygous coding mutation was

identified that qualified as pathogenic based on current classifications standards. By cDNA sequencing we could confirm a functional impact for additional non-coding mutations in these patients and we argue that this extended work-up increases the diagnostic yield. Considering all molecularly confirmed cases of Mabry syndrome in our lab over the last five years *PGAP3* has now become the second most prevalent disease gene for this phenotypic series after *PIGV*.

All patients with genetic alterations in *PGAP3* have a combination of severe global developmental delay and elevated levels of alkaline phosphatase activity, which are the most indicative features for HMPRS (Supp. Table S1). However, we also observe that there is some variability within the phenotypes and we will therefore describe the clinical features of the patients of this report in detail. Two individuals started to walk at a normal age, but the others did not walk until the age of between 3 and 7 years and one individual was not able to walk at all at the age of 16 years. Five individuals did not achieve verbal communication, and three other patients used only single words. Furthermore, six individuals developed seizures with variable onset and severity. Muscular hypotonia was found in four individuals. The presence of ataxia or unsteady gait was striking in 7 patients (patients of family B, C, D, E and F)

Six patients showed particular behavioral problems. Among them sleep disturbance was described as most frequently reported feature (patients A, B, F, E), one patient (D) exhibited long lasting episodes of hypersomnolence classified as Klein-Levine syndrome. Additionally, hyperactivity, autistic features and obsessive-compulsive disorder were documented in patients A and D. In patient B, MRI revealed a mild brain anomaly, namely a small capsula interna. The siblings of family E also showed brain atrophy of the temporal lobes. A megacisterna magna was found in patient F. Hearing loss was documented in three individuals (patients from family E and F)

At birth normal growth parameters and head circumferences were observed in all patients.

During infancy and childhood, growth parameters were found to be variable but within the normal range in most patients. However two individuals showed an increased and one a decreased weight at the last physical examination. The postnatal occipitofrontal head circumference varied between -0.4 and +3.2 SD with three affected individuals who showed macrocephaly. No distinct pattern of facial anomalies was present in this cohort. But five of them showed some facial dysmorphisms compatible with other forms of HPMRS such as short nose with a broad nasal bridge and tip as well as a thin and tented upper lip. Apart from broad fingers and toe nails in four individuals (families B, D, E) no other anomalies of the hands and feet were found. A cleft palate was documented in three patients (families A, D, F). Despite a substantial clinical variability in our patient cohort, all patients showed global developmental delay as well as hyperphosphatasia and thus fulfilled the criteria for Mabry syndrome.

All affected individuals were first analyzed for rare coding variants in known exons of the GPI-anchor synthesis pathway on genomic DNA as previously described (Krawitz, et al., 2013) or through related sequencing techniques. Genomic sequencing alone was able to identify the molecular cause of the disease for the affected individuals in family D, E and F, identifying the following homozygous or compound heterozygous missense mutations: D-II-1: p.Ser107Leu, p.Asp305Gly, E-II-3 and E-II-4: p.Asp282Gly, F-II-1: p.Cys171Arg, p.Trp287Cys (Fig. 2). All these missense mutations caused the decreased activity of PGAP3 (Supp. Figure S7). This finding also confirms that bi-allelic missense mutations represent the most common cause of Mabry syndrome in all known disease genes, *PIGV*, *PIGO*, *PGAP2* and *PGAP3*.

In 4/8 patients only single heterozygous mutations could be identified, that have a detrimental effect on the protein level or its activity (A-II-1: p.Ser107Leu, B-II-2: p.Met135Hisfs*28, C-II-1/2: p.Trp287Cys) (Supp. Figure S8). As hypomorphic promoter mutations have been described in two other genes of the GPI-anchor synthesis pathway, *PIGM* and *PIGY*, we

hypothesized that the missing second mutations could also be non-coding variants (Almeida, et al., 2006; Ilkovski, et al., 2015). In contrast to the classification of coding mutations, predicting the effect of variants that are deeply intronic or in untranslated regions is challenging from a bioinformatics perspective. We have therefore further developed our gene-panel screening approach in such a way that it is suitable for the analysis of transcripts involved in the GPI-anchor synthesis and remodeling. Before we subjected the samples to a quantitative analysis of cDNA we confirmed a reduction of GPI-linker markers on the cell surface.

In the subsequent analysis of the cDNA we achieved optimal results in target specific enrichment with a mean fragment size around 200 bp. Most reads of the correctly spliced mRNAs were exon-spanning and fragments mapping to intronic sequences were rare.

A considerable amount of sequence reads that map to intron 5 in *PGAP3* were found in the affected individuals of families A and B. In A-II-1 there is a sharp drop in coverage at the intron-exon boundary to almost 50% and in B-II-2 to about 70% indicating that a heterozygous allele is causing a splicing defect. Most of the sequence fragments that reach into intron 5, show the intronic variant c.588-10G>A, while this variant is a clear heterozygous call on the genomic level (Fig. 3). In all heterozygous carriers of the c.588-10G>A mutation as well as in all healthy controls there is a low rate of intron 5 fragments with the wild type allele c.588-10G. We therefore assume that even in the wild type, intron 5 is not always spliced out, but that the mutation c.588-10G>A reduces the splicing efficiency dramatically. The single base pair duplication c.402dupC in the father of family B (B-I-1) results in a premature stop codon. The resulting transcript including the c.402dupC is thus subject to nonsense-mediated decay, that is confirmed by qPCR expression analysis of PGAP3 in fibroblasts. The second heterozygous mutation of the index (B-II-2) c.588-10G>A, results in an expression level of only 10% (Supp. Figure S9). This also explains the less prominent reduction of coverage in B-II-2 at the exon-intron-boundary (Fig. 3, panel 4).

In affected individuals C-II-1 and C-II-2 we identified a heterozygous missense mutation in exon 7 of *PGAP3*, c.861G>T, p.Trp287Cys. The only sequence variant that would qualify as pathogenic second *PGAP3* mutation based on its allele frequency is a novel 3'UTR mutation, c.*559C>T. On the cDNA level this mutation only occurs in less than a fifth of the reads, indicating a more than threefold reduction of this transcript (Fig. 4A). This is in agreement with the contrary ratio of the compound missense mutation c.861G>T that is present in the majority of the sequence reads. The low expression of *PGAP3* for the haplotype with the 3'UTR mutation can be quantified by qPCR from fibroblast RNA. The father, C-I-1, who is a heterozygous carrier of the missense mutation p.Trp287Cys, shows expression levels comparable to a healthy control, while the index (C-II-2) and her mother (C-I-2), who are carrier of c.*559C>T, have a markedly reduced expression of *PGAP3* (Supp. Figure S9).

In summary, we have four patients with non-coding variants in our cohort that are likely to retain a residual level of functional PGAP3. However, we suspected that the amount of wild type PGAP3 is pathologically low and in consequence it should have the same detrimental impact on GPI-anchored markers, GPI-APs, as seen for pathogenic coding variants. So far flow cytometry is used in a qualitative manner to assess GPI-anchor deficiencies on a functional level. FACS analysis of the peripheral granulocytes is very helpful in the diagnostic procedure of inherited GPI deficiencies. Many IGD's show decreased expression of CD16 or FLAER compared to healthy controls. But the limitation is that the blood should be analyzed within two days without fixation, otherwise the expression levels gradually decrease which makes the results unreliable. For more quantitatively applicable results we established a flow cytometry protocol for fibroblasts and assessed the cell surface levels for GPI-APs for different patients. In all three patients with non-coding mutations in *PGAP3* the mean fluorescent intensity (MFI) of the GPI-linked proteins CD55, CD59 as well as FLAER was markedly reduced compared to healthy controls (Fig. 5). The reduction was similar in

PGAP3 deficient fibroblasts with compound heterozygous mutations (QM-100:[p.Asp305Gly; p.Leu147Profs*16])(Howard, et al., 2014).

Discussion

HPMRS represents the largest subgroup of IGDs. The clinical variability of the expressivity of this syndrome is wide and little is known about gene- or genotype-phenotype correlations. In our current study group intellectual disability as well as elevated ALP are the only consistent features across patients compared with other individuals affected with HPMRS caused by mutations in *PIGV, PIGW, PIGY*, *PIGO* and *PGAP2*. Speech development, especially expressive language, was more affected than motor skills in the majority of patients (Table 1, supplemental material). Seizures are present in the majority of this cohort. Behavioral problems, in particular sleep disturbances and autistic features as well as ataxia tend to be frequent. Most patients of this cohort presented with some facial dysmorphism compatible with HPMRS. Furthermore, brachytelephalangy, which is an important diagnostic sign in other types of HPMRS, is not present in any of the affected individuals with *PGAP3* mutations. Cleft palate as the only associated malformation found in this cohort has been previously documented in other individuals with HPMRS due to mutations in *PGAP3* but also in the other groups of Mabry syndrome. Variability regarding the postnatal growth, body weight and OFC has already been observed in individuals carrying *PIGV*, *PIGO*, and *PGAP2* mutations.

For all known HPMRS disease genes, the majority of pathogenic variants are missense mutations, a finding that is also supported by our data. Frame-shift mutations, that result most likely in a complete loss of function, have only been observed in a compound heterozygous

state with missense mutations and individuals with such combinations seem to be affected more severely.

Flow cytometry of GPI-anchored markers on the cell surface of peripheral granulocytes has been used in many patients with suspected IGDs for confirmatory diagnostic purposes. However, FACS measurements on blood cells are known to be variable in time and expression levels are difficult to compare between samples. In a measurement of granulocytes from F-II-3 we did for instance not observe a marked reduction of GPI-makers although the mutations have been shown to be pathogenic in the CHO test assay (supplemental material). In other cases repeated measurements of ALP in the same patient have also shown values that were only borderline high in some instances. Thus also unremarkable results in flow cytometry of blood cells do not rule out HPMRS.

For a better reproducibility and comparability of different pathogenic mutations we established a FACS protocol for fibroblasts and tested cells with non-coding as well as coding mutations in *PGAP3* and *PIGV*. Although the numbers for which we were able to perform FACS analysis on fibroblasts are still too small to be statistically significant, there seems to be no obvious correlation between the MFIs of the tested markers and the severity of the phenotype. The reduction in MFI in fibroblasts with impaired PGAP3 is also comparable to cells with pathogenic mutations in *PIGV* that we previously assessed (PIGV-X-II-1: [p.Ala341Glu; p.Ala341Glu], PIGV-Y-II-1:[p.Ala165Glu; p.Arg460*], PIGV-Z-II-2: [p.Cys156Tyr; p.Ala341Glu]). In two of these patients intellectual disability is the predominant clinical feature (Horn, et al., 2011; Krawitz, et al., 2010), whereas in patient PIGV-Y-II-1 (not reported so far) the most prominent manifestation is treatment-resistant epilepsy. Seizures are a common feature in HPMRS and in some cases they are intractable and life-threatening (Nakamura, et al., 2014); PIGV-Y-II-1 thus represents a severely affected case with frequent status epilepticus. Still no quantitative differences of the MFIs between the milder and more severe PIGV cases could be observed in the fibroblast cultures.

Most pathogenic mutations in genes of the GPI-anchor synthesis primarily decrease the surface expression of GPI-anchored proteins (e.g. *PIGV*), whereas deficiencies in *PGAP2 or PGAP3* genes, which involve in lipid remodeling in the Golgi result in expression of GPI-APs that are more prone to cleavage (Maeda, et al., 2007). *PGAP3* is among putative membrane-bound hydrolases called CREST superfamily proteins and it removes unsaturated fatty acid from the sn-2 position of lipid moiety of GPI anchored protein in the Golgi, the first step of fatty acid remodeling, followed by the attachment of saturated fatty acid through *PGAP2* involvement (Pei, et al., 2011). This fatty acid remodeling reaction is necessary for association of GPI-APs to lipid raft. In PGAP3 deficient cells GPI-APs are expressed at normal level but could not localize on lipid rafts because of their non-remodeled lipid structure, which might cause the symptoms of the patients.

For a better understanding of genotype-phenotype correlations in Mabry syndrome it might be worthwhile to extend the flow cytometric profiling to more GPI-APs and to further tissues. A deeper insight into the dynamics of GPI-APs on the cell surface might also help us to design experiments for analyzing the conjectured feedback mechanism that regulates the expression of genes of the GPI-anchor synthesis.

Our study also shows that new screening approaches, such as cDNA sequencing, will help to increase the diagnostic yield for inherited GPI-anchor deficiencies further. With a quantitative and allele specific analysis of transcripts regulatory variants can be identified, extending the pathogenic mutation spectrum of Mabry Syndrome.

Figures

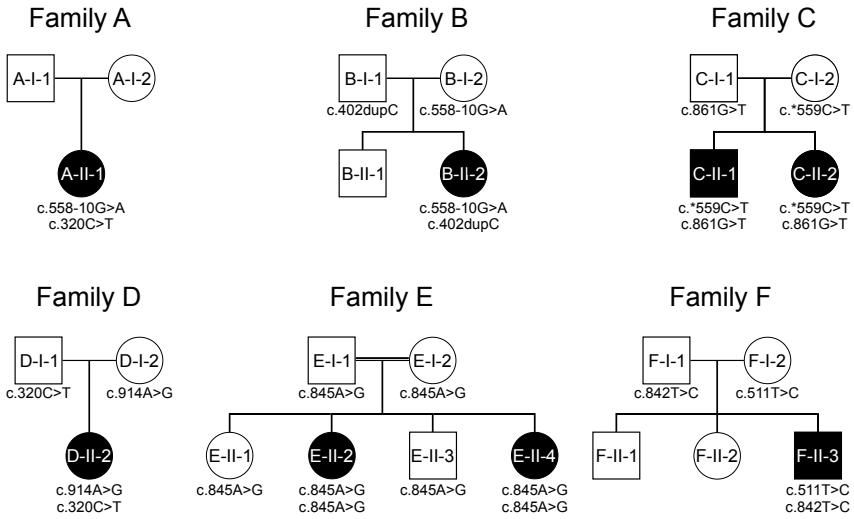

Figure 1: Pedigrees and segregation of identified mutations.

Families A, B, C, and D, are of European descent, family E are Palestinians, and patient F is from Japan. For detailed clinical information and high resolution photographs of patients, see supplemental material.

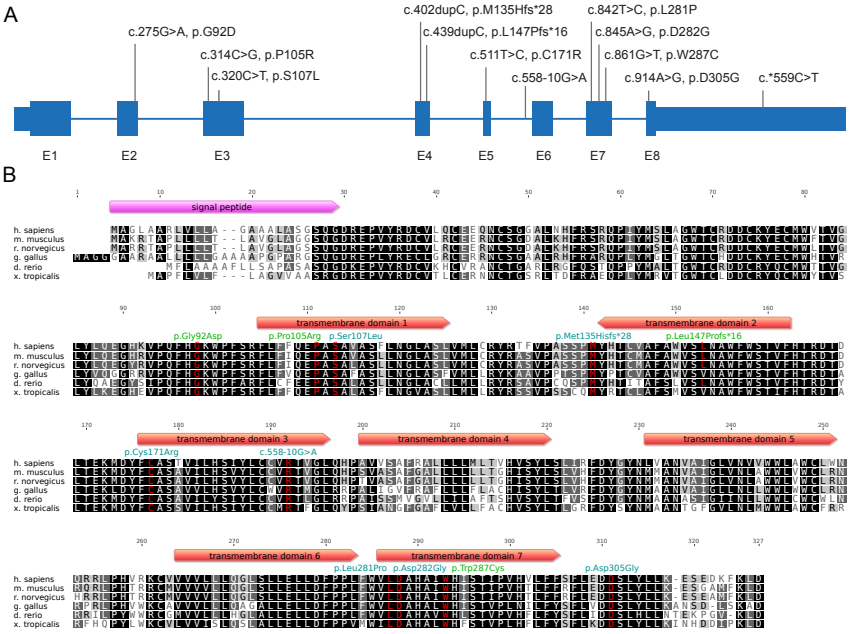

Figure 2: Overview of pathogenic mutations in PGAP3.

A) The coding sequence of PGAP3 is organised in 8 exons. The majority of pathogenic mutations in PGAP3 are missense mutations without a specific pattern for the distribution of pathogenic variants. The intronic mutation c.558-10G>A impairs the splicing of intron 5 and the 3'UTR mutation c.*559C>T is associated with a reduced expression. Mutation numbering is based on cDNA level.

B) The protein has 7 predicted transmembrane domains (TDs) and the mutations affect highly conserved amino acid residues in TDs as well as in the intracellular and extracellular sites.

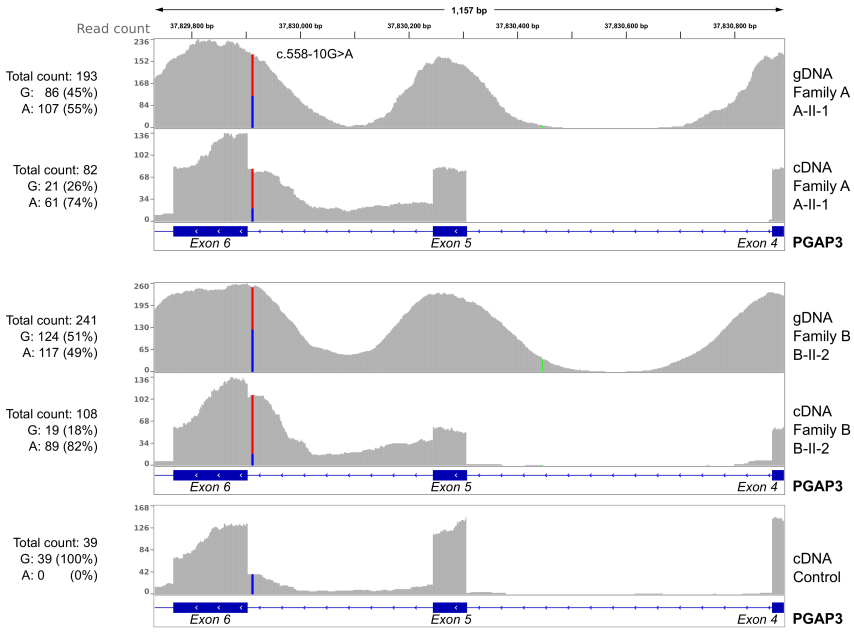

Figure 3: Intronic mutation causing aberrant splicing.

The coverage is shown for g- and cDNA of PGAP3 for exons 5, 6 and partly 4, as well as for introns 4 and 5 of individuals A-II-1 (panel 1 gDNA and panel 2 cDNA), B-II-2 (panel 3 gDNA and panel 4 cDNA) and one control (panel 5 cDNA). gDNA sequence reads of the affected individuals of family A and B show the heterozygous intronic mutation c.558-10G>A with the expected ratio of about 50%.

Intron 4 is correctly spliced out in the cDNA of all samples. A low rate of reads map into intron 5 in the healthy control (panel 5), suggesting that intron 5 is not removed in all transcripts. However, the two affected individuals, show a high increase of reads from intron 5 in the cDNA. While about half of the enriched fragments of genomic DNA show the c.558-10G>A mutation, the fraction of the mutation increases to about four fifth in the cDNA. The heterozygous mutation c.558-10G>A thus impedes correct splicing of intron 5 from the pre-mRNA and results in an aberrant splice product.

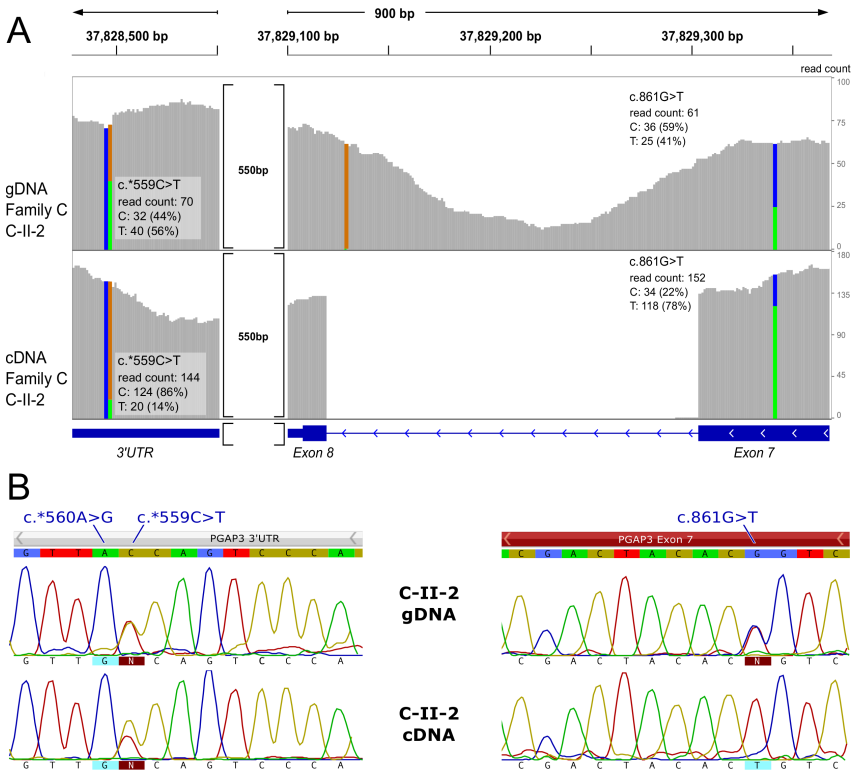

Figure 4: Effect of 3' UTR mutation on transcript level.

A) The ratio of reads on gDNA of the compound heterozygous mutations c.861G>T and c.*559C>T are comparable (upper panel) in the affected individual from family C. For cDNA data the allelic balance deviates in opposite directions. On cDNA level the ratio of the mutant allele at the 3'-UTR position drops below one fifth, while most of the sequence reads show the mutant allele at the position of the missense mutation.

B) Sanger sequencing of gDNA and cDNA of individual C-II-2. A quantitative measurement of transcripts carrying the mutations is not possible via Sanger sequencing.

References

Almeida AM, Murakami Y, Layton DM, Hillmen P, Sellick GS, Maeda Y, Richards S, Patterson S, Kotsianidis I, Mollica L and others. 2006. Hypomorphic promoter mutation in PIGM causes inherited glycosylphosphatidylinositol deficiency. Nature medicine 12(7):846-51.

Chiyonobu T, Inoue N, Morimoto M, Kinoshita T, Murakami Y. 2014. Glycosylphosphatidylinositol (GPI) anchor deficiency caused by mutations in PIGW is associated with West syndrome and hyperphosphatasia with mental retardation syndrome. J Med Genet 51(3):203-7.

Freeze HH, Chong JX, Bamshad MJ, Ng BG. 2014. Solving Glycosylation Disorders: Fundamental Approaches Reveal Complicated Pathways. Am J Hum Genet 94(2):161-175.

Hansen L, Tawamie H, Murakami Y, Mang Y, ur Rehman S, Buchert R, Schaffer S, Muhammad S, Bak M, Nothen MM and others. 2013. Hypomorphic mutations in PGAP2, encoding a GPI-anchor-remodeling protein, cause autosomal-recessive intellectual disability. Am J Hum Genet 92(4):575-83.

Horn D, Krawitz P, Mannhardt A, Korenke GC, Meinecke P. 2011. Hyperphosphatasia-mental retardation syndrome due to PIGV mutations: expanded clinical spectrum. American journal of medical genetics. Part A 155A(8):1917-22.

Horn D, Schottmann G, Meinecke P. 2010. Hyperphosphatasia with mental retardation, brachytelephalangy, and a distinct facial gestalt: Delineation of a recognizable syndrome. European journal of medical genetics 53(2):85-8.

Howard MF, Murakami Y, Pagnamenta AT, Daumer-Haas C, Fischer B, Hecht J, Keays DA, Knight SJ, Kolsch U, Kruger U and others. 2014. Mutations in PGAP3 Impair GPI-Anchor Maturation, Causing a Subtype of Hyperphosphatasia with Mental Retardation. Am J Hum Genet.

Ilkovski B, Pagnamenta AT, O'Grady GL, Kinoshita T, Howard MF, Lek M, Thomas B, Turner A, Christodoulou J, Sillence D and others. 2015. Mutations in PIGY: expanding the phenotype of inherited glycosylphosphatidylinositol (GPI) deficiencies. Hum Mol Genet.

Kinoshita T, Fujita M, Maeda Y. 2008. Biosynthesis, remodelling and functions of mammalian GPI-anchored proteins: recent progress. Journal of biochemistry 144(3):287-94.

Krawitz PM, Murakami Y, Hecht J, Kruger U, Holder SE, Mortier GR, Delle Chiaie B, De Baere E, Thompson MD, Roscioli T and others. 2012. Mutations in PIGO, a member of the GPI-anchor-synthesis pathway, cause hyperphosphatasia with mental retardation. Am J Hum Genet 91(1):146-51.

Krawitz PM, Murakami Y, Riess A, Hietala M, Kruger U, Zhu N, Kinoshita T, Mundlos S, Hecht J, Robinson PN and others. 2013. PGAP2 mutations, affecting the GPI-anchor-synthesis pathway, cause hyperphosphatasia with mental retardation syndrome. Am J Hum Genet 92(4):584-9.

Krawitz PM, Schweiger MR, Rodelsperger C, Marcelis C, Kolsch U, Meisel C, Stephani F, Kinoshita T, Murakami Y, Bauer S and others. 2010. Identity-by-descent filtering of exome sequence data identifies PIGV mutations in hyperphosphatasia mental retardation syndrome. Nature genetics 42(10):827-9.

Mabry CC, Bautista A, Kirk RF, Dubilier LD, Braunstein H, Koepke JA. 1970. Familial hyperphosphatase with mental retardation, seizures, and neurologic deficits. The Journal of pediatrics 77(1):74-85.

Maeda Y, Tashima Y, Houjou T, Fujita M, Yoko-o T, Jigami Y, Taguchi R, Kinoshita T. 2007. Fatty acid remodeling of GPI-anchored proteins is required for their raft association. Mol Biol Cell 18(4):1497-506.

Nakamura K, Osaka H, Murakami Y, Anzai R, Nishiyama K, Kodera H, Nakashima M, Tsurusaki Y, Miyake N, Kinoshita T and others. 2014. PIGO mutations in intractable epilepsy and severe developmental delay with mild elevation of alkaline phosphatase levels. Epilepsia 55(2):e13-7.

Nozaki M, Ohishi K, Yamada N, Kinoshita T, Nagy A, Takeda J. 1999. Developmental abnormalities of glycosylphosphatidylinositol-anchor-deficient embryos revealed by Cre/loxP system. Lab Invest 79(3):293-9.

Pei J, Millay DP, Olson EN, Grishin NV. 2011. CREST--a large and diverse superfamily of putative transmembrane hydrolases. Biol Direct 6:37.

Tarutani M, Itami S, Okabe M, Ikawa M, Tezuka T, Yoshikawa K, Kinoshita T, Takeda J. 1997. Tissue-specific knockout of the mouse Pig-a gene reveals important roles for GPI-anchored proteins in skin development. Proc Natl Acad Sci U S A 94(14):7400-5.

Thompson MD, Nezarati MM, Gillessen-Kaesbach G, Meinecke P, Mendoza-Londono R, Mornet E, Brun-Heath I, Squarcioni CP, Legeai-Mallet L, Munnich A and others. 2010. Hyperphosphatasia with seizures, neurologic deficit, and characteristic facial features: Five new patients with Mabry syndrome. Am J Med Genet A 152A(7):1661-9.

Supplemental Material

Clinical Data

Patient A-II-1

Supplementary Figure 1: A-II-1

This patient is an adult female, the first child of non-consanguineous parents of European American origin. The further family history was unremarkable. She was delivered spontaneously at 40 weeks of gestation with a length of 49.5 cm (-1 SD), weight of 3175 g (-0.7 SD) and occipitofrontal head circumference (OFC) of 35 cm (mean). After birth, physical examination revealed a cleft palate which had been surgically corrected in the first months of life. At that time, abdominal ultrasound and ultrasound examinations of the brain were normal. Echocardiogram revealed a small PDA that closed spontaneously.
Early developmental milestones were reported as normal with sitting at 6 months, walking at 13 months and first words at 9 months. At 2 years she has had regression in her vocabulary skills. Later on she had no verbal communication. At 3 years she developed attention deficit disorder with hyperactivity and significant sleeping problems. At 19 years, she was noted to have obsessive-compulsive disorder in addition to autistic features and constant sleep disturbance. At 20 years she has begun having seizures which corresponded well to anticonvulsants.
During infancy and childhood, weight and length progressed in the normal range but head circumference was above the normal range. At age of 25 years, her length was 161.3 cm (- 0.6 SD), weight 87 kg, BMI 33.3 (obese range) and her OFC 58.2 cm (+3.2 SD). Her facial signs included synophris, deep set eyes, up-slanting palpebral fissures, a broad nasal bridge, high and prominent cheekbones, a short philtrum, thin upper and lower lips as well as bifid uvula (S. Fig. 1). Her hands and feet were normal as well as her nails. X-ray of the hands revealed normal findings.
Apart from a variety of normal metabolic tests, AP activity was raised (469 U/L, upper limit of the normal range 136 U/L) in repeated tests.

Patient B-II-2

This girl is the second child of German parents. This pregnancy was complicated by gestational diabetes, and prolonged delivery necessitated caesarean delivery at week 38. Birth weight was 3950 g (+1.1 SD), length 49 cm (-0.5 SD) and normal head circumference.
Her early psychomotor development was normal. At age 16 months, she started walking. At age 12 months, the girl spoke her first word. Later on psychomotor retardation became evident with pronounced speech delay. Since the age of 18 months, myoclonic seizures occurred. At that age she developed significant sleep disturbance.
Physical examination of the 3-year-old patient showed a height of 97 cm (+0.4 SD), a weight of 18 kg (+ 2.4 SD), and an OFC of 50 cm (+0.4 SD) as well as muscular hypotonia and ataxia. Facial dysmorphism was subtle with up-slanting palpebral fissures, a short nose, broad nasal bridge and tip, tented upper lip and small teeth. Hands and feet showed broad finger and toe nails.

Apart from a small capsula interna the MRI investigation of the brain at age of 2 years gave a normal result. Serum alkaline phosphatase level was elevated with 333 U/L, upper normal range is 297 U/L at this age.

Patient C-II-1 and C-II-2

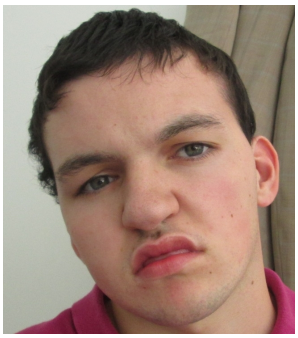

Supplementary Figure 2:C-II-1

Patients C-II-1 and C-II-2 were first described by (Thompson, et al., 2010). The boy was born to unrelated healthy French parents after a term pregnancy and normal delivery (birth weight: 3370 g, height: 50 cm, OFC: 37 cm; +1.7 SD). His ability to sit unaided (12 months) and walk was delayed (after 3 years). After two years of age he received valproate and diazepam for iterative episodes of myoclonic jerks. At 5 years, examination showed normal height and weight but enlarged OFC (56.5 cm, +3 SD), coarse facies, long palpebral fissures, prominent cheeks, a large mouth with a tented upper lip, a short philtrum, and mild joint hypermobility (S. Fig. 2). His gait was unstable with mild cerebellar ataxia. He had weak deep tendon reflexes. Oculomotor apraxia was noted. EEG and brain MRI were normal. Metabolic work up detected very high levels of total alkaline phosphatases (830-1000 U/l, normal range 125-410). Array CGH and metabolic tests were otherwise normal. He is now a 22 years-old man living in a home for disabled adults. He has limited autonomy, no speech development but he understands simple orders.

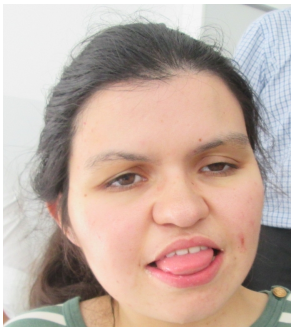

Supplementary Figure 3:C-II-2

His younger sister was born after a term pregnancy and normal delivery (birth weight: 3300 g, height: 49 cm, OFC: 36.5 cm, +1.2SD). Her ability to sit unaided and walk was also delayed (3.5 years). At that age, her facial appearance was quite similar to that of her brother, with enlarged head circumference (53 cm, +2 SD), normal height and weight, long palpebral fissures, small ears and teeth, large mouth, full cheeks and mild joint hypermobility (S. Fig. 3). She also had oculomotor apraxia and no speech development. Her gait was unstable with mild cerebellar ataxia. Her total plasma alkaline phosphatases were markedly elevated (830-900 U/l, normal range 125-410). Histopathological analyses of cultured skin fibroblasts and bone biopsies taken during hip surgery at 10 years revealed accumulation of mixed lipid and carbohydrate storage material of unknown nature in enlarged vacuoles within swollen cultured cells. At the age of 22 years, she had limited autonomy and no speech development.

Patient D-II-1

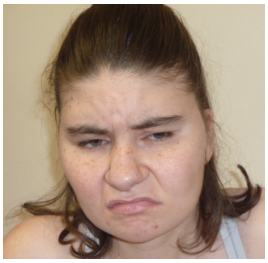

Supplementary Figure 4: D-II-1

Her mother had four miscarriages but also a healthy son. In the pregnancy with the patient the mother described reduced fetal movements. The patient was delivered by planned Caesarean section at 40 weeks, weighing 4300 g (+2 SD). A Cleft soft palate was repaired at 7 months of age. She sat unstably at 9 months and walked at three years, but was extremely unsteady and slow. She has never spoken and is not continent. Abdominal pain and chronic constipation led to the diagnosis of intestinal malrotation which was repaired at the age of 9 years, but constipation did not improve. She started her menses at the age of 12 years. During her teenage years she developed autistic features and episodes of hypersomnolence classified as Kleine-Levin syndrome. Therefore she was treated with carbamazepine for 10 years. After stopping of this therapy at age of 23 years, she developed seizures. Examination at this age showed normal OFC (55.6 cm, +1.2 SD), slightly coarse face with deep set eyes and prominent cheeks (S. Fig. 4). Her hands and feet appeared normal, however her second toenail was broad. In repeated tests she has been found to have increased AP (667 U/L with normal range 35-105).

Patient E-II-2 and E-II-4

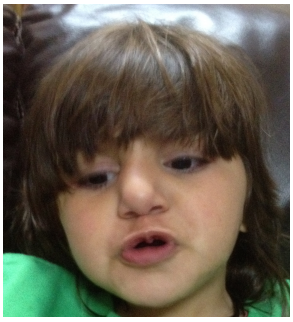

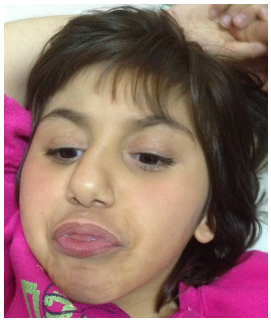

Supplementary Figure 5: E-II-2 and E-II-4

These two girls are the second and forth child of consanguineous Palestinian parents. Both pregnancies were normal with spontaneous term delivery without complications, length, weight and OFC within normal limits. Both affected siblings had early developmental delay with severe lax ligaments and muscular hypotonia. Psychomotor retardation became evident with pronounced speech delay and later on they developed severe spastic quadriparesis.E-II-2 remained bed ridden and can use her hand only for simple tasks. E-II-4 started walking with help at age of 7 years. Brain MRIs of both patients at age of 2 and 3 years showed brain atrophy of temporal lobes partially due to vascular events. Since the age of 5 years tonic clonic seizures occurred in E-II-2 and had been very difficult to manage by different anti-epileptic drugs (Lamotrigene, clonazepam). At that E-II-2 also developed significant sleep disturbance treated by melatonin. EEG showed generalized slowing of the background with spike/slow wave activityand. focal epileptic activity most highlighted in occipital area. Facial features included a broad nasal tip and a tented upper lip in both patients (S. Fig. 5)

Patient F-II-3

This boy is the third child of non-consanguineous Japanese parents. His brother and sister are both healthy. He was born at 34 weeks gestation by caesarean section. Cleft palate without cleft lip, macroglossia, micrognathia, and ear lobe anomaly were noticed at birth. Due to respiratory distress and poor sucking, he needed intensive medical care, and required tube feeding until 1.5 months. He had severe muscular hypotonia and sensorineural hearing loss. There was no brachytelephalangy. His psychomotor development was severely delayed. He learned to roll over at 8 months. At last examination at age of 4 years and 4 months he could not sit alone. He was always very irritable and had no meaningful words. No seizure occurred. Sleep disturbance and bruxism were noted. He had recurrent episodes of pneumonia and suffered from severe food allergy and eczema.
Increased serum alkaline phosphatase was persistent (1,848 to 5,275 IU/L, compared to normal range 115 to 335 IU/L). High serum IgE was also noted (220 to 680 IU/mL, compared to normal range <170 IU/mL). Flow cytometry showed normal expression of GPI-APs on blood cells including erythrocytes, granulocytes, lymphocytes, and monocytes (S. Fig. 6.) Head MRI revealed megacisterna magna. Body CT scan and ultrasonography revealed no apparent morphological anomaly.

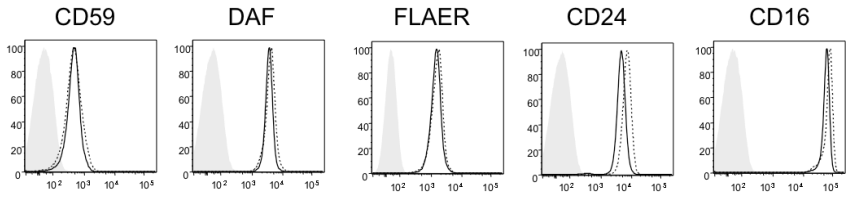

Supplementary Figure 6: Flow cytometric measurements of GPI-linked markers on cell surface of blood cells. No marked reduction of expression levels compared to wildtype controls. Black line: affected individual, dotted line: wildtype control, gray area: unstained cells, background.

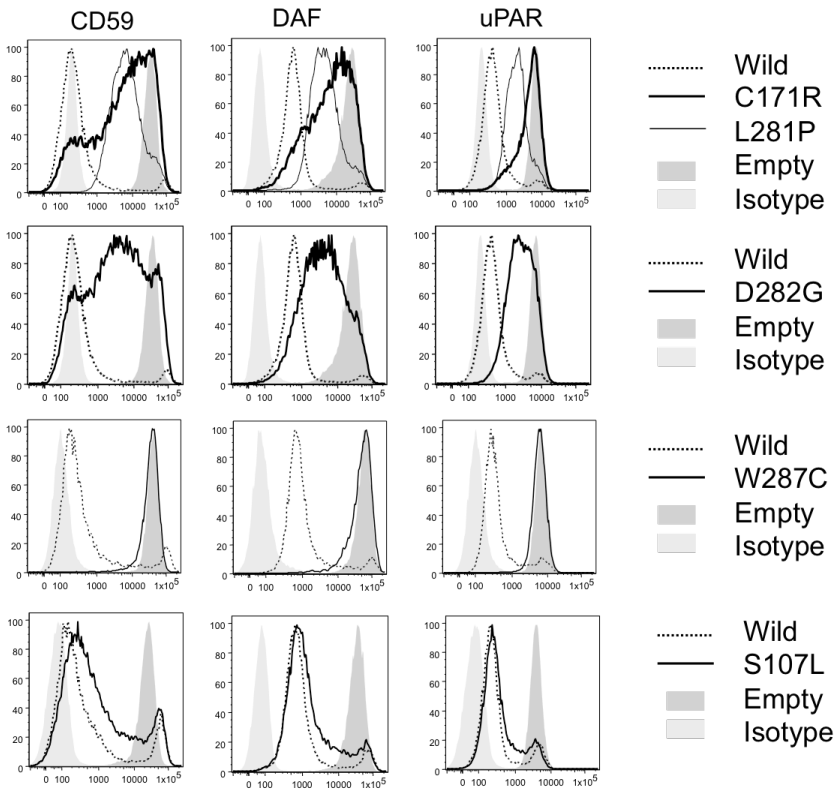

Supplementary Figure 7: PGAP3/2 double deficient CHO cells (C84 DM-C2, *Mol. Biol. Cell* vol.18 1497-1506,2007) were transiently transfected with HA-tagged wild type and suggested mutant PGAP3 driven by the strong promoter SRalpha (pME HA-PGAP3). Two days later, the surface expressions of GPI-anchored proteins, CD59, DAF and uPAR were assessed by flow cytometry. PGAP2/3 double deficient cells which showed normal expression of GPI-APs (dark gray shadows) became PGAP2 single deficient cells when it was transfected with wild type PGAP3 expression vector and surface expression of GPI-APs were decreased (dotted lines). The activity of each mutant was decreased (thick lines).

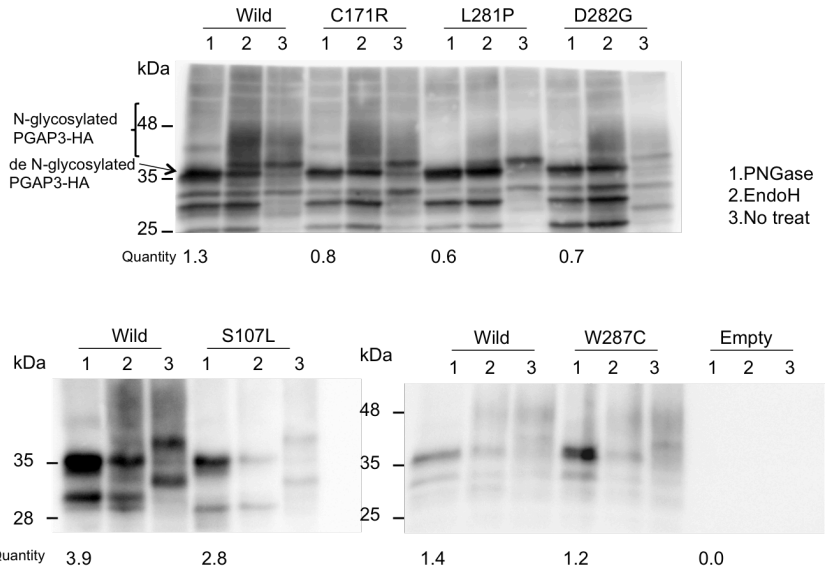

Supplementary Figure 8: Protein expression levels of PGAP3 wt and mutant transcripts. Two days after transfection of each PGAP3 construct, lysates were immunoprecipitated with anti-HA beads (H-7, Sigma). The protein expression levels all mutants with the novel missense mutations C171R, L281P, D282G, S107L and W287C were significantly reduced. These results are comparable to mutant constructs with pathogenic mutations, that have already been reported in (Howard, et al., 2014). The precipitates were digested with Endoglycosidase H or PNGase F. Only mature PGAP3 is resistant to Endo H. Thus a reduction of the smear of N-glycosylated PGAP3 after Endo H indicates also a higher fraction of immature PGAP3 that resides in the ER.

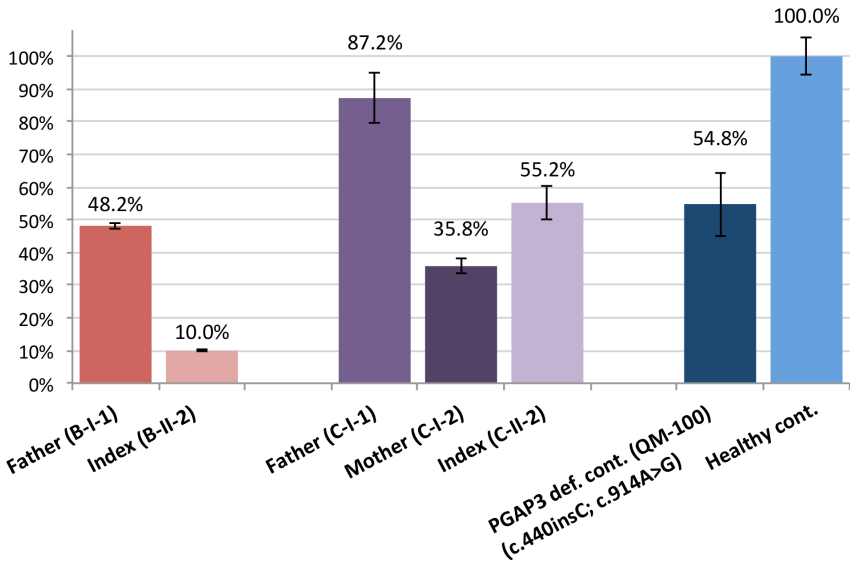

Supplementary Figure 9: *PGAP3* expression measured by RT qPCR from fibroblast total RNA. Patient and control fibroblasts were cultured in 6-wells for four days to reach full confluency. Total RNA was isolated with Trizol and 200ng of total RNA were used for reverse transcription to cDNA. GAPDH was used for normalization. Two biological replicates of RNA were used and qPCR were performed with triplicates. The expression of *PGAP3* in the father of family B (B-I-1) is reduced by half, probably due to nonsense-mediated decay of the transcript resulting from the c.402dupC mutation. The index (B-II-2) with the second mutation c.588-10G>A shows a reduction of *PGAP* expression to only 10%. In family C the father (C-I-1) with the missense variant c.861G>T expresses PGAP3 at a similar level as healthy controls, while the mother (C-I-2) and the index (C-II-2) with the 3' UTR mutation have substantially reduced expression of PGAP3. QM-100 from Howard et al. (individual II-1 from family B) shows also a reduction of PGAP3 expression by half, compared to pooled healthy controls.

Howard MF, Murakami Y, Pagnamenta AT, Daumer-Haas C, Fischer B, Hecht J, Keays DA, Knight SJ, Kolsch U, Kruger U and others. 2014. Mutations in PGAP3 Impair GPI-Anchor Maturation, Causing a Subtype of Hyperphosphatasia with Mental Retardation. Am J Hum Genet.

Thompson MD, Nezarati MM, Gillessen-Kaesbach G, Meinecke P, Mendoza-Londono R, Mornet E, Brun-Heath I, Squarcioni CP, Legeai-Mallet L, Munnich A and others. 2010. Hyperphosphatasia with seizures, neurologic deficit, and characteristic facial features: Five new patients with Mabry syndrome. Am J Med Genet A 152A(7):1661-9.

3.1.1 Contribution

The manuscript was handed in on 18th November 2015. It was accepted on 3rd of April 2016, and published online on 27th of April 2016 in the journal *Human Mutation*, Vol. 37, No. 8, pages 737 – 744.

Sequencing and functional analyses were performed by the joint first authors (Knaus, A. and Awaya, T.). The coauthors (Afawi, Z., Pendziwiat, M., Abu-Rachma, J., Thompson, M.D., Cole, D.E., Skinner, S., Annese, F., Canham, N., Munnich, A., and Horn, D.,) contributed the patient data, patient images and clinical information. Group leaders and supervisors (Helbig, I., Robinson, P.N., Schweiger, M.R., Mundlos, S., Kinoshita, T., and Murakami, Y.) designed and provided resources for the experiments. The last authors (Horn, D., Krawitz, P.M.) evaluated the clinical information and designed the manuscript. The manuscript was written by the first and last author (Knaus A. and Krawitz, P.M.). All authors were involved in correction and final approval of the manuscript during the revision process.

3.1.2 Discussion

This work broadens the phenotypic spectrum of individuals affected by mutations in *PGAP3* and highlights the difficulties in identification and interpretation of pathogenic variants in the recessive disorder HPMRS4. The phenotypic features hyperphosphatasia and intellectual disability in combination with hypotonia and seizures are characteristic for HPMRS. In the genetic workup of such cases the genes *PIGV* (HPMRS1), *PIGO* (HPMRS2), *PGAP2* (HPMRS3), *PGAP3* (HPMRS4), *PIGQ* (HPMRS5), and *PIGY* (HPMRS6) should be carefully analyzed. In cases where one known or probably pathogenic variant is found, the challenge remains in the identification of the second hit. The application of NGS based RNA sequencing facilitated the identification and characterization of non-coding pathogenic mutations. NGS based panel sequencing is cost efficient and frequently applied in diagnosis of rare monogenic disorders. Extension of the panel sequencing protocol from DNA to RNA can be accomplished in routine diagnostic settings. However, for analysis and interpretation of the results from RNA panel sequencing no computational tools are yet available.

Interpretation is dependent on experienced evaluation of the sequencing reads in the IGV browser or by summary statistics of reads in coding and non-coding regions. The identified non-coding mutations in the 3' UTR provide a target for development of personalized therapeutics. In contrast to other coding mutations the PGAP3 protein is not affected, but its expression. This work laid ground for the development of a target site blocker (TSB) to block the miRNA binging site, leading to down regulation of the *PGAP3* transcript in individuals with the c.*559C>T mutation. The allele frequency of 0.003826 (120 heterozygous carriers out of 31.364 sequenced genomes: https://gnomad.broadinstitute.org/variant/17-37828497-G-A) of the 3' UTR mutation indicates a high clinical relevance for HPMRS4, as homozygous or compound heterozygous carriers in outbred populations may occur with a rate about 1:50.000.

3.2 Zhao *et al.,* Reduced cell surface levels of GPI-linked markers in a new case with PIGG loss of function, 2017

Jin James Zhao, Jonatan Halvardson, Alexej Knaus, Patrik Georgii-Hemming, Peter Baeck, Peter M. Krawitz, Ann-Charlotte Thuresson, and Lars Feuk,
Published in *Human Mutation*, 2017 October;38(10):1394–1401,
doi: https://doi.org/10.1002/humu.23268

PIGG deficiency was first described by Makrythanasis et al. (2015) as cause of an autosomal recessive form of mental retardation 53 (MIM #616917) in five individuals. In this work two siblings from one family with a homozygous missense mutation in *PIGG* are described, broadening the phenotypic spectrum of *PIGG* associated GPIBD. Consistent with previous findings, flow cytometric analysis of blood did not reveal an impairment of GPI-AP. However, in contrast to the work by Makrythanasis et al. (2015), a reduction of GPI-AP expression was found in fibroblasts. These findings suggest that correct processing of GPI-APs might be cell type specific and that the expression of some GPI-APs on fibroblasts could be more sensitive to pathogenic mutations in genes of the GPI anchor biosynthesis pathway. Thus, the choice of cells to analyze by flow cytometry should be made thoughtfully.

Reduced cell surface levels of GPI-linked markers in a new case with PIGG loss of function

Jin James Zhao[1], Jonatan Halvardson[1], Alexej Knaus[2,3], Patrik Georgii-Hemming[1,4], Peter Baeck[5], Peter Krawitz[2], Ann-Charlotte Thuresson[1*#], Lars Feuk[1*#]

[1]Department of Immunology, Genetics and Pathology, Science for Life Laboratory, Uppsala University, Sweden
[2]Institute for Medical Genetics and Human Genetics, Charité Universitätsmedizin Berlin, Berlin, Germany
[3]Berlin-Brandenburg School for Regenerative Therapies (BSRT), Charitè Universitätsmedizin Berlin, Germany
[4]Department of Molecular Medicine and Surgery, Karolinska Institute, Karolinska University Hospital Solna, Stockholm, Sweden
[5]Childrens Clinic, County Hospital, Kalmar, Sweden, [5]Clinical Genetics, Uppsala University Hospital, Uppsala, Sweden

*Equal author contribution

[#]Corresponding authors:

Lars Feuk
Department of Immunology, Genetics and Pathology
Box 815,
BMC B11:4, Uppsala University
SE-751 08 Uppsala, Sweden

Email: lars.feuk@igp.uu.se

Ann-Charlotte Thuresson
Department of Immunology, Genetics and Pathology
Rudbeck Laboratory, Uppsala University
SE-751 85 Uppsala
Sweden

Email: ann-charlotte.thuresson@igp.uu.se

Abstract

Glycosylphosphatidylinositol (GPI) is a glycolipid that tethers more than 150 different proteins to the cell surface. Aberrations in biosynthesis of GPI anchors cause congenital disorders of glycosylation with clinical features including intellectual disability, seizures and facial dysmorphism. Here we present two siblings with intellectual disability, cerebellar hypoplasia, cerebellar ataxia, early onset seizures and minor facial dysmorphology. Using exome sequencing, we identified a homozygous nonsense variant (NM_001127178.1:c.1640G>A, p.Trp547*) in the gene Phosphatidylinositol Glycan Anchor Biosynthesis, Class G (*PIGG*) in both the patients. Variants in several other GPI anchor synthesis genes lead to a reduced expression of GPI anchored proteins that can be measured by flow cytometry. No significant differences in GPI anchored proteins could be detected in patient granulocytes, consistent with recent findings. However, fibroblasts showed a reduced global level of GPI anchors and of specific GPI-linked markers. These findings suggest that fibroblasts might be more sensitive to pathogenic variants in GPI synthesis pathway and are well suited to screen for GPI-anchor deficiencies. Based on genetic and functional evidence we confirm that pathogenic variants in *PIGG* cause an intellectual disability syndrome and we find that loss of function of *PIGG* is associated with GPI deficiency.

Keywords
PIGG, GPI deficiency, Intellectual disability, Exome sequencing

Introduction

Glycosylphosphatidylinositol (GPI) is a glycolipid that tethers proteins to the cell surface. Proteins that are anchored to the outer leaflet of plasma membrane are termed GPI-anchored proteins (GPI-APs). More than 150 human GPI-APs have been identified and have been shown to have important structural, catalytic and regulatory functions (Kinoshita, 2014). The synthesis of GPI anchors includes 12 reaction steps and involves at least 26 genes, including 22 Phosphatidyl Inositol Glycan (PIG) genes (Kinoshita, 2014). Pathogenic variants in several genes involved in the maturation of GPI anchors have been associated with a group of congenital disorders of glycosylation referred to as inherited GPI deficiencies, IGDs. Common clinical features of these disorders include intellectual disability (ID), seizures and facial dysmorphism. To date, pathogenic variants in 14 genes in the GPI anchor pathway have been reported to cause GPI deficiencies, including nine PIG genes, namely *PIGA, PIGM, PIGV, PIGL, PIGT, PIGN, PIGO, PIGQ* and *PIGW* (Martin, et al., 2014) (Almeida, et al., 2006; Chiyonobu, et al., 2014; Johnston, et al., 2012; Krawitz, et al., 2012; Krawitz, et al., 2010; Kvarnung, et al., 2013; Maydan, et al., 2011). *PIGA* is the only X-linked PIG gene, while the remaining PIG genes are autosomal and recessively inherited (Takeda, et al., 1993).

Part of the core backbone of GPI-AP is three mannoses: Man1, Man2, and Man3. Each of the three mannoses is modified with one ethanol-amine phosphate (EtNP) group (Kinoshita, 2014). While the EtNPs on Man1 and Man2 are side branches, the third EtNP on Man3 is a core component, for it makes an amide-bond with the C-terminus of the protein (Hong, et al., 1999). The transfer of EtNPs to Man1, Man2 and Man3 is catalyzed by human GPI-EtNP transferase I, II and III, of which the catalytic components are *PIGN*, *PIGG*, *PIGO*, respectively (Hong, et al., 2000; Hong, et al., 1999; Shishioh, et al., 2005). Pathogenic variants in both *PIGN* and *PIGO* have been repeatedly reported to cause ID syndromes, and variants in *PIGN* (MIM# 606097) were initially identified as a cause of multiple congenital anomalies-hypotonia-seizures syndrome 1 (MCAHS1, MIM# 614080) in seven individuals from a consanguineous family (Maydan, et al., 2011). Three additional families have since been reported to carry causative variants in *PIGN,* and patients all have congenital disorders including ID (Brady, et al., 2014; Couser, et al., 2015; Ohba, et al., 2014). Impairments of *PIGO*

(MIM# 614730), that transfers the 'bridging' EtNP to the third mannose residue, was first reported to cause Hyperphosphatasia with mental retardation syndrome 2 (HPMRS2, MIM# 614749) in three individuals from two families (Krawitz, et al., 2012), and has later been reported in two additional studies (Kuki, et al., 2013; Nakamura, et al., 2014).
The *PIGG* (MIM# 616918) gene was identified as one of the three mammalian homologs of yeast GPI7 gene (the other two are *PIGN* and *PIGO*). *PIGG* is the catalytic component of GPI-EtNP transferase II, and is the only PIG gene that adds an intermediate EtNP to the second mannose on GPI (Shishioh, et al., 2005). Recently, variants in *PIGG* were reported to cause ID with seizures and hypotonia. Interestingly, flow cytometry tests showed that normal levels of GPI-AP were expressed in granulocytes and lymphoblastoid cell lines (LCL) from the patients. This raised questions regarding the mechanism of pathogenesis of *PIGG* variants (Makrythanasis, et al., 2016).

In this study we report the identification of homozygous nonsense variants (NM_001127178.1:c.1640G>A, p.Trp547*) in the *PIGG* (MIM# 616918) gene in two affected siblings. The patients harbored several large stretches of homozygosity in their genomes, and the variant was identified in a 5.6 Mb homozygous region on chromosome 4. The siblings have ID, cerebellar hypoplasia, cerebellar ataxia, frontal bossing, hypertelorism, hyperopia, depressed nasal bridge and frequent seizures until the age of six months. The seizures then became sparser and eventually ceased entirely. In agreement with the previous report on pathogenic *PIGG* variants, flow cytometry showed that GPI-AP levels are normal in patients' granulocytes. However, a clear reduction of GPI-AP expression was found in fibroblast cells from these patients. Our findings provide a first independent validation that pathogenic variants in *PIGG* cause a congenital ID syndrome. Our results further show that *PIGG* is essential for normal cell surface expression GPI-APs, but that this effect of loss of function of *PIGG* is limited to certain cell types.

Material and Methods

Microarray analysis

Chromosomal microarray (CMA) analysis was performed using Affymetrix CytoScan HD (Affymetrix Inc, Santa Clara, California, USA), according to the manufactures instructions. Data analysis was carried out using Chromosome Analysis Suite 3.1.

Exome sequencing

Exome enrichment was performed using SureSelect (Agilent) version 5 following the manufacturer's protocol and samples were sequenced on Illumina HiSeq Sequencer. The sequencing was performed to achieve at least 30x coverage of the captured regions. Reads were mapped against the Hg19 version of the human reference genome using BWA (http://bio-bwa.sourceforge.net/) Programs used for mapping were run using default settings. Vcf files from the GATK pipeline was annotated using the GEMINI software.

Sanger sequencing was performed in both patients and parents to validate the variant in the *PIGG* gene detected by exome sequencing. Primers were designed using Primers3 for the PCR to flank the mutation sites.

Flow Cytometry

Peripheral blood was drawn from both affected siblings and the parents into Cyto-Chex® BCT (Streck Laboratories, Omaha, USA) and delivered at 4°C within 72h. 50µl whole blood was used to stain with FLAER

(fluorescein-labeled proaerolysin), and fluorescently conjugated antibodies (CD55-PE, CD24-PC5, CD16-PE, CD14-ECD), respectively for 30,I at room temperature. Erythrocytes were removed with lysis buffer followed by centrifugation. Samples were washed twice and resuspended in 200µl FACS buffer for flow cytometric analysis on a Navios 10/3 (Beckmann Coulter GmbH, Krefeld, Germany).

Fibroblasts derived from small skin biopsies were cultured in DMEM supplemented with 10% FCS, 1% Ultraglutamine and 1% penicillin and streptomycin. For GPI-AP expression analysis by flow cytometry a single cell solution of confluently grown fibroblasts from both affected individuals and the parents were prepared. Cells were washed twice with PBS, removed from the dish with 2mM EDTA, and resuspended in FACS buffer (2mM HEPES, 2mM EDTA, 2% FCS in PBS). To ensure a single cell suspension cells were thoroughly pipetted, filtered through a 40µm sieve and counted using Countess II FL Automated Cell Counter. 50,000 cells were stained with fluorescently conjugated antibodies (CD55-FITC (BD #555694), CD59-PE (BD #555763), CD73-PE (BD #550257), CD90-FITC (BD #555595) and FLAER, respectively) in 30µl FACS buffer for 30min at room temperature, washed twice, and resuspended in 100µl FACS buffer for flow cytometric analysis on a MacsQuant VYB (Miltenyi Biotec GmbH, Gladbach, Germany). Triplicates of each sample were analysed. FlowJo ™ v. 9.9.5.(FlowJo LLC, Ashland, USA) was used for data visualization. The median fluorescent intensity (MFI) of the isotype control was subtracted from the MFI of the sample to obtain the absolute MFI (abs MFI). Standard deviation bars result from triplicates. A t-test was performed to determine significant reduction of marker expression.

AmpliSeq

Total RNA extracted from fibroblast cells was reverse transcribed according to Ion AmpliSeq™ Transcriptome Human Gene Expression kit Preparation protocol (Revision A.0, Thermo Fisher Scientific). The cDNA was amplified using Ion AmpliSeq™ Transcriptome Human Gene Expression core panel (Thermo Fisher Scientific) and the primer sequences were then partially digested, before ligation of Ion P1 Adapters and Ion Xpress™ Barcode Adapters (Thermo Fisher Scientific). Adaptor ligated amplicons were purified using Agencourt® AMPure® XP reagent (Beckman Coulter) and eluted in amplification mix (Platinum® PCR SuperMix High Fidelity and Library Amplification Primer Mix, Thermo Fisher Scientific) and amplified. Size-selection and purification was conducted using Agencourt® AMPure® XP reagent (Beckman Coulter). The amplicons were quantified using Agilent® Bioanalyzer™ instrument with Agilent® High Sensitivity DNA kit (Agilent® Technologies).
Samples were then pooled five and five, followed by template preparation on the Ion Chef system using the Ion PI Hi-Q Chef Kit (ThermoFisher). Samples were sequenced on the Ion Proton™ system using the Ion PI Hi-Q Sequencing 200 Kit on Ion PI v3 chips (200 bp read length, ThermoFisher).

Results

Clinical report

In this family, originating from Palestine, two of four siblings are affected by a non-progressive severe generalized ataxia and tonic clonic seizures (Figure 1). The parents report that they are unrelated. The maternal aunt has a child with delayed development. Both siblings have a delayed development, with moderate (girl) to mild (boy) ID. Speech is severely delayed, especially the expressive speech, which could be an effect of the ataxia. They both have an ataxic gait and balance difficulties, but do not show any spasticity. Because of the ataxia they also have feeding difficulties. Furthermore both siblings have hypotonia, hypertelorism, hyperopia,

depressed nasal bridge, broad nose, thin upper lip, bilateral valgus foot deformity, pes planus and hypermobile joints of the fingers, toes and feet. At age two months tonic seizures appeared 3-4 times a day and lasted for approximately 30 minutes. Seizures slowly diminished from age 6 months and vanished completely at around 9 months. Additionally, the boy also suffered from absence-like seizures up to 30 minutes. Brain MRI shows clear signs of cerebellar atrophy with prominent sulci, atrophic cortex and white matter loss in both siblings. Vermis cerebelli is comparatively spared (Suppl. Figure S1). However, brain MRI performed in the boy's first year of life was normal. Serum alkaline phosphatase (ALP) levels, taken at age 6 years, were within normal range. Although being a GPI-linked protein, this has also been reported for other IGDs (Nakagawa, et al., 2016).

The boy, who now is 7 years old, was born with co-arctation of aorta with hypoplastic aortic arch and an atrial septal defect, which was corrected by cardiac surgery at two months of age. He sat at 10-11 month and crawled just after his first birthday. He was a late walker (approximately 5.5 years) and still has difficulties walking independently and now uses a wheelchair. Apart from the symptoms shared between the siblings, he has mild ptosis, discretely stubby feet and short thumbs and joint laxity. The now 9-year-old sister also shows the following dysmorphic features; frontal bossing, epicanthal folds, strabismus and a prominent chin. She crawled at the age of 2.5 years and started walking approximately at 4 years of age. At the age of 2.5 years she was diagnosed with Medium-chain acyl-CoA dehydrogenase (MCAD) deficiency, (MIM# 201550) with an identified pathogenic homozygous frame-shift variant in *ACADM* (NM_000016.5: c.431_434delAGTA; p.Lys144Ilefs*5) (MIM# 607008). The parents are heterozygous carriers of the variant. However, MCAD could not explain the dysmorphic features and developmental delay also present. Moreover, her brother who is presenting with similar features, is a heterozygous carrier of this variant, and thereby MCAD could not explain the phenotype of the siblings.

Molecular results

CMA was carried out on the affected girl, but the analysis did not show any pathogenic copy number variants. Parents had reported no known consanguinity, but the CMA showed that regions of homozygosity cover 4% of the genome, which is a slightly higher than what would be expected in second-order cousins. To follow up on the CMA, exome sequencing was performed on both affected siblings and their parents. Analysis was performed, primarily focusing on recessive inheritance and assuming that both siblings would be homozygous for the disease-causing mutation. Variants were filtered to keep only variants in coding sequence and splice sites. A single homozygous loss of function variant (NM_001127178.1:c.1640G>A, p.Trp547*) was identified in both siblings, with both parents being heterozygous carriers, in the gene Phosphatidylinositol Glycan Anchor Biosynthesis, Class G (*PIGG*) (MIM# 616918). The *PIGG* gene is located on chromosome 4, within a 5.6 Mb region of homozygosity, as determined by CMA on the affected girl (Suppl. Figure S2). We note that this variant is present in the Database of Single Nucleotide Polymorphism (dbSNP; rs547951371) based on reports of one heterozygous carrier in the 1000 Genomes Project and five heterozygous carriers in the Exome Aggregation Consortium (ExAC) data (allele frequency: 4.223e-05), while no homozygous healthy individuals have been reported. This is an allele prevalence that is comparable to other pathogenic variants of the molecular pathway.

To investigate the effect of the nonsense variants in *PIGG* we used primary fibroblast cell lines and granulocytes from the two siblings and their parents, as well as independent controls, to measure the expression of GPI-APs on the cell surface. Using flow cytometry the GPI-anchored proteins CD90, CD73, CD59, and

CD55 were tested, as well as fluorescein-labeled proaerolysin (FLAER), which binds specifically to GPI anchors. The analysis showed decreased levels of GPI anchors in fibroblasts (Figure 2, Suppl. Figure S3A). Interestingly, the surface levels of the GPI-anchored markers CD59, CD73, and CD90 showed a more prominent reduction than CD55 and FLAER. On the contrary, flow cytometric analysis of blood samples did not show an altered GPI-anchored marker expression on granulocytes (Suppl. Figure S3B.). Based on these experiments we hypothesize that GPI-anchored proteins are affected differently depending on the cell type.

In order to further investigate the expression of *PIGG* in the family we first performed transcriptome analysis using AmpliSeq, an amplification based method providing an expression value for each gene in the genome. The data shows that the expression of *PIGG* is approximately half in the patients compared to their parents (Figure 3A). In contrast, all other genes in the GPI anchor synthesis pathway showed equal expression in patients and parents (Figure 4). These results indicate that transcripts containing the loss of function variant are most likely degraded by nonsense-mediated decay. To further validate the lower transcript levels of the nonsense allele we performed Sanger sequencing of cDNA from the heterozygous parents. The results clearly show a significantly lowered expression of the mutated allele (Figure 3B), further supporting that transcripts containing the loss of function allele are degraded prior to translation.

Discussion

Here we report two patients with a novel homozygous nonsense variant (NM_001127178.1:c.1640G>A, p.Trp547*) in the *PIGG* gene (MIM# 616918). The patients are two siblings with symptoms including ID, cerebellar hypoplasia, cerebellar ataxia, early onset seizures, hypotonia and minor facial dysmorphology. The patients thus display similar phenotypes to other IGDs, but with milder dysmorphology and no detectable change in ALP. The symptoms are consistent with the phenotypes associated with pathogenic variants in *PIGG*, as reported by Makrythanasis et al.(Makrythanasis, et al., 2016)

While serum ALP levels were found to be within the normal range in patients with pathogenic variants in *PIGG*, changes in serum ALP levels is otherwise a common symptom in IGDs. ALP precursor protein is initially located on ER and contains GPI attachment signal. GPI transamidase recognizes the GPI attachment signal, cleaves ALP precursor protein, and hydrolyzes ALP to GPI anchor. The GPI-anchored ALP is subsequently transported to cell membrane, where a fraction of ALP is released into serum (Murakami, et al., 2012). Elevated serum ALP has been associated with pathogenic variants in *PIGL*, *PIGW*, *PIGV*, and *PIGO*, which are responsible for synthesizing backbone-components of the GPI-anchor.(Chiyonobu, et al., 2014; Fujiwara, et al., 2015; Krawitz, et al., 2012; Krawitz, et al., 2010). GPI anchor with defect structure could not form a stable connection with ALP and cause an excess of ALP released into serum (Murakami, et al., 2012). Decreased levels of serum ALP were reported with pathogenic variants in *PIGT*, which is a subunit of the GPI transamidase complex (Kvarnung, et al., 2013). Aberrant transamidase could not cleave the ALP precursor protein, resulting in the degradation of ALP precursor protein within the cells (Kvarnung, et al., 2013). Pathogenic variants in *PIGN* cause GPI deficiency, but was reported not to be associated an abnormal level of serum ALP. PIGN adds a side modification of EtNP similar to the function of PIGG, which presumably could have less impact in the release of ALP (Nakagawa, et al., 2016). It is therefore not surprising that pathogenic variants in *PIGG* gene leads to a serum ALP level within the normal range. In the absence of elevated ALP, flow cytometry of multiple GPI-anchored markers is considered the gold standard for diagnosis of IGDs.

Cells with defective *PIGG* could still express normal GPI-AP proteins, as the EtNP added by *PIGG* is often later removed. This may explain why normal GPI-AP surface levels were found in granulocytes, which is

consistent with the recent investigation by Makrythansis et al., reporting that both lymphoblastoid cells generated from patients with pathogenic variants and *PIGG*-knockout HEK293 cells showed normal surface levels of GPI-AP (Makrythanasis, et al., 2016). However, the patients in our study showed decreased surface level of GPI-APs in fibroblast cells. One explanation may be that the addition of EtNP on second mannose could be critical for efficient sorting and transporting of GPI-APs from ER to cell surface. GPIs are not only structural anchors for cell surface proteins, but also act as signals and regulates ER-exit and transporting of GPI-APs. Previous human cell studies show that interactions between GPI and PGAP5 are crucial for efficient transport of GPI-AP from ER to Golgi (Fujita, et al., 2009). It is possible that different cell types are differentially affected by PIGG deficiency, potentially depending on the distance from the ER to the cell membrane. That might explain why a GPI reduction could be seen in fibroblasts but not in granulocytes. One can speculate that larger cells such as neurons, where the GPI must be transported further, would be even more severely affected. Nonetheless, our results show that the choice of cells to study the effect of variants on GPI-AP cell surface levels is important. In our study, we find that fibroblasts are worthwhile studying in a suspected IGD if flow cytometry on blood cells is inconclusive. Further studies will be required to determine if this is representative for GPI deficiencies in general, or whether *PIGG* represents an exception.

The purpose of the addition and subsequent removal of EtNP on the second mannose is not yet clear, and it may be that variants in PIGG exert their main effect through other mechanisms than reduced GPI-AP cell surface level expression. First, not all EtNP on the second mannose is removed on GPI-APs. For instance, a previous test on GPI anchors of porcine renal membrane di-peptidase and human placental alkaline phosphatase showed the presence of EtNP on the second mannose in 50% and 40% of the GPI, respectively (Brewis, et al., 1995). It is possible that a balanced fraction of EtNP on second mannose is important for normal function of certain GPI-APs. The EtNP on the second mannose that reaches the cell surface might also be important for the organization of GPI-anchored proteins in the membrane. It is known that deleterious mutations in genes that catalyze modifications of the fatty acid residues of the GPI-anchor make them more prone to cleavage. Interestingly, in a cohort of patients with pathogenic variants in *PGAP3*, one case also showed normal levels of GPI-markers on blood cells, but reduced levels in fibroblasts (Knaus, et al., 2016).

Finally, *PIGG* could also have additional functions besides processing GPI, for instance, adding EtNP side chains on other cellular molecules (Benachour, et al., 1999). In general, the role of *PIGG* has not been thoroughly investigated in human or mammalian cell systems. Deletion of the yeast ortholog, *GP17*, does have significant effects on cell separation and cell growth (Benachour, et al., 1999).

While both siblings have a homozygous loss of function variant in *PIGG* gene, an additional pathogenic homozygous variant (NM_000016.5: c.431_434delAGTA; p.Lys144Ilefs*5) in *ACADM* gene was identified in only the sister, which caused MCADD. MCADD is a fatty acid oxidation disorder caused by mutations in *ACADM* gene, which encodes the medium chain acyl-CoA dehydrogenase enzyme that catalyzes the beta-oxidation of medium-chain fatty acid (Matsubara, et al., 1986). It was reported that among children with MCADD, 7% to 8% of the patients also had ID (Grosse, et al., 2006). The combination of MCADD and IGD could be the reason the sister has moderate ID and the brother mild ID. Brain MRI showed cerebellar atrophy and atrophic cortex in both patients, but MRI performed in the brother's first year was normal (Suppl. Figure S1). Cerebral palsy (CP) has been reported in 9% of MCADD children (Grosse, et al., 2006). This could potentially explain why the sister had a more delayed motor development during her first years of life, crawling at the age of 2.5 years, compared to her brother who crawled at one year of age.

Our results confirm that pathogenic variants in *PIGG* are associated with a congenital ID syndrome, adding

PIGG to the growing list of genes in the GPI biosynthesis pathway where loss of function causes disease. More than 25 different genes associated with the pathway have now been associated with human phenotypes, and it is likely that further genes remain to be identified. Our finding that loss of function of *PIGG* leads to a cell type specific reduction in GPI-APs provides novel insights and may contribute towards an increased understanding of how disruption of the GPI biosynthesis pathway gives rise to intellectual disability syndromes.

Footnotes

Parental consent obtained. Patients have been submitted to DECIPHER (#332268) (https://decipher.sanger.ac.uk/).

Acknowledgements

We are very grateful to the participating family for their cooperation. Sequencing was performed using the SciLifeLab National Genomics Infrastructure at Uppsala Genome Center and the Uppsala SNP & Seq Facility. Computational analyses were performed on resources provided by SNIC through Uppsala Multidisciplinary Center for Advanced Computational Science (UPPMAX).

This work was supported by grants from the Föreningen Margarethahemmet, the Sävstaholm Society and the "Regionala forskningsrådet" (to ACT), and the European Research Council ERC Starting Grant Agreement n. 282330 and the Swedish Medical Research Council (to LF).

Author contributions

ACT and LF designed and planned the study. JZ and JH analyzed the exome and transcriptome data. JZ performed gene expression and validation experiments. AK and PK performed and analyzed the flow cytometry experiments. PGH, PB, and ACT diagnosed the patients, performed clinical assessments and collected patient samples. JZ, ACT and LF wrote the manuscript. All authors read, commented on and approved the manuscript.

References

Almeida AM, Murakami Y, Layton DM, Hillmen P, Sellick GS, Maeda Y, Richards S, Patterson S, Kotsianidis I, Mollica L, Crawford DH, Baker A and others. 2006. Hypomorphic promoter mutation in PIGM causes inherited glycosylphosphatidylinositol deficiency. Nat Med. p 846-51.

Benachour A, Sipos G, Flury I, Reggiori F, Canivenc-Gansel E, Vionnet C, Conzelmann A, Benghezal M. 1999. Deletion of GPI7, a yeast gene required for addition of a side chain to the glycosylphosphatidylinositol (GPI) core structure, affects GPI protein transport, remodeling, and cell wall integrity. J Biol Chem 274(21):15251-61.

Brady PD, Moerman P, De Catte L, Deprest J, Devriendt K, Vermeesch JR. 2014. Exome sequencing identifies a recessive PIGN splice site mutation as a cause of syndromic congenital diaphragmatic hernia. Eur J Med Genet 57(9):487-93.

Brewis IA, Ferguson MA, Mehlert A, Turner AJ, Hooper NM. 1995. Structures of the glycosyl-phosphatidylinositol anchors of porcine and human renal membrane dipeptidase. Comprehensive

structural studies on the porcine anchor and interspecies comparison of the glycan core structures. J Biol Chem 270(39):22946-56.

Chiyonobu T, Inoue N, Morimoto M, Kinoshita T, Murakami Y. 2014. Glycosylphosphatidylinositol (GPI) anchor deficiency caused by mutations in PIGW is associated with West syndrome and hyperphosphatasia with mental retardation syndrome. J Med Genet 51(3):203-7.

Couser NL, Masood MM, Strande NT, Foreman AK, Crooks K, Weck KE, Lu M, Wilhelmsen KC, Roche M, Evans JP, Berg JS, Powell CM. 2015. The phenotype of multiple congenital anomalies-hypotonia-seizures syndrome 1: report and review. Am J Med Genet A 167A(9):2176-81.

Fujita M, Maeda Y, Ra M, Yamaguchi Y, Taguchi R, Kinoshita T. 2009. GPI glycan remodeling by PGAP5 regulates transport of GPI-anchored proteins from the ER to the Golgi. Cell 139(2):352-65.

Fujiwara I, Murakami Y, Niihori T, Kanno J, Hakoda A, Sakamoto O, Okamoto N, Funayama R, Nagashima T, Nakayama K, Kinoshita T, Kure S and others. 2015. Mutations in PIGL in a patient with Mabry syndrome. Am J Med Genet A 167A(4):777-85.

Grosse SD, Khoury MJ, Greene CL, Crider KS, Pollitt RJ. 2006. The epidemiology of medium chain acyl-CoA dehydrogenase deficiency: an update. Genet Med 8(4):205-12.

Hong Y, Maeda Y, Watanabe R, Inoue N, Ohishi K, Kinoshita T. 2000. Requirement of PIG-F and PIG-O for transferring phosphoethanolamine to the third mannose in glycosylphosphatidylinositol. J Biol Chem 275(27):20911-9.

Hong Y, Maeda Y, Watanabe R, Ohishi K, Mishkind M, Riezman H, Kinoshita T. 1999. Pig-n, a mammalian homologue of yeast Mcd4p, is involved in transferring phosphoethanolamine to the first mannose of the glycosylphosphatidylinositol. J Biol Chem 274(49):35099-106.

Johnston JJ, Gropman AL, Sapp JC, Teer JK, Martin JM, Liu CF, Yuan X, Ye Z, Cheng L, Brodsky RA, Biesecker LG. 2012. The phenotype of a germline mutation in PIGA: the gene somatically mutated in paroxysmal nocturnal hemoglobinuria. Am J Hum Genet 90(2):295-300.

Kinoshita T. 2014. Biosynthesis and deficiencies of glycosylphosphatidylinositol. Proc Jpn Acad Ser B Phys Biol Sci 90(4):130-43.

Knaus A, Awaya T, Helbig I, Afawi Z, Pendziwiat M, Abu-Rachma J, Thompson MD, Cole DE, Skinner S, Annese F, Canham N, Schweiger MR and others. 2016. Rare Noncoding Mutations Extend the Mutational Spectrum in the PGAP3 Subtype of Hyperphosphatasia with Mental Retardation Syndrome. Hum Mutat.

Krawitz PM, Murakami Y, Hecht J, Kruger U, Holder SE, Mortier GR, Delle Chiaie B, De Baere E, Thompson MD, Roscioli T, Kielbasa S, Kinoshita T and others. 2012. Mutations in PIGO, a member of the GPI-anchor-synthesis pathway, cause hyperphosphatasia with mental retardation. Am J Hum Genet 91(1):146-51.

Krawitz PM, Schweiger MR, Rodelsperger C, Marcelis C, Kolsch U, Meisel C, Stephani F, Kinoshita T, Murakami Y, Bauer S, Isau M, Fischer A and others. 2010. Identity-by-descent filtering of exome sequence data identifies PIGV mutations in hyperphosphatasia mental retardation syndrome. Nat Genet 42(10):827-9.

Kuki I, Takahashi Y, Okazaki S, Kawawaki H, Ehara E, Inoue N, Kinoshita T, Murakami Y. 2013. Vitamin B6-responsive epilepsy due to inherited GPI deficiency. Neurology 81(16):1467-9.

Kvarnung M, Nilsson D, Lindstrand A, Korenke GC, Chiang SC, Blennow E, Bergmann M, Stodberg T, Makitie O, Anderlid BM, Bryceson YT, Nordenskjold M and others. 2013. A novel intellectual disability syndrome caused by GPI anchor deficiency due to homozygous mutations in PIGT. J Med Genet 50(8):521-8.

Makrythanasis P, Kato M, Zaki MS, Saitsu H, Nakamura K, Santoni FA, Miyatake S, Nakashima M, Issa MY, Guipponi M, Letourneau A, Logan CV and others. 2016. Pathogenic Variants in PIGG Cause Intellectual Disability with Seizures and Hypotonia. Am J Hum Genet 98(4):615-26.

Martin HC, Kim GE, Pagnamenta AT, Murakami Y, Carvill GL, Meyer E, Copley RR, Rimmer A, Barcia G, Fleming MR, Kronengold J, Brown MR and others. 2014. Clinical whole-genome sequencing in severe early-onset epilepsy reveals new genes and improves molecular diagnosis. Hum Mol Genet 23(12):3200-11.

Matsubara Y, Kraus JP, Yang-Feng TL, Francke U, Rosenberg LE, Tanaka K. 1986. Molecular cloning of cDNAs encoding rat and human medium-chain acyl-CoA dehydrogenase and assignment of the gene to human chromosome 1. Proc Natl Acad Sci U S A 83(17):6543-7.

Maydan G, Noyman I, Har-Zahav A, Neriah ZB, Pasmanik-Chor M, Yeheskel A, Albin-Kaplanski A, Maya I, Magal N, Birk E, Simon AJ, Halevy A and others. 2011. Multiple congenital anomalies-hypotonia-seizures syndrome is caused by a mutation in PIGN. J Med Genet 48(6):383-9.

Murakami Y, Kanzawa N, Saito K, Krawitz PM, Mundlos S, Robinson PN, Karadimitris A, Maeda Y, Kinoshita T. 2012. Mechanism for release of alkaline phosphatase caused by glycosylphosphatidylinositol deficiency in patients with hyperphosphatasia mental retardation syndrome. J Biol Chem 287(9):6318-25.

Nakagawa T, Taniguchi-Ikeda M, Murakami Y, Nakamura S, Motooka D, Emoto T, Satake W, Nishiyama M, Toyoshima D, Morisada N, Takada S, Tairaku S and others. 2016. A novel PIGN mutation and prenatal diagnosis of inherited glycosylphosphatidylinositol deficiency. Am J Med Genet A 170A(1):183-8.

Nakamura K, Osaka H, Murakami Y, Anzai R, Nishiyama K, Kodera H, Nakashima M, Tsurusaki Y, Miyake N, Kinoshita T, Matsumoto N, Saitsu H. 2014. PIGO mutations in intractable epilepsy and severe developmental delay with mild elevation of alkaline phosphatase levels. Epilepsia 55(2):e13-7.

Ohba C, Okamoto N, Murakami Y, Suzuki Y, Tsurusaki Y, Nakashima M, Miyake N, Tanaka F, Kinoshita T, Matsumoto N, Saitsu H. 2014. PIGN mutations cause congenital anomalies, developmental delay, hypotonia, epilepsy, and progressive cerebellar atrophy. Neurogenetics 15(2):85-92.

Shishioh N, Hong Y, Ohishi K, Ashida H, Maeda Y, Kinoshita T. 2005. GPI7 is the second partner of PIG-F and involved in modification of glycosylphosphatidylinositol. J Biol Chem 280(10):9728-34.

Takeda J, Miyata T, Kawagoe K, Iida Y, Endo Y, Fujita T, Takahashi M, Kitani T, Kinoshita T. 1993. Deficiency of the GPI anchor caused by a somatic mutation of the PIG-A gene in paroxysmal nocturnal hemoglobinuria. Cell 73(4):703-11.

10

Figures

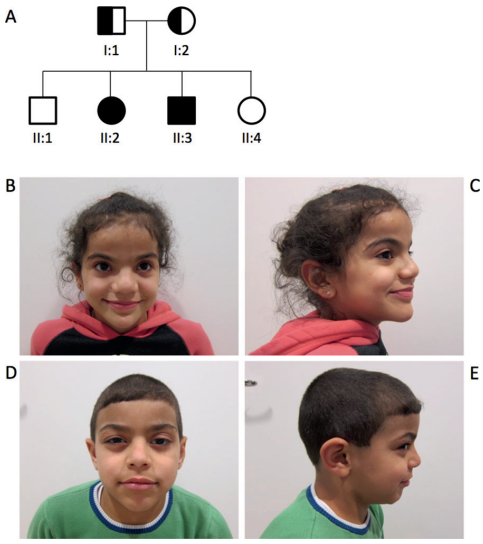

Figure 1 (A) Pedigree of the family. (B, C) Patient II:2 and (D, E) II:3 at ages 9 and 7 years respectively.

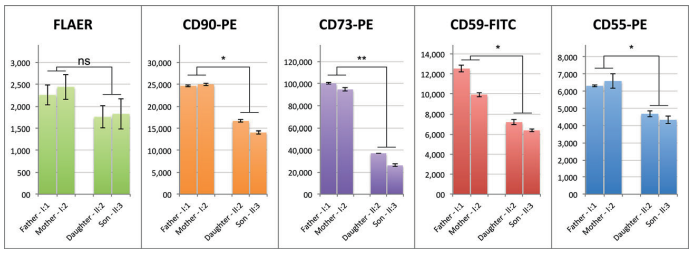

Figure 2 GPI-anchors and protein levels of GPI-anchored markers CD55, CD59, CD73, and CD90 are reduced on fibroblast cell surfaces in affected siblings compared to healthy parents. Measurements were performed in triplicates. Significant reduction of marker expression was assessed with a t-test, $p \leq 0.05$ are marked with *; $p \leq 0.01$are marked with **.

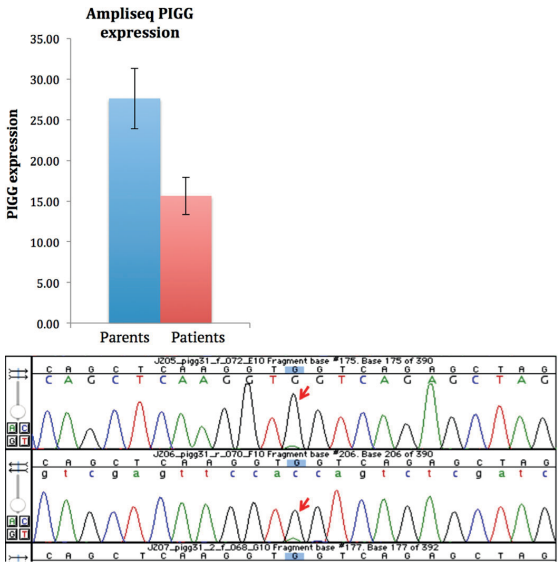

Figure 3 A. PIGG transcript levels are significantly lower in the two patients compared to their parents. **B.** Sanger sequencing of the variant in the heterozygous parents shows that the levels of mutated allele are very low, indicating that the transcripts with the mutation are degraded by nonsense mediated decay.

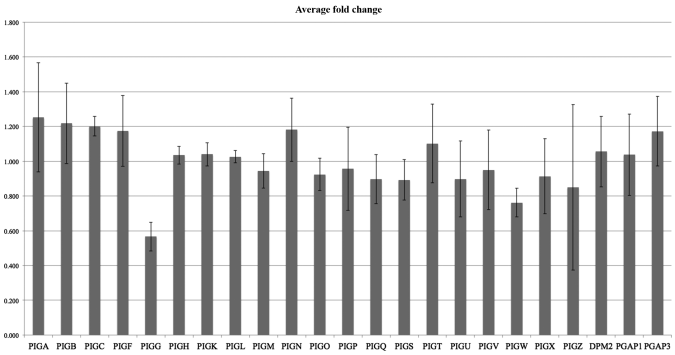

Figure 4 Figure showing the relative fold change in the expression between patients and parents for genes in the GPI synthesis pathway. *PIGG* stands out by showing a significant reduction in the patients.

12

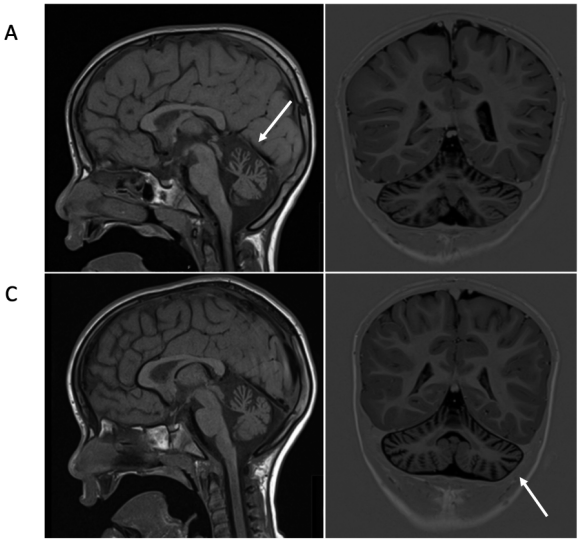

Supplementary Figure S1
MRI image of (A, B) II:2 at age 5 years and 9 months and (C, D) II:3 at age 2 years and 9 months showing cerebellar atrophy with prominent sulci, atrophic cortex and white matter loss.

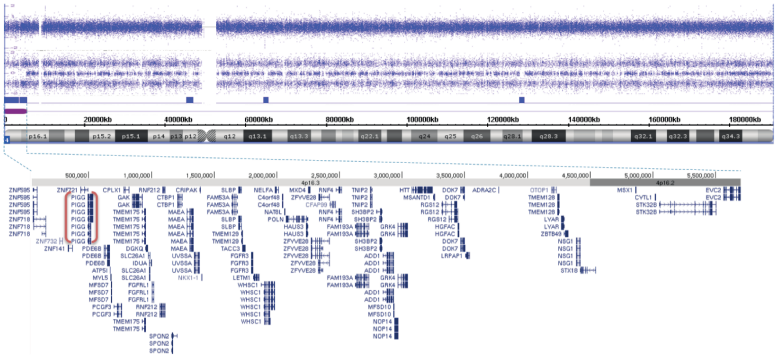

Supplementary Figure S2
Chromosomal microarray results from patient II:2 of the detected homozygous region at 4p16.3p16.2, with a focused view of the genes encompassed by the homozygous stretch (adapted from UCSC genome browser, assembly GRCh37/hg19).

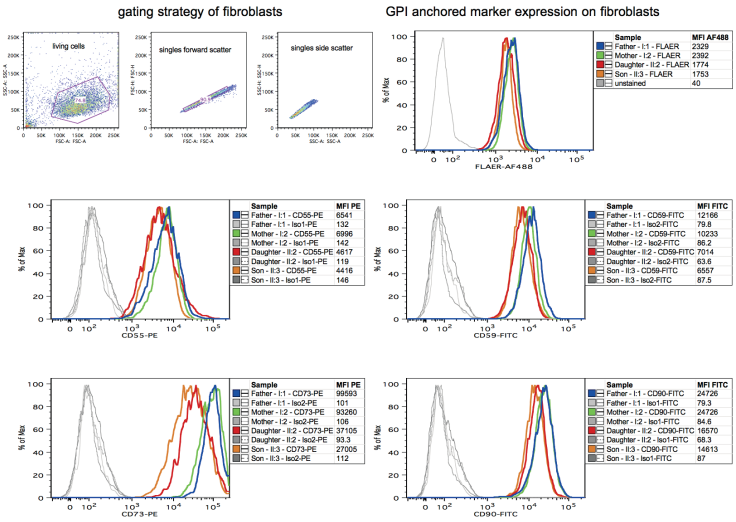

Supplementary Figure S3A

Flow cytometry gating strategy for single fibroblasts and histograms representing median fluorescence intensity (MFI) of GPI anchored marker expression. Patient fibroblasts and control fibroblasts were stained with anti-CD55, anti-CD59, anti-CD73, anti-CD90, and fluorescence-labeled aerolysin (FLAER).

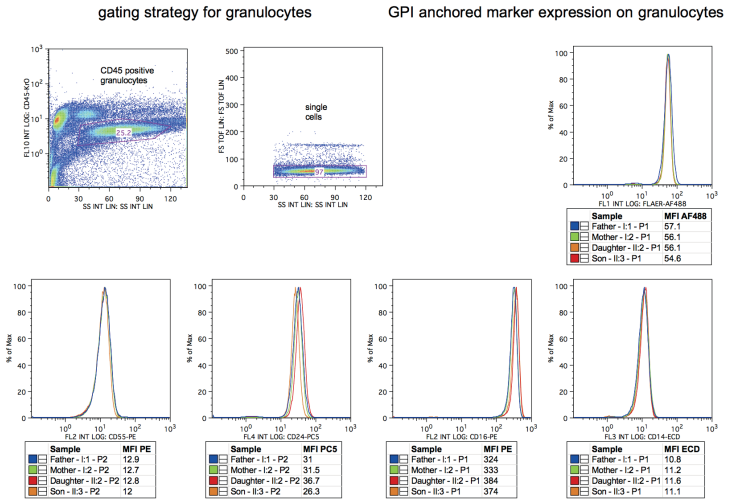

Supplementary Figure S3B

Flow cytometry gating strategy for granulocytes from blood samples and histograms representing median fluorescence intensity (MFI) of GPI anchored marker expression.

3.2.1 Contribution

The manuscript was handed in on 29th of August 2016, the revised article was accepted on 3rd of May 2017 and printed on 21st of May 2017 in *Human Mutation*, Vol. 38, No. 10, pages 1394 – 1401

The study was planned and designed by Thuresson, A.C. and Feuk, L. – the last authors. Zhao, J.J. and Halvardson, J. performed analyses of exome and transcriptome data. Zhao, J.J. performed gene expression and validation experiments. Knaus, A. and Krawitz, P.M. organized and performed functional analyses on blood and fibroblasts by flow cytometry. Georgii-Hemming, P., Baeck, P., and Thuresson, A.C. diagnosed the patients, performed clinical assessments, and collected patient samples. Zhao, J.J., Thuresson, A.C., and Feuk, L. composed the manuscript. All authors read, commented on, and approved the manuscript.

3.2.2 Discussion

The gene products of *PIGG* and *PIGF* associate to form the EtNP transferase II protein complex and orchestrate the addition of the second EtNP to the second mannose of the GPI anchor in the ER (Shishioh et al., 2005). Although during GPI anchor maturation the EtNP2 is removed from Man2 by MPPE1 (encoded by *PGAP5*, Figure 2) in the Golgi, it is important for correct sorting and transport of GPI-APs (Fujita et al., 2009). Yet, it has not been shown that this process of GPI anchor modification is cell type specific. This study reveals, for the first time, that incorrect modification of the GPI anchor leads to diverse GPI-AP expression in different cell types. Consistent with the findings by Makrythanasis et al. (2015) no reduction of GPI-AP expression was measured in blood. However, fibroblasts showed decreased expression of CD55, CD59, CD73, and CD90. The aberrant expression of the same GPI-APs in different cell types indicates that GPI anchored proteins are not equally processed in all cell types. Hence, the correct choice of cell types for studying GPIBDs is very important.

ALP is a characteristic marker for diagnosis of various GPIBDs; while ALP levels in the serum are increased in HPMRS, patients with MCAHS do not show an increased re-

lease of ALP into the blood serum. Therefore, hyper- and hypophosphatasia are associated with different gene mutations of the GPI anchors biosynthesis pathway and measurement of ALP levels in the serum can be used to confirm identified mutations. The intracellular degradation or extracellular release of ALP depends on the completion of GPI anchor synthesis (Murakami et al., 2012). This second report of individuals with *PIGG* deficiency confirms that the missing EtNP on Man2 during GPI anchor biosynthesis does not alter the expression of ALP or its degree of shedding from the cell surface, as affected individuals showed normal ALP levels in serum. Therefore, identification and confirmation of *PIGG* deficiency can so far only be made by combination of DNA sequencing, segregation analysis, in depth phenotypic evaluation, and flow cytometry of fibroblasts.

A thorough analysis of *PIGG* deficiency should be performed in model organisms *in vivo* or in cultured cell lines (e.g. neuronal cell lines) *in vitro* to better understand the underlying pathomechanism.

3.3 Knaus *et al*., Characterization of glycosylphosphatidylinositol biosynthesis defects by clinical features, flow cytometry, and automated image analysis, 2018

***Alexej Knaus**, Jean Tori Pantel, Manuela Pendziwiat, Nurulhuda Hajjir, Max Zhao, Tzung-Chien Hsieh, Max Schubach, Yaron Gurovich, Nicole Fleischer, Marten Jäger, Sebastian Köhler, Hiltrud Muhle, Christian Korff, Rikke S. Møller, Allan Bayat, Patrick Calvas, Nicolas Chassaing, Hannah Warren, Steven Skinner, Raymond Louie, Christina Evers, Marc Bohn, Hans-Jürgen Christen, Myrthe van den Born, Ewa Obersztyn, Agnieszka Charzewska, Milda Endziniene, Fanny Kortüm, Natasha Brown, Peter N. Robinson, Helenius J. Schelhaas, Yvonne Weber, Ingo Helbig, Stefan Mundlos, Denise Horn, and Peter M. Krawitz*

Published in *Genome Medicine*, 2018 January;10(3):1-13,
doi: https://doi.org/10.1186/s13073-017-0510-5

The application of NGS in the routine diagnostic for rare disorders over the past years lead to the identification of further individuals with mutations in the GPI anchor biosynthesis pathway. HPMRS and MCAHS are two of the most prevalent disease entities of the GPIBDs. Phenotypically HPMRS and MCAHS share common features such as global developmental delay, seizures, and hypotonia. However, a variability of congenital anomalies has been described in HPMRS and MCAHS individuals. Noticeably, increased ALP levels were reported in some cases of MCAHS (Johnston et al., 2012; van der Crabben et al., 2014) as well as normal ALP levels in individuals with HPMRS (Knaus et al., 2016). The overlapping phenotypic spectrum of the most prevalent GPIBDs makes it difficult to discriminate affected individuals solely based on clinical features. Although, well-experienced clinical geneticists stated that individuals affected by HPMRS and MCAHS, respectively, presented with a characteristic facial gestalt. In this work, we reviewed data of all published and novel cases of the five most prevalent GPIBDs (*PIGA*, *PIGN*, *PIGT*, *PIGV*, and *PGAP3*).

In order to investigate a genotype phenotype correlation on a functional level flow cytometric data from published and novel cases was collected and thoroughly reanalyzed. In addition, frontal facial images of published and novel individuals with mo-

lecularly confirmed GPIBDs were aggregated. To explore whether a gene specific facial gestalt was present, we applied automated facial analysis in the RESEARCH application of Face2Gene (FDNA Inc., Boston, USA).

The major results of this work were the broadening of the phenotypic spectrum of the five most prevalent GPIBDs by summarizing published and novel cases. Facial analysis allowed delineation of the two disease entities MCAHS and HPMRS. Correct gene interference by facial analysis achieved a mean accuracy of 52.2%. While a genotype phenotype correlation between the disease entities by flow cytometry was not possible.

Although the discrimination between the disease entities is based on historical reasons, it reflects phenotypic similarity. Deep phenotyping of affected individuals, however, may identify subtle and gene specific characteristics, that may be overlooked by humans. Therefore, a gene-centered classification of GPIBDs is recommended.

Knaus *et al. Genome Medicine* (2018) 10:3
DOI 10.1186/s13073-017-0510-5

Genome Medicine

RESEARCH Open Access

Characterization of glycosylphosphatidylinositol biosynthesis defects by clinical features, flow cytometry, and automated image analysis

Alexej Knaus[1,2,3,4], Jean Tori Pantel[1], Manuela Pendziwiat[5], Nurulhuda Hajjir[1], Max Zhao[1], Tzung-Chien Hsieh[1,4], Max Schubach[1,6], Yaron Gurovich[7], Nicole Fleischer[7], Marten Jäger[1,6], Sebastian Köhler[1], Hiltrud Muhle[5], Christian Korff[8], Rikke S. Møller[9,10], Allan Bayat[11], Patrick Calvas[12], Nicolas Chassaing[12], Hannah Warren[13], Steven Skinner[13], Raymond Louie[13], Christina Evers[14], Marc Bohn[15], Hans-Jürgen Christen[16], Myrthe van den Born[17], Ewa Obersztyn[18], Agnieszka Charzewska[18], Milda Endziniene[19], Fanny Kortüm[20], Natasha Brown[21,22], Peter N. Robinson[23], Helenius J. Schelhaas[24], Yvonne Weber[25], Ingo Helbig[4,26], Stefan Mundlos[1,2], Denise Horn[1*†] and Peter M. Krawitz[1,2,4*†]

Abstract

Background: Glycosylphosphatidylinositol biosynthesis defects (GPIBDs) cause a group of phenotypically overlapping recessive syndromes with intellectual disability, for which pathogenic mutations have been described in 16 genes of the corresponding molecular pathway. An elevated serum activity of alkaline phosphatase (AP), a GPI-linked enzyme, has been used to assign GPIBDs to the phenotypic series of hyperphosphatasia with mental retardation syndrome (HPMRS) and to distinguish them from another subset of GPIBDs, termed multiple congenital anomalies hypotonia seizures syndrome (MCAHS). However, the increasing number of individuals with a GPIBD shows that hyperphosphatasia is a variable feature that is not ideal for a clinical classification.

Methods: We studied the discriminatory power of multiple GPI-linked substrates that were assessed by flow cytometry in blood cells and fibroblasts of 39 and 14 individuals with a GPIBD, respectively. On the phenotypic level, we evaluated the frequency of occurrence of clinical symptoms and analyzed the performance of computer-assisted image analysis of the facial gestalt in 91 individuals.

Results: We found that certain malformations such as Morbus Hirschsprung and diaphragmatic defects are more likely to be associated with particular gene defects (*PIGV*, *PGAP3*, *PIGN*). However, especially at the severe end of the clinical spectrum of HPMRS, there is a high phenotypic overlap with MCAHS. Elevation of AP has also been documented in some of the individuals with MCAHS, namely those with *PIGA* mutations. Although the impairment of GPI-linked substrates is supposed to play the key role in the pathophysiology of GPIBDs, we could not observe gene-specific profiles for flow cytometric markers or a correlation between their cell surface levels and the severity of the phenotype. In contrast, it was facial recognition software that achieved the highest accuracy in predicting the disease-causing gene in a GPIBD.
(Continued on next page)

* Correspondence: denise.horn@charite.de; pkrawitz@uni-bonn.de
†Equal contributors
[1]Institut für Medizinische Genetik und Humangenetik, Charité Universitätsmedizin Berlin, 13353 Berlin, Germany
Full list of author information is available at the end of the article

(Continued from previous page)

Conclusions: Due to the overlapping clinical spectrum of both HPMRS and MCAHS in the majority of affected individuals, the elevation of AP and the reduced surface levels of GPI-linked markers in both groups, a common classification as GPIBDs is recommended. The effectiveness of computer-assisted gestalt analysis for the correct gene inference in a GPIBD and probably beyond is remarkable and illustrates how the information contained in human faces is pivotal in the delineation of genetic entities.

Keywords: GPI, Anchor biosynthesis defects, Automated image analysis, Gene, Prediction

Background

Inherited deficiencies of glycosylphosphatidylinositol (GPI) biosynthesis are a heterogeneous group of recessive Mendelian disorders that all share a common feature: the function of GPI-linked proteins is compromised due to a defect in GPI anchor synthesis or modification. Most of the enzymes involved in this molecular pathway are known and the biochemical steps are well described [1]. With respect to the effect of genetic mutations on the anchor and the GPI-linked substrate, several subdivisions of the pathway have been in use: 1) early GPI anchor synthesis, 2) late GPI anchor synthesis, 3) GPI transamidase, and 4) remodeling of fatty acids of the GPI anchor after attachment to proteins (Additional file 1: Figure S1).

The last two groups are defined by their molecular actions and comprise the genes *GPAA1*, *PIGK*, *PIGU*, *PIGS*, and *PIGT* for the GPI-transamidase and *PGAP1*, *PGAP2*, *PGAP3*, *MPPE1*, and *TMEM8* for fatty acid remodeling. The differentiation between early and late GPI anchor synthesis considers the molecular consequence of the glycosylphosphatidylinositol biosynthesis defect (GPIBD), which was suggested after an important finding from Murakami et al. [2] regarding the release of alkaline phosphatase (AP), a GPI anchor marker: if anchor synthesis is stuck at an earlier step, the transamidase is not activated and the hydrophobic signal peptide of GPI anchor substrates is not cleaved. As soon as the first mannose residue on the GPI anchor has been added by PIGM, the transamidase tries to attach the substrate to the anchor. However, if subsequent steps are missing, the GPI anchored proteins (GPI-APs) might be less stable and hyperphosphatasia was hypothesized to be a consequence thereof.

The activity of the AP was regarded as such a discriminatory feature that it resulted in the phenotypic series of hyperphosphatasia with mental retardation syndrome (HPMRS) 1 to 6, currently comprising the six genes *PGAP2*, *PGAP3*, *PIGV*, *PIGO*, *PIGW*, and *PIGY* [3–9]. Whenever a pathogenic mutation was discovered in a new gene of the GPI pathway and the developmentally delayed individuals showed elevated AP in the serum, the gene was simply added to this phenotypic series. If hyperphosphatasia was missing, the gene was linked to another phenotypic series, multiple congenital anomalies hypotonia seizures (MCAHS), that currently consists of *PIGA*, *PIGN*, and *PIGT* [10–12]. However, the convention of dividing newly discovered GPIBDs over these two phenotypic subgroups is only reasonable if they really represent distinguishable entities. This practice is now challenged by a growing number of exceptions. The expressivity of most features is variable and even the AP seems to be a biomarker with some variability: some individuals with mutations in *PIGA* also show elevated AP levels [10, 13–15], and some individuals with mutations in *PIGO*, *PIGW*, *PGAP2*, and *PGAP3* show AP levels that are only borderline high [16–20].

Recently, deleterious mutations were identified in *PIGC*, *PIGP*, and *PIGG* in individuals with intellectual disability (ID), seizures, and muscular hypotonia, but other features considered to be a prerequisite for MCAHS or HPMRS were missing [21–23]. Despite the large phenotypic overlap with most GPIBDs, a flow cytometric analysis of granulocytes in individuals with *PIGG* mutations did not show reduced surface levels for GPI-APs [21–23]. However, Zhao et al. [24] showed that an impairment of PIGG in fibroblasts affects the marker expression, indicating that there might also be variability depending on the tissue. In concordance with these finding, a case report of an individual with ID and seizures that has mutations in *PIGQ* seems suggestive of a GPIBD in spite of negative FACS results [25].

The work of Makrythanasis et al. [23] can also be considered as a turning point in the naming convention of phenotypes that are caused by deficiencies of the molecular pathway as OMIM has now started referring to them as GPIBDs (see OMIM entry #610293 for a discussion). In this work we go one step further in this direction and ask whether the phenotypic series MCAHS and HPMRS should also be abandoned in favor of a more gene-centered description of the phenotype, which would also be in accordance with what Jaeken [26] already suggested for other congenital disorders of glycosylation. Referring to GPIBD phenotypes in a gene-specific manner makes particular sense if the gene can be predicted from the phenotypic level with some accuracy. For this purpose, we systematically analyzed the discriminatory power for GPIBDs for previously reported individuals as well as 23 novel cases that were identified through routine diagnostics. This also adds novel FACS results for 16 patients

(blood or fibroblasts) as well as 19 novel mutations (Additional file 1: Figure S2).

Apart from founder effects that explain the reoccurrence of certain mutations at higher frequency, pathogenic mutations have now been reported in many exons (Additional file 1: Figure S2). However, not much is known about genotype–phenotype correlations in these genes, which makes bioinformatics interpretation of novel variants challenging. The phenotypic analysis, for which we received ethics approval from the Charité University and obtained informed consent from the responsible persons on behalf of all study participants, is based on three different data sources: 1) a comprehensive clinical description of the phenotypic features in human phenotype ontology terminology [27]; 2) flow cytometric profiles of multiple GPI-linked markers; and 3) computer-assisted pattern recognition on frontal photos of individuals with a molecularly confirmed diagnosis.

The rationale behind flow cytometry and image analyses is that GPIBDs might differ in their effect on GPI-APs and their trafficking pathways, resulting in distinguishable phenotypes. Interestingly, we found that the facial gestalt was well suited for delineating the molecular entity. The high information content of facies has become accessible recently through advanced phenotypic tools that might also be used for the analysis of other pathway disorders. Before we present the flow cytometry and automated image analysis results we review the most important phenotypic features of GPIBDs in the old schema of phenotypic series HPMRS and MCAHS.

Methods

Clinical overview of HPMRS

HPMRS, which is also sometimes referred to as Mabry syndrome (HPMRS1-6: MIM 239300, MIM 614749, MIM 614207, MIM 615716, MIM 616025, MIM 616809), can present as an apparently non-syndromic form of ID at one end of the clinical spectrum but also as a multiple congenital malformation syndrome at the other end (Table 1). The distinct pattern of facial anomalies of Mabry syndrome consist of wide set eyes, often with a large appearance and upslanting palpebral fissures, a short nose with a broad nasal bridge and tip, and a tented upper lip. The results of a computer-assisted comparison of the gene-specific facial gestalt is given in the "Comparison of the facial gestalt of GPIBDs" section.

Psychomotor delay, ID, and variable AP elevation are the only consistent features of all individuals with pathogenic mutations in *PIGV* [9, 28–34], *PIGO* [7, 16, 17, 31, 35–37], *PGAP2* [4, 8, 18, 38], *PGAP3* [5, 19, 39–41], and *PIGY* [6]. Speech development, especially expressive language, is more severely affected than motor skills in the majority of the affected individuals (Table 1). Absent speech development was observed in more than half of the affected individuals. Speech difficulties may be complicated by hearing loss, which is present in a minority of affected individuals. In the different genetic groups, seizures of various types and onset are present in about 65% of affected individuals. Most affected individuals show a good response to anticonvulsive drugs, but a few affected individuals are classified as drug resistant and represent the clinically severe cases (individual 14-0585). Muscular hypotonia is common in all types of HPMRS (about 85%). Behavioral problems, in particular sleep disturbances and autistic features, tend to be frequent (81%) in affected individuals with *PGAP3* mutations and are described in a few affected individuals with *PIGY* mutations but are not documented in affected individuals with mutations in the other four genes. Furthermore, ataxia and unsteady gait have been documented in almost half of the affected individuals carrying *PGAP3* mutations and about a third of this group did not achieve free walking at all.

Elevated values of AP were the key finding in affected individuals. However, a few cases are documented with only minimal elevation of this parameter. The degree of persistent hyperphosphatasia in the reported affected individuals varies over a wide range between about 1.1 and 17 times the age-adjusted upper limit of the normal range. The mean elevation of AP is about five to six times the upper limit. Measurements at different ages of one individual show marked variability of this value, for example, from two to seven times the upper limit. There is no association between the AP activity and the degree of neurological involvement. Furthermore, there is no correlation between the mutation class and genes with the level of elevation of AP.

Growth parameters at birth are usually within the normal range. Most affected individuals remain in the normal range, although there is evidence of a skewed distribution towards the upper centiles and a few affected individuals become overweight. In contrast, about 8% of the affected individuals develop postnatal short stature and fail to thrive. About 28% of affected individuals develop microcephaly, whereas less than 10% become macrocephalic. Abnormalities of growth and head size do not correlate with a specific mutation or gene within this group of genes.

Involvement of other organ systems varies among the genetically different groups. *PIGV*, *PIGO*, and *PGAP2* affected individuals frequently suffer from a variety of different malformations. Anorectal malformations, such as anal atresia or anal stenosis, are the most frequent anomalies with almost 30% penetrance in the group of affected individuals. The second most frequent anomaly is Hirschsprung disease with a frequency of about 26% in the same group of affected individuals. Vesicoureteral or renal malformations occur with a similar frequency;

Table 1 Summary of clinical findings in patients carrying *PIGV*, *PIGO*, *PGAP2*, *PGAP3*, *PIGW*, and *PIGY* mutations

	HPMRS1 *PIGV* (*n* = 26, excluding 2 fetus)	HPMRS2 *PIGO* (*n* = 16)	HPMRS3 *PGAP2* (*n* = 12)	HPMRS4 *PGAP3* (*n* = 26)	HPMRS5 *PIGW* (*n* = 3)	HPMRS6 *PIGY* (*n* = 4)
Hyperphosphatasia	26/26	14/14, ND in 2	6/6, ND in 6	25/26	1/3	4/4
Growth parameters						
OFC	Normal in 22/26 (microcephaly in 2/26, macrocephaly in 2/26)	Normal in 2/6 (microcephaly in 4, macrocephaly in 2, ND in 8)	Normal in 5/12 (microcephaly in 7)	Normal in 17/26 (microcephaly in 7, macrocephaly in 2)	Normal in 2 (ND in 1)	Normal in 2/4 (microcephaly in 2)
Height	Normal in 24/26	Normal in 3/5 (short stature in 2, ND in 11)	Normal in 2/2, ND in 10	Normal in 25/26 (short stature in 1/26)	Normal in 2 (ND in 1)	Normal in 2/4 (short stature in 2/4)
Weight	Normal in 24/26	Normal in 4/5 (dystrophy in 1, ND in 11)	Normal in 2/2, ND in 10	Normal in 21/26 (overweight in 2/26, dystrophy in 3/26)	Normal in 2 (ND in 1)	ND
Neurological phenotype						
Global developmental delay	26/26	16/16	2/2	26/26	3/3	4/4
Motor delay	26/26	16/16	12/12 (mild in 5)	26/26	3/3	4/4
Speech and language developmental delay	26/26 (no speech in 6/10)	16 (no speech in 5/16)	11/12	26/26 (no speech in 20/26)	3/3	4/4
Muscular hypotonia	18/24, ND in 2	11/11, ND in 5	5/6, ND in 6	23/26	2/2, ND in 1	ND
Seizures	20/26	11/12, ND in 4	8/12	17/26	Autistic traits 1/3	2/4
Behavioral abnormalities	ND	ND	ND	21/26	ND	2/4
Other neurological abnormalitites	Hearing loss	Hearing impairment (5/16), thin corpus callosum	Hearing impairment	Ataxia (10/26); no walking in 8/26	-	Regression of acquired skills (2/4)
	HPMRS1 (PIGV)	HPMRS2 (PIGO)	HPMRS3 (PGAP2)	HPMRS4 (PGAP3)	HPMRS5 (PIGW)	HPMRS6 (PIGY)
Malformations						
Cleft palate	8/26	4/16	1/12	15/26	-	0/4
Megacolon	8/26	5/16	1/12	0/26	-	0/4
Anorectal malformations	9/26	3/16	1/12	0/26	-	0/4
Vesicoureteral/ renal malformations	6/10	2/16	ND	0/26	-	1/4
Heart defect	5/26	2/16	2/12	2/26	-	0/4
Facial gestalt						
Apparent hypertelorism	26/26	6/6, ND in 10	1/12	12/13, ND in 13	ND	1/4
Up-slanting palpebral fissure	26/26	10/11, ND in 5	ND in 12	2/26	ND	0/4
Broad nasal bridge	26/26	5/6, ND in 10	2/12	13/13, ND in 13	1/3 ND in 2	1/4
Broad nasal tip	26/26	5/6, ND in 10	1/12	4/14, ND in 12	ND	1/4
Short nose	26/26	5/6, ND in 10	1/12	14/24, ND in 2	ND	ND
Tented upper lip vermilion	26/26	7/8, ND in 8	2/12	17/24, ND in 21	3/3	ND

Table 1 Summary of clinical findings in patients carrying *PIGV*, *PIGO*, *PGAP2*, *PGAP3*, *PIGW*, and *PIGY* mutations *(Continued)*

	HPMRS1 *PIGV* ($n = 26$, excluding 2 fetus)	HPMRS2 *PIGO* ($n = 16$)	HPMRS3 *PGAP2* ($n = 12$)	HPMRS4 *PGAP3* ($n = 26$)	HPMRS5 *PIGW* ($n = 3$)	HPMRS6 *PIGY* ($n = 4$)
Large, fleshy ear lobes	-	1/16		18/24, ND in 21	ND	4/4
Brachytelephalangy	26/26	10/10, ND in 6	0/12 (broad nails in 1/12)	0/26 (broad nails in 6/26)	-	1/4
Further anomalies (rare)	Gastroesophageal reflux, optic atrophy bilateral, scoliosis, hip subluxation (right), thin corpus callosum, gingiva hyperplasia	Coronal synostosis, keratoderma, micrognathia, auricular malformations		Thin corpus callosum (9/26), ventriculomegaly (3/26), vermis hypoplasia (4/26)	Inguinal hernia (1/3)	Cataracts (2/4) Rhizomelic shortness of limbs (2/4) Contractures (2/4) Hip dysplasia (2/4)
Published cases	Rabe et al. 1991 [33]	Krawitz et al. 2012 [7]	Hansen et al. 2013 [4]	Howard et al. 2014 [5]	Chiyonobu et al. 2014 [3]	Ilkovski et al. 2015 [6]
	Marcelis et al. 2007 [34]	Kuki et al. 2013 [36]	Krawitz et al. 2013 [8]	Knaus et al. 2016 [19]	Hogrebe et al. 2016 [20]	
	Krawitz et al. 2010 [9] and Horn et al. 2010 [60]	Nakamura et al. 2014 [16]	Jezela-Stanek et al. 2016 [18]	Pagnamenta et al. 2017 [40]		
	Horn et al. 2011 [28]	Xue et al. 2016 [31]	Naseer et al. 2016 [38]	Nampoothiri et al. 2017 [41]		
	Thompson et al. 2012 [29]	Morren et al. 2017 [35]		Abdel-Hamid et al. 2017 [39]		
	Horn et al. 2014 [30]	Zehavi et al. 2017 [17]		2 unpublished cases		
	Xue et al. 2016 [31]	Tanigawa 2017 [37]				
	Reynolds et al. 2017 [32]					
	6 unpublished cases					

ND not documented; *OFC* occipitofrontal head circumference

among these are congenital hydronephrosis, megaureter, and vesicoureteral reflux. Our data revealed a frequency of heart defects of about 20% in the group of affected individuals with *PIGV*, *PIGO*, and *PGAP2* mutations; however, the type of cardiac abnormality is variable. Only 2 of 26 affected individuals carrying *PGAP3* mutations have variable congenital heart defects. Cleft palate is the malformation with the highest frequency in the group of affected individuals with *PGAP3* mutations with a prevalence of almost 60%, whereas other malformations are rarely observed. Exceptional is a group of ten Egyptian individuals with the same founder mutation and a high incidence of structural brain anomalies (thin corpus callosum (8/10), vermis hypoplasia (4/10), ventriculomegaly (3/10), and Dandy-Walker malformation (1/10)) [39]. To date these are the few individuals with a presumably complete loss of function for this gene (NM_033419.3:c.402dupC, p.Met135Hisfs*28; c.817_820 delGACT, p.Asp273Serfs*37).

Malformations had not been observed in the single reported affected individual with *PIGW* mutations [3]. Apart from dilation of renal collecting systems, affected individuals with *PIGY* mutations presented with a new spectrum of organ involvement such as cataracts, rhizomelic shortness of limbs, contractures and hip dysplasia [6].

All affected individuals with *PIGV* and *PIGO* mutations had a variable degree of distal hand anomalies, namely brachytelephalangy. They showed hypoplastic finger nails as well as hypoplastic distal phalanges in hand X-rays. Often, they displayed broad and short distal phalanges of the thumbs and halluces, including short and broad corresponding nails of the affected digits. Brachytelephalangy is not present in any of the affected individuals with *PGAP3*, *PGAP2*, and *PIGW* mutations, respectively, although one-third showed broad nails without radiological abnormalities in the available X-rays. One of four affected individuals with *PIGY* mutations showed brachytelephalangy.

A multidisciplinary approach is required to manage the GPIBDs described in this section, as the clinical variability is broad. It is recommended that all affected individuals have at least one baseline renal ultrasound investigation as

well as echocardiography to rule out any obvious malformations. In case of chronic obstipation, Hirschsprung disease, as well as anal anomalies, should be excluded. Hearing evaluation is recommended in all affected individuals. Individuals with behavioral problems may benefit from a review by a clinical psychologist. Regular developmental assessments and EEG investigations are required to ensure that affected individuals get optimal support. The tendency towards epilepsies has been reported to decrease in some affected individuals with age and if the affected individual and physician agree to a trial discontinuation of therapy, medications could be tapered.

Clinical overview of MCAHS

MCAHS comprises a group of genetically different disorders characterized by early onset forms of different types of epilepsies with poor prognosis, missing or minimal psychomotor development, and often, early death (Table 2). The phenotypic series include individuals with *PIGA* (MIM 300868) [10, 13–15, 42–46], *PIGN* (MIM 614080) [12, 18, 47–53], and *PIGT* (MIM 615398) [11, 40, 54–57] mutations.

Neonatal muscular hypotonia is often present. The variable congenital anomalies affect the renal/vesicoureteral, cardiac, and gastrointestinal systems. Brain imaging showed variable abnormalities, for example, thin corpus callosum, cerebellar atrophy/hypoplasia, cerebral atrophy, and delayed myelination, but also normal findings in other affected individuals. There is overlap with the spectrum of malformations seen in HPMRS. Exceptions are megacolon, which is only reported in individuals with *PIGV*, *PIGO*, and *PGAP2* mutations, and diaphragmatic defects, which are only documented in three fetuses with *PIGN* mutations [51]. In addition, joint contractures and hyperreflexia are documented in some individuals with *PIGA* and *PIGN* mutations [10, 13–15,

Table 2 Comparison of phenotypic data and biomarkers in different types of MCAHS

GPIBDs: affected gene (individuals)	MCAHS2 PIGA ($n = 26$)	MCAHS1 PIGN ($n = 20$, including three fetuses)	MCAHS3 PIGT ($n = 14$)
Hyperphosphatasia	+/–	+/–	+
Seizures with early onset	+	+	+
Early death	+/–	+/–	–
Profound ID	+	+	+
Neonatal muscular hypotonia	+/–	+/–	+
Macrocephaly or macrosomia	+/–	+/–	+/–
Variable brain anomalies	+/–	+	+
Hyperreflexia/contractures	+/–	+/–	ND
Variable facial anomalies	+/–	+/–	+/–
Renal/vesicoureteral anomalies	+/–	+/–	+/–
Gastrointestinal anomalies	+/–	+/–	ND
Cardiovascular abnormalities	ND	+/–	ND
Cleft palate	+	+/–	–
Diaphragmatic defect	–	+/–	–
Short distal phalanges	–	+/–	–
Elevated alkaline phosphatase (AP)	+/– (5/23 elevated AP)	–	Decreased AP
Abnormal flow cytometry results	+/ND	+/ND	+/ND
Published cases	Johnston et al. 2012 [10]	Maydan et al. 2011 [12]	Kvarnung 2013 [11]
	van der Crabben et al. 2014 [15]	Brady et al. 2014 [48]	Nakashima 2014 [54]
	Swoboda et al. 2014 [43]	Ohba et al. 2014 [47]	Lam 2015 [55]
	Kato et al. 2014 [14]	Couser et al. 2015 [49]	Skauli 2015 [56]
	Belet et al. 2014 [42]	Fleming et al. 2015 [52]	Kohashi 2017 [57]
	Tarailo-Graovac et al. 2015 [44]	Khayat et al. 2015 [53]	Pagnamenta 2017 [40]
	Joshi et al. 2016 [46]	Nakagawa et al. 2016 [50]	3 unpublished cases
	Fauth et al. 2016 [13]	Jezela-Stanek et al. 2016 [18]	
	Kim et al. 2016 [45]	McInerney-Leo et al. 2016 [51]	
	9 unpublished cases		

ND not documented

42–46]. Macrocephaly or macrosomia occur in some of these individuals, whereas microcephaly occurs in others. No distinct facial phenotype is recognizable in comparison within and between the genetically different groups of MCAHS.

Interestingly, 5 out of 23 individuals with *PIGA* mutations had elevated AP measurements, whereas only one individual with *PIGN* mutations was reported with borderline high AP activity [52]. In contrast, some of the individuals with *PIGT* mutations showed decreased AP [11, 54].

HPMRS and MCAHS display an overlapping clinical spectrum but MCAHS has a considerably worse prognosis due to early onset and often intractable seizures as well as early death in the majority of affected individuals. However, facial dysmorphisms do not appear to be characteristic in the different types of MCAHS in contrast to HPMRS. Importantly, elevation of AP and reduced surface levels of GPI-linked substrates are not restricted to HPMRS.

Flow cytometry

Flow cytometry analysis of blood

Flow cytometry was performed on granulocytes extracted from peripheral blood draws that were sampled in BCT CytoChex tubes (Streck, NE, USA), shipped, and analyzed in less than 72 h. Whole blood (50 μl) was mixed with 20 μl of an antibody panel:

1. 4 μl CD55-PE (BD #555694), 4 μl CD59-FITC (BD #555763), 2 μl CD45-PacBlue (Beckman Coulter, clone J.33), and 10 μl FACS buffer.
2. 2 μl CD16-PE (Beckman Coulter, clone 3G8), 4 μl FLAER-AF488 (FL2S-C; Burlington, Canada,), 2 μl CD45-PacBlue (Beckman Coulter, clone J.33), and 12 μl FACS buffer.
3. 2 μl CD24-APC (MiltenyiBiotec Clone REA832), 2 μl CD45-PacBlue (Beckman Coulter, clone J.33), and 16 μl FACS buffer.

The staining was incubated for 30 min at room temperature followed by an incubation with 500 μl red blood cell lysis buffer for 10 min. Debris was removed by discarding the supernatant after centrifugation and the cell pellet was washed twice with 200 μl and resuspended in 100 μl FACS buffer for flow cytometry analysis on a MACSQuant VYB (MiltenyiBiotec, Bergisch Gladbach, Germany).

Gating for living cells was based on forward and side scatter (FSC-A vs. SSC-A). Single cells were gated on a diagonal (FSC-A vs. FSC-H). Granulocytes were identified as granular (SSC-A high) and CD45-positive cells.

The reduction of GPI-AP expression was assessed by the ratio of the median fluorescence intensity (MFI) of the patient to the MFI of a shipped healthy control. Heterozygous carriers of pathogenic mutations (parents) were used as controls when unrelated healthy controls were not available. It is noteworthy that differences in GPI-AP expression were subtle in healthy parents compared to unrelated controls. To compare marker reduction of published and unpublished cases only FLAER and CD16 were used.

Flow cytometric analysis of fibroblast cells

Fibroblasts derived from skin biopsies of patients, parents, and healthy control individuals were cultured in DMEM supplemented with 10% FCS, 1% ultraglutamine, 1% penicillin/streptomycin. For flow cytometry analysis confluently grown cells were washed twice with PBS (-Ca^{2+}, -Mg^{2+}); the cells were gently detached from the coulter dish with Trypsin-EDTA (0.01%). The single cell suspension was washed with FACS buffer, counted, diluted (100.000 cells/stain), and centrifuged, after which the supernatant was discarded and the cell pellet was resuspended in the following antibody mix.

1. 4 μl CD55-PE (BD #555694), 4 μl CD59-FITC (BD #555763), and 12 μl FACS buffer.
2. 4 μl CD73-PE (BD#550257), 4 μl FLAER-AF488 (Cedarlane, FL2S-C), and 12 μl FACS buffer.

The staining was incubated for 30 min at room temperature followed by two washing steps with 200 μl FACS buffer. For flow cytometry analysis on a MACSQuant VYB the cells were resuspended in 100 μl FACS buffer.

Reduction of GPI-AP expression was calculated as a ratio between the median fluorescence intensity (MFI) of the patient against the mean of MFIs from healthy parents and a healthy unrelated control. It is noteworthy that heterozygous carriers of pathogenic mutations (parents) and unrelated healthy controls had only subtle differences in GPI-AP expression.

Computer-assisted phenotype comparison

Facial images of all individuals with a molecularly confirmed GPIBD were assessed with the Face2Gene Research Application (FDNA Inc., Boston MA, USA). This software tool set allows the phenotypic comparison of user-defined cohorts with ten or more individuals. The classification model of Face2Gene Research uses a neural network architecture that consists of ten convolutional layers, each but the last followed by batch normalization. The original collections are split into training and test sets for cross-validation and mean accuracies for the classification process are computed. The result of a single experiment is a confusion matrix that describes the performance of the

classification process. As cohort size is a known confounder, we randomly sampled all cohorts down to the same size ($n = 10$) and computed the mean true positive and error rates as well as the standard deviation from ten iterations [58]. The scripts for the simulations are available on request and can be used to reproduce the results.

Results

Flow cytometric assessment of GPIBDs

We acquired fibroblast cultures of affected individuals to perform measurements under the same experimental conditions repeatedly. The marker FLAER, which binds to the GPI anchor directly, as well as the GPI-APs CD55, CD59, and CD73, which show high expression levels on fibroblasts, were assessed (Fig. 1). We hypothesized that measuring cell surface levels of GPI-linked substrates directly by flow cytometry might be more suitable to quantify the severity of a GPIBD or to predict the affected gene. No significant differences between patients with MCAHS were observed compared to patients with HPMRS (Fig. 1a). Furthermore, the cell surface levels of CD55 and CD59 were on average lower in cells that were derived from individuals with mutations in *PGAP3* compared to individuals with mutations in *PIGV* (Additional file 1: Table S1), although this did not correspond to a higher prevalence of seizures or a more severe developmental delay. CD55 and CD59 are of particular interest as they protect cells from an attack on the activated complement system and the membrane attack complex that has also been shown to be involved in the pathogenesis of seizures [59].

The samples with pathogenic mutations in *PIGV* are noteworthy as they are derived from individuals that differ considerably in the severity of their phenotype: 14-0585 was born with multiple malformations and his seizures are resistant to treatment, whereas the other three individuals, A2, A3, and P1, are considered to be moderately affected. The flow cytometric profiles, however, do not show marked differences. Furthermore, the cell surface levels of CD55 and CD59 were on average lower in cells that were derived from individuals with mutations in *PGAP3*.

While the reproducibility of the flow cytometric data on fibroblasts is attractive, the small size of the sample set is clearly a disadvantage in the assessment of potential differences between the phenotypic subgroups of GPIBDs. Most flow cytometric analyses have been performed on granulocytes of affected individuals with the markers CD16 and FLAER and we added a comparison of the relative median fluorescent intensities (rMFI) for a total of 39 individuals of the phenotypic series MCAHS and HPMRS (Additional file 1: Table S2). Although individuals of the MCAHS spectrum are usually more severely affected than individuals of the HPMRS spectrum, we did not observe any significant differences for the tested markers (Fig. 1b). Thus, no significant correlation between FACS profiles of the two phenotypic series was found.

Comparison of the facial gestalt of GPIBDs

The craniofacial characteristics of many Mendelian disorders are highly informative for clinical geneticists and have also been used to delineate gene-specific phenotypes of several GPIBDs [3–5, 10, 12, 19, 28–30, 32, 39, 40, 43, 44, 60, 61]. However, our medical terminology is often not capable of describing subtle differences in the facial gestalt. Therefore, computer-assisted analysis of the gestalt has recently received much attention in syndromology and several groups have shown that the clinical face phenotype space (CFPS) can also be exploited

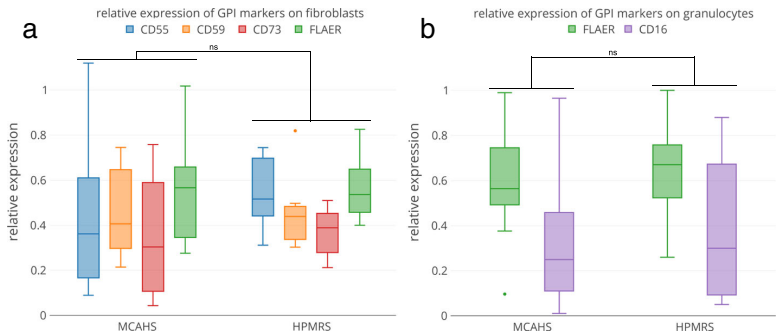

Fig. 1 Flow cytometric profiling for GPIBDs. Cell surface levels of FLAER and tissue-specific GPI-anchored proteins were assessed on fibroblasts (**a**) as well as on granulocytes (**b**) of individuals affected by GPIBDs. The relative expression was grouped for GPIBDs of the same phenotypic series, MCAHS (*PIGA*, *PIGN*, *PIGT*) and HPMRS (*PGAP3*, *PIGV*, *PIGO*, *PIGW*), but showed no significant differences (significance was tested with Wilcoxon-Mann-Whitney test; the *p* value was corrected for sample size (Bonferoni))

by machine learning approaches [62]. If a recognizable gestalt exists, a classifier for facial patterns can be trained to infer likely differential diagnoses. Conversely, if photos of affected individuals with disease-causing mutations in different genes of a pathway form separate clusters, it indicates that the gestalt is distinguishable to a certain extent. FDNA's recently launched RESEARCH application is a deep learning tool for exactly this purpose (https://app.face2gene.com/research): a classification model is generated on two or more collections of frontal images and the performance is reported as a confusion matrix. If true positive rates for the single gene–phenotypes are achieved that are significantly better than for a random assignment of photos to cohorts, there is some phenotypic substructure and the null hypothesis of perfect heterogeneity may be rejected.

We used the RESEARCH app of the Face2Gene suite to evaluate a classifier for the five most prevalent GPIBDs, *PIGA* ($n = 20$), *PIGN* ($n = 11$), *PIGT* ($n = 12$), *PIGV* ($n = 25$), and *PGAP3* ($n = 23$). Our original sample set thus consists of frontal facial photos of 91 individuals with a molecularly confirmed diagnosis of HPMRS or MCAHS, including cases that have been previously published [5, 9–11, 13–15, 19, 28–30, 32–34, 39, 43, 47, 49, 50, 52–56, 60, 63]. The mean accuracy that was achieved on this original sample set was 52.2%, which is significantly better than random. In order to compare the performance for the single gene classes we had to exclude confounding effects from unbalanced cohort sizes and sampled the cohorts down to the same size of $n = 10$. Although this decreases the overall performance, the mean accuracy of 45.8% is still significantly better than the 20% that would be achieved by chance in a five-class problem for evenly sized cohorts (Fig. 2). Furthermore, for every single gene–phenotype, the true positive rate (TPR) was better than randomly expected, with *PIGV* achieving the highest value (59%).

Interestingly, we observed the highest false negative rate in the confusion matrix for *PGAP3* (HPMRS4): on average 32% of these cases are erroneously classified as *PIGV* (HPMRS1) cases. This finding is in good agreement with the phenotypic delineation from syndromologists that grouped these to genes in the same subclass. A cluster analysis of the confusion matrix actually reproduces the two phenotypic series as shown by the dendrogram in Fig. 2.

While the confusion matrix on the entire sample set can be used to decide whether there are gene-specific substructures in the GPI pathway, pairwise comparisons are better suited to derive phenotypic differences between genes even inside a phenotypic series. We therefore evaluated the area under the receiver operating characteristics curve (AUC) and found the correct gene prediction more often than randomly expected, including *PIGV* versus *PGAP3* (Additional file 1: Figure S3). The differences in pair-wise comparison between *PIGV* and *PGAP3* could be confounded by the large number of Egyptian cases in the *PGAP3* cohort [39], the effect of which we could not further analyze due to the limited set of patient photos.

Discussion

The identification of multiple affected individuals with GPIBDs has enabled the analysis of genotype–phenotype relationships for the molecular pathway of GPI anchor synthesis. Besides a developmental delay and seizures, which are common findings in most affected individuals with a GPIBD, the clinical variability and the variation in expressivity is wide. So far, recognizable gene-specific phenotypes seem to be accepted for *PIGL* and are discussed for *PIGM* [64, 65]. For other GPIBDs the phenotypic series HPMRS and MCAHS have been used to subgroup the pathway and the activity of AP in serum was the main classification criterion. However, these disease entities are increasingly cumbersome as some cases are now known to not follow this oversimplified rule.

We therefore compared GPIBDs based on deep phenotyping data and flow cytometric profiles of GPI-APs. Among the 16 genes of the GPI pathway with reports of affected individuals, mutations in *PIGA*, *PIGN*, *PIGT*, *PIGV*, and *PGAP3* were most numerous and these GPIBDs were also suitable for automated image analysis.

A systematic evaluation of the phenotypic features showed that certain malformations occur with a higher frequency in specific GPIBDs. To date, megacolon has only been found to be associated with *PIGV*, *PIGO*, and *PGAP2* mutations. Diaphragmatic defects have only been documented in affected individuals with *PIGN* mutations. Only in individuals with *PGAP3* mutations are behavioral problems, especially sleep disturbances and autistic features, present, in about 90%. In addition, ataxia and unsteady gait are also frequently documented in this group but not in the others. An accurate classification that is merely based on clinical symptoms is, however, not possible due to their high variability. Also, flow cytometric analysis of GPI marker expression was not indicative for the gene defect and did not correlate with the severity of the phenotype. Of note, however, an assessment of the GPI-AP expression levels seems more sensitive in fibroblasts than in blood cells [24]. This might also be related to the trafficking pathways of GPI-APs through endoplasmic reticulum and Golgi that differ for cell types and substrates [66, 67].

The overlapping clinical spectrum of both HPMRS and MCAHS, the findings of elevated AP, and the reduced surface levels of GPI-linked proteins in some of the MCAHS cases favor a common classification as GPIBDs.

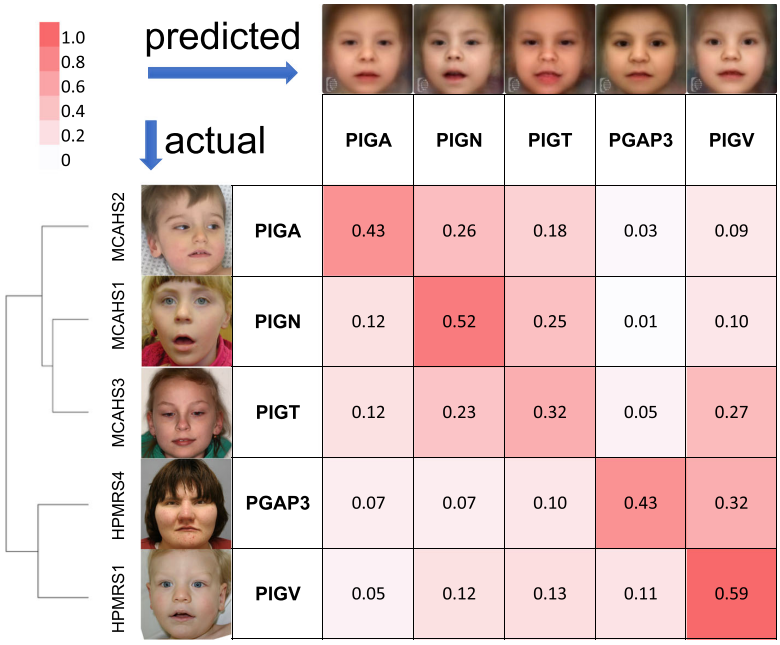

Fig. 2 Automated image analysis for five of the most prevalent GPIBDs. A model for the classification of the gene–phenotypes was repeatedly trained and cross-validated on patient subsets that were randomly down-sampled to the same cohort size of n = 10. A mean accuracy of 0.44 was achieved, which is significantly better than random (0.20). For explanatory purposes, the rows of the confusion matrix start with instances of previously published or newly identified individuals with GPIBDs. If the predicted gene matches the molecularly confirmed diagnosis, such a test case would contribute to the true positive rate, shown on the diagonal. Actual affected individual photographs were used to generate an averaged and de-identified composite photo and are shown at the top of the columns. The performance of computer-assisted image classification is significantly better than expected under the null model of perfect heterogeneity and indicates a gene-specific phenotypic substructure for the molecular pathway disease. Higher false positive error rates occur between genes of the same phenotypic series, HPMRS and MCAHS, as indicated by the dendrogram

In light of the high variability and expressivity of the clinical findings and the weak genotype–phenotype correlation, the most surprising finding of our study was the high discriminatory power that facial recognition technology achieved. In spite of the similarity of the pathophysiology, differences in the gestalt are still perceptible. This illustrates the remarkable information content of human faces and advocates for the power of computer-assisted syndromology in the definition of disease entities.

Automated image analysis of syndromic disorders is a comparably new field of research and the approach that we used requires photos of at least ten individuals per cohort. However, it is currently not known if there is a minimum number of cases that is required to assess whether a gene–phenotype is recognizable. Furthermore, for every rare disorder with a characteristic gestalt there is possibly a maximum value for the recognizability. So far, the approximation of this upper limit has not systematically been studied depending on the number of individuals that were used in the training process and should definitely be a focus for future research.

Conclusions

A gene-centered classification of GPIBDs is recommended due to the overlapping clinical spectrum of both HPMRS and MCAHS in the majority of affected individuals. Measuring AP serum activity and cell surface levels of GPI-linked markers is still regarded as an imperative in the diagnostic work-up of GPIBDs, especially when dealing with mutations that have not been reported previously. In addition, next-generation phenotyping tools can add another layer of information in the interpretation of novel mutations in the GPI anchor pathway, particularly if the flow cytometric data are inconclusive.

Additional file

Additional file 1: Supplemental tables and figures. (DOCX 1270 kb)

Abbreviations

AP: Alkaline phophatase; APC: Allophycocyanin; AUC: Area under the curve; DMEM: Dulbecco's modified Eagle medium; DPDL: Deep Phenotyping for Deep Learning; EEG: Electroencephalography; FACS: Fluorescence-activated cell sorting; FCS: Fetal calf serum; FITC: Fluorescein isothiocyanate;

FLAER: Fluorescein-labeled proaerolysin; FSC-A: Forward scatter area; FSC-H: Forward scatter area hight; GPI: Glycosylphosphatidylinositol; GPI-AP: GPI-anchored protein; GPIBD: GPI biosynthesis defect; HPMRS: Hyperphosphatasia with mental retardation syndrome; ID: Intellectual disability; MCAHS: Multiple congenital anomalies hypotonia seizures; MFI: Media fluorescent intensity; OFC: Occipitofrontal head circumference; PBS: Phosphate buffered saline; PE: Phycoerythrin; SSC-A: Side scatter area; TPR: true positive rate

Acknowledgments
The authors thank the patients and their families who participated in this study.

Funding
This work was supported by grants from the German Ministry of Research and Education to M.S. (BMBF project number 01EC1402B), and the German Research Foundation to I.H. (HE 5415/6-1), Y.W. (WE 4896/3-1), and P.M.K (KR3985/7-3).

Availability of data and materials
Data supporting the findings of this study are available within the article and Additional file 1. All data that were used for the phenotypic analysis is part of a larger effort, called DPDL, that serves as a case-centered data collection for benchmarking of automated imaging technology. DPDL is accessible at http://www.dpdl.org and requires registration. On Face2Gene registered users can run the experiments for phenotypic comparison in the RESEARCH app (https://app.face2gene.com/research). Registration at Face2Gene is free, but is designated to be used by healthcare professionals.

Authors' contributions
AK performed flow cytometry analysis and interpretation. AK, JTP, NH, MZ, TCH, MS, YG, and NF contributed to facial picture acquisition, analysis, and bioinformatics interpretation of the data. MJ and SK performed variant analysis of sequencing data. HM, CK, RSM, AB, PC, NC, HW, SS, RL, CE, MB, HJC, MvdB, EO, AC, ME, FK, NB, HJS, YW, and DH were involved in recruitment of participants, genotyping, and/or phenotypic characterization and interpretation. AK, PNR, SM, DH, IH, and PK were involved in study design and patient data analysis. AK, DH, and PK wrote the manuscript. All authors were involved in interpreting and drafting this manuscript and read and approved the final manuscript.

Ethics approval and consent to participate
The Charité – Universitätsmedizin Berlin ethics board approved this study, which was carried out in accordance with the principles of the Declaration of Helsinki. Written informed consent to participate was obtained before enrolment from the responsible persons (parents) on behalf of all study participants.

Consent for publication
Written informed consent was obtained before enrolment from the responsible persons (parents) on behalf of all study participants to publish their photographs as well as their clinical data for scientific purposes.

Competing interests
PMK is a member of the scientific advisory board of FDNA, the company providing the Face2Gene platform. YG and NF are employees of FNDA. The remaining authors declare that they have no competing interests.

Publisher's Note

Author details
[1]Institut für Medizinische Genetik und Humangenetik, Charité Universitätsmedizin Berlin, 13353 Berlin, Germany. [2]Max Planck Institute for Molecular Genetics, 14195 Berlin, Germany. [3]Berlin-Brandenburg School for Regenerative Therapies, Charité Universitätsmedizin Berlin, 13353 Berlin, Germany. [4]Institute for Genomic Statistics and Bioinformatics, University Hospital Bonn, Rheinische Friedrich-Wilhelms-Universität Bonn, 53127 Bonn, Germany. [5]Department of Neuropediatrics, University Medical Center Schleswig Holstein, 24105 Kiel, Germany. [6]Berlin Institute of Health (BIH), 10178 Berlin, Germany. [7]FDNA Inc., Boston, MA, USA. [8]Unité de Neuropédiatrie, Université de Genève, CH-1211 Genève, Switzerland. [9]Danish Epilepsy Centre, DK-4293 Dianalund, Denmark. [10]Institute for Regional Health Services Research, University of Southern Denmark, DK-5000 Odense, Denmark. [11]Department of Pediatrics, University Hospital of Hvidovre, 2650 Hvicovre, Denmark. [12]Service de Génétique Médicale, Hôpital Purpan, CHU, 31059 Toulouse, France. [13]Greenwood Genetic Center, SC29646 Greenwood, USA. [14]Genetische Poliklinik, Universitätsklinik Heidelberg, 69120 Heidelberg, Germany. [15]St. Bernward Krankenhaus, 31134 Hildesheim, Germany. [16]Kinderkrankenhaus auf der Bult, Hannoversche Kinderheilanstalt, 30173 Hannover, Germany. [17]Department for Clinical Genetics, Erasmus MC, 3000 Rotterdam, Netherlands. [18]Institute of Mother and Child Department of Molecular Genetics, 01-211 Warsaw, Poland. [19]Neurology Department, Lithuanian University of Health Sciences, 50009 Kaunas, Lithuania. [20]Institute of Human Genetics, University Medical Center Hamburg-Eppendorf, 20246 Hamburg, Germany. [21]Victorian Clinical Genetics Services, Royal Children's Hospital, MCRI, Parkville, Australia. [22]Department of Clinical Genetics, Austin Health, Heidelberg, Australia. [23]The Jackson Laboratory for Genomic Medicine, 06032 Farmington, USA. [24]Departement of Neurology, Academic Center for Epileptology, 5590 Heeze, The Netherlands. [25]Department of Neurology and Epileptology and Hertie Institute for Clinical Brain Research, University Tübingen, 72076 Tübingen, Germany. [26]Pediatric Neurology, Children's Hospital of Philadelphia, 3401 Philadelphia, USA.

Received: 2 August 2017 Accepted: 11 December 2017
Published online: 09 January 2018

References

1. Kinoshita T, Fujita M, Maeda Y. Biosynthesis, remodelling and functions of mammalian GPI-anchored proteins: recent progress. J Biochem. 2008;144(3): 287–94.
2. Murakami Y, Kanzawa N, Saito K, Krawitz PM, Mundlos S, Robinson PN, Karadimitris A, Maeda Y, Kinoshita T. Mechanism for release of alkaline phosphatase caused by glycosylphosphatidylinositol deficiency in patients with hyperphosphatasia-mental retardation syndrome. J Biol Chem. 2012;287(9):6318-6325.
3. Chiyonobu T, Inoue N, Morimoto M, Kinoshita T, Murakami Y. Glycosylphosphatidylinositol (GPI) anchor deficiency caused by mutations in PIGW is associated with West syndrome and hyperphosphatasia with mental retardation syndrome. J Med Genet. 2014;51(3):203–7.
4. Hansen L, Tawamie H, Murakami Y, Mang Y, ur Rehman S, Buchert R, Schaffer S, Muhammad S, Bak M, Nothen MM, et al. Hypomorphic mutations in PGAP2, encoding a GPI-anchor-remodeling protein, cause autosomal-recessive intellectual disability. Am J Hum Genet. 2013;92(4):575–83.
5. Howard MF, Murakami Y, Pagnamenta AT, Daumer-Haas C, Fischer B, Hecht J, Keays DA, Knight SJ, Kolsch U, Kruger U, et al. Mutations in PGAP3 impair GPI-anchor maturation, causing a subtype of hyperphosphatasia with mental retardation. Am J Hum Genet. 2014;94(2):278-287.
6. Ilkovski B, Pagnamenta AT, O'Grady GL, Kinoshita T, Howard MF, Lek M, Thomas B, Turner A, Christodoulou J, Sillence D, et al. Mutations in PIGY: expanding the phenotype of inherited glycosylphosphatidylinositol (GPI) deficiencies. Hum Mol Genet. 2015;24(21):6146-6159.
7. Krawitz PM, Murakami Y, Hecht J, Kruger U, Holder SE, Mortier GR, Delle Chiaie B, De Baere E, Thompson MD, Roscioli T, et al. Mutations in PIGO, a member of the GPI-anchor-synthesis pathway, cause hyperphosphatasia with mental retardation. Am J Hum Genet. 2012;91(1):146–51.
8. Krawitz PM, Murakami Y, Riess A, Hietala M, Kruger U, Zhu N, Kinoshita T, Mundlos S, Hecht J, Robinson PN, et al. PGAP2 mutations, affecting the GPI-anchor-synthesis pathway, cause hyperphosphatasia with mental retardation syndrome. Am J Hum Genet. 2013;92(4):584–9.
9. Krawitz PM, Schweiger MR, Rodelsperger C, Marcelis C, Kolsch U, Meisel C, Stephani F, Kinoshita T, Murakami Y, Bauer S, et al. Identity-by-descent filtering of exome sequence data identifies PIGV mutations in hyperphosphatasia mental retardation syndrome. Nat Genet. 2010;42(10):827–9.
10. Johnston JJ, Gropman AL, Sapp JC, Teer JK, Martin JM, Liu CF, Yuan X, Ye Z, Cheng L, Brodsky RA, et al. The phenotype of a germline mutation in PIGA: the gene somatically mutated in paroxysmal nocturnal hemoglobinuria. Am J Hum Genet. 2012;90(2):295–300.
11. Kvarnung M, Nilsson D, Lindstrand A, Korenke GC, Chiang SC, Blennow E, Bergmann M, Stodberg T, Makitie O, Anderlid BM et al. A novel intellectual disability syndrome caused by GPI anchor deficiency due to homozygous mutations in PIGT. J Med Genet. 2013;50(8):521-528.

12. Maydan G, Noyman I, Har-Zahav A, Neriah ZB, Pasmanik-Chor M, Yeheskel A, Albin-Kaplanski A, Maya I, Magal N, Birk E, et al. Multiple congenital anomalies-hypotonia-seizures syndrome is caused by a mutation in PIGN. J Med Genet. 2011;48(6):383–9.
13. Fauth C, Steindl K, Toutain A, Farrell S, Witsch-Baumgartner M, Karall D, Joset P, Bohm S, Baumer A, Maier O, et al. A recurrent germline mutation in the PIGA gene causes Simpson-Golabi-Behmel syndrome type 2. Am J Med Genet A. 2016;170A(2):392–402.
14. Kato M, Saitsu H, Murakami Y, Kikuchi K, Watanabe S, Iai M, Miya K, Matsuura R, Takayama R, Ohba C, et al. PIGA mutations cause early-onset epileptic encephalopathies and distinctive features. Neurology. 2014;82(18):1587–96.
15. van der Crabben SN, Harakalova M, Brilstra EH, van Berkestijn FM, Hofstede FC, van Vught AJ, Cuppen E, Kloosterman W, van Amstel HKP, van Haaften G, et al. Expanding the spectrum of phenotypes associated with germline PIGA mutations: a child with developmental delay, accelerated linear growth, facial dysmorphisms, elevated alkaline phosphatase, and progressive CNS abnormalities. Am J Med Genet A. 2014;164A(1):29–35.
16. Nakamura K, Osaka H, Murakami Y, Anzai R, Nishiyama K, Kodera H, Nakashima M, Tsurusaki Y, Miyake N, Kinoshita T, et al. PIGO mutations in intractable epilepsy and severe developmental delay with mild elevation of alkaline phosphatase levels. Epilepsia. 2014;55(2):e13–17.
17. Zehavi Y, von Renesse A, Daniel-Spiegel E, Sapir Y, Zalman L, Chervinsky I, Schuelke M, Straussberg R, Spiegel R. A homozygous PIGO mutation associated with severe infantile epileptic encephalopathy and corpus callosum hypoplasia, but normal alkaline phosphatase levels. Metab Brain Dis. 2017;32(6):2131-2137.
18. Jezela-Stanek A, Ciara E, Piekutowska-Abramczuk D, Trubicka J, Jurkiewicz E, Rokicki D, Mierzewska H, Spychalska J, Uhrynowska M, Szwarc-Bronikowska M, et al. Congenital disorder of glycosylphosphatidylinositol (GPI)-anchor biosynthesis–The phenotype of two patients with novel mutations in the PIGN and PGAP2 genes. Eur J Paediatr Neurol. 2016;20(3):462–73.
19. Knaus A, Awaya T, Helbig I, Afawi Z, Pendziwiat M, Abu-Rachma J, Thompson MD, Cole DE, Skinner S, Annese F, et al. Rare noncoding mutations extend the mutational spectrum in the PGAP3 subtype of hyperphosphatasia with mental retardation syndrome. Hum Mutat. 2016;37(8):737–44.
20. Hogrebe M, Murakami Y, Wild M, Ahlmann M, Biskup S, Hortnagel K, Gruneberg M, Reunert J, Linden T, Kinoshita T, et al. A novel mutation in PIGW causes glycosylphosphatidylinositol deficiency without hyperphosphatasia. Am J Med Genet A. 2016;170(12):3319–22.
21. Edvardson S, Murakami Y, Nguyen TT, Shahrour M, St-Denis A, Shaag A, Damseh N, Le Deist F, Bryceson Y, Abu-Libdeh B, et al. Mutations in the phosphatidylinositol glycan C (PIGC) gene are associated with epilepsy and intellectual disability. J Med Genet. 2017;54(3):196–201.
22. Johnstone DL, Nguyen TT, Murakami Y, Kernohan KD, Tetreault M, Goldsmith C, Doja A, Wagner JD, Huang L, Hartley T, et al. Compound heterozygous mutations in the gene PIGP are associated with early infantile epileptic encephalopathy. Hum Mol Genet. 2017;26(9):1706–15.
23. Makrythanasis P, Kato M, Zaki MS, Saitsu H, Nakamura K, Santoni FA, Miyatake S, Nakashima M, Issa MY, Guipponi M, et al. Pathogenic variants in PIGG cause intellectual disability with seizures and hypotonia. Am J Hum Genet. 2016;98(4):615–26.
24. Zhao JJ, Halvardson J, Knaus A, Georgii-Hemming P, Baeck P, Krawitz PM, Thuresson AC, Feuk L. Reduced cell surface levels of GPI-linked markers in a new case with PIGG loss of function. Hum Mutat. 2017;38(10):1394-1401.
25. Martin HC, Kim GE, Pagnamenta AT, Murakami Y, Carvill GL, Meyer E, Copley RR, Rimmer A, Barcia G, Fleming MR, et al. Clinical whole-genome sequencing in severe early-onset epilepsy reveals new genes and improves molecular diagnosis. Hum Mol Genet. 2014;23(12):3200–11.
26. Jaeken J. Congenital disorders of glycosylation (CDG): it's (nearly) all in it! J Inherit Metab Dis. 2011;34(4):853–8.
27. Robinson PN, Kohler S, Bauer S, Seelow D, Horn D, Mundlos S. The Human Phenotype Ontology: a tool for annotating and analyzing human hereditary disease. Am J Hum Genet. 2008;83(5):610–5.
28. Horn D, Krawitz P, Mannhardt A, Korenke GC, Meinecke P. Hyperphosphatasia-mental retardation syndrome due to PIGV mutations: expanded clinical spectrum. Am J Med Genet A. 2011;155A(8):1917–22.
29. Thompson MD, Roscioli T, Marcelis C, Nezarati MM, Stolte-Dijkstra I, Sharom FJ, Lu P, Phillips JA, Sweeney E, Robinson PN, et al. Phenotypic variability in hyperphosphatasia with seizures and neurologic deficit (Mabry syndrome). Am J Med Genet A. 2012;158A(3):553–8.
30. Horn D, Wieczorek D, Metcalfe K, Baric I, Palezac L, Cuk M, Petkovic Ramadza D, Kruger U, Demuth S, Heinritz W, et al. Delineation of PIGV mutation spectrum and associated phenotypes in hyperphosphatasia with mental retardation syndrome. Eur J Hum Genet. 2014;22(6):762–7.
31. Xue J, Li H, Zhang Y, Yang Z. Clinical and genetic analysis of two Chinese infants with Mabry syndrome. Brain Dev. 2016;38(9):807–18.
32. Reynolds KK, Juusola J, Rice GM, Giampietro PF. Prenatal presentation of Mabry syndrome with congenital diaphragmatic hernia and phenotypic overlap with Fryns syndrome. Am J Med Genet A. 2017;173(10):2776–81.
33. Rabe P, Haverkamp F, Emons D, Rosskamp R, Zerres K, Passarge E. Syndrome of developmental retardation, facial and skeletal anomalies, and hyperphosphatasia in two sisters: nosology and genetics of the Coffin-Siris syndrome. Am J Med Genet. 1991;41(3):350–4.
34. Marcelis CL, Rieu P, Beemer F, Brunner HG. Severe mental retardation, epilepsy, anal anomalies, and distal phalangeal hypoplasia in siblings. Clin Dysmorphol. 2007;16(2):73–6.
35. Morren MA, Jaeken J, Visser G, Salles I, Van Geet C, BioResource N, Simeoni I, Turro E, Freson K. PIGO deficiency: palmoplantar keratoderma and novel mutations. Orphanet J Rare Dis. 2017;12(1):101.
36. Kuki I, Takahashi Y, Okazaki S, Kawawaki H, Ehara E, Inoue N, Kinoshita T, Murakami Y. Vitamin B6-responsive epilepsy due to inherited GPI deficiency. Neurology. 2013;81(16):1467–9.
37. Tanigawa J, Mimatsu H, Mizuno S, Okamoto N, Fukushi D, Tominaga K, Kidokoro H, Muramatsu Y, Nishi E, Nakamura S, et al. Phenotype-genotype correlations of PIGO deficiency with variable phenotypes from infantile lethality to mild learning difficulties. Hum Mutat. 2017;38(7):805–15.
38. Naseer MI, Rasool M, Jan MM, Chaudhary AG, Pushparaj PN, Abuzenadah AM, Al-Qahtani MH. A novel mutation in PGAP2 gene causes developmental delay, intellectual disability, epilepsy and microcephaly in consanguineous Saudi family. J Neurol Sci. 2016;371:121–5.
39. Abdel-Hamid MS, Issa MY, Otaify GA, Abdel-Ghafar SF, Elbendary HM, Zaki MS. PGAP3-related hyperphosphatasia with mental retardation syndrome: report of 10 new patients and a homozygous founder mutation. Clin Genet. 2017;93(1):84–91.
40. Pagnamenta AT, Murakami Y, Taylor JM, Anzilotti C, Howard MF, Miller V, Johnson DS, Tadros S, Mansour S, Temple IK, et al. Analysis of exome data for 4293 trios suggests GPI-anchor biogenesis defects are a rare cause of developmental disorders. Eur J Hum Genet. 2017;25(6):669–79.
41. Nampoothiri S, Hebbar M, Roy AG, Kochumon SP, Bielas S, Shukla A, Girisha KM. Hyperphosphatasia with mental retardation syndrome due to a novel mutation in PGAP3. J Pediatr Genet. 2017;6(3):191–3.
42. Belet S, Fieremans N, Yuan X, Van Esch H, Verbeeck J, Ye Z, Cheng L, Brodsky BR, Hu H, Kalscheuer VM, et al. Early frameshift mutation in PIGA identified in a large XLID family without neonatal lethality. Hum Mutat. 2014;35(3):350–5.
43. Swoboda KJ, Margraf RL, Carey JC, Zhou H, Newcomb TM, Coonrod E, Durtschi J, Mallempati K, Kumanovics A, Katz BE, et al. A novel germline PIGA mutation in Ferro-Cerebro-Cutaneous syndrome: a neurodegenerative X-linked epileptic encephalopathy with systemic iron-overload. Am J Med Genet A. 2014;164A(1):17–28.
44. Tarailo-Graovac M, Sinclair G, Stockler-Ipsiroglu S, Van Allen M, Rozmus J, Shyr C, Biancheri R, Oh T, Sayson B, Lafek M, et al. The genotypic and phenotypic spectrum of PIGA deficiency. Orphanet J Rare Dis. 2015;10:23.
45. Kim YO, Yang JH, Park C, Kim SK, Kim MK, Shin MG, Woo YJ. A novel PIGA mutation in a family with X-linked, early-onset epileptic encephalopathy. Brain Dev. 2016;38(8):750–4.
46. Joshi C, Kolbe DL, Mansilla MA, Mason S, Smith RJ, Campbell CA. Ketogenic diet - A novel treatment for early epileptic encephalopathy due to PIGA deficiency. Brain Dev. 2016;38(9):848–51.
47. Ohba C, Okamoto N, Murakami Y, Suzuki Y, Tsurusaki Y, Nakashima M, Miyake N, Tanaka F, Kinoshita T, Matsumoto N, et al. PIGN mutations cause congenital anomalies, developmental delay, hypotonia, epilepsy, and progressive cerebellar atrophy. Neurogenetics. 2014;15(2):85–92.
48. Brady PD, Moerman P, De Catte L, Deprest J, Devriendt K, Vermeesch JR. Exome sequencing identifies a recessive PIGN splice site mutation as a cause of syndromic congenital diaphragmatic hernia. Eur J Med Genet. 2014;57(9):487–93.
49. Couser NL, Masood MM, Strande NT, Foreman AK, Crooks K, Weck KE, Lu M, Wilhelmsen KC, Roche M, Evans JP, et al. The phenotype of multiple

congenital anomalies-hypotonia-seizures syndrome 1: report and review. Am J Med Genet A. 2015;167A(9):2176–81.
50. Nakagawa T, Taniguchi-Ikeda M, Murakami Y, Nakamura S, Motooka D, Emoto T, Satake W, Nishiyama M, Toyoshima D, Morisada N, et al. A novel PIGN mutation and prenatal diagnosis of inherited glycosylphosphatidylinositol deficiency. Am J Med Genet A. 2016;170A(1):183–8.
51. McInerney-Leo AM, Harris JE, Gattas M, Peach EE, Sinnott S, Dudding-Byth T, Rajagopalan S, Barnett CP, Anderson LK, Wheeler L, et al. Fryns syndrome associated with recessive mutations in PIGN in two separate families. Hum Mutat. 2016;37(7):695–702.
52. Fleming L, Lemmon M, Beck N, Johnson M, Mu W, Murdock D, Bodurtha J, Hoover-Fong J, Cohn R, Bosemani T, et al. Genotype-phenotype correlation of congenital anomalies in multiple congenital anomalies hypotonia seizures syndrome (MCAHS1)/PIGN-related epilepsy. Am J Med Genet A. 2016;170A(1):77–86.
53. Khayat M, Tilghman JM, Chervinsky I, Zalman L, Chakravarti A, Shalev SA. A PIGN mutation responsible for multiple congenital anomalies-hypotonia-seizures syndrome 1 (MCAHS1) in an Israeli-Arab family. Am J Med Genet A. 2016;170A(1):176–82.
54. Nakashima M, Kashii H, Murakami Y, Kato M, Tsurusaki Y, Miyake N, Kubota M, Kinoshita T, Saitsu H, Matsumoto N. Novel compound heterozygous PIGT mutations caused multiple congenital anomalies-hypotonia-seizures syndrome 3. Neurogenetics. 2014;15(3):193–200.
55. Lam C, Golas GA, Davids M, Huizing M, Kane MS, Krasnewich DM, Malicdan MCV, Adams DR, Markello TC, Zein WM, et al. Expanding the clinical and molecular characteristics of PIGT-CDG, a disorder of glycosylphosphatidylinositol anchors. Mol Genet Metab. 2015;115(2-3):128–40.
56. Skauli N, Wallace S, Chiang SC, Baroy T, Holmgren A, Stray-Pedersen A, Bryceson YT, Stromme P, Frengen E, Misceo D. Novel PIGT variant in two brothers: expansion of the multiple congenital anomalies-hypotonia seizures syndrome 3 phenotype. Genes (Basel). 2016;7(12):E108.
57. Kohashi K, Ishiyama A, Yuasa S, Tanaka T, Miya K, Adachi Y, Sato N, Saitsu H, Ohba C, Matsumoto N et al. Epileptic apnea in a patient with inherited glycosylphosphatidylinositol anchor deficiency and PIGT mutations. Brain Dev. 2017;40(1):53-57.
58. Pantel JT, Zhao M, Mensah MA, Hajjir N, Hsieh T-c, Hanani Y, Fleischer N, Kamphans T, Mundlos S, Gurovich Y. Advances in computer-assisted syndrome recognition and differentiation in a set of metabolic disorders. https://doi.org/10.1101/219394.
59. Xiong ZQ, Qian W, Suzuki K, McNamara JO. Formation of complement membrane attack complex in mammalian cerebral cortex evokes seizures and neurodegeneration. J Neurosci. 2003;23(3):955–60.
60. Horn D, Schottmann G, Meinecke P. Hyperphosphatasia with mental retardation, brachytelephalangy, and a distinct facial gestalt: Delineation of a recognizable syndrome. European J Med Gen. 2010;53(2):85–8.
61. Ihara S, Nakayama S, Murakami Y, Suzuki E, Asakawa M, Kinoshita T, Sawa H. PIGN prevents protein aggregation in the endoplasmic reticulum independently of its function in the GPI synthesis. J Cell Sci. 2017;130(3):602–13.
62. Ferry Q, Steinberg J, Webber C, FitzPatrick DR, Ponting CP, Zisserman A, Nellaker C. Diagnostically relevant facial gestalt information from ordinary photos. Elife. 2014;3:e02020.
63. Thompson MD, Nezarati MM, Gillessen-Kaesbach G, Meinecke P, Mendoza-Londono R, Mornet E, Brun-Heath I, Squarcioni CP, Legeai-Mallet L, Munnich A, et al. Hyperphosphatasia with seizures, neurologic deficit, and characteristic facial features: Five new patients with Mabry syndrome. Am J Med Genet A. 2010;152A(7):1661–9.
64. Ng BG, Hackmann K, Jones MA, Eroshkin AM, He P, Wiliams R, Bhide S, Cantagrel V, Gleeson JG, Paller AS, et al. Mutations in the Glycosylphosphatidylinositol Gene PIGL Cause CHIME Syndrome. Am J Hum Genet. 2012;90(4):685–8.
65. Almeida AM, Murakami Y, Layton DM, Hillmen P, Sellick GS, Maeda Y, Richards S, Patterson S, Kotsianidis I, Mollica L, et al. Hypomorphic promoter mutation in PIGM causes inherited glycosylphosphatidylinositol deficiency. Nat Med. 2006;12(7):846–51.
66. Davis EM, Kim J, Menasche BL, Sheppard J, Liu X, Tan AC, Shen J. Comparative haploid genetic screens reveal divergent pathways in the biogenesis and trafficking of glycophosphatidylinositol-anchored proteins. Cell Rep. 2015;11(11):1727–36.
67. Muniz M, Riezman H. Trafficking of glycosylphosphatidylinositol anchored proteins from the endoplasmic reticulum to the cell surface. J Lipid Res. 2016;57(3):352–60.

3.3.1 Contribution

The manuscript was submitted on the 2nd of August 2017. The article was accepted on the 11th of December 2017 and published online on the 9th of January 2018 in *Genome Medicine*, Vol. 10, No. 3

The research study was carried out by the first author (Knaus, A.). Krawitz, M. P. and Horn, D. contributed to the design and concept of the work. Pantel, J. T., Hajjir, N. and Pendziwiat, M. assisted in facial data collection. Facial data analysis was performed by Knaus, A., Hsieh, T.-C., and Schubach, M. and was supported by Gurovich, Y. and Fleischer, N. from FDNA. Jäger M. and Köhler S. contributed to variant and phenotype data interpretation. Muhle, H., Korff, C., Møller, R., Bayat, A., Calvas, P., Chassain, N., Warren H., Skinner, S., Loui, R., Evers, C., Bohn, M., Christen, H.-J., van den Bonr, M., Robinson, P. N., Schelhaas, H. J., and Weber, Y. diagnosed the patients, performed clinical assessments, and collected patient samples. The group leaders (Helbig, I. and Mundlos, S.) funded the work, provided resources for the experiments, and assisted in the formation of the manuscript. The manuscript was read, commented, approved by all authors.

3.3.2 Discussion

Analysis of individual data has limited potential to identify genotype phenotype correlation in rare Mendelian disorders. In this multi-centered effort we collected data of novel and published cases of the most prevalent GPIBDs. Detailed phenotypic characterization allowed broadening of the phenotypic spectrum of GPIBDs and revealed a dichotomy between HPMRS and MCAHS. Thereby, a basis for differential diagnosis of individuals suspected for a GPIBD was provided to the community of syndromologists. Further delineation within the phenotypic series was achieved with an accuracy of 52.2% by automated facial analysis using Face2Gene's DeepGestalt algorithm (Gurovich et al., 2018). Although, the similarity of the individuals' gestalt between HPMRS1 and 4 as well as MCAHS1, 2, and 3 resembled the dichotomy in the feature analysis, due to the overlapping clinical spectrum of both HPMRS and MCAHS, the findings of elevated AP, and the reduced surface levels of GPI-APs in

MCAHS cases favor a common classification as GPIBD that should be further delineated on gene level.

The performance of correct gene inference from facial analysis was confounded by ethnicity, age, sex, and an uneven distribution of the data set. To address the latter, a random down sampling and leave one out cross validation was performed that reduced accuracy to 44%, which was still significantly better than random chance (20%).

Due to the rarity of the GPIBDs, suspected individuals are reported across ethnic boundaries and at varying age. Therefore, further research on the major confounding factors of ethnicity and age should be carried out.

Although flow cytometry is the gold standard for functional validation of pathogenic variants in genes of the GPI anchor biosynthesis pathway, the collected data did not reveal a gene characteristic pattern. Different research laboratories use various GPI-linked markers in flow cytometric analysis of blood to assess the functional implication of identified variants. CD16 was commonly used across different studies, as these markers are also analyzed in for PNH diagnosis. Although CD16 shows the highest sensitivity to GPI anchor deficiency, its expression on granulocytes however, may be up-regulated under inflammatory conditions (Kimura et al., 2003; Middelhoven, van Buul, Kleijer, Roos, & Hordijk, 1999; Romee et al., 2013), reducing the specificity of the marker. Analysis of CD55, CD59, and CD66b expression in combination with FLAER is also widely used in diagnosis of PNH (Alfinito et al., 1996; Hill et al., 2017). However, only FLAER was applied in almost all studies on congenitally inherited GPIBDs. Hence, meta-analysis of relative reduction only of CD16 and FLAER expression was possible. The effect of hypomorphic variants that reduce activity in enzymes of the GPI anchor biosynthesis pathway is variable, thus different pathogenic mutations in the same gene probably lead to varying reduction of GPI-AP expression. This fluctuation has been also observed in the collection of fibroblasts from multiple individuals. Nevertheless, a larger collection of GPIBD cases and an extended as well as standardized multicolor flow cytometry panel may reveal a gene specific pattern of reduced marker expression. Potentially, a thorough rescue experimental analysis of a multitude of pathogenic variants per gene in cultured cell lines may provide grounds for a gene specific pattern of flow cytometric results.

Finally, the combination of deep phenotyping, flow cytometry analysis, and NGS add layers of information for the interpretation of variants in genes of the GPI anchor biosynthesis pathway. Facial data can be easily applied in the decision guidance for single gene sequencing, while flow cytometry is inevitable for functional validation.

3.4 Höchsmann *et al.*, Complement- and inflammasome-mediated autoinflammation-paroxysmal nocturnal hemoglobinuria, 2019

Britta Höchsmann, *Yoshiko Murakami*, *Makiko Osato*, ***Alexej Knaus***, *Michi Kawamoto*, *Norimitsu Inoue*, *Tetsuya Hirata*, *Shogo Murata*, *Markus Anliker*, *Thomas Eggerman*, *Severin Dicks*, *Marten Jäger*, *Ricarda Flöttmann*, *Alexander Hoellein*, *Sho Murase*, *Yasutaka Ueda*, *Jun-ichi Nishimura*, *Yuzuru Kanakura*, *Nobuo Kohara*, *Hubert Schrezenmeier*, *Peter M. Krawitz*, and *Taroh Kinoshita*

Published in *Journal of Clinical Investigation*, under the title: **Complement and inflammasome overactivation mediates paroxysmal nocturnal hemoglobinuria with autoinflammation**, 2019 August, pii: 123501. (Epub ahead of print),
doi: https://doi.org/10.1172/JCI123501.

Since the identification of *PIGA* as the cause of PNH (paroxysmal nocturnal hemoglobinuria, Takeda et al.) in 1993 and further elucidation of the genes that act in the formation of the GPI anchor, clinicians and researchers speculated whether PNH might be caused by mutations in any other gene of the GPI anchor biosynthesis pathway. In this work a novel disease entity of PNH with autoinflammatory clinical features has been described through the application of NGS, flow cytometry and intensive molecular analyses. The first patient with wild type *PIGA*, but affected by PNH has been identified by Krawitz et al., twenty years later, followed by a case report by Murakami et al. (2016). Both patients carried a predisposing germline mutation in *PIGT*. The acquisition of a somatic deletion of 8 MB that encompassed the wild type *PIGT* allele caused loss of heterozygosity in a hematopoietic stem cell (HSC). Clinical manifestation of PNH occurred after a growth advantage, leading to clonal expansion, of the *PIGT* deficient HSC followed by differentiation, and generation of mature, GPI transamidase deficient blood cells that lack expression of GPI linked CD55 and CD59. The absence of CD55 and CD59 in turn leads to susceptibility of erythrocytes to the complement system. However, intravascular hemolysis and thrombosis were observed in combination with arthralgia, headache, urticaria, abdominal pain, and diarrhea (Krawitz et al., 2013). Similar symptoms were noted in the Japanese patient, who additionally suffered from frequent aseptic meningitis ac-

companied by massive release of inflammatory cytokines such as IL6, TNF-α and IL1β in the serum (Murakami et al., 2016).

In this work the mechanistic bases of a novel disease entity, autoinflammation PNH (AIF-PNH), in the above-mentioned patients and identification of two novel patients with mutations in *PIGT* was elucidated.

Moreover, inflammasome activation was confirmed by high levels of IL18 in serum and secretion of IL1β, and fragments of the complement cascade in *in vitro* assays from different cultured cell lines. The results showed that free GPI anchor in *PIGT* deficient, but not the absence of the GPI anchor itself (in *PIGA* deficient cells), lead to AIF-PNH.

NGS revealed a large deletion 8 – 18 Mb encompassing the wild type PIGT allele and a common deleted region (CDR) seen in patients with myeloproliferative neoplasms (MPN) and myelodysplastic syndrome (MDS). Loss of the CDR was shown to be causally related to clonal expansion of myeloid cells in these 20q-deletion syndromes (Aziz et al., 2013). Suppressor-like gene *L3MBTL1* and a kinase gene *SGK2* located within the myeloid CDR are expressed only in the paternal allele due to gene imprinting (J. Li et al., 2004). GPI transamidase deficient cells lost the maternal copy of these genes as revealed by bisulfite sequencing and qPCR analysis.

Patients with GPI transamidase deficiency can be detected by flow cytometric analysis using T5 antibody directed against an epitope of the free GPI anchor (Y. Wang et al., 2019). Treatment of the patients with eculizumab, an anti-complement C5 drug, prevented both hemolysis and autoinflammation.

Complement- and inflammasome-mediated autoinflammation-paroxysmal nocturnal hemoglobinuria

Britta Hoechsmann[1+], Yoshiko Murakami[2,3+], Makiko Osato[2,4+], Alexej Knaus[5], Michi Kawamoto[6], Norimitsu Inoue[7], Tetsuya Hirata[2], Shogo Murata[2,8], Markus Anliker[1], Thomas Eggerman[9], Severin Dicks[9], Marten Jaeger[10], Ricarda Floettmann[10], Alexander Hoellein[11], Sho Murase[6], Yasutaka Ueda[4], Jun-ichi Nishimura[4], Yuzuru Kanakura[4], Nobuo Kohara[6], Hubert Schrezenmeier[1*], Peter M. Krawitz[5*], and Taroh Kinoshita[2,3*].

[1] Institute of Transfusion Medicine, University of Ulm and Institute of Clinical Transfusion Medicine and Immunogenetics, German Red Cross Blood Transfusion Service and University Hospital Ulm, Ulm, Germany; [2] Research Institute for Microbial Diseases, Osaka University, Japan; [3] WPI Immunology Frontier Research Center, Osaka University, Japan; [4] Department of Hematology and Oncology, Graduate School of Medicine, Osaka University, Japan; [5] Institute for Genomic Statistics and Bioinformatics, Rheinische Friedrich-Wilhelms-Universität Bonn, Germany; [6] Department of Neurology, Kobe City Medical Center General Hospital, Japan; [7] Department of Tumor Immunology, Osaka International Cancer Institute, Japan; [8] Department of Hematology/Oncology, Wakayama Medical University, Japan; [9] Institute for Human Genetics, RWTH, Aachen, Germany; [10] Department of Medical Genetics, Charite Hospital, University of Berlin, Germany; [11] MLL Muenchner Leukaemielabor GmbH, Munich, Germany.

[+]Equally contributed authors; *equally contributed corresponding authors.

Corresponding authors:

Taroh Kinoshita, PhD.

Yabumoto Department of Intractable Disease Research, Research Institute for Microbial Diseases, Osaka University, 3-1 Yamada-oka, Suita, Osaka 565-0871, Japan

eMail: tkinoshi@biken.osaka-u.ac.jp Tel.: +81-6-6879-8328

Peter M. Krawitz, PhD.

Institute for Genomic Statistics and Bioinformatics, Rheinische Friedrich-Wilhelms-Universität, Sigmund-Freud-Str. 25, 53127 Bonn, Germany

eMail: pkrawitz@uni-bonn.de Tel.: +49-228-287-14799

Hubert Schrezenmeier, MD.

Institute of Transfusion Medicine, University of Ulm and Institute of Clinical Transfusion Medicine and Immunogenetics, German Red Cross Blood Transfusion Service and University Hospital Ulm, Helmholtzstrasse 10, 89081 Ulm, Germany

eMail: h.schrezenmeier@blutspende.de Tel.: +49-731-150-550

Short title: PIGT mutations in autoinflammation-PNH

Category: Red Cells, iron, and Erythropoiesis

Key Points

Autoinflammation-paroxysmal nocturnal hemoglobinuria is characterized by intravascular hemolysis and inflammasome-mediated autoinflammation.

Germline and somatic mutations in *PIGT* cause CD59 deficiency and cell surface display of free glycosylphosphatidylinositol.

Abstract

Paroxysmal nocturnal hemoglobinuria (PNH) is an acquired hematopoietic stem cell disorder characterized by complement-mediated hemolysis and thrombosis, and bone marrow failure. Affected cells harbor a somatic mutation in X-linked *PIGA* gene, essential for the initial step in glycosylphosphatidylinositol (GPI) biosynthesis. A loss of GPI biosynthesis results in the defective cell surface expression of GPI-anchored complement regulators CD59 and DAF/CD55. The affected stem cells generate large numbers of abnormal blood cells after clonal expansion that occurs under bone marrow failure. Here, we report mechanistic bases of a disease entity, autoinflammation - paroxysmal nocturnal hemoglobinuria (AIF-PNH) caused by germline and somatic mutations in *PIGT* localized in chromosome 20q. Consistent with PIGT's essential role in attachment of synthesized GPI to precursor proteins, free GPIs appeared on the surface of PIGT-defective cells. AIF-PNH is characterized by intravascular hemolysis and recurrent autoinflammation, such as urticaria, arthralgia, fever and aseptic meningitis. Eculizumab, an anti-complement C5 drug, prevented both hemolysis and autoinflammation. PIGT-defective cells accumulated higher levels of C3 fragments and C5b-9 complexes, and secreted more IL-1β than PIGA-defective cells after the alternative pathway activation. IL-1β secretion was dependent upon C5b-9 complex. These results suggest that non-protein-linked free GPIs enhance complement activation and inflammasome-mediated IL-1β secretion. The "myeloid common deleted region" implicated in clonal expansion mechanism of 20q- myeloproliferative syndromes was always lost together with *PIGT* from the paternal chromosome 20. Taken together with a lack of bone marrow failure in AIF-PNH, clonal expansion mechanisms in PNH and AIF-PNH appeared to be different.

Introduction

Paroxysmal nocturnal hemoglobinuria (PNH) is an acquired hematopoietic stem cell disorder characterized by complement-mediated hemolysis, thrombosis and bone marrow failure.[1,2] Affected cells harbor a somatic mutation in *PIGA* gene, essential for the initial step in glycosylphosphatidylinositol (GPI) biosynthesis.[3] A loss of GPI biosynthesis results in the defective expression of GPI-anchored proteins (GPI-APs) including complement inhibitors CD59 and DAF/CD55. The affected stem cells generate large numbers of abnormal blood cells after clonal expansion that occurs under bone marrow failure. The affected erythrocytes are defective in complement regulation and destroyed by the membrane attack complex (MAC or C5b-9) upon complement activation.[1] Eculizumab, a humanized anti-complement component 5 (C5) monoclonal antibody (mAb), has been used to prevent intravascular hemolysis and thrombosis.[4,5] Eculizumab binds to C5 and inhibits its activation and

subsequent generation of MAC.

Among more than 20 genes involved in GPI biosynthesis and transfer to proteins, *PIGA* is X-linked whereas all others are autosomal.[6] Because of X-linkage, one somatic mutation in *PIGA* causes GPI deficiency in both males and females.[3] In contrast, two mutations are required for autosomal genes, however a probability of somatic mutations in both alleles at the same locus is extremely low. Here we describe four patients with PNH caused by germline and somatic mutations in *PIGT* gene. Because PIGT acts in transfer of GPI to proteins [7], free GPI remains in PIGT-defective cells. Correspondingly, patients with *PIGT*-defect unusually had complement- and inflammasome-dependent autoinflammation in addition to typical PNH symptoms, representing a distinct disease entity, autoinflammation-paroxysmal nocturnal hemoglobinuria (AIF-PNH).

Methods

Blood samples and flow cytometry

Peripheral blood samples were obtained from patients J1[8], G1[9], G2 and G3 with AIF-PNH, and six patients with PNH after informed consent. Peripheral blood leukocytes (Figure S1**A**), erythrocytes and reticulocytes were stained for GPI-APs. T5-4E10 mAb (T5 mAb) of IgM isotype against free GPI of *Toxoplasma gondii* was a gift from Dr. J. F. Dubremetz[10]. T5 mAb recognizes mammalian free GPI bearing N-acetylgalactosamine (GalNAc) side-chain linked to the first mannose (Figure S1**B**)[11]. T5 mAb does not bind to free GPI when galactose (Gal) is attached to GalNAc. Therefore, reactivity of T5 mAb to free GPI is affected by an expression level of Gal transferase that attaches Gal to the GalNAc. Cells were analyzed by a flow cytometer (MACSQuant Analyzer VYB, Miltenyi Biotec or FACSCalibur, BD) and FlowJo software.

DNA and RNA analyses

Granulocytes with PNH phenotype were separated from normal granulocytes by cell sorting after staining by fluorescence-labeled non-lytic aerolysin (FLAER). DNA was analyzed for mutations in genes involved in GPI-AP biosynthesis by target exome sequencing, followed by confirmation by Sanger sequencing.[9] DNA was also analyzed by array comparative genomic hybridization for deletion.[9] Methylation status of CpG was determined by bisulfite sequencing and a SNuPE assay.[12] Total RNA was extracted with the RNeasy Mini Kit (Qiagen) including DNase digestion and DNA cleanup, and reverse transcription was performed with the SuperScript VILO cDNA Synthesis Kit (Invitrogen). Levels of *L3MBTL1*, *SGK2*, *IFT52*, *MYBL2, ABL* and *GAPDH* mRNAs were analyzed by quantitative real-time PCR (Table S1).

Cell lines

PIGT-defective Chinese hamster ovary (CHO) cells and *PIGL*-defective CHO cells were derived from CHOK1 (ATCC) cells and reported previously.[13,14] CRISPR/Cas 9 system was used to generate *PIGT* and *PIGA* knockout (KO) human monocytic THP-1 cells (ATCC) (Table S1 for guide RNA sequences). KO cells were FACS sorted for

GPI-AP negative cells. Each knockout cell was rescued by transfection of a corresponding cDNA. *SLC35A2* gene was knocked out in PIGTKO THP-1 cells by CRISPR/Cas9 system.

Inflammasome activation and IL1β measurements

Toll-like receptor 2 (TLR2) ligands, Pam_3CSK4 and *Staphylococcus aureus* lipoteichoic acid (LTA), are from InvivoGen.[15,16] ATP and monosodium urate (MSU) for activating inflammasomes are from Enzo Life Sciences and InvivoGen.[15,17] Peripheral blood mononuclear cells were stimulated by Pam_3CSK4 or LTA for 4 hr at 37℃ and after washing by ATP or MSU for 4 hr at 37℃. IL1β ELISA kit (BioLegend) was used to measure IL1β secreted into the supernatants. Polyclonal rabbit anti-IL1β antibody for western blotting was from Cell Signaling Technology. PIGAKO, PIGTKO and wild-type THP-1 cells were differentiated into adherent macrophages in complete RPMI 1640 medium containing 100 ng/ml phorbol 12-myristate 13-acetate (PMA; InvivoGen) for 3 hr, and then with fresh complete medium for overnight.[18] For stimulation, medium was replaced with serum free medium with Pam_3CSK_4 (200 ng/ml), followed 4hr-later by ATP stimulation for 4 hr (5 mM).

Stimulation of THP-1-derived macrophages with complement

As a source of complement, whole blood was collected from healthy donors after informed consent, and serum separated, aliquoted and stored at -80°C prior to use. Inactivation of complement was carried out by heating serum at 56°C for 30 min. To prepare acidified serum (AS) that allows activation of the alternative pathway on the cell surface, 21 volumes of serum was mixed with 1 volume of 0.4 M HCl to have pH of approximately 6.7. C6- and C7-depleted sera and purified C6 and C7 proteins were purchased from Complement Technology. Differentiated cells were stimulated with acidified normal serum, or acidified C6-depleted and C7-depleted sera, and those reconstituted with C6 and C7, respectively, at 37°C for 5hr and secreted IL1β was measured by ELISA. C5 was inhibited by addition of 35 μg/ml anti-C5 mAb (eculizumab, Alexion Pharmaceuticals).

For ex vivo blockade of human C5aR, anti-human C5aR (CD88) or nonpeptide C5aR antagonist W-54011 (5 μM, Merck Millipore)[19] was used. Complement C3 fragments and MAC deposited on the cells were measured by flow cytometry. THP-1 cells were suspended in 20 μl FACS buffer (PBS, 1% BSA, 0.05% sodium azide) with 1:20 human TruStain FcX™ (Fc receptor blocking solution) at room temperature for 10 min. Cells were stained with anti-complement C3/C3b/iC3b/C3d mAb (clone 1H8, BioLegend) or rabbit anti-human SC5b-9 (MAC) polyclonal antibodies (Complement Technology) in FACS buffer. After washing twice, cells were incubated with the PE-conjugated goat anti-mouse IgG (BioLegend) or Alexa Fluor488-conjugated goat anti-rabbit IgG (Thermo Fisher) secondary antibody. The anti-human SC5b-9 polyclonal antibodies positively stained PMA-differentiated THP-1 cells without incubation in AS. The same antibodies did not stain similarly differentiated PIGTKO and PIGAKO THP-1 cells, suggesting that the antibody product contained antibodies reacted with some GPI-AP expressed on THP-1-derived macrophages (Figure S8**B**, **C**). Because of this reactivity to non-MAC antigen(s), the anti-SC5b-9 antibodies were used for PIGTKO and PIGAKO cells but not for WT cells in experiments shown in Figure 5**D** and **F**.

Statistical analyses

All experiments with THP-1 cells were performed at least three times. All values were expressed as the mean ± SD of individual samples. For two-group comparisons between PIGTKO and PIGAKO cells, Student's *t*-test was used. *P* values below 0.05 were considered statistically significant.

Study approval

This study was approved by institutional review boards of Osaka University (approval number 681), University of Ulm (approval numbers 279/09 and 188/16) and University of Berlin (approval number EA2/077/12).

Data Sharing Statement

All data supporting the findings are available from the corresponding authors.

Results

Case Report

Japanese patient J1[8], and German patients G1[9], G2 and G3 were diagnosed as PNH at ages of 68, 49, 65 and 66, respectively. Changes in PNH clone sizes in J1, G1 and G3 after PNH diagnosis are shown in Figure 1**A**. They were treated with eculizumab with effective prevention of intravascular hemolysis. Blood cell counts for G1 and G3 are shown in Figure S1**C**. Before diagnosis of PNH, J1, G1 and G3 had inflammatory symptoms including urticaria, arthralgia and fever since ages of 30, 26 and 48, respectively (Table 1). Urticaria in J1 was associated with neutrophil infiltration[8] and in G3 with a mixed inflammatory infiltrate (Figure 1**B**). J1[8] and G3 suffered from recurrent aseptic meningitis characterized by neutrophil dominant cerebrospinal fluid. After eculizumab treatment began 3–5 years ago for hemolysis, J1[8] and G3 had no episode of meningitis (Figure 1**C**). Urticaria and arthralgia were also settled in all three by eculizumab treatment. Whether G2 had autoinflammatory symptoms is unclear and is not able to confirm because the patient deceased.

Genetic basis of GPI-AP deficiency

Four patients did not have *PIGA* somatic mutations but had a germline mutation in one allele of *PIGT* located in chromosome 20q: J1, NM_015937: c.250G>T; G1, c.1401-2A>G; G2, c.761_764delGAAA; and G3, c.197delA (Figure S2**A**). They cause E84X, exon 11 skipping, frame-shift after G254 and frame-shift after Y66, respectively. Functional activities of variant *PIGT* found in J1 and G1 were reported to be very low.[9,13] Variants in G2 and G3 causing frame-shifts should also be severely deleterious to PIGT function. In addition to the germline *PIGT* mutation, all four had in the other allele a somatic 8 Mb to 18 Mb deletion that includes entire *PIGT* gene (Figure S2**B**). [8,9] Therefore, in contrast to GPI-AP-deficiency caused by single *PIGA* somatic mutation in PNH, GPI-AP-deficiency in all four is caused by a combination of a germline loss-of-function *PIGT* mutation and a somatic loss of entire *PIGT* in hematopoietic stem cells (Figure 2**A**).

A possible mechanism of clonal expansion in AIF-PNH

Deletion of chromosome 20q represents the most common chromosomal abnormality associated with the myeloproliferative disorders. The 8 Mb to 18 Mb deleted region included a "myeloid common deleted region (CDR)"[20] (Figure 2**A**). A fraction (approximately 10 %) of patients with myeloproliferative neoplasm (MPN) such as polycythemia vera commonly have a 2.7 Mb deletion in chromosome 20q.[20] A fraction (approximately 4 %) of patients with myelodysplastic syndrome (MDS) also have a 2.6 Mb deletion in this region.[20] The CDR region shared by MPN and MDS spanning approximately 1.9 Mb has been called "myeloid CDR" (Figure 2**B**) and its loss was shown to be causally related to clonal expansion of the affected myeloid cells in these 20q$^-$ syndromes.[12] In contrast to previous cytogenetic analysis on classical PNH cases that showed no aberrations on 20q[21,22], one allele of the myeloid CDR was lost in PNH cells of all four patients (Figure S2**B**). [8,9]

A tumor suppressor-like gene *L3MBTL1* and a kinase gene *SGK2* located within the myeloid CDR (Figure 2**A**,**B**) are expressed only in the paternal allele due to gene imprinting.[23] It was shown that losses of active paternal alleles of these two genes had a causal relationship with clonal expansion of these 20q$^-$ myeloid cells.[12] *L3MBTL1* and *SGK2* transcripts were undetectable in GPI-AP-defective granulocytes from J1 and extremely low in whole blood cells from G1 whereas they were found in granulocytes from healthy individuals (Figure 2**C**). Transcripts of two non-imprinted genes *IFT52* and *MYBL2* were detected in both GPI-AP-defective granulocytes from J1 and normal granulocytes (Figure 2**C**, top). The results therefore indicate that expression of *L3MBTL1* and *SGK2* are lost in GPI-AP-defective cells in J1 and G1.

The results shown in Figure 2**C** also indicate that the somatically deleted region in J1 and G1 included active *L3MBTL1* and *SGK2*, hence was in the paternal chromosome. Due to unavailability of mRNA from patients G2 and G3, we determined the methylation status of *L3MBTL1* gene using DNA from blood leukocytes, in which the large majority of cells were of PNH phenotype. *L3MBTL1* in G1 and G3 samples were hypermethylated (Figure 2**D** and Figure S3**A**), indicating that the myeloid CDR allele remaining in their PNH clones were imprinted. In contrast G2 sample was hypomethylated. It was reported that in some MPN patients with myeloid CDR deletion, the remained allele was hypomethylated, nevertheless, its transcription was suppressed.[12] G2 might be in a similar situation although it was not possible to draw a definitive conclusion by RT-PCR analysis as the patient deceased. These results indicate that the loss of expressed myeloid CDR allele is associated with clonal expansion of *PIGT*-defective cells similar to 20q- MPN and MDS.

Appearance of free GPI on the surface of PIGT-defective cells

PIGA is required for the first step in GPI biosynthesis[24], therefore no GPI intermediate is generated in *PIGA*-defective cells (Figure 3**A**, middle). *PIGT* is involved in attachment of GPI to proteins. GPI is synthesized in the endoplasmic reticulum but is not used as protein anchors in *PIGT*-defective cells (Figure 3**A**, bottom). We used T5 mAb that recognizes free GPI, but not protein-bound GPI, as a probe to determine a fate of the unused free GPI

(see Methods for epitope and other characteristics of this antibody).[10,11] Using T5 mAb we analyzed *PIGT*-defective CHO cells by western blotting and flow cytometry. T5 mAb revealed a strong band of free GPI at around 10 kDa position in lysates of *PIGT*-defective cells (Figure 3**B**). Free GPI was not detected in lysates of *PIGL*-defective cells used as a reference instead of *PIGA*-defective cells (PIGL acts next to PIGA). DAF and CD59 were not detected in either mutant cells, confirming that un-GPI-anchored precursor proteins were degraded (Figure 3**B**).[25] T5 mAb stained *PIGT*-defective CHO cells strongly, indicating that free GPI is transported to the cell surface (Figure 3**C**). As expected, T5 mAb did not stain *PIGL*-defective CHO cells that do not generate free GPI reactive to T5 mAb.

We next analyzed blood cells from J1, G1 and G3, and from patients with *PIGA*-PNH by flow cytometry. All four patients had PNH-type blood cells defective in various GPI-APs (Figure 3**D**, **E**, **F** and Figure S4**A**, **B**). Erythrocytes from J1, G1 and G3 contained 3%, 84% and 60% of PNH cells, respectively and a sizable fraction of them (36%, 87% and 87%, respectively) were stained by T5 mAb (Figure 3**D**). J1 had PNH cells in granulocytes (81%), monocytes (87%) and B-lymphocytes (54%) but not T-lymphocytes (<2%) as revealed by anti-CD59 and GPI-binding probe FLAER. Affected monocytes and B-lymphocytes were strongly stained by T5 mAb whereas affected granulocytes were weakly but clearly stained (Figures 3**E** and S4**B**). Normal populations in granulocytes, monocytes and B-lymphocytes were not stained by T5 mAb (Figure 3**E**). Similar results, showing strong T5 staining of affected monocytes and granulocytes, were obtained with leukocytes from G1 and G3 (Figure 3**F**). In contrast, PNH cells from *PIGA*-PNH patients and cells from healthy individuals were not positively stained by T5 mAb (Figures 3**E**, **F**). A small fraction of wild-type erythrocytes from J1, G1 and G3 (0.13, 9.7 and 9.5%, respectively) were positively stained by T5 mAb (Figure 3**D**). Free GPI might be transferred from PNH erythrocytes to wild-type erythrocytes in vivo[26,27] although an exact mechanism needs to be clarified. Thus, the surface expression of T5 mAb epitope is specific for *PIGT*-defective cells and T5 mAb is useful to diagnose AIF-PNH.

We then asked whether GPI-AP-defective clone existed in the stage with autoinflammation only. After determining the break points causing the 18 Mbp deletion in J1 (Figure S5), we quantitatively analyzed blood DNA samples for the presence of the break. It was estimated that approximately 3% of total leukocytes obtained four months before the onset of recurrent hemolysis had the break, i.e., were GPI-AP-defective cells (Figure 3**G**).

Inflammasome- and complement-mediated autoinflammation, a feature of AIF-PNH

IL18 levels were elevated in serum samples taken from J1 before and after commencement of eculizumab therapy (Table 2), suggesting a complement-independent phenomenon. Serum amyloid A was also elevated before eculizumab therapy but was within normal range after commencement of eculizumab therapy (Table 2), suggesting the elevation was complement-dependent. In G3, increased levels of soluble IL2-receptor and thymidine kinase before, but not after, start of eculizumab therapy suggested autoinflammation (Table 2). Serum amyloid A (up to 10.5 μg/ml; normal range <5 μg/ml) was also elevated. Combination therapies of prednisolone with anakinra, an IL1 receptor antagonist, or canakinumab, a mAb against IL1β, were effective in reducing

urticaria（but not arthralgia and meningitis episodes） of G3. In G1, IL18 level was above normal range during eculizumab therapy (195 pg/ml; normal range <150 pg/ml). These lines of evidence suggest that autoinflammatory symptoms are associated with inflammasome activation. We also measured IL18, serum amyloid A and LDH in serum samples from 4 patients with *PIGA*-PNH who were not with eculizumab therapy. Levels of IL18 (263−443 pg/ml; normal range <211 pg/ml) and serum amyloid A (5.0−8.3 μg/ml) were within or slightly higher than the normal ranges whereas LDH levels were much elevated (Table 2). These results suggest that autoinflammation is a feature of AIF-PNH.

We next compared mononuclear cells from J1, patients with *PIGA*-PNH and healthy donors for IL1β production upon stimulation by NLRP3-inflammasome activators.[15] Cells from three *PIGA*-PNH patients secreted only very low IL1β after stimulation by Pam_3CSK4 (TLR2 ligand) and ATP or MSU (Figure 4**A** right and 4**B**). In contrast, cells from J1 secreted 45- to 60-times as much IL1β and the levels were even higher than those from healthy control cells (Figure 4**A** left and 4**B**). Similar difference between PIGT- and PIGA-defective cells was seen upon stimulation by LTA (another TLR2 ligand) and ATP or MSU (Figure 4**B**). Low IL1β response of PIGA-defective cells was predicted because they lack CD14, a GPI-anchored co-receptor of TLRs. However, PIGT-defective cells also lacking CD14 showed strong IL1β response. These results indicate that NLRP3-inflammasomes are easily activated and support the idea that the presence of non-protein-linked free GPI is associated with efficient activation of NLRP3-inflammasomes, contributing to autoinflammatory symptoms in AIF-PNH.

To investigate roles of complement in inflammasome activation in AIF-PNH, we switched to a model cell system because patients' blood cells were easily damaged in vitro under complement activation conditions. PIGTKO and PIGAKO cells were generated from human monocytic THP-1 cells (Figure S6**A**) and were differentiated to macrophages. They showed comparable IL1β response to authentic inflammasome activators (Figure S6**B**). To analyze inflammasome response to activated complement, these THP-1-derived macrophages were stimulated with AS in that the alternative complement pathway is activated. PIGTKO and PIGAKO cells but not WT cells secreted IL1β (1221.8±91.6, 568.2±101 and 23.7±2.2 pg/ml for PIGTKO, PIGAKO and WT cells, respectively) (Figure 5**A**). This result is consistent with impaired complement regulatory activities on PIGTKO and PIGAKO cells, and normal complement regulatory activity on WT cells. PIGTKO cells secreted approximately 2-fold more IL1β than PIGAKO cells (p<0.01). IL1β production returned near to WT cell levels after transfection of *PIGT* and *PIGA* cDNAs into PIGTKO and PIGAKO cells, respectively (Figure 5**B**). Levels of IL1β mRNA and protein were comparable in WT, PIGTKO and PIGAKO cells (Figure S7**A** and S7**B**). Therefore, PIGT KO enhanced secretion but not generation of IL1β.

Heat-inactivation of complement and an addition of anti-C5 mAb to AS almost completely inhibited IL1β secretion (Figure 5**A**). These results indicate that IL1β secretion requires activation of C5 on PIGTKO and PIGAKO cells. Activation of C5 leads to two biologically active products, C5a and MAC.[28] To address which of them is important for IL1β secretion, cells were treated with C5aR antagonist W-54011[19] or anti-C5aR mAb to inhibit the signal

transduction through C5aR. WT, PIGTKO and PIGAKO cells expressed C5aR at similar levels (Figure S7**C**). Two ways of functional inhibition of C5aR had little effect on IL1β secretion, indicating that the signal through C5aR plays no major role in this cell system (Figure 5**C**). Next, AS treated cells were analyzed for surface binding of C3b fragments and MAC. Exposure to AS resulted in the higher binding of C3b fragments and MAC on PIGTKO cells compared to PIGAKO cells (Figure 5**D** and Figure S8**A**, **B**). The level of MAC was several times higher on PIGTKO cells than PIGAKO cells, suggesting that complement activation was enhanced leading to enhanced formation of MAC on PIGTKO cells. To confirm the role of MAC in IL1β secretion, PIGTKO cells were treated with acidified C6- and C7-depleted sera, in which C5a generation is intact whereas the MAC formation is impaired. IL1β secretion was greatly reduced by C6 or C7 depletion and was restored by replenishment of C6 or C7 (Figure 5**E**). These results suggest that the MAC but not C5a plays a critical role in secretion of IL1β. It is also suggested that free GPI plays some role in complement activation leading to enhanced binding of C3b fragments and MAC formation.

Finally, to see whether the structure of free GPI (presence or absence of Gal capping) affects complement activation and subsequent IL1β secretion, we knocked out SLC35A2 in PIGTKO THP-1 cells. PIGT-SLC35A2 double KO THP-1 cells were strongly stained by T5 mAb as expected (Figure S6**C**). Both bindings of C3 fragments and MAC increased approximately 5-times after SLC35A2 KO (Figure 5**F**). Concomitantly, secretion of IL1β increased more than twice (Figure 5**G**). These results indicate that structure of free GPI influenced complement activation efficiency and subsequent IL1β secretion.

Discussion

We report patients with PNH caused by *PIGT* mutations and propose that they represent a disease entity, AIF-PNH. AIF-PNH caused by *PIGT* mutations is distinct from PNH in four points. First, GPI-AP deficiency in PNH is caused by somatic mutations of X-linked *PIGA* gene in hematopoietic stem cells whereas GPI-AP deficiency in AIF-PNH is caused by a germline mutation in *PIGT* gene on chromosome 20q in combination with a somatic deletion of the entire *PIGT* gene in hematopoietic stem cells. Second, *PIGA*-mutations cause a defect in the initial step in GPI biosynthesis whereas *PIGT*-mutations cause a defect in transfer of preassembled GPI to proteins. Therefore, free GPI remains in *PIGT*-defective cells but not in *PIGA*-defective cells. Third, expansion of *PIGA*-defective clone in PNH is caused by selective survival under autoimmune bone marrow failure with or without acquisition of benign tumor characteristics by additional somatic mutations (Figure S3**B**).[29-32] In contrast, none of the patients with AIF-PNH had documented bone marrow failure (Figure S1**C**).[8,9] In addition, the myeloid CDR is lost in *PIGT*-defective clone in AIF-PNH similar to the clonal cells in myeloproliferative 20q- syndromes associated with a loss of the myeloid CDR. The causal relation between the myeloid CDR loss in AIF-PNH and the clonal expansion needs to be proven, particularly because boosted lineages under L3MBTL1 and SGK2 loss are different between in vitro study[12] and AIF-PNH patients. Nevertheless, this unique deletion occurs in AIF-PNH but not in PIGA-PNH. Taken together, clonal expansion mechanism for AIF-PNH seems to be distinct from that

for *PIGA*-PNH cells. Fourth, whereas AIF-PNH shares intravascular hemolysis and thrombosis with PNH, AIF-PNH is characterized by autoinflammatory symptoms including recurrent urticaria, arthralgia and aseptic meningitis. AIF-PNH was first manifested with autoinflammatory symptoms alone and symptoms of PNH became apparent many years later. Perhaps, different clinical symptoms appear depending on the size of *PIGT*-defective clone. When the clone size is small, autoinflammation but not PNH may occur and when a clone size becomes sufficiently large, PNH may become apparent. It is important to consider GPI-AP-deficiency for patients with autoinflammatory symptoms because eculizumab may be effective.

Inflammatory symptoms, recurrent urticaria, arthralgia, fever and especially meningitis, seen in AIF-PNH are shared by children with cryopyrinopathies or cryopyrin-associated periodic syndrome (reviewed by Neven et al[33]). Cryopyrinopathies are caused by a gain-of-function mutation in *NLRP3* that leads to easy activation of NLRP3-inflammasomes in monocytes and autoinflammatory symptoms[33], further supporting that inflammasomes are activated in monocytes from AIF-PNH patients. It was reported that autoinflammation occurs in patients having mosaicism with *NLRP3*-mutant cells even when a mutant clone size is small.[34] This is relevant to the symptoms-clone size relationship in AIF-PNH. The idea that a size of *PIGT*-defective clone is small when only the autoinflammation is seen was supported by analyzing J1 DNA obtained before the start of recurrent hemolysis (Figure 3G).

C5 activation must be involved in the autoinflammatory symptoms in AIF-PNH because they were suppressed by eculizumab. Involvement of complement in inflammasome activation has been shown in various blood cell systems.[35-38] Because DAF and CD59 are missing on *PIGT*-defective monocytes, C5a and MAC might be generated, once complement activation is initiated. Indeed, in the THP-1 cell model system, IL1β secretion was induced by complement in both PIGTKO and PIGAKO cells and more strongly in PIGTKO cells mainly through MAC formation. It appeared that complement activation is enhanced in PIGTKO cells although a mechanism is unclear. AIF-PNH mononuclear cells were activated by conventional stimulators of inflammasomes similar to or even stronger than healthy control cells. Because blood mononuclear cells were easily lysed by acidified serum and the effect of complement on inflammasome activation in mononuclear cells could not be addressed. Together with the results of THP-1 cells, we speculate that *PIGT*-deficient monocytes show enhanced inflammasome response when complement is activated. How free GPI is involved in inflammasome and complement activation needs to be clarified to fully understand mechanistic basis of AIF-PNH.

Acknowledgments

We thank Drs. Morihisa Fujita (Jiangnan University), Tatsutoshi Nakahata (Kyoto University), Hidenori Ohnishi (Gifu University), Tatsuya Saitoh (Tokushima University) and Yusuke Maeda (Osaka University) for discussion, Dr. Jean-Francois Dubremetz (Montpellier University) for T5-4E10 mAb, and Keiko Kinoshita, Kana Miyanagi, Saori Umeshita and Miguel Rodriguez de los Santos for technical help and Dr. med. Lisa A. Gerdes (Munich University) for collaboration regarding patients G3 as well as the patients for providing blood samples and

pictures. This work was supported by JSPS and MEXT KAKENHI grants (JP16H04753 and JP17H06422) and a grant from the Japan Society of Complement Research.

Authorship Contributions

BH, YM, NI, HS, PMK, and TK designed the study. YM, MO, AK, TH, Shogo M, TE, SD, MJ, RF, and AH conducted experiments. BH, MK, MA, Sho M, YU, and NK acquired the data. BH, YM, MO, MK, JN, YK, NK, HS, and PMK analyzed the data. BH, YM, MO, HS, PMK, and TK wrote the manuscript.

Conflict-of-interest statements

The authors have declared that no conflict of interest exists.

References

1. Parker C, Omine M, Richards S, et al. Diagnosis and management of paroxysmal nocturnal hemoglobinuria. *Blood*. 2005;106(12):3699-3709.

2. Hill A, DeZern AE, Kinoshita T, Brodsky RA. Paroxysmal nocturnal haemoglobinuria. *Nat Rev Dis Primers*. 2017;3:17028.

3. Takeda J, Miyata T, Kawagoe K, et al. Deficiency of the GPI anchor caused by a somatic mutation of the PIG-A gene in paroxysmal nocturnal hemoglobinuria. *Cell*. 1993;73:703-711.

4. Hillmen P, Young NS, Schubert J, et al. The complement inhibitor eculizumab in paroxysmal nocturnal hemoglobinuria. *N Engl J Med*. 2006;355(12):1233-1243.

5. Hillmen P, Muus P, Roth A, et al. Long-term safety and efficacy of sustained eculizumab treatment in patients with paroxysmal nocturnal haemoglobinuria. *Br J Haematol*. 2013;162(1):62-73.

6. Kinoshita T. Biosynthesis and deficiencies of glycosylphosphatidylinositol. *Proc Jpn Acad Ser B Phys Biol Sci*. 2014;90(4):130-143.

7. Ohishi K, Inoue N, Kinoshita T. PIG-S and PIG-T, essential for GPI anchor attachment to proteins, form a complex with GAA1 and GPI8. *EMBO J*. 2001;20:4088-4098.

8. Kawamoto M, Murakami Y, Kinoshita T, Kohara N. Recurrent aseptic meningitis with PIGT mutations: a novel pathogenesis of recurrent meningitis successfully treated by eculizumab. *BMJ Case Rep*. 2018;2018.

9. Krawitz PM, Hochsmann B, Murakami Y, et al. A case of paroxysmal nocturnal hemoglobinuria caused by a germline mutation and a somatic mutation in PIGT. *Blood*. 2013;122(7):1312-1315.

10. Tomavo S, Couvreur G, Leriche MA, et al. Immunolocalization and characterization of the low molecular weight antigen (4-5 kDa) of Toxoplasma gondii that elicits an early IgM response upon primary infection. *Parasitology*. 1994;108 (Pt 2):139-145.

11. Hirata T, Mishra SK, Nakamura S, et al. Identification of a Golgi GPI-N-acetylgalactosamine transferase with tandem transmembrane regions in the catalytic domain. *Nat Commun*. 2018;9(1):405.

12. Aziz A, Baxter EJ, Edwards C, et al. Cooperativity of imprinted genes inactivated by acquired chromosome 20q deletions. *J Clin Invest*. 2013;123(5):2169-2182.

13. Nakashima M, Kashii H, Murakami Y, et al. Novel compound heterozygous PIGT mutations caused multiple congenital anomalies-hypotonia-seizures syndrome 3. *Neurogenetics*. 2014;15(3):193-200.

14. Nakamura N, Inoue N, Watanabe R, et al. Expression cloning of PIG-L, a candidate N-acetylglucosaminyl-phosphatidylinositol deacetylase. *J Biol Chem*. 1997;272:15834-15840.

15. Parzych K, Zetterqvist AV, Wright WR, Kirkby NS, Mitchell JA, Paul-Clark MJ. Differential role of pannexin-1/ATP/P2X7 axis in IL-1beta release by human monocytes. *FASEB J*. 2017.

16. Morath S, Geyer A, Hartung T. Structure-function relationship of cytokine induction by lipoteichoic acid from Staphylococcus aureus. *J Exp Med*. 2001;193(3):393-397.

17. Martinon F, Petrilli V, Mayor A, Tardivel A, Tschopp J. Gout-associated uric acid crystals activate the NALP3 inflammasome. *Nature*. 2006;440(7081):237-241.

18. Zhou R, Yazdi AS, Menu P, Tschopp J. A role for mitochondria in NLRP3 inflammasome activation. *Nature*. 2011;469(7329):221-225.

19. Sumichika H, Sakata K, Sato N, et al. Identification of a potent and orally active non-peptide C5a receptor antagonist. *J Biol Chem*. 2002;277(51):49403-49407.

20. Bench AJ, Nacheva EP, Hood TL, et al. Chromosome 20 deletions in myeloid malignancies: reduction of the common deleted region, generation of a PAC/BAC contig and identification of candidate genes. UK Cancer Cytogenetics Group (UKCCG). *Oncogene*. 2000;19(34):3902-3913.

21. Araten DJ, Swirsky D, Karadimitris A, et al. Cytogenetic and morphological abnormalities in paroxysmal nocturnal haemoglobinuria. *Br J Haematol*. 2001;115(2):360-368.

22. Sloand EM, Fuhrer M, Keyvanfar K, et al. Cytogenetic abnormalities in paroxysmal nocturnal haemoglobinuria usually occur in haematopoietic cells that are glycosylphosphatidylinositol-anchored protein (GPI-AP) positive. *Br J Haematol*. 2003;123(1):173-176.

23. Li J, Bench AJ, Vassiliou GS, Fourouclas N, Ferguson-Smith AC, Green AR. Imprinting of the human L3MBTL gene, a polycomb family member located in a region of chromosome 20 deleted in human myeloid malignancies. *Proc Natl Acad Sci U S A*. 2004;101(19):7341-7346.

24. Miyata T, Takeda J, Iida Y, et al. Cloning of PIG-A, a component in the early step of GPI-anchor biosynthesis. *Science*. 1993;259:1318-1320.

25. Murakami Y, Kanzawa N, Saito K, et al. Mechanism for release of alkaline phosphatase caused by glycosylphosphatidylinositol deficiency in patients with hyperphosphatasia mental retardation syndrome. *J Biol Chem*. 2012;287(9):6318-6325.

26. Kooyman DL, Byrne GW, McClellan S, et al. In vivo transfer of GPI-linked complement restriction factors from erythrocytes to the endothelium. *Science*. 1995;269:89-92.

27. Dunn DE, Yu J, Nagarajan S, et al. A knock-out model of paroxysmal nocturnal hemoglobinuria: Pig-a-hematopoiesis is reconstituted following intercellular transfer of GPI-anchored proteins. *Proc Natl Acad Sci USA*. 1996;93:7938-7943.

28. Ricklin D, Hajishengallis G, Yang K, Lambris JD. Complement: a key system for immune surveillance and homeostasis. *Nat Immunol*. 2010;11(9):785-797.

29. Rotoli B, Luzzatto L. Paroxysmal nocturnal hemoglobinuria. *Seminars in Hematology*. 1989;26:201-207.

30. Young NS. The problem of clonality in aplastic anemia: Dr Dameshek's riddle, restated. *Blood*. 1992;79:1385-1392.

31. Inoue N, Izui-Sarumaru T, Murakami Y, et al. Molecular basis of clonal expansion of hematopoiesis in 2 patients with paroxysmal nocturnal hemoglobinuria (PNH). *Blood*. 2006;108(13):4232-4236.

32. Shen W, Clemente MJ, Hosono N, et al. Deep sequencing reveals stepwise mutation acquisition in paroxysmal nocturnal hemoglobinuria. *J Clin Invest*. 2014;124(10):4529-4538.

33. Neven B, Prieur AM, Quartier dit Maire P. Cryopyrinopathies: update on pathogenesis and treatment. *Nat Clin Pract Rheumatol*. 2008;4(9):481-489.

34. Saito M, Nishikomori R, Kambe N, et al. Disease-associated CIAS1 mutations induce monocyte death, revealing low-level mosaicism in mutation-negative cryopyrin-associated periodic syndrome patients. *Blood*. 2008;111(4):2132-2141.

35. An LL, Mehta P, Xu L, et al. Complement C5a potentiates uric acid crystal-induced IL-1beta production. *Eur J Immunol*. 2014;44(12):3669-3679.

36. Samstad EO, Niyonzima N, Nymo S, et al. Cholesterol crystals induce complement-dependent inflammasome activation and cytokine release. *J Immunol*. 2014;192(6):2837-2845.

37. Laudisi F, Spreafico R, Evrard M, et al. Cutting edge: the NLRP3 inflammasome links complement-mediated inflammation and IL-1beta release. *J Immunol*. 2013;191(3):1006-1010.

38. Arbore G, West EE, Spolski R, et al. T helper 1 immunity requires complement-driven NLRP3 inflammasome activity in CD4(+) T cells. *Science*. 2016;352(6292):aad1210.

39. Kohashi K, Ishiyama A, Yuasa S, et al. Epileptic apnea in a patient with inherited glycosylphosphatidylinositol anchor deficiency and PIGT mutations. *Brain Dev*. 2018;40(1):53-57.

Table 1. Summary of clinical and genetic findings

	J1[1]	**G1**[2]	**G2**[3]	**G3**[4]
Age at diagnosis of PNH	68	49	65	66
Gender	Male	Female	Male	Male
Origin	Japanese	Caucasian	Caucasian	Caucasian
Signs and symptoms (age of onset)				
Urticaria	+ (30)[5]	+ (26)		+ (48)
Arthralgia	+ (30)	+ (27)		+ (61)
Myalgia		+ (27)		+ (61)
Aseptic meningitis	+ (53)			+ (61)
Fever	+ (53)			+ (61)
Headache	+ (53)	+ [6]		
Intravascular hemolysis	+ (67)	+ (44)[7]	+	+ (61)[8]
Abdominal pain				
Ulcerative colitis		+ (39) + (52)[9]		+ (61)
Previous therapy	Corticosteroids Colchicine (for symptoms of autoinflammation)	Corticosteroids Diphenhydramine Cromoglycin Azathioprine (for symptoms of autoinflammation)	Corticosteroids (for residual hemolysis after start of eculizumab)	Corticosteroids Mycophenolate mofetil Dapsone Anakinra Canakinumab (for symptoms of autoinflammation)
Eculizumab	+ (69)	+ (52)	+ (66)	+ (66)
M[10] allele of *PIGT*	c.250G>T[11][12] (p.E84*)	c.1401-2A>G (exon 11 del)	c.761_764delGAAA[13] (p.G254fs)	c.197delA[13] (p.Y66fs)
P[10] allele of *PIGT*	Entire deletion (18 Mb) [14]	Entire deletion (8 Mb)	Entire deletion (12Mb) [13][14]	Entire deletion (15 Mb) [13]

[1] J1 had recurrent urticaria and arthralgia since 30 years of age. At 53 years of age, he had first aseptic meningitis and since then had meningitis several times a year. A cerebrospinal fluid sample taken during an episode of meningitis had approximately 2,000 polymorphonuclear leukocytes per microliter. Since 58 years of age, frequencies of meningitis increased to twice a month. At 67 years of age, intravascular hemolysis was first noted. His white blood cell counts during asymptomatic period and after commencement of eculizumab therapy

were within a normal range. Refer to Kawamoto M et al., *BMJ Case Rep.* 2018;2018[8] for more detailed description of J1.

2) Refer to Supplemental Data in Krawitz PM et al., Blood 2013; 122:1312-1315[9] for detailed description of G1.

3) 96% of granulocytes and 19% of erythrocytes of G2 were GPI-AP-defective. Additional diagnosis and symptoms: Coronary heart disease, myocardial infarction (49 years); recurrent left brain transient ischemic attacks (66 years), recurrent confusion symptoms, disturbance of memory; cholecystectomy (43 years) in the following years remitting cholangitis; elevation of indirect bilirubin; B chronic lymphocytic leukemia (64 years), treatment with rituximab (Whether leukemic cells were from PNH clone was not known.); hemochromatosis (compound heterozygous), diagnosed at age of 66 because of elevation of ferritin, prostate adenoma. The patient died for cardiac decompensation with fulminant pulmonal edema and massive general arteriosclerosis with ulcerated plaques.

4) Additional diagnosis and symptoms of G3: Cholecystolithiasis (65 years); metabolic syndrome with obesity, diabetes and dyslipoproteinemia; sensorineural hearing loss (61 years); peripheral arterial occlusive disease; JAK2 V617F mutation (age of 66)(Whether the mutation occurred in PNH clone was not known.), neurinoma left side (52 years), increasingly personality changes and disturbance of memory since the beginning of the meningitis episodes until start of eculizumab.

5) Numbers in parentheses indicate age when the symptom first recognized or eculizumab treatment started.

6) Headache often occurred associated with urticaria (first urticaria, followed by severe headache).

7) First time of significantly elevated lactate dehydrogenase (LDH).[9]

8) Patient reported on dark urine (panel d of Figure 1**B**).

9) G1 developed ulcerative colitis/proctitis about 5 years after diagnosis of PNH. Eculizumab was not effective to ulcerative colitis/proctitis in G1.

10) M, maternal; P, paternal.

11) Based on NM_015937.

12) The same variant c.250G>T in J1[8] was found in two Japanese patients with inherited GPI deficiency (IGD) suffering from developmental delay, seizures and skeletal abnormality (Table S2).[13,39]

13) Data are shown in Figure S2.

14) Deletions of J1 and G2 included entire *PIGU* gene as well as *PIGT*.

were within a normal range. Refer to Kawamoto M et al., *BMJ Case Rep.* 2018;2018[8] for more detailed description of J1.

2) Refer to Supplemental Data in Krawitz PM et al., Blood 2013; 122:1312-1315[9] for detailed description of G1.

3) 96% of granulocytes and 19% of erythrocytes of G2 were GPI-AP-defective. Additional diagnosis and symptoms: Coronary heart disease, myocardial infarction (49 years); recurrent left brain transient ischemic attacks (66 years), recurrent confusion symptoms, disturbance of memory; cholecystectomy (43 years) in the following years remitting cholangitis; elevation of indirect bilirubin; B chronic lymphocytic leukemia (64 years), treatment with rituximab (Whether leukemic cells were from PNH clone was not known.); hemochromatosis (compound heterozygous), diagnosed at age of 66 because of elevation of ferritin, prostate adenoma. The patient died for cardiac decompensation with fulminant pulmonal edema and massive general arteriosclerosis with ulcerated plaques.

4) Additional diagnosis and symptoms of G3: Cholecystolithiasis (65 years); metabolic syndrome with obesity, diabetes and dyslipoproteinemia; sensorineural hearing loss (61 years); peripheral arterial occlusive disease; JAK2 V617F mutation (age of 66)(Whether the mutation occurred in PNH clone was not known.), neurinoma left side (52 years), increasingly personality changes and disturbance of memory since the beginning of the meningitis episodes until start of eculizumab.

5) Numbers in parentheses indicate age when the symptom first recognized or eculizumab treatment started.

6) Headache often occurred associated with urticaria (first urticaria, followed by severe headache).

7) First time of significantly elevated lactate dehydrogenase (LDH).[9]

8) Patient reported on dark urine (panel d of Figure 1**B**).

9) G1 developed ulcerative colitis/proctitis about 5 years after diagnosis of PNH. Eculizumab was not effective to ulcerative colitis/proctitis in G1.

10) M, maternal; P, paternal.

11) Based on NM_015937.

12) The same variant c.250G>T in J1[8] was found in two Japanese patients with inherited GPI deficiency (IGD) suffering from developmental delay, seizures and skeletal abnormality (Table S2).[13,39]

13) Data are shown in Figure S2.

14) Deletions of J1 and G2 included entire *PIGU* gene as well as *PIGT*.

Figure 1

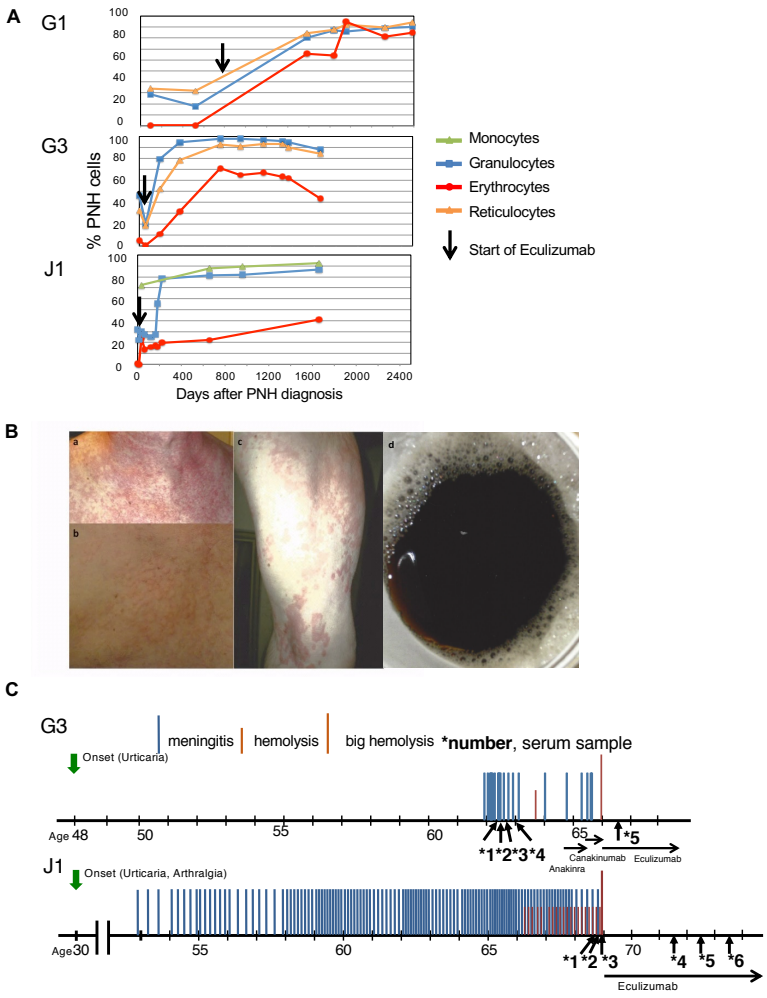

Figure 1. Clinical features of AIF-PNH. A. Time course of PNH clone sizes in patients G1, G3 and J1. Percentages of PNH cells in monocytes, granulocytes, erythrocytes and reticulocytes are plotted as a function of time in days. Arrows, start of eculizumab therapy. **B**. Examples of urticaria in patient G3 before the start of the anakinra treatment: (a) and (b), chest; (c), left upper leg. Brightness in (b) was adjusted to more clearly show raised skin in the affected area. The pictures were kindly made available by the patient. (d) hemoglobinuria of patient G3. **C**. Clinical courses of patients G3 in comparison to J1 (Fig. 1 in Kawamoto M et al[8] was modified with additional data) including effective treatments. G3 (top) had meningitis 19 times since 62 years of age to 65 years of age. Eculizumab therapy started at 66 years of age after a severe hemolysis. J1 (bottom) had meningitis 121 times since 53 years of age to 69 years of age when eculizumab therapy started.[8] Downward green arrows, onset of urticaria and/or arthralgia; Blue middle height bars, meningitis; Orange short bars, hemolysis; Orange long bars, severe hemolysis; horizontal arrows of various lengths, treatment periods of effective therapies (Anakinra and canakinumab were given with prednisolone); upward arrows with number and asterisk, serum samples taken for cytokine and other protein determination.

Figure 2

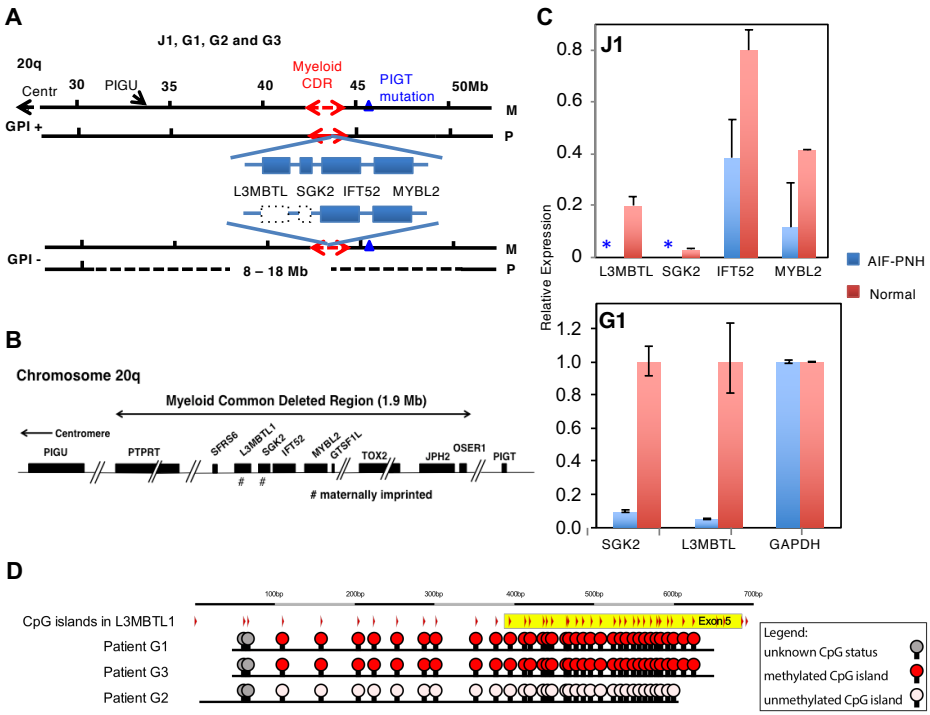

Figure 2. Genetic abnormalities in patients with AIF-PNH. A. PIGT mutations in GPI-positive (GPI +) and -defective (GPI -) cells from patients with AIF-PNH. (Top) GPI + cells from patients with AIF-PNH J1, G1, G2 and G3 had a germline *PIGT* mutation (triangle) in the maternal (M) allele. Two maternally imprinted genes, *L3MBTL1* and *SGK2*, within myeloid Common Deleted Region (CDR) are expressed from the paternal (P) allele. Solid and broken red double arrows, P and M alleles of myeloid CDR, respectively. (Bottom) GPI - blood cells from AIF-PNH patients had an 8 Mb to 18 Mb deletion spanning myeloid CDR and *PIGT* and/or *PIGU* in the P chromosome 20q leading to losses of expression of two maternally imprinted *L3MBTL1* and *SGK2* genes (dotted boxes). **B**. Myeloid Common Deleted Region. A 1.9-Mb region in chromosome 20q spanning *PTPRT* gene to *OSER1* gene is termed "myeloid common deleted region (CDR)". *PIGT* and *PIGU* genes are approximately 1.2 Mb telomeric and 7.4 Mb centromeric to the myeloid CDR, respectively. *L3MBTL1* and *SGK2* genes marked # are maternally imprinted. **C**. qRT-PCR analysis of genes within myeloid CDR in GPI-AP-defective granulocytes from J1 and granulocytes from a healthy control (top) and whole blood cells from G1 and a healthy control (bottom). L3MBTL1 and SGK2, maternally imprinted genes; IFT52 and MYBL2, non-imprinted genes. Relative expression is determined taking means of ABL levels as 1 (J1) or of GAPDH as 1 (G1). Blue bars, cells from J1 and G1; orange bars, cells from healthy individuals; asterisks (*), below detection limits. Mean +/- SD of duplicate (JI) and triplicate (G1) samples in one of the two independent experiments. **D**. Methylation status of the CpG islands in *L3MBTL1* in G1, G2 and G3. Red, methylated CpG islands; pink, unmethylated CpG islands; gray, unknown CpG islands. Bisulfite sequencing data are shown in Figure S3**A**.

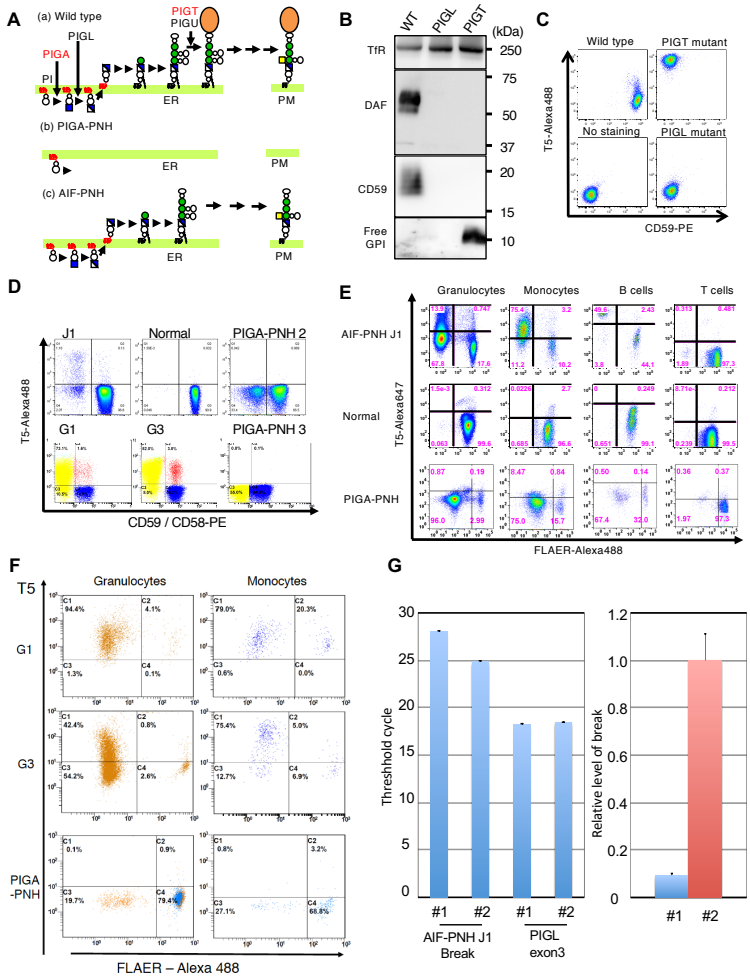

Figure 3. Biochemical abnormalities in PIGT-defective cells. A. Schematics of normal and defective biosynthesis of GPI anchors. (a) Normal biosynthesis of GPI-APs. GPI is synthesized in the endoplasmic reticulum (ER) from phosphatidylinositol (PI) by sequential reactions and assembled GPI is attached to proteins (orange oval). PIGA acts in the first step of GPI biosynthesis whereas PIGT acts in attachment of GPI to proteins. GPI-APs are transported from the ER to the plasma membrane (PM). (b) No GPI biosynthesis in PNH caused by *PIGA* defect. (c) Accumulation of free GPI in PNH cells caused by *PIGT* defect. GPI is not attached to proteins because of PIGT defect and is transported to the cell surface. **B**. Western blotting analysis of *PIGT*-defective and *PIGL*-defective CHO cells with T5 mAb for free GPI, anti-CD59 and anti-DAF mAbs, and anti-transferrin receptor (TfR) as loading controls. **C**. Flow cytometry of *PIGT*-defective and *PIGL*-defective CHO cells with T5 mAb and anti-CD59 mAb. **D**. Flow cytometry of erythrocytes from J1, G1, G3, a healthy individual and two patients with *PIGA*-PNH with T5 mAb and anti-CD59 (top panels) or anti-CD58 (bottom panels). **E**. Flow cytometry of blood cells from JI, a healthy individual and a patient with *PIGA*-PNH with T5 mAb and FLAER. **F**. Granulocytes and monocytes from G1 and G3, and a patient with *PIGA*-PNH, stained by T5 mAb and FLAER. **G**. Determination of the PNH clone size in J1 by qPCR analysis of the break causing 18 Mbp deletion. (Left) Threshold cycle in PCR for the break and exon 3 of PIGL as a reference. #1, DNA from whole blood leukocytes taken in a stage with autoinflammation only (four months before the onset of recurrent hemolysis); #2, DNA from granulocytes (29% of cells were GPI-AP-defective) taken one month after start of eculizumab therapy. (Right) Relative levels of the break in samples #1 and #2 by setting the level in #2 as 1. Data are shown in mean + SD of triplicate samples in one experiment.

Figure 4

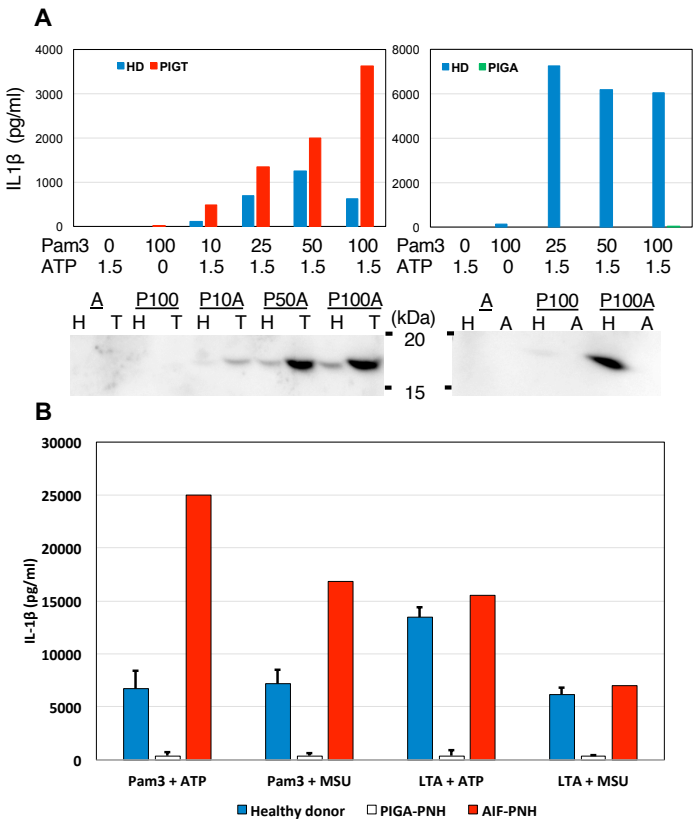

Figure 4. IL1β secretion from AIF-PNH and PIGA-PNH cells. A. The peripheral blood mono- nuclear cells from JI, PIGA-PNH4 and a healthy individual were incubated with 10 to 100 ng/ml Pam_3CSK4 (Pam3) at 37℃ for 4 hr, and then were incubated with 1.5 mM ATP for 30 min. IL1β in the supernatants was measured by ELISA (top) and western blotting (bottom). (Left) J1 (red bars) and a healthy individual (blue bars). (Right) PIGA-PNH4 (green bars) and a healthy individual (blue bars). A, ATP only; P100, 100 ng/ml Pam_3CSK4 only; P10A, P50A and P100A, 10, 50 and 100 ng/ml Pam_3CSK4, respectively and ATP; H, healthy donors; T, AIF-PNH; A, PIGA-PNH. **B**. The peripheral blood mononuclear cells from J1 and two or three patients with *PIGA*-PNH and three healthy controls were stimulated with 200 ng/ml of Pam3 or 1 μg/ml of lipoteichoic acid (LTA) from *Staphylococcus aureus* for 4 hr at 37℃ and after washing were incubated with 3mM ATP or 200 μg/ml monosodium ureate (MSU) for 4 hr at 37℃. IL1β secreted into the medium was determined by ELISA. Data for healthy donors and *PIGA*-PNH were shown as mean + SD. Cells from three patients with *PIGA*-PNH (PIGA-PNH4-6) secreted very low levels of IL1β (403+/-326 pg/ml) after stimulation of NLRP3-inflammasomes with Pam_3CSK4 and ATP under these strong conditions. In contrast, cells from AIF-PNH J1 secreted IL1β at a high level (25,000 pg/ml) that is higher than levels from three healthy donors (6,693+/-1,711 pg/ml). Similar results were obtained by stimulation with Pam_3CSK4 and MSU instead of ATP. Moreover, similar results were obtained by stimulation with LTA plus ATP or MSU.

Figure 5

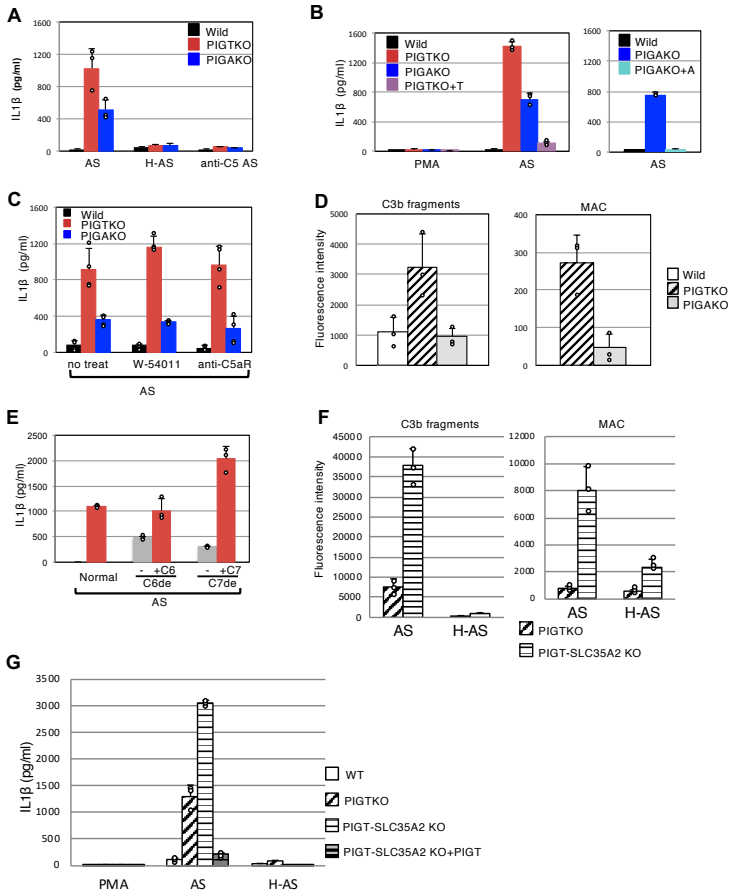

Figure 5. IL1β secretion from PIGT- and PIGA-defective THP-1 cells. **A**. Complement-mediated IL1β secretion from THP-1-derived macro- phages. WT, PIGTKO and PIGAKO cells were incubated with acidified serum (AS), heat-inactivated AS (H-AS), or AS containing anti-C5 mAb. Supernatant samples were collected after 5-hr incubation and analyzed for IL1β by ELISA. Mean + SD of three independent experiments. **B**. Reductions of IL1β secretion by transfection of *PIGT* and *PIGA* cDNAs into PIGTKO and PIGAKO cells (PIGTKO+T and PIGAKO+A, respectively). Cells differentiated by PMA were either left untreated (PMA) or incubated with AS (AS) under similar conditions as described in **A** and supernatants analyzed for IL1β. Mean + SD of three independent experiments. **C**. Effect of inhibiting C5aR on IL1β secretion from THP-1-derived macrophages. Cells were incubated with AS alone (no treat), or AS containing C5aR antagonist (W-54011) or anti-C5aR mAb. Supernatant was collected after 5 hr and analyzed for IL1β by ELISA. Mean + SD of duplicate samples from two independent experiments. **D**. Detection of C3b fragments (left) and MAC (right) by flow cytometry on PMA-differentiated THP-1 macrophages after incubation with AS. Geometric mean fluorescence intensity of medium-treated cells was subtracted from that of AS-treated cells. Mean + SD of three independent experiments. **E**. IL1β secretion from PIGTKO THP-1 macrophages stimulated with C6- or C7-depleted AS. PIGTKO THP-1 macrophages were incubated with AS, C6-depleted AS (-/C6de), C6de restored by C6 (+C6/C6de), C7-depleted AS (-/C7de), or C7de restored by C7 (+C7/C7de). Supernatant was collected after overnight incubation. Mean + SD of triplicate samples from two independent experiments (normal and C6-depleted sera) and one experiment (C7-depleted serum). **F**. Binding of C3b fragments (left) and MAC (right) on PIGTKO and PIGT-SLC35A2 double KO THP-1 macrophages after AS treatments. **G**. IL1β secretion from PIGTKO and PIGT-SLC35A2 double KO THP-1 macrophages after AS treatments.

3.4.1 Contribution

The manuscript was accepted in *Journal of Clinical Investigation* 20th of August 2019 under the title “Complement and inflammasome overactivation mediates paroxysmal nocturnal hemoglobinuria with autoinflammation” after completion of this thesis.

The first authors Höchsmann, B. and Murakami, Y. designed the study together with Inoue, N., Schrezenmeier, H., Krawitz, M. P., and Kinoshita, T. Functional experiments were conducted by T. Murakami, Y., Osato, M., Hirata, T., and Murata, S. Sequencing, qPCR, methylation analysis, and bioinformatic data processing was carried out by Knaus, A., and Jäger, M., Eggerman, T., and Dicks S. The patients were examined by Flöttmann, R., Hoellein, A., Schrezenmeier, H., Höchsmann, B., Kawamoto, M., Kanakura Y., and Nishimura J. Flow cytometry analysis and data interpretation was carried out by Anliker, M., Knaus, A., Murata, S., Ueda, Y., and Kohara N. The manuscript was composed by Höchsmann, B., Murakami, Y., Schrezenmeier, H., Krawitz, M. P., and Kinoshita, T. All authors read, commented and approved the final version of the manuscript.

3.4.2 Discussion

In this work a total of four patients with PNH caused by *PIGT* mutations were reported and a new disease entity was proposed: AIF-PNH. Although, PNH caused by *PIGA* and *PIGT* mutations, respectively, can be both treated by eculizumab, four major differences have been discovered between AIF-PNH and PNH.

First, GPI deficiency in PNH is caused by somatic mutations of the X-linked gene *PIGA* in hematopoietic stem cells, whereas AIF-PNH is caused by a predisposing germline mutation in *PIGT* and an acquired somatic deletion on chromosome 20q encompassing the wild type allele of *PIGT* and other proto-oncogenes in hematopoietic stem cells.

Second, *PIGA*-mutations impair the function of the GPI-GlcNAc transferase (an initial step of the GPI biosynthesis pathway) whereas *PIGT*-mutations cause GPI transami-

dase deficiency. Therefore, free GPI remains on the surface of *PIGT*-defective cells and the cells lack GPI-APs, whereas *PIGA*-defective cells lack GPI anchor and GPI-APs. This can be used to discriminated PIGT-PNH from PIGA-PNH by flow cytometry. Hoechsmann et al., (2019) showed that granulocytes and B-cells express the free GPI anchor on the cell surface carrying the N-acetylgalactosamine side branch of the first mannose. This side branch of the GPI anchor serves as an epitope for a monoclonal IgG antibody: T5-4E10 (T5-antibody) (Azzouz et al., 2006; B Striepen et al., 1992; Boris Striepen et al., 1997; Y. Wang et al., 2019). In contrast granulocytes and B-cells from patients with PIGA-PNH do not react with the T5-antibody (Hoechsmann et al., 2019).

Third, the expansion of the *PIGA*-defective HSC clone in PNH is caused by selective survival under autoimmune bone marrow failure with or without acquisition of benign tumor characteristics by additional somatic mutations (Brodsky, 2008; Shen et al., 2014). In contrast, none of the patients with AIF-PNH had documented bone marrow failure (Krawitz et al., 2013; Murakami et al., 2016). Additionally, loss of myeloid CDR in *PIGT*-defective AIF-PNH cells is similar to the myeloproliferative 20q deletion syndromes. Further investigations are needed to determine the relation between the loss of myeloid CDR in AIF-PNH and the clonal expansion, as *in vitro* studies showed clonal growth advantage for different lineages under *L3MBTL1* and *SGK2* loss compared to AIF-PNH patients. Hence, this unique deletion in AIF-PNH provides a clonal expansion mechanism for AIF-PNH cells that is distinct from PIGA-PNH cells.

Fourth, whereas PNH patients share intravascular hemolysis and thrombosis with AIF-PNH patients, autoinflammatory symptoms including recurrent urticaria, arthralgia and aseptic meningitis, were reported in AIF-PNH patients even before onset of hemolysis and thrombosis. Perhaps different clinical symptoms appear depending on the size of *PIGT*-defective clone. Interestingly autoinflammatory symptoms disappeared after treatment with eculizumab. This suggests the involvement of C5 activation in the autoinflammation. Consequently, the autoinflammatory symptoms of some patients might be explained by GPI transamidase deficiency. A potential treatment with eculizumab and its derivates might be considered, after confirmation of a low fraction of GPI transamidase deficient cells by flow cytometry.

The role of free GPI in inflammasome and complement activation needs to be clarified in further studies to fully understand the mechanistic basis of AIF-PNH.

The discovery of a novel disease entity AIF-PNH raises the question whether, similar to congenital GPIBDs, also acquired GPIBDs can result due to mutations in any of the genes of the GPI anchor biosynthesis pathway in HSCs. Furthermore, it remains unknown whether individuals with acquired GPIBDs might present with a different clinical manifestation. Most likely the complement mediated hemolysis will persist as a clinical characteristic due to the lack of complement regulating factors (CD55 and CD59).

4 Summary and Discussion

4.1 PNH and complement dysregulation

Although PNH is a rare disorder, it has been already described in the late 19th century (Strübing, 1882). PNH is an acquired disorder of the hematopoietic system and the only GPIBD whose pathomechanism is well understood. In most of the cases mutations in the X-linked gene *PIGA* lead to a complete loss of the GPI anchor. Males and females are equally frequently affected by PIGA-PNH, because females have only one active X-chromosome and acquired mutations only need to affect this copy of *PIGA*, while males have only one X-chromosome.

Lately, mutations in *PIGT* were discovered in patients with PNH that presented with autoinflammatory symptoms. Both disease entities share a clonal expansion of GPI deficient HSC cells. Consequently, blood cells originating from the mutated HSC are vulnerable to complement mediated attack, due to missing or reduced expression of complement regulating factors CD55 and CD59 (Takeda et al., 1993). However, there is still debate about the molecular mechanism of clonal expansion of the mutated HSC. While, immune mechanisms may mediate clonal selection by survival advantage that is dependent on GPI-AP deficiency, it is probably insufficient for the clonal dominance necessary for PNH to become clinically apparent (Inoue et al., 2006). Several case reports suggest that further mutations in genes associated with aplastic anemia or myeloid malignancies such as MPN or MDS could be responsible for the clonal expansion in PIGA-PNH (Shen et al., 2014; Teye et al., 2017) as well as PIGT-PNH. It is also possible that various mechanisms lead to clonal expansion and multiple genes, if mutated, drive the clonal expansion. Deep sequencing of DNA from GPI deficient blood cells from more cases might reveal the underlying mechanism of clonal expansion and dominance.

The high prevalence of PIGA-PNH in comparison to PIGT PNH is most likely due to the X chromosomal location of *PIGA*. Thus, the acquisition of a pathogenic variant on one allele in an HSC might lead to development of PNH. But in AIF-PNH all patients identified were heterozygous carriers of a known pathogenic variant, that led to

predisposition to AIF-PNH. Hence, the question arises whether predisposing mutations in compound heterozygosity with acquired mutations in genes of the GPI anchor biosynthesis pathway might cause different forms of PNH. Potentially the acquired mutations can be large deletions that lead to loss of heterozygosity and might affect nearby genes commonly mutated in hematopoietic or lymphoid malignancies.

In both disease entities (PNH and AIF-PNH) the disbalance of complement regulation (due to absence of CD55 and CD59) leads to episodes of hemolytic events that are linked to complement pathway activation either initiated by spontaneous C3 hydrolysis ('tick-over') under steady-state conditions (Pangburn & Müller-Eberhard, 1983) or aggravated by pathogen-driven activation in response to infections (bystander effect) (Risitano, 2013). Additionally, the clinical manifestation of complement mediated intravascular hemolysis is accompanied by thrombosis and consequently infarction (Hill et al., 2017, 2013).

The discovery of the monoclonal antibody eculizumab that binds to C5 and prevents cleavage by C5 convertase, thereby inhibiting terminal complement activation, was a milestone in PNH therapy (Rother et al., 2007; Thomas et al., 1996). Furthermore, eculizumab can be applied to also treat other disorders where complement suppression is necessary (Rother et al., 2007).

Such an example is congenital CD59 deficiency. Yamashina et al., (1990) reported a patient with PNH-like symptoms, but normal CD55 expression. Subsequently, further reports broadened the spectrum of CD59 deficiency that include hemolysis, immune-mediated polyneuropathy, and strokes (Anliker et al., 2014; Ben-Zeev et al., 2015; Haliloglu et al., 2015; Klemann et al., 2018; Mevorach, 2015; Nevo et al., 2013). All of the symptoms are related to complement misregulation and attack of CD59 deficient cells by activated complement system. Neurological findings such as demyelination of sensory and motor nerves and neuropathy were demonstrated to be a result of membrane attack complex deposition and terminal activation of the complement cascade (Nevo et al., 2013). The clinical manifestation was reverted after treatment with eculizumab (reviewed by Höchsmann & Schrezenmeier, 2015). Interestingly, individuals with a congenital CD55 deficiency do not develop any of the above mentioned clinical symptoms (Daniels et al., 1998; Reid et al., 1991; L. Wang et al., 1998). This leads to the hypothesis that CD59 expression is potentially dominating over

CD55 expression in complement regulation and highlights the importance of eculizumab that blocks complement at C5 (upstream of CD59 but downstream of CD55, compare Rother et al., 2007).

An adverse effect of PNH treatment, during bacterial or viral infections, is the accumulation of C3 fragments on erythrocytes. Thereafter, opsonized erythrocytes are cleared in the spleen (Risitano et al., 2009). The increase hemolysis and thrombosis even under eculizumab treatment can be life threating, but the complications resolve after clearance of infections.

4.2 Inherited GPIBDs

Before the human genome was deciphered and next generation sequencing technologies were available GPIBDs were delineated as a clinical entity based on characteristic clinical and facial features (Horn et al., 2010; Kruse et al., 1988; Mabry et al., 1970; Rabe et al., 1991; M. Thompson et al., 2010). HPMRS was defined by hyperphosphatasia, severe to profound intellectual disability, brachtelephangely, seizures, and a characteristic facial appearance with elongated palpebral fissures, a broad nasal bridge, tented upper lip with downturned corners of the mouth, and a long philtrum.

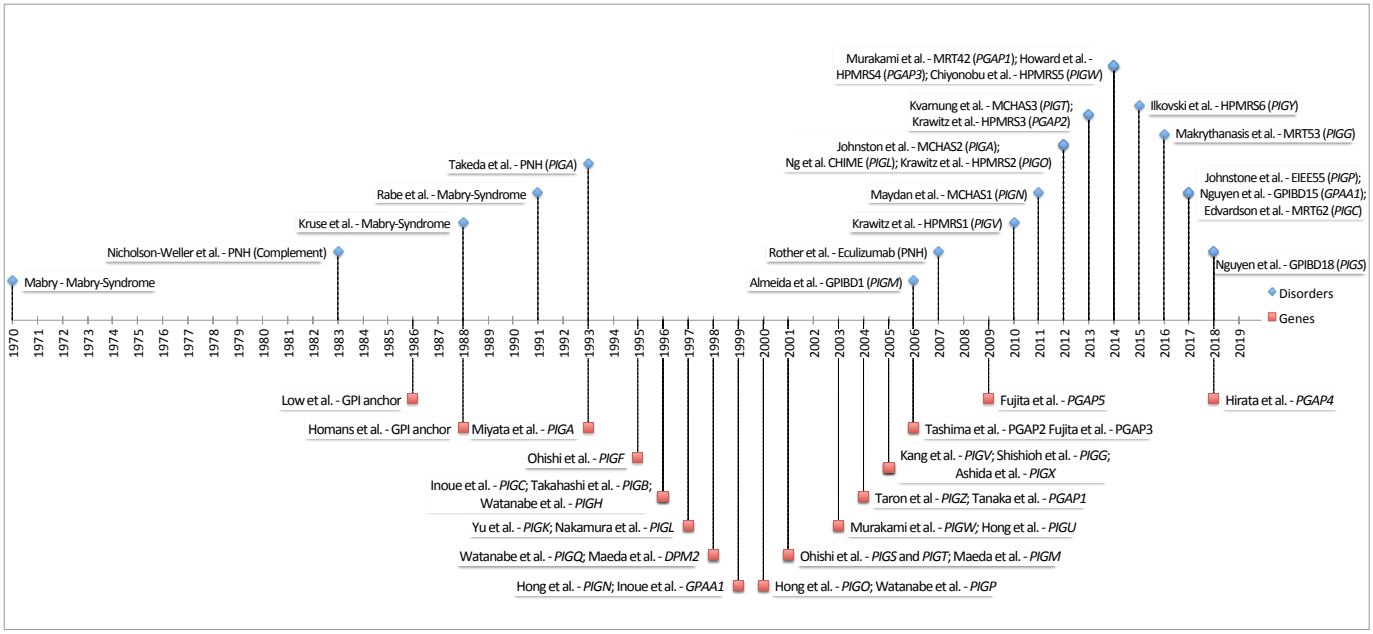

Figure 9. Timeline of the first publications in the field of GPI and GPIBDs. First author and identified disorder or syndrome (blue; upper part). First author and identified gene of the GPI pathway (red, lower part)

It was speculated that the cause of HPMRS is the result of increased tissue nonspecific ALP activity measured in blood (Cole & Whyte, 1997) or that mutations of the *ALPL* gene might be the cause of the syndrome. The hypothesis was not maintained after no variants were identified in the gene (Thompson et al., 2010).

The biochemical structure of the GPI anchor and its function was described in the mid to late 1980s (Homans et al., 1988; Low et al., 1986) and most genes of the GPI anchor biosynthesis pathway had been discovered by 2006 (Figure 9).

Interestingly, the first two individuals with GPI anchor deficiency were reported by Almeida et al. (2006). Due to the portal vein thrombosis in the affected individuals at

a very young age, the researchers speculated a congenitally inherited PNH like phenotype. But then, homozygosity mapping in the two affected individuals from two consanguineous families reduced the search space dramatically to only one gene of the GPI anchor biosynthesis pathway: *PIGM*. Finally, sanger sequencing and flow cytometry analysis confirmed the GPIBD.

However, the genetic cause of HPMRS had remained undiscovered until 2010, when Krawitz et al. identified a founder mutation in *PIGV* by WES and identity-by-descent linkage analysis in a family with three affected individuals. Soon after the GPI anchor biosynthesis pathway was associated to syndromic forms of intellectual disability with hypotonia, seizures and various congenital malformations new reports emerged that utilized linkage analysis and flow cytometry (Maydan et al., 2011; Ng et al., 2012).

The era of exome sequencing led to the identification of individuals, with mutation in 20 of the 29 genes of the GPI anchor pathway that were affected by a range of different syndromes (Figure 9). A major difficulty is the broad heterogeneity of the phenotypic spectrum of GPIBDs. The cardinal features shared between all GPIBDs are intellectual disability, developmental delay, seizures, and muscular hypotonia. Less frequently expressed and partially gene-specific congenital malformations range from cleft lip, over brain anomalies, abnormalities of the hand and feet to gastrointestinal anomalies and genitourinary malformations, (Bellai-Dussault et al., 2018). Although, over 200 individuals with mutations in the GPI biosynthesis and processing pathway have been identified, for nine genes no pathogenic mutations have yet been reported (*PIGB*, *PIGF*, *PIGK*, *PIGU*, *PIGX*, *PIGZ*, *PGAP4*, *PGAP5*, and *PGAP6*). The missing gene-phenotype links might be due to the rareness of the disease. Alternatively, it might also be possible that even hypomorphic mutations in certain of the remaining genes are not compatible with life and lead to early embryonic death (McKean & Niswander, 2012). So far, homozygous lof variants in these genes have not been observed in the large sequencing projects of healthy individuals and for all known GPIBD genes a residual function has been shown (Bellai-Dussault et al., 2018; Knaus et al., 2018); only in *PGAP3* biallelic lof mutations have been identified in individuals from the same ethnic descent (Abdel-hamid et al., 2017). The high evolutionary conservation and compactness (ranging from 1kb (*PIGF*) to 5kb (*PGAP4*)) of genes

that are not yet described to cause GPIBDs may explain why it is difficult to find multiple unrelated individuals in outbred populations with mutations in the same gene. This difficulty may be overcome by initiatives such as MatchMaker Exchange (Sobreira et al., 2017) or GeneTalk (Kamphans & Krawitz, 2012). However, matching individuals on the genetic and feature level might not be sufficient, since clinicians have to provide manually curated information to the platform and might forget to submit candidate variants or would not provide all clinical features. In recent studies, computer assisted facial analysis was used to demonstrate a shared facial gestalt in individuals affected by the most prevalent GPIBDs (Hsieh et al., 2018; Knaus et al., 2018). Hence, such technology could be applied to match individuals affected by yet unknown GPIBDs on the level of facial gestalt and phenotypic features. It is noteworthy that patient matching is a different task than clustering individuals by facial similarity and comparing it to other clusters (Marbach et al., 2019). The future initiatives such as gestaltmatch.org or face2gene are going investigate the promising potential.

Biallelic mutations in genes, which products act in protein complexes with known disease genes, such as *PIGM* with *PIGX* (that form the mannosyltransferase I, with *PIGM* as known GPIBD1 gene), are more likely to be associated to novel GPIBD. The same holds true for *PIGF* (as part of the EtNP transferase II and III with pathogenic mutations identified in *PIGO* and *PIGG*), and *PIGK* and *PIGU* (as part of the GPI transamidase, with pathogenic mutations identified in *PIGS*, *PIGT*, and *GPAA1*).

For the other genes (*PIGB*, *PIGZ*, *PGAP4*, *PGAP5*, and *PGAP6*) predictions are more difficult. The evolutionary conservation over multiple species down to yeast of *PIGB* and *PIGZ* and high similarity to the other mannosyltransferases (*PIGV* and *PIGM*) (B. Eisenhaber, Sinha, Wong, & Eisenhaber, 2018) might implicate their role in yet undiscovered GPIBDs. PIGB function is indispensable for correct GPI anchor synthesis and its ubiquitous expression also suggests universal importance, making it a promising disease gene candidate for HPMRS similar to *PIGV*. The mannosyltransferase IV, encoded by *PIGZ*, adds Man4 to the core mannose structure of the GPI anchor and is likely not required for the attachment of all substrates. However, *PIGZ* is highly expressed in the brain and colon and during embryonic development (Taron et al., 2004) where it might play crucial roles. Further evidence for *PIGZ* as a promising

GPIBD candidate gene is its importance in yeast (Grimme et al., 2001) and it is currently not known whether PIGZ deficiency might lethal or tolerated in humans.

For the enzymes encoded by *PGAP4* (*TMEM246*), *PGAP5* (*MPPE1*), and *PGAP6* (*TMEM8A*) that act in the late stages of GPI maturation, modification, and GPI-AP release, respectively, it is difficult to predict what consequences a functional impairment would have in humans.

Deficiency of PGAP1 leads to diminished deacylation of the fatty acid at the inositol and results in a phospholipase resistant GPI anchor (Fujita et al., 2011; Murakami et al., 2014; Tanaka et al., 2004). Affected individuals do not show a reduced GPI-AP expression, thus, the neurological features are most probably due to insufficient release of specific GPI-APs in neuronal tissues. Coherently, the dysfunction of *PGAP6*, that encodes the phospholipase A2, which releases particular GPI-APs during embryogenesis in neuronal tissues, might be associated to neurological disorders (Lee et al., 2016).

Liu et al., (2018) stated that "GPI–glycan remodeling by *PGAP5* is critical for binding of GPI-APs to their cargo receptors, the p24 family of proteins, for efficient sorting into the ER exit sites". Potentially, PGAP5 deficiency might affect various but not all GPI-APs (similar to *PGAP1*). The same applies to *PGAP4*: the addition of the GalNAc side branch of Man1 by *PGAP4* is GPI-AP and tissue specific. Therefore, proteomics or *in vivo* analysis of knock-out or knock-in mice may elucidate in more detail the implications of *PGAP4, PGAP5*, and *PGAP6* deficiency, respectively.

For the recessive GPIBDs the identification of heterozygous potentially deleterious variants may guide further analysis. In cases where the second hit is a non-coding variant, which is potentially not covered by targeted sequencing, orthologous methods of DNA, RNA, or protein analysis are necessary. Non-coding variants may be identified by WGS (Gloss & Dinger, 2018). While consequences of non-coding variants (such as 3'UTR mutations or splice site mutations) may be discovered by RNA sequencing (Almeida et al., 2006; Knaus et al., 2016) and western blotting of proteins can confirm RNA based analysis.

The functional characterization of pathogenic mutations in *PIGM* and *PIGV* has been performed in a similar manner as for acquired mutations in *PIGA* in PNH patients: by flow cytometry. The preceding reports of reduced expression of GPI-APs (namely

CD55 and CD59) in PNH patients (Hillmen et al., 1992) and identification of somatic mutations in *PIGA* as cause for PNH (Takeda et al., 1993) have paved the way for the diagnostic workup of inherited GPIBDs. Especially for functional characterization of pathogenic mutations in genes that are expressed in all tissues and play crucial roles in the biosynthesis of the GPI anchor, flow cytometric analyses are inevitable. This accounts also for genes such as *PIGB*, *PIGF*, *PIGK*, *PIGU*, and *PIGX* for which pathogenic mutations in individuals affected by GPIBDs have yet not been identified.

Due to the broad range of GPI-APs expressed on different cells and a lack of standardized flow cytometry panels for GPIBDs, analyses were performed on various markers and different cell types, which resulted in comparison difficulties. Hence, the attempt to identify a syndrome specific pattern of marker expression by flow cytometry in GPIBDs was unsuccessful on a gene-specific level (Knaus et al., 2018). Notably, however is, that mothers, who are heterozygous carriers of pathogenic *PIGA* mutations may show a bimodal distribution of GPI marker expression in histogram analysis (unpublished observations). This may be explained by random X chromosome inactivation in hematopoietic stem cells that give rise to two types of blood cells that transcribe either the wild type or the pathogenic *PIGA* allele.

Despite that GPI-APs are similarly tethered to the plasma membrane in nearly all cells, a recent study demonstrated that not all GPI-APs are processed in the same manner (Davis et al., 2015). Thus, GPI-AP specific variances may result depending on the gene mutated in the GPI anchor biosynthesis pathway.

Recent observations and thorough literature review indicates that PIGT deficiency results in a relative decrease of CD16 and CD24 expression, while CD55 and CD59 expression and staining with FLAER were not affected (Lam et al., 2015; Nakashima et al., 2014; and unpublished cases). Furthermore, the T5-4E10 antibody that recognizes the GlcNAc side branch of the GPI anchor can be used to discriminate between GPI transamidase and GPI anchor deficiency (Hoechsmann et al., 2019; Y. Wang et al., 2019). It could be also applied in the functional characterization of inherited GPIBDs.

Ideally, the following investigations on patient derived samples should be performed in order to establish genotype phenotype correlation between mutations in a gene of the GPI biosynthesis pathway and marker expression measured by flow cytome-

try. First, a cohort of individuals with a common ethnic background and the same mutation in a gene should be analyzed at multiple points in time using a standardized multicolor flow cytometry panel. The obtained marker expression profiles and their variability would serve as a baseline. Next, individuals with various hypomorphic mutations in the same domain of the gene (and thus variable residual function of the protein) should be compared to the baseline to determine the domain specific variability. Only thereafter, a comparison of marker expression from individuals with various mutations over the entire gene can be made to identify a gene specific expression pattern. However, it is very challenging in the field of ultra-rare monogenic disorders, such as GPIBDs, to collect large numbers of individuals for such studies. A deeper understanding of the transamidation process of different GPI-APs and effects of different GPI signal sequences may explain why GPI-AP expression pattern may be specific to different gene mutations (B. Eisenhaber & Eisenhaber, 2007).
Flow cytometric analyses in some examples might reach its limitations: In a prospective investigation of *PIGZ* as a potential candidate gene in a suspected GPIBD, blood samples would most likely not be a suitable source for flow cytometric analysis. Firstly, *PIGZ* is expressed in only minimal quantities in blood. Secondarily, expression of the commonly tested markers (such as CD55, CD59) is most probably not affected by the absence of the Man4 on the GPI anchor. Likewise, in potential cases with *PGAP4* or *PGAP5* deficiencies it is difficult to predict the effect on GPI-AP expression in blood. In such cases functional analysis should be performed on appropriate tissues and marker.
In vitro analysis can be applied to identify relevant variants in known and novel GPIBD genes. From knock-out and knock-in experiments in CHO cell lines almost all genes that play a role in the GPI biosynthesis and maturation pathway have been discovered (Maeda et al., 2006). Furthermore, genetic screens of haploid cell lines *in vitro* demonstrated its applicability in forward genetics and GPI pathway analysis (Davis et al., 2015). Selection of positions based on allele frequency (e.g. from gnomAD) and deleteriousness scores (e.g. CADD), massively parallel permutation of the positions of a given gene in a vector by CRISPR/Cas (Clustered Regularly Interspaced Short Palindromic Repeats/CRISPR associated), transfection, and subsequent analysis by flow cytometry could reveal potentially pathogenic variants, even before they are

found in individuals (Menasche et al., 2019; Timms et al., 2016). Functional validation might be performed in knock-in mice.

The decreasing costs and low error rate of NGS, fast and standardized processing of NGS data, and increasing diagnostic yield of exome and genome analysis are shifting the challenge towards variant interpretation (Cooper & Shendure, 2011; Vissers et al., 2017). But due to the involvement of GPI-APs in many pathways and developmental events (Fujita & Kinoshita, 2012), defects in the genes of the GPI anchor synthesis and processing can result in a variety of genetic disorders for which affected individuals display a wide spectrum of features (Bellai-Dussault et al., 2018). Hence, multiple layers of information are needed for precise and fast processing of future cases. Deep and automated phenotyping by image analysis and feature extraction from clinical reports add supplementary layers of information to the rapidly generated and annotated NGS data (Knaus et al., 2018; Jean T. Pantel et al., 2018). The combination of various scores and multiple layers of information will decrease the turnaround time and increase the diagnostic yield in the future (Hsieh et al., 2018).

Despite of the recent advancement in the diagnosis of suspected GPIBDs, clinicians and geneticists should be aware of the following differential diagnosis that can mimick HPMRS. The HPO term “increased alkaline phosphatase” (HP:0003155) is related to 43 genes, “intellectual disability” (ID; HP:0001249) and “developmental delay”, (DD, HP:0001263) yields a total of 1344 genes from the HPO. Even though the selected set of genes from the HPO may be incomplete, it illustrates that the intersect does not only contain genes associated with GPIBDs. Although, a combination of the three phenotypic feature terms reduces the search space dramatically to only 14 genes, not all belong to the (Figure 10). Eight genes in the intersect are syndromic ID genes that are also linked to elevated ALP rather as a consequence of abnormalities in the bone metabolism (COG4, *FAM20C*, *HNF4A*, *LBR*, *RB1*, *SOST*, *SLC2A2* and *TNFRSF11A*). Furthermore, *COG4* should be considered for differential diagnosis of cases suspected for HPMRS. Furthermore a large retrospective study recently showed, that in more than 2 % of the cases the clinical symptoms of a patient are probably explained by mutations in more than just one Mendelian gene (Smith et al., 2019). A recently identified individual suspected for HPMRS turned out to have a mutation in one of the 30 genes causing

hyperphosphatasia and a second mutation causative for intellectual diasability (unpublished data). In such a case, deep phenotyping and analysis of the facial gestalt provide pivotal information for the guidance of the diagnosis.

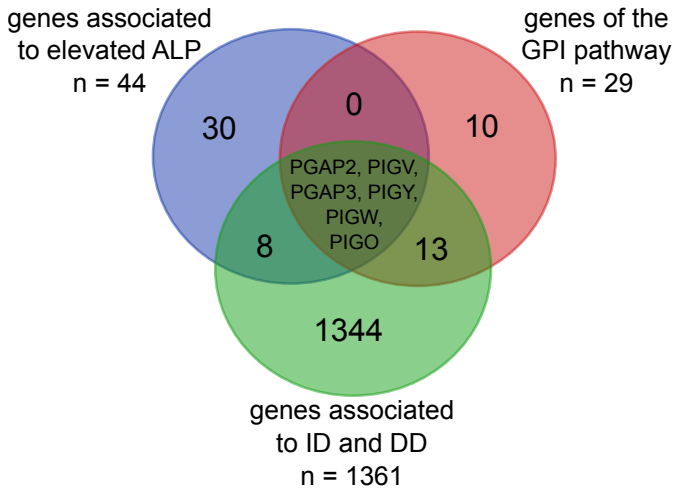

Figure 10. Venn diagram of genes linked to three different HPO terms.
30 genes associated to "increased alkaline phosphatase" are not related to "intellectual disability" nor "global developmental delay". 10 genes of the GPI pathway are not yet associated to any clinical feature.

Therefore, NGS data interpretation should be completed either in collaboration with experienced syndromologists or aided by automated facial analysis and deep phenotyping.

Although the diagnosis of GPIBDs improved over recent years, treatment thereof remained unchanged. Seizures are commonly treated with anticonvulsants such as valproic acid or clonazepam (Thompson et al., 2012) but often remain intractable (Nakamura et al., 2014; Zehavi et al., 2017). However, other reports demonstrated that seizures of individuals affected by HPMRS were controlled by administration of pyridoxine (a precursor of vitamin B6) (Kuki et al., 2013; Sakaguchi et al., 2018; Thompson et al., 2010). Interestingly, pyridoxine is taken up in the liver where it is phosphorylated and released into the blood. Dephosphorylation of pyridoxal 5'-phosphate (PLP) by ALP is important for uptake of pyridoxal into the central nervous system (CNS) where it is critical for gamma-aminobutyric acid (GABA) production (Dakshinamurti, Sharma, & Geiger, 2003) and other biochemical reactions. It remains speculative whether individuals affected by HPMRS or other GPIBDs are suffering from seizures due to impaired vitamin B6 metabolism. Analysis of PLP levels in plas-

ma and cerebro-spinal fluid in GPIBD individuals might reveal whether distorted ALP expression correlates with PLP uptake into the CNS.

As discussed by Manea, (2018) many GPI-APs act in multiple pathways that are important for proper neuronal function. Deficiencies of GPI-APs within the pathways might provide clues for the underlying pathomechanism in GPIBDs and targets for therapeutic intervention. But, in most GPIBD cases the hypomorphic mutations lead to a systemic reduction of GPI-AP expression that may be tissue and GPI-AP specific.

A hypomorphic mutation in *PIGA* has been deeply studied in regard of the pathophysiology of GPIBDs and linked in particular to impaired neuronal differentiation, neuronal dysfunction, and susceptibility to complement-mediated cytotoxicity (Yuan et al., 2017). The combination of variable expression of multiple GPI-APs in various pathways that are altered explain the complex phenotype observed by (Yuan et al., 2017) in PIGA deficient iPSCs (induced pluripotent cells).

Taken together, these data may suggest that the neurological impairment that accompanies inherited GPIBDs may be in part explained by complement-mediated neurodegeneration similar to germline CD59 deficiency. Further iPSC models with different mutated genes of the GPI pathway may elicit which GPI-APs are accountable for neuronal features observed in individuals affected by GPIBDs.

4.3 Conclusion

In this thesis novel techniques for NGS data acquisition and evaluation were developed that aided in the publication of 29 novel cases affected by GPIBDs. The application of these techniques could also be extended to the diagnostic workup of many other rare monogenic disorders and could improve the diagnostic yield of genetic testing in general.

As presented in my publications the application of NGS in combination with facial image analysis and flow cytometry is highly valuable in the identification of yet unknown disease-causing genes and characterization of novel VOUCS in cases of suspected inherited GPIBDs. My work showed that gene-centered classification of GPIBDs should be favored over phenotypic series, as the clinical spectrum within a series can be very broad.

Analogously to inherited GPIBDs, I demonstrated that, flow cytometric analysis with an advanced multicolor panel including T5 antibody should be applied in the diagnosis of PNH in order to determine the disease entity. Furthermore, NGS of patients' blood should be performed to discover driving mutation of the proliferative HSC clone. Hence, therapeutic treatment could be adjusted to the molecular diagnosis.

The current change from gene panel sequencing towards WES and WGS in monogenic disorder diagnostics will return a higher diagnostic yield when the bottleneck of massive data interpretation is tackled by artificial intelligence. Hence, clinicians will be guided by deep phenotyping and automated facial analysis in their diagnostic process. As applied in my work multiple levels of evidence (variant prediction and classification, flow cytometry, biochemical analysis of blood, facial analysis, etc.) should be collected to determine the disease-causing mutation.

Although, the genetic cause of GPIBDs is well understood and further individuals with mutations in genes of the GPI pathway are reported on an annual basis, the main pathomechanisms remain unclear. Significant similarities on the phenotypic level were described for HPMRS and MCAHS, but it is still puzzling why mutations in genes from different parts of the GPI pathway result in similar phenotypic series (cf. HPMRS1 – 4).

Many of the potential biological and biochemical explanations that were discussed in the last part of this thesis will require a more comprehensive analysis in animal

models. Deep phenotyping, as described in this work, might help to elucidate further details of the underlying pathomechanism of GPIBDs.

Finally, based of my research, targets might be identified that are urgently needed for the development of therapeutic approaches.

5 Appendix

5.1 Literature

Abdel-hamid, M. S. S., Issa, M. Y. Y., Otaify, G. . A., Abdel-ghafar, S. F. F., Elbendary, H. M., & Zaki, M. S. (2017). PGAP3-related hyperphosphatasia with mental retardation syndrome: Report of 10 new patients and a homozygous founder mutation. *Clinical Genetics*. https://doi.org/10.1111/cge.13033

Acuna-Hidalgo, R., Veltman, J. A., & Hoischen, A. (2016). New insights into the generation and role of de novo mutations in health and disease. *Genome Biology*, *17*(1), 241. https://doi.org/10.1186/s13059-016-1110-1

Adzhubei, I., Jordan, D. M., & Sunyaev, S. R. (2015). *Predicting Functional Effect of Human Missense Mutations Using PolyPhen-2*. *Current Protocols in Human Genetics* (Vol. 7). https://doi.org/10.1002/0471142905.hg0720s76.Predicting

Akgün Doğan, Ö., Demir, G. Ü., Kosukcu, C., Taskiran, E. Z., Simsek-Kiper, P. Ö., Utine, G. E., … Boduroğlu, K. (2018). Hyperphosphatasia with mental retardation syndrome type 4 In two siblings-expanding the phenotypic and mutational spectrum. *European Journal of Medical Genetics*.

Alfinito, F., Del Vecchio, L., Rocco, S., Boccuni, P., Musto, P., & Rotoli, B. (1996). Blood cell flow cytometry in paroxysmal nocturnal hemoglobinuria: a tool for measuring the extent of the PNH clone. *Leukemia*, *10*(8), 1326–1330.

Almeida, A. M., Murakami, Y., Layton, D. M., Hillmen, P., Sellick, G. S., Maeda, Y., … Karadimitris, A. (2006). Hypomorphic promoter mutation in PIGM causes inherited glycosylphosphatidylinositol deficiency. *Nat Med*, *12*(7), 846–851. https://doi.org/10.1038/nm1410

Altassan, R., Fox, S., Poulin, C., & Buhas, D. (2018). Hyperphosphatasia with mental retardation syndrome, expanded phenotype of PIGL related disorders. *Molecular Genetics and Metabolism Reports*, *15*(December 2017), 46–49. https://doi.org/10.1016/j.ymgmr.2018.01.007

Andrey, G., & Mundlos, S. (2017). The three-dimensional genome: regulating gene expression during pluripotency and development. *Development*, *144*(20), 3646 LP – 3658.

Anliker, M., von Zabern, I., Höchsmann, B., Kyrieleis, H., Dohna-Schwake, C., Flegel, W. A., … Weinstock, C. (2014). A new blood group antigen is defined by anti-CD59, detected in a CD59-deficient patient. *Transfusion*, *54*(7), 1817–1822.

Ashida, H., Hong, Y., Murakami, Y., Shishioh, N., Sugimoto, N., Kim, Y. U., … Kinoshita, T. (2005). Mammalian PIG-X and Yeast Pbn1p Are the Essential Components of Glycosylphosphatidylinositol-Mannosyltransferase I. *Molecular Biology of the Cell*, *16*(3), 1439–1448. https://doi.org/10.1091/mbc.E04-09-0802

Aziz, A., Baxter, E. J., Edwards, C., Cheong, C. Y., Ito, M., Bench, A., … Green, A. R. (2013). Cooperativity of imprinted genes inactivated by acquired chromosome 20q deletions. *Journal of Clinical Investigation*, *123*(5), 2169–2182. https://doi.org/10.1172/JCI66113

Azzouz, N., Shams-Eldin, H., Niehus, S., Debierre-Grockiego, F., Bieker, U., Schmidt, J., … Schwarz, R. T. (2006). Toxoplasma gondii grown in human cells uses GalNAc-containing glycosylphosphatidylinositol precursors to anchor surface antigens while the immunogenic Glc-GalNAc-containing precursors remain free at the parasite cell surface. *International Journal of Biochemistry and Cell Biology*, *38*(11), 1914–1925. https://doi.org/10.1016/j.biocel.2006.05.006

Baldwin, M. A. (2006). Analysis of glycosylphosphatidylinositol protein anchors: The prion protein. *Methods in Enzymology*, *405*(05), 172–187. https://doi.org/10.1016/S0076-6879(05)05008-1

Balobaid, A., Ben-Omran, T., Ramzan, K., Altassan, R., Almureikhi, M., Musa, S., … Al-Sayed, M. (2018). Delineating the phenotypic spectrum of hyperphosphatasia with mental retardation syndrome 4 in 14 patients of Middle-Eastern origin. *American Journal of Medical Genetics Part A*. https://doi.org/10.1002/ajmg.a.40627

Barone, R., Aiello, C., Race, V., Morava, E., Foulquier, F., Riemersma, M., … Lefeber, D. J. (2012). DPM2-CDG: A muscular dystrophy-dystroglycanopathy syndrome with severe epilepsy. *Annals of Neurology*, *72*(4), 550–558. https://doi.org/10.1002/ana.23632

Bauer, S., Köhler, S., Schulz, M. H., & Robinson, P. N. (2012). Bayesian ontology querying for accurate and noise-tolerant semantic searches. *Bioinformatics (Oxford, England)*, *28*(19), 2502–2508.

https://doi.org/10.1093/bioinformatics/bts471

Belet, S., Fieremans, N., Yuan, X., Van Esch, H., Verbeeck, J., Ye, Z., … Froyen, G. (2014). Early frameshift mutation in PIGA identified in a large XLID family without neonatal lethality. *Human Mutation*, *35*(3), 350–355. https://doi.org/10.1002/humu.22498

Bellai-Dussault, K., Nguyen, T. T. M., Baratang, N. V., Jimenez-Cruz, D. A., & Campeau, P. M. (2018). Clinical variability in inherited glycosylphosphatidylinositol deficiency disorders. *Clinical Genetics*, *95*(1), 112–121. https://doi.org/10.1111/cge.13425

Ben-Zeev, B., Tabib, A., Nissenkorn, A., Garti, B.-Z., Gomori, J. M., Nass, D., … Mevorach, D. (2015). Devastating recurrent brain ischemic infarctions and retinal disease in pediatric patients with CD59 deficiency. *European Journal of Paediatric Neurology : EJPN : Official Journal of the European Paediatric Neurology Society*, *19*(6), 688–693.

Bentley, D. R., Balasubramanian, S., Swerdlow, H. P., Smith, G. P., Milton, J., Brown, C. G., … Smith, A. J. (2008). Accurate whole human genome sequencing using reversible terminator chemistry. *Nature*, *456*(7218), 53–59. https://doi.org/10.1038/nature07517

Besenbacher, S., Liu, S., Izarzugaza, J. M. G., Grove, J., Belling, K., Bork-Jensen, J., … Rasmussen, S. (2015). Novel variation and de novo mutation rates in population-wide de novo assembled Danish trios. *Nature Communications*, *6*, 5969. https://doi.org/10.1038/ncomms6969

Bessler, M., Mason, P. J., Hillmen, P., Miyata, T., Yamada, N., & Takeda, J. (1994). Paroxysmal nocturnal haemoglobinuria (PNH) is caused by somatic mutations in the PIG-A gene. *EMBO J*, *13*.

Bonnon, C., Wendeler, M. W., Paccaud, J.-P., & Hauri, H.-P. (2010). Selective export of human GPI-anchored proteins from the endoplasmic reticulum. *Journal of Cell Science*, *123*(Pt 10), 1705–1715. https://doi.org/10.1242/jcs.062950

Bosch, D. G. M., Boonstra, F. N., Kinoshita, T., Jhangiani, S., De Ligt, J., Cremers, F. P. M., … De Vries, B. B. A. (2015). Cerebral visual impairment and intellectual disability caused by PGAP1 variants. *European Journal of Human Genetics*, *23*(12), 1689–1693. https://doi.org/10.1038/ejhg.2015.42

Boyle, A. P., Hong, E. L., Hariharan, M., Cheng, Y., Schaub, M. A., Kasowski, M., … Snyder, M. (2012). Annotation of functional variation in personal genomes using RegulomeDB. *Genome Research*, *22*(9), 1790–1797. https://doi.org/10.1101/gr.137323.112

Brady, P. D., Moerman, P., De Catte, L., Deprest, J., Devriendt, K., & Vermeesch, J. R. (2014). Exome sequencing identifies a recessive PIGN splice site mutation as a cause of syndromic Congenital Diaphragmatic Hernia. *European Journal of Medical Genetics*, *57*(9), 487–493. https://doi.org/10.1016/j.ejmg.2014.05.001

Brodsky, R. A. (2008). Paroxysmal nocturnal hemoglobinuria: stem cells and clonality. *Hematology / the Education Program of the American Society of Hematology. American Society of Hematology. Education Program*, 111–115. https://doi.org/10.1182/asheducation-2008.1.111

Brodsky, R. A., Mukhina, G. L., Li, S., Nelson, K. L., Chiurazzi, P. L., Buckley, J. T., & Borowitz, M. J. (2000). Improved detection and characterization of paroxysmal nocturnal hemoglobinuria using fluorescent aerolysin. *American Journal of Clinical Pathology*, *114*(3), 459–466. https://doi.org/10.1093/ajcp/114.3.459

Bronner, I. F., Quail, M. A., Turner, D. J., & Swerdlow, H. (2009). *Europe PMC Funders Group Improved Protocols for Illumina Sequencing*. *Current Protocols in Human Genetics* (Vol. 18). https://doi.org/10.1002/0471142905.hg1802s62.Improved

Brunt, J. Van. (1988). What's in a face? *Nature*, *6*(10), 1151–1156.

Ceroni, J. R., Yamamoto, G. L., Honjo, R. S., Kim, C. A., Passos-Bueno, M. R., & Bertola, D. R. (2018). Large deletion in PIGL: a common mutational mechanism in CHIME syndrome? *Genetics and Molecular Biology*, *41*(1), 85–91. https://doi.org/10.1590/1678-4685-GMB-2017-0172

Chiyonobu, T., Inoue, N., Morimoto, M., Kinoshita, T., & Murakami, Y. (2014). Glycosylphosphatidylinositol (GPI) anchor deficiency caused by mutations in PIGW is associated with West syndrome and hyperphosphatasia with mental retardation syndrome. *Journal of Medical Genetics*, *51*(3), 203–207. https://doi.org/10.1136/jmedgenet-2013-102156

Cole, D. E. C., & Whyte, M. P. (1997). Hyperphosphatasia syndromes, Chapter 15. In *Studies in Stomatology and Craniofacial Biology* (pp. 245–272).

Consortium, Gte. (2015). The Genotype-Tissue Expression (GTEx) pilot analysis:

Multitissue gene regulation in humans. *Science (New York, N.Y.)*, *348*(6235), 648–660. https://doi.org/10.1126/science.1262110

Consortium, T. 1000 G. P. (2015). A global reference for human genetic variation. *Nature*, *526*, 68.

Consortium, T. U. (2015). The UK10K project identifies rare variants in health and disease. *Nature*, *526*, 82.

Cooper, G. M., & Shendure, J. (2011). Needles in stacks of needles: Finding disease-causal variants in a wealth of genomic data. *Nature Reviews Genetics*, *12*(9), 628–640. https://doi.org/10.1038/nrg3046

Dakshinamurti, K., Sharma, S. K., & Geiger, J. D. (2003). Neuroprotective actions of pyridoxine. *Biochimica et Biophysica Acta*, *1647*(1–2), 225–229.

Danecek, P., Auton, A., Abecasis, G., Albers, C. A., Banks, E., DePristo, M. A., … Durbin, R. (2011). The variant call format and VCFtools. *Bioinformatics*, *27*(15), 2156–2158. https://doi.org/10.1093/bioinformatics/btr330

Daniels, Green, Mallinson, Okubo, Hori, Kataoka, & Kaihara. (1998). Decay-accelerating factor (CD55) deficiency phenotypes in Japanese. *Transfusion Medicine*, *8*(2), 141–147. https://doi.org/10.1046/j.1365-3148.1998.00145.x

Davis, E. M., Kim, J., Menasche, B. L., Sheppard, J., Liu, X., Tan, A. C., & Shen, J. (2015). Comparative Haploid Genetic Screens Reveal Divergent Pathways in the Biogenesis and Trafficking of Glycophosphatidylinositol-Anchored Proteins. *Cell Reports*, *11*(11), 1727–1736. https://doi.org/10.1016/j.celrep.2015.05.026

Edvardson, S., Murakami, Y., Nguyen, T. T. M., Shahrour, M., St-Denis, A., Shaag, A., … Elpeleg, O. (2017). Mutations in the phosphatidylinositol glycan C (PIGC) gene are associated with epilepsy and intellectual disability. *Journal of Medical Genetics*, *54*(3), 196–201. https://doi.org/10.1136/jmedgenet-2016-104202

Eisenhaber, B., & Eisenhaber, F. (2007). Posttranslational modifications and subcellular localization signals: indicators of sequence regions without inherent 3D structure? *Current Protein & Peptide Science*, *8*(2), 197–203. https://doi.org/10.2174/138920307780363424

Eisenhaber, B., Sinha, S., Wong, W.-C., & Eisenhaber, F. (2018). Function of a membrane-embedded domain evolutionarily multiplied in the GPI lipid anchor pathway proteins PIG-B, PIG-M, PIG-U, PIG-W, PIG-V, and PIG-Z. *Cell Cycle*

(Georgetown, Tex.), *17*(7), 874–880. https://doi.org/10.1080/15384101.2018.1456294

Eisenhaber, F., Eisenhaber, B., Kubina, W., Maurer-Stroh, S., Neuberger, G., Schneider, G., & Wildpaner, M. (2003). Prediction of lipid posttranslational modifications and localization signals from protein sequences: Big-Π, NMT and PTS1. *Nucleic Acids Research*, *31*(13), 3631–3634. https://doi.org/10.1093/nar/gkg537

Enneking, J. (1928). Eine Neue form Intermittierender Hämoglobinurie. *Klinische Wochenschrift*, *7*(43), 2045–2047. https://doi.org/10.1007/BF01846778

Fauth, C., Steindl, K., Toutain, A., Farrell, S., Witsch-Baumgartner, M., Karall, D., … Rauch, A. (2016). A recurrent germline mutation in the PIGA gene causes Simpson-Golabi-Behmel syndrome type 2. *American Journal of Medical Genetics Part A*, *170*(2), 392–402. https://doi.org/10.1002/ajmg.a.37452

Felekkis, K., Touvana, E., Stefanou, C., & Deltas, C. (2010). microRNAs: a newly described class of encoded molecules that play a role in health and disease. *Hippokratia*, *14*(4), 236–240.

Ferry, Q., Steinberg, J., Webber, C., Fitzpatrick, D. R., Ponting, C. P., Zisserman, A., & Nellåker, C. (2014). Diagnostically relevant facial gestalt information from ordinary photos. *ELife*, 1–22. https://doi.org/10.7554/eLife.02020

Fleming, L., Lemmon, M., Beck, N., Johnson, M., Mu, W., Murdock, D., … Hamosh, A. (2016). Genotype-phenotype correlation of congenital anomalies in multiple congenital anomalies hypotonia seizures syndrome (MCAHS1)/PIGN -related epilepsy. *American Journal of Medical Genetics Part A*, *170*(1), 77–86. https://doi.org/10.1002/ajmg.a.37369

Fletcher, M., Whitby, L., Whitby, A., & Barnett, D. (2016). Current international flow cytometric practices for the detection and monitoring of paroxysmal nocturnal haemoglobinuria clones: A UK NEQAS survey. *Cytometry Part B: Clinical Cytometry*, n/a-n/a. https://doi.org/10.1002/cyto.b.21368

Fokkema, I. F. A. C., Taschner, P. E. M., Schaafsma, G. C. P., Celli, J., Laros, J. F. J., & den Dunnen, J. T. (2011). LOVD v.2.0: The next generation in gene variant databases. *Human Mutation*, *32*(5), 557–563. https://doi.org/10.1002/humu.21438

Fu, L., Liu, Y., Chen, Y., Yuan, Y., & Wei, W. (2019). Mutations in the PIGW gene associated with hyperphosphatasia and mental retardation syndrome: a case report. *BMC Pediatrics*, *19*(1), 68. https://doi.org/10.1186/s12887-019-1440-8

Fujihara, Y., & Ikawa, M. (2015). GPI-AP release in cellular, developmental, and reproductive biology. *Journal of Lipid Research*.

Fujita, M., & Kinoshita, T. (2012). GPI-anchor remodeling: Potential functions of GPI-anchors in intracellular trafficking and membrane dynamics. *Biochimica et Biophysica Acta - Molecular and Cell Biology of Lipids*, *1821*(8), 1050–1058. https://doi.org/10.1016/j.bbalip.2012.01.004

Fujita, M., Maeda, Y., Ra, M., Yamaguchi, Y., Taguchi, R., & Kinoshita, T. (2009). GPI Glycan Remodeling by PGAP5 Regulates Transport of GPI-Anchored Proteins from the ER to the Golgi. *Cell*, *139*(2), 352–365. https://doi.org/10.1016/j.cell.2009.08.040

Fujita, M., Watanabe, R., Jaensch, N., Romanova-Michaelides, M., Satoh, T., Kato, M., … Kinoshita, T. (2011). Sorting of GPI-anchored proteins into ER exit sites by p24 proteins is dependent on remodeled GPI. *The Journal of Cell Biology*, *194*(1), 61–75.

Fujiwara, I., Murakami, Y., Niihori, T., Kanno, J., Hakoda, A., Sakamoto, O., … Aoki, Y. (2015). Mutations in PIGL in a patient with Mabry syndrome. *American Journal of Medical Genetics, Part A*, *167*(4). https://doi.org/10.1002/ajmg.a.36987

Garrison, E., & Marth, G. (2012). Haplotype-based variant detection from short-read sequencing.

Gloss, B. S., & Dinger, M. E. (2018). Realizing the significance of noncoding functionality in clinical genomics. *Experimental & Molecular Medicine*, *50*(8), 97. https://doi.org/10.1038/s12276-018-0087-0

Grimme, S. J., Westfall, B. A., Wiedman, J. M., Taron, C. H., & Orlean, P. (2001). The essential Smp3 protein is required for addition of the side-branching fourth mannose during assembly of yeast glycosylphosphatidylinositols. *The Journal of Biological Chemistry*, *276*(29), 27731–27739. https://doi.org/10.1074/jbc.M101986200

Gripp, K. W., Baker, L., Telegrafi, A., & Monaghan, K. G. (2016). The role of objective facial analysis using FDNA in making diagnoses following whole exome analysis.

Report of two patients with mutations in the BAF complex genes. *American Journal of Medical Genetics Part A*, *170*(7), 1754–1762. https://doi.org/10.1002/ajmg.a.37672

Gurovich, Y., Hanani, Y., Bar, O., Fleischer, N., Gelbman, D., Basel-Salmon, L., … Gripp, K. W. (2018). DeepGestalt - Identifying Rare Genetic Syndromes Using Deep Learning.

Haliloglu, G., Maluenda, J., Sayinbatur, B., Aumont, C., Temucin, C., Tavil, B., … Aumont, C. (2015). Early-onset chronic axonal neuropathy, strokes, and hemolysis: Inherited CD59 deficiency. *Neurology*, *84*(12), 1220–1225. https://doi.org/10.1212/WNL.0000000000001391

Hansen, L., Tawamie, H., Murakami, Y., Mang, Y., ur Rehman, S., Buchert, R., … Abou Jamra, R. (2013). Hypomorphic mutations in PGAP2, encoding a GPI-anchor-remodeling protein, cause autosomal-recessive intellectual disability. *American Journal of Human Genetics*, *92*(4), 575–583. https://doi.org/10.1016/j.ajhg.2013.03.008

Hennekam, R. C. M., & Biesecker, L. G. (2012). Next Generation Sequencing Demands Next Generation Phenotyping. *Human Mutation*, *33*(5), 884–886. https://doi.org/10.1002/humu.22048

Hill, A., DeZern, A. E., Kinoshita, T., & Brodsky, R. A. (2017). Paroxysmal nocturnal haemoglobinuria. *Nature Reviews Disease Primers*, *3*, 17028. https://doi.org/10.1038/nrdp.2017.28

Hill, A., Kelly, R. J., & Hillmen, P. (2013). Thrombosis in paroxysmal nocturnal hemoglobinuria. *Blood*, *121*(25), 4985–96. https://doi.org/10.1182/blood-2012-09-311381.PNH

Hillmen, P., Hows, J. M., & Luzzatto, L. (1992). Two distinct patterns of glycosylphosphatidylinositol (GPI) linked protein deficiency in the red cells of patients with paroxysmal nocturnal haemoglobinuria. *British Journal of Haematology*, *80*(3), 399–405. https://doi.org/10.1111/j.1365-2141.1992.tb08151.x

Hirata, T., Mishra, S. K., Nakamura, S., Saito, K., Motooka, D., Takada, Y., … Kinoshita, T. (2018). Identification of a Golgi GPI-N-acetylgalactosamine transferase with tandem transmembrane regions in the catalytic domain. *Nature*

Communications 2018 9:1, *9*(1), 405. https://doi.org/10.1038/s41467-017-02799-0

Höchsmann, B., & Schrezenmeier, H. (2015). Congenital CD59 Deficiency. *Hematology/Oncology Clinics of North America*, *29*(3), 495–507.

Hoechsmann, B., Murakami, Y., Osato, M., Knaus, A., Kawamoto, M., Inoue, N., … Kinoshita, T. (2019). *Complement- and inflammasome-mediated autoinflammation-paroxysmal autoinflammation-paroxysmal nocturnal hemoglobinuria*. *PNAS* (Vol. in review).

Hogrebe, M., Murakami, Y., Wild, M., Ahlmann, M., Biskup, S., Hörtnagel, K., … Marquardt, T. (2016). A novel mutation in PIGW causes glycosylphosphatidylinositol deficiency without hyperphosphatasia. *American Journal of Medical Genetics. Part A*, *170*(12), 3319–3322. https://doi.org/https://dx.doi.org/10.1002/ajmg.a.37950

Homans, S. W., Ferguson, M. a, Dwek, R. a, Rademacher, T. W., Anand, R., & Williams, a F. (1988). Complete structure of the glycosyl phosphatidylinositol membrane anchor of rat brain Thy-1 glycoprotein. *Nature*, *333*(6170), 269–272. https://doi.org/10.1038/333269a0

Hong, Y., Maeda, Y., Watanabe, R., Inoue, N., Ohishi, K., & Kinoshita, T. (2000). Requirement of PIG-F and PIG-O for Transferring Phosphoethanolamine to the Third Mannose in Glycosylphosphatidylinositol. *Journal of Biological Chemistry*, *275*(27), 20911–20919. https://doi.org/10.1074/jbc.M001913200

Hong, Y., Maeda, Y., Watanabe, R., Ohishi, K., Mishkind, M., Riezman, H., & Kinoshita, T. (1999). Pig-n, a mammalian homologue of yeast Mcd4p, is involved in transferring phosphoethanolamine to the first mannose of the glycosylphosphatidylinositol. *Journal of Biological Chemistry*, *274*(49), 35099–35106. https://doi.org/10.1074/jbc.274.49.35099

Hong, Y., Ohishi, K., Kang, J. Y., Tanaka, S., Inoue, N., Nishimura, J., … Kinoshita, T. (2003). Human PIG-U and Yeast Cdc91p Are the Fifth Subunit of GPI Transamidase That Attaches GPI-Anchors to Proteins. *Molecular Biology of the Cell*, *14*(5), 1780–1789. https://doi.org/10.1091/mbc.E02-12-0794

Horn, D., Krawitz, P., Mannhardt, A., Korenke, G. C., & Meinecke, P. (2011). Hyperphosphatasia-mental retardation syndrome due to PIGV mutations:

expanded clinical spectrum. *American Journal of Medical Genetics Part A*, *155A*(8), 1917–1922.

Horn, D., Schottmann, G., & Meinecke, P. (2010). Hyperphosphatasia with mental retardation, brachytelephalangy, and a distinct facial gestalt: Delineation of a recognizable syndrome. *European Journal of Medical Genetics*, *53*(2), 85–88.

Howard, M. F., Murakami, Y., Pagnamenta, A. T., Daumer-Haas, C., Fischer, B., Hecht, J., … Krawitz, P. M. (2014). Mutations in PGAP3 Impair GPI-Anchor Maturation, Causing a Subtype of Hyperphosphatasia with Mental Retardation. *The American Journal of Human Genetics*, *94*(2), 278–287. https://doi.org/10.1016/j.ajhg.2013.12.012

Hsieh, T.-C., Mensah, M. A., Pantel, J. T., consortium, P., & Krawitz, P. (2018). PEDIA: Prioritization of Exome Data by Image Analysis. *BioRxiv*, 473306. https://doi.org/10.1101/473306

Ihara, S., Nakayama, S., Murakami, Y., Suzuki, E., Asakawa, M., Kinoshita, T., & Sawa, H. (2017). PIGN prevents protein aggregation in the endoplasmic reticulum independently of its function in the GPI synthesis. *Journal of Cell Science*, *130*(3).

Ikezawa, H. (2002). Glycosylphosphatidylinositol (GPI)-anchored proteins. *Biological & Pharmaceutical Bulletin*, *25*(4), 409–417.

Ilkovski, B., Pagnamenta, A. T., O'Grady, G. L., Kinoshita, T., Howard, M. F., Lek, M., … Clarke, N. F. (2015). Mutations in PIGY: expanding the phenotype of inherited glycosylphosphatidylinositol deficiencies. *Human Molecular Genetics*, *24*(21), 6146–6159. https://doi.org/10.1093/hmg/ddv331

Inoue, N., Izui-Sarumaru, T., Murakami, Y., Endo, Y., Nishimura, J.-I., Kurokawa, K., … Kinoshita, T. (2006). Molecular basis of clonal expansion of hematopoiesis in 2 patients with paroxysmal nocturnal hemoglobinuria (PNH). *Blood*, *108*(13), 4232–4236. https://doi.org/10.1182/blood-2006-05-025148

Jäger, M., Wang, K., Bauer, S., Smedley, D., Krawitz, P., & Robinson, P. N. (2014). Jannovar: A Java Library for Exome Annotation. *Human Mutation*, *35*(5), 548–555. https://doi.org/10.1002/humu.22531

Jezela-Stanek, A., Ciara, E., Piekutowska-Abramczuk, D., Trubicka, J., Jurkiewicz, E., Rokicki, D., … Pronicka, E. (2016). Congenital disorder of

glycosylphosphatidylinositol (GPI)-anchor biosynthesis - The phenotype of two patients with novel mutations in the PIGN and PGAP2 genes. *European Journal of Paediatric Neurology*, *20*(3), 462–473. https://doi.org/10.1016/j.ejpn.2016.01.007

Johnston, J. J. J., Gropman, A. L. L., Sapp, J. C. C., Teer, J. K. K., Martin, J. M. M., Liu, C. F. F., … Biesecker, L. G. (2012). *The Phenotype of a Germline Mutation in PIGA: The Gene Somatically Mutated in Paroxysmal Nocturnal Hemoglobinuria*. *The American Journal of Human Genetics* (Vol. 90). https://doi.org/10.1016/j.ajhg.2011.11.031

Johnstone, D. L., Nguyen, T.-T.-M., Murakami, Y., Kernohan, K. D., Tétreault, M., Goldsmith, C., … Campeau, P. M. (2017). Compound heterozygous mutations in the gene PIGP are associated with early infantile epileptic encephalopathy. *Human Molecular Genetics*, *26*(9), 1706–1715. https://doi.org/10.1093/hmg/ddx077

Kamphans, T., & Krawitz, P. M. (2012). GeneTalk: An expert exchange platform for assessing rare sequence variants in personal genomes. *Bioinformatics*, *28*(19), 2515–2516. https://doi.org/10.1093/bioinformatics/bts462

Kamphans, T., Sabri, P., Zhu, N., Heinrich, V., Mundlos, S., Robinson, P. N., … Krawitz, P. M. (2013). Filtering for Compound Heterozygous Sequence Variants in Non-Consanguineous Pedigrees. *PLoS ONE*, *8*(8), 1–6. https://doi.org/10.1371/journal.pone.0070151

Kang, J. Y., Hong, Y., Ashida, H., Shishioh, N., Murakami, Y., Morita, Y. S., … Kinoshita, T. (2005). PIG-V Involved in Transferring the Second Mannose in Glycosylphosphatidylinositol. *Journal of Biological Chemistry*, *280*(10), 9489–9497. https://doi.org/10.1074/jbc.M413867200

Kato, M., Saitsu, H., Murakami, Y., Kikuchi, K., Watanabe, S., Iai, M., … Matsumoto, N. (2014). PIGA mutations cause early-onset epileptic encephalopathies and distinctive features. *Neurology*, *82*(18), 1587–1596. https://doi.org/10.1212/WNL.0000000000000389

Kawamoto, M., Murakami, Y., Kinoshita, T., & Kohara, N. (2018). Recurrent aseptic meningitis with PIGT mutations: a novel pathogenesis of recurrent meningitis successfully treated by eculizumab. *BMJ Case Reports*, *2018*.

https://doi.org/10.1136/bcr-2018-225910

Kettwig, M., Elpeleg, O., Wegener, E., Dreha-Kulaczewski, S., Henneke, M., Gärtner, J., & Huppke, P. (2016). Compound heterozygous variants in PGAP1 causing severe psychomotor retardation, brain atrophy, recurrent apneas and delayed myelination: a case report and literature review. *BMC Neurology*, *16*, 74. https://doi.org/10.1186/s12883-016-0602-7

Khayat, M., Tilghman, J. M., Chervinsky, I., Zalman, L., Chakravarti, A., & Shalev, S. A. (2016). A PIGN mutation responsible for multiple congenital anomalies-hypotonia-seizures syndrome 1 (MCAHS1) in an Israeli-Arab family. *American Journal of Medical Genetics, Part A*, *170*(1), 176–182. https://doi.org/10.1002/ajmg.a.37375

Kim, Y. O., Yang, J. H., Park, C., Kim, S. K., Kim, M.-K., Shin, M.-G., & Woo, Y. J. (2016). A novel PIGA mutation in a family with X-linked, early-onset epileptic encephalopathy. *Brain and Development*, *38*(8), 750–754. https://doi.org/10.1016/j.braindev.2016.02.008

Kimura, H., Kato, M., Ikeda, M., Nagai, A., Okada, Y., Naito, S., … Morikawa, A. (2003). Sulfonated human immunoglobulin enhances CD16-linked CD11b expression on human neutrophils. *Cell Biology International*, *27*(11), 913–919.

Kinoshita, T. (2014). Biosynthesis and deficiencies of glycosylphosphatidylinositol. *Proceedings of the Japan Academy. Series B, Physical and Biological Sciences*, *90*(4), 130–143. https://doi.org/10.2183/pjab.90.130

Kinoshita, T., & Fujita, M. (2015). Biosynthesis of GPI-anchored proteins: special emphasis on GPI lipid remodeling. *Journal of Lipid Research*.

Kinoshita, T., Fujita, M., & Maeda, Y. (2008). Biosynthesis, remodelling and functions of mammalian GPI-anchored proteins: recent progress. *Journal of Biochemistry*, *144*(3), 287–294.

Kircher, M., Witten, D. M., Jain, P., O'Roak, B. J., Cooper, G. M., Shendure, J., … Shendure, J. (2014). A general framework for estimating the relative pathogenicity of human genetic variants. *Nature Genetics*, *46*(3), 310–315. https://doi.org/10.1038/ng.2892

Klemann, C., Kirschner, J., Ammann, S., Urbach, H., Moske-Eick, O., Zieger, B., … Korinthenberg, R. (2018). CD59 deficiency presenting as polyneuropathy and

Moyamoya syndrome with endothelial abnormalities of small brain vessels. *European Journal of Paediatric Neurology*, *22*(5), 870–877. https://doi.org/10.1016/j.ejpn.2018.04.003

Knaus, A., Awaya, T., Helbig, I., Afawi, Z., Pendziwiat, M., Abu-Rachma, J., … Krawitz, P. M. (2016). Rare Noncoding Mutations Extend the Mutational Spectrum in the PGAP3 Subtype of Hyperphosphatasia with Mental Retardation Syndrome. *Human Mutation*, *37*(8), 737–744. https://doi.org/10.1002/humu.23006

Knaus, A., Pantel, J. T., Pendziwiat, M., Hajjir, N., Zhao, M., Hsieh, T. C., … Krawitz, P. M. (2018). Characterization of glycosylphosphatidylinositol biosynthesis defects by clinical features, flow cytometry, and automated image analysis. *Genome Medicine*, *10*(1), 3. https://doi.org/10.1186/s13073-017-0510-5

Köhler, S., Schulz, M. H., Krawitz, P., Bauer, S., Dölken, S., Ott, C. E., … Robinson, P. N. (2009). Clinical Diagnostics in Human Genetics with Semantic Similarity Searches in Ontologies. *The American Journal of Human Genetics*, *85*(4), 457–464. https://doi.org/10.1016/j.ajhg.2009.09.003

Köhler, S., Vasilevsky, N. A., Engelstad, M., Foster, E., McMurry, J., Aymé, S., … Robinson, P. N. (2017). The human phenotype ontology in 2017. *Nucleic Acids Research*, *45*(D1). https://doi.org/10.1093/nar/gkw1039

Krawitz, P. M. (2016). *Aufklärung der genetischen Ursache von Glykosylphosphatidylinositol (GPI)-Ankerstörungen mittels Hochdurchsatz-Sequenzierung*. Freie Universität Berlin, Germany.

Krawitz, P. M., Höchsmann, B., Murakami, Y., Teubner, B., Krüger, U., Klopocki, E., … Schrezenmeier, H. (2013). A case of paroxysmal nocturnal hemoglobinuria caused by a germline mutation and a somatic mutation in PIGT. *Blood*, *122*(7), 1312–1315. https://doi.org/10.1182/blood-2013-01-481499

Krawitz, P. M., Murakami, Y., Hecht, J., Krüger, U., Holder, S. E., Mortier, G. R., … Horn, D. (2012). Mutations in PIGO, a member of the GPI-anchor-synthesis pathway, cause hyperphosphatasia with mental retardation. *American Journal of Human Genetics*, *91*(1), 146–151. https://doi.org/10.1016/j.ajhg.2012.05.004

Krawitz, P. M., Schweiger, M. R., Rödelsperger, C., Marcelis, C., Kölsch, U., Meisel, C., … Robinson, P. N. (2010). Identity-by-descent filtering of exome sequence data identifies PIGV mutations in hyperphosphatasia mental retardation syndrome.

Nature Genetics, *42*(10), 827–829. https://doi.org/10.1038/ng.653

Kruse, K., Hanefeld, F., Kohlschütter, A., Rosskamp, R., & Gross-Selbeck, G. (1988). Hyperphosphatasia with mental retardation. *The Journal of Pediatrics*, *112*(3), 436–439. https://doi.org/10.1016/S0022-3476(88)80331-7

Kuki, I., Takahashi, Y., Okazaki, S., Kawawaki, H., Ehara, E., Inoue, N., … Murakami, Y. (2013). Vitamin B6-responsive epilepsy due to inherited GPI deficiency. *Neurology*, *81*(16), 1467–1469. https://doi.org/10.1212/WNL.0b013e3182a8411a

Kumar, P., Henikoff, S., & Ng, P. C. (2009). Predicting the effects of coding non-synonymous variants on protein function using the SIFT algorithm. *Nat Protoc*, *4*. https://doi.org/10.1038/nprot.2009.86

Kuru, K., Niranjan, M., Tunca, Y., Osvank, E., & Azim, T. (2014). Biomedical visual data analysis to build an intelligent diagnostic decision support system in medical genetics. *Artificial Intelligence in Medicine*, *62*(2), 105–118. https://doi.org/https://doi.org/10.1016/j.artmed.2014.08.003

Kvarnung, M., Nilsson, D., Lindstrand, A., Korenke, G. C., Chiang, S. C. C., Blennow, E., … Nordgren, A. (2013). A novel intellectual disability syndrome caused by GPI anchor deficiency due to homozygous mutations in PIGT. *Journal of Medical Genetics*, *50*(8), 521–528. https://doi.org/10.1136/jmedgenet-2013-101654

Lam, C., Golas, G. A., Davids, M., Huizing, M., Kane, M. S., Krasnewich, D. M., … Wolfe, L. A. (2015). Expanding the clinical and molecular characteristics of PIGT-CDG, a disorder of glycosylphosphatidylinositol anchors. *Molecular Genetics and Metabolism*, *115*(2–3), 128–140.

Landrum, M. J., Lee, J. M., Riley, G. R., Jang, W., Rubinstein, W. S., Church, D. M., & Maglott, D. R. (2014). ClinVar: Public archive of relationships among sequence variation and human phenotype. *Nucleic Acids Research*, *42*(D1), 1–6. https://doi.org/10.1093/nar/gkt1113

Langmead, B., Trapnell, C., Pop, M., & Salzberg, S. L. (2009). Ultrafast and memory-efficient alignment of short DNA sequences to the human genome. *Genome Biology*, *10*(3). https://doi.org/10.1186/gb-2009-10-3-r25

Lee, G.-H., Fujita, M., Takaoka, K., Murakami, Y., Fujihara, Y., Kanzawa, N., … Kinoshita, T. (2016). A GPI processing phospholipase A2, PGAP6, modulates

Nodal signaling in embryos by shedding CRIPTO. *Journal of Cell Biology*, *215*(5), 705–718. https://doi.org/10.1083/jcb.201605121

Lee, T. I., & Young, R. A. (2013). Transcriptional Regulation and its Misregulation in Disease. *Cell*, *152*(6), 1237–1251. https://doi.org/10.1016/j.cell.2013.02.014

Lek, M., Karczewski, K. J., Minikel, E. V., Samocha, K. E., Banks, E., Fennell, T., … MacArthur, D. G. (2016). Analysis of protein-coding genetic variation in 60,706 humans. *Nature*, *536*(7616), 285–291. https://doi.org/10.1038/nature19057

Li, H., & Durbin, R. (2009). Fast and accurate short read alignment with Burrows-Wheeler transform. *Bioinformatics*, *25*(14), 1754–1760. https://doi.org/10.1093/bioinformatics/btp324

Li, H., Handsaker, B., Wysoker, A., Fennell, T., Ruan, J., Homer, N., … Durbin, R. (2009). The Sequence Alignment/Map format and SAMtools. *Bioinformatics*, *25*(16), 2078–2079. https://doi.org/10.1093/bioinformatics/btp352

Li, J., Bench, A. J., Vassiliou, G. S., Fourouclas, N., Ferguson-Smith, A. C., & Green, A. R. (2004). Imprinting of the human L3MBTL gene, a polycomb family member located in a region of chromosome 20 deleted in human myeloid malignancies. *Proceedings of the National Academy of Sciences of the United States of America*, *101*(19), 7341–7346. https://doi.org/10.1073/pnas.0308195101

Lin, W. De, Chou, I. C., Tsai, F. J., & Hong, S. Y. (2018). A novel PIGA mutation in a Taiwanese family with early-onset epileptic encephalopathy. *Seizure*, *58*, 52–54. https://doi.org/10.1016/j.seizure.2018.03.025

Liu, Y. S., Guo, X. Y., Hirata, T., Rong, Y., Motooka, D., Kitajima, T., … Fujita, M. (2018). N-Glycan-dependent protein folding and endoplasmic reticulum retention regulate GPI-anchor processing. *Journal of Cell Biology*, *217*(2), 585–599. https://doi.org/10.1083/jcb.201706135

Lohmann, K., & Klein, C. (2014). Next Generation Sequencing and the Future of Genetic Diagnosis. *Neurotherapeutics*, *11*(4), 699–707. https://doi.org/10.1007/s13311-014-0288-8

Loos, H. S., Wieczorek, D., Würtz, R. P., von der Malsburg, C., & Horsthemke, B. (2003). Computer-based recognition of dysmorphic faces. *European Journal of Human Genetics*, *11*(8), 555–560. https://doi.org/10.1038/sj.ejhg.5200997

Low, K. J., James, M., Sharples, P. M., Eaton, M., Jenkinson, S., Study, D. D. D., &

Smithson, S. F. (2018). A novel PIGA variant associated with severe X-linked epilepsy and profound developmental delay. *Seizure*, *56*, 1–3. https://doi.org/10.1016/j.seizure.2018.01.013

Low, M. G., Ferguson, M. A. ., Futerman, A. H., & Silman, I. (1986). Covalently attached phosphatidylinositol as a hydrophobic anchor for membrane proteins. *Trends in Biochemical Sciences*, *11*(5), 212–215. https://doi.org/10.1016/0968-0004(86)90009-5

Mabry, C. C., Bautista, A., Kirk, R. F., Dubilier, L. D., Braunstein, H., & Koepke, J. A. (1970). Familial hyperphosphatase with mental retardation, seizures, and neurologic deficits. *The Journal of Pediatrics*, *77*(1), 74–85. https://doi.org/10.1016/S0022-3476(70)80047-6

MacArthur, D. G., Manolio, T. A., Dimmock, D. P., Rehm, H. L., Shendure, J., Abecasis, G. R., … Gunter, C. (2014). Guidelines for investigating causality of sequence variants in human disease. *Nature*, *508*(7497), 469–476. https://doi.org/10.1038/nature13127

Maeda, Y., Ashida, H., & Kinoshita, T. (2006). CHO Glycosylation Mutants: GPI Anchor. In *Methods in enzymology* (Vol. 416, pp. 182–205). https://doi.org/10.1016/S0076-6879(06)16012-7

Maeda, Y., Tashima, Y., Houjou, T., Fujita, M., Yoko-o, T., Jigami, Y., … Kinoshita, T. (2007). Fatty acid remodeling of GPI-anchored proteins is required for their raft association. *Molecular Biology of the Cell*, *18*(4), 1497–1506. https://doi.org/10.1091/mbc.E06-10-0885

Makrythanasis, P., Kato, M., Zaki, M. S., Saitsu, H., Nakamura, K., Santoni, F. A., … Murakami, Y. (2015). Pathogenic Variants in PIGG Cause Intellectual Disability with Seizures and Hypotonia. *American Journal of Human Genetics*, 1–12. https://doi.org/10.1016/j.ajhg.2016.02.007

Manea, E. (2018). A step closer in defining glycosylphosphatidylinositol anchored proteins role in health and glycosylation disorders. *Molecular Genetics and Metabolism Reports*, *16*(April), 67–75. https://doi.org/10.1016/j.ymgmr.2018.07.006

Marbach, F., Rustad, C. F., Riess, A., Đukić, D., Hsieh, T.-C., Jobani, I., … Netzer, C. (2019). The Discovery of a LEMD2-Associated Nuclear Envelopathy with Early

Progeroid Appearance Suggests Advanced Applications for AI-Driven Facial Phenotyping. *The American Journal of Human Genetics*. https://doi.org/10.1016/j.ajhg.2019.02.021

Marinov, I., Illingworth, A. J., Benko, M., & Sutherland, D. R. (2016). Performance characteristics of a non-fluorescent aerolysin-based paroxysmal nocturnal hemoglobinuria (PNH) assay for simultaneous evaluation of PNH neutrophils and PNH monocytes by flow cytometry, following published PNH guidelines. *Cytometry Part B: Clinical Cytometry*, *94*(1), 31–36. https://doi.org/10.1002/cyto.b.21389

Martin, H. C., Kim, G. E., Pagnamenta, A. T., Murakami, Y., Carvill, G. L., Meyer, E., … Taylor, J. C. (2014). Clinical whole-genome sequencing in severe early-onset epilepsy reveals new genes and improves molecular diagnosis. *Human Molecular Genetics*, *23*(12), 3200–3211. https://doi.org/10.1093/hmg/ddu030

Masuishi, Y., Endo, S., Kasuga, H., Hidaka, T., Kakamu, T., & Fukushima, T. (2018). Identification of ω -sites of Glycosylphosphatidylinositol Anchored Proteins. *Journal of Immunological Sciences*, *25*(5), 1–5.

Maydan, G., Noyman, I., Har-Zahav, A., Neriah, Z. Ben, Pasmanik-Chor, M., Yeheskel, A., … Basel-Vanagaite, L. (2011). Multiple congenital anomalies-hypotonia-seizures syndrome is caused by a mutation in PIGN. *Journal of Medical Genetics*, *48*(6), 383–389. https://doi.org/10.1136/jmg.2010.087114

McInerney-Leo, A. M., Harris, J. E., Gattas, M., Peach, E. E., Sinnott, S., Dudding-Byth, T., … Duncan, E. L. (2016). Fryns Syndrome Associated with Recessive Mutations in PIGN in two Separate Families. *Human Mutation*. https://doi.org/10.1002/humu.22994

McKeage, K. (2019). Ravulizumab: First Global Approval. *Drugs*, *79*(3), 347–352. https://doi.org/10.1007/s40265-019-01068-2

McKean, D. M., & Niswander, L. (2012). Defects in GPI biosynthesis perturb Cripto signaling during forebrain development in two new mouse models of holoprosencephaly. *Biology Open*, *1*(9), 874–883. https://doi.org/10.1242/bio.20121982

McKenna, A., Hanna, M., Banks, E., Sivachenko, A., Cibulskis, K., Kernytsky, A., … DePristo, M. A. (2010). The Genome Analysis Toolkit: A MapReduce framework

for analyzing next-generation DNA sequencing data. *Genome Research*, *20*(9), 1297–1303. https://doi.org/10.1101/gr.107524.110

McLaren, W., Gil, L., Hunt, S. E., Riat, H. S., Ritchie, G. R. S., Thormann, A., … Cunningham, F. (2016). The Ensembl Variant Effect Predictor. *Genome Biology*, *17*(1), 1–14. https://doi.org/10.1186/s13059-016-0974-4

Menasche, B. L., Crisman, L., Gulbranson, D. R., Davis, E. M., Yu, H., & Shen, J. (2019). Fluorescence Activated Cell Sorting (FACS) in Genome-Wide Genetic Screening of Membrane Trafficking. *Current Protocols in Cell Biology*, *82*(1), e68. https://doi.org/10.1002/cpcb.68

Meola, N., Gennarino, V. A., & Banfi, S. (2009). microRNAs and genetic diseases. *PathoGenetics*, *2*, 7. https://doi.org/10.1186/1755-8417-2-7

Metz, C. N., Schenkman, S., & Davitz, M. A. (1991). Characterization of the plasma glycosylphosphatidylinositol-specific phospholipase D (GPI-PLD). *Cell Biology International Reports*, *15*(9, Part 1), 875–882. https://doi.org/https://doi.org/10.1016/0309-1651(91)90039-L

Mevorach, D. (2015). Paroxysmal nocturnal hemoglobinuria (PNH) and primary p.Cys89Tyr mutation in CD59: Differences and similarities. *Molecular Immunology*, *67*(1), 51–55.

Middelhoven, P. J., Ager, A., Roos, D., & Verhoeven, A. J. (1997). Involvement of a metalloprotease in the shedding of human neutrophil Fc??RIIIB. *FEBS Letters*, *414*(1), 14–18. https://doi.org/10.1016/S0014-5793(97)00959-9

Middelhoven, P. J., van Buul, J. D., Kleijer, M., Roos, D., & Hordijk, P. L. (1999). Actin polymerization induces shedding of FcgammaRIIIb (CD16) from human neutrophils. *Biochemical and Biophysical Research Communications*, *255*(3), 568–574. https://doi.org/10.1006/bbrc.1999.0244

Morren, M.-A., Jaeken, J., Visser, G., Salles, I., Van Geet, C., Simeoni, I., … Freson, K. (2017). PIGO deficiency: palmoplantar keratoderma and novel mutations. *Orphanet Journal of Rare Diseases*, *12*(1), 101. https://doi.org/10.1186/s13023-017-0654-9

Müller, A., Klöppel, C., Smith-Valentine, M., Van Houten, J., & Simon, M. (2012). Selective and programmed cleavage of GPI-anchored proteins from the surface membrane by phospholipase C. *Biochimica et Biophysica Acta (BBA) -*

Biomembranes, *1818*(1), 117–124. https://doi.org/10.1016/j.bbamem.2011.10.009

Muñiz, M., & Riezman, H. (2015). Trafficking of glycosylphosphatidyl inositol anchored proteins from the endoplasmic reticulum to the cell surface. *Journal of Lipid Research*, *57*, 76–81. https://doi.org/10.1194/jlr.R062760

Muñiz, M., & Zurzolo, C. (2014). Sorting of GPI-anchored proteins from yeast to mammals--common pathways at different sites? *Journal of Cell Science*, *127*(Pt 13), 2793–2801.

Murakami, Y., Inoue, N., Kawamoto, M., Kohara, N., & Kinoshita, T. (2016). Paroxysmal nocturnal hemoglobinuria caused by PIGT mutations: Atypical PNH. *Immunobiology*, *221*(10), 1159. https://doi.org/10.1016/j.imbio.2016.06.079

Murakami, Y., Kanzawa, N., Saito, K., Krawitz, P. M., Mundlos, S., Robinson, P. N., … Kinoshita, T. (2012). Mechanism for release of alkaline phosphatase caused by glycosylphosphatidylinositol deficiency in patients with hyperphosphatasia mental retardation syndrome. *The Journal of Biological Chemistry*, *287*(9), 6318–6325. https://doi.org/10.1074/jbc.M111.331090

Murakami, Y., Siripanyaphinyo, U., Hong, Y., Tashima, Y., Maeda, Y., & Kinoshita, T. (2005). The Initial Enzyme for Glycosylphosphatidylinositol Biosynthesis Requires PIG-Y, a Seventh Component. *Molecular Biology of the Cell*, *16*(11), 5236–5246. https://doi.org/10.1091/mbc.E05-08-0743

Murakami, Y., Siripanyapinyo, U., Hong, Y., Kang, J. Y., Ishihara, S., Nakakuma, H., … Kinoshita, T. (2003). PIG-W Is Critical for Inositol Acylation but Not for Flipping of Glycosylphosphatidylinositol-Anchor. *Molecular Biology of the Cell*, *14*(10), 4285–4295. https://doi.org/10.1091/mbc.E03-03-0193

Murakami, Y., Tawamie, H., Maeda, Y., Büttner, C., Buchert, R., Radwan, F., … Jamra, R. A. (2014). Null mutation in PGAP1 impairing Gpi-anchor maturation in patients with intellectual disability and encephalopathy. *PLoS Genetics*, *10*(5), e1004320. https://doi.org/http://dx.doi.org/10.1371/journal.pgen.1004320

Nafa, K., Bessler, M., Castro-Malaspina, H., Jhanwar, S., & Luzzatto, L. (1998). The spectrum of somatic mutations in the PIG-A gene in paroxysmal nocturnal hemoglobinuria includes large deletions and small duplications. *Blood Cells, Molecules, and Diseases*, *24*(3), 370–384.

https://doi.org/10.1006/bcmd.1998.0203

Nakagawa, T., Taniguchi-Ikeda, M., Murakami, Y., Nakamura, S., Motooka, D., Emoto, T., … Iijima, K. (2016). A novel PIGN mutation and prenatal diagnosis of inherited glycosylphosphatidylinositol deficiency. *American Journal of Medical Genetics Part A*, *170*(1), 183–188. https://doi.org/10.1002/ajmg.a.37397

Nakamura, K., Osaka, H., Murakami, Y., Anzai, R., Nishiyama, K., Kodera, H., … Saitsu, H. (2014). PIGO mutations in intractable epilepsy and severe developmental delay with mild elevation of alkaline phosphatase levels. *Epilepsia*, *55*(2), 13–17. https://doi.org/10.1111/epi.12508

Nakashima, M., Kashii, H., Murakami, Y., Kato, M., Tsurusaki, Y., Miyake, N., … Matsumoto, N. (2014). Novel compound heterozygous PIGT mutations caused multiple congenital anomalies-hypotonia-seizures syndrome 3. *Neurogenetics*, *15*(3), 193–200. https://doi.org/10.1007/s10048-014-0408-y

Nampoothiri, S., Hebbar, M., Roy, A. G., Kochumon, S. P., & Bielas, S. (2017). Hyperphosphatasia with Mental Retardation Syndrome Due to a Novel Mutation in PGAP3, 2–4.

Naseer, M. I., Rasool, M., Jan, M. M., Chaudhary, A. G., Pushparaj, P. N., Abuzenadah, A. M., & Al-Qahtani, M. H. (2016). A novel mutation in PGAP2 gene causes developmental delay, intellectual disability, epilepsy and microcephaly in consanguineous Saudi family. *Journal of the Neurological Sciences*, *371*, 121–125. https://doi.org/10.1016/j.jns.2016.10.027

Neveling, K., Feenstra, I., Gilissen, C., Hoefsloot, L. H., Kamsteeg, E.-J., Mensenkamp, A. R., … Nelen, M. R. (2013). A Post-Hoc Comparison of the Utility of Sanger Sequencing and Exome Sequencing for the Diagnosis of Heterogeneous Diseases. *Human Mutation*, *34*(12), 1721–1726. https://doi.org/10.1002/humu.22450

Nevo, Y., Ben-Zeev, B., Tabib, A., Straussberg, R., Anikster, Y., Shorer, Z., … Elpeleg, O. (2013). CD59 deficiency is associated with chronic hemolysis and childhood relapsing immune-mediated polyneuropathy. *Blood*, *121*(1), 129–135.

Ng, B. G., Hackmann, K., Jones, M. A., Eroshkin, A. M., He, P., Wiliams, R., … Freeze, H. H. (2012). *Mutations in the Glycosylphosphatidylinositol Gene PIGL Cause CHIME Syndrome*. *The American Journal of Human Genetics* (Vol. 90).

https://doi.org/10.1016/j.ajhg.2012.02.010

Nguyen, T T M, Mahida, S. D., Smith-Hicks, C., & Campeau, P. M. (2018). A PIGH mutation leading to GPI deficiency is associated with developmental delay and autism. *Human Mutation*, *39*(6), 827–829. https://doi.org/10.1002/humu.23426

Nguyen, Thi Tuyet Mai, Murakami, Y., Sheridan, E., Ehresmann, S., Rousseau, J., St-Denis, A., … Campeau, P. M. (2017). Mutations in GPAA1 , Encoding a GPI Transamidase Complex Protein, Cause Developmental Delay, Epilepsy, Cerebellar Atrophy, and Osteopenia. *The American Journal of Human Genetics*, *101*(5), 856–865. https://doi.org/10.1016/j.ajhg.2017.09.020

Nguyen, Thi Tuyet Mai, Murakami, Y., Wigby, K. M., Baratang, N. V., Rousseau, J., St-Denis, A., … Campeau, P. M. (2018). Mutations in PIGS, Encoding a GPI Transamidase, Cause a Neurological Syndrome Ranging from Fetal Akinesia to Epileptic Encephalopathy. *The American Journal of Human Genetics*, *103*(4), 602–611. https://doi.org/10.1016/J.AJHG.2018.08.014

Novoalign. (2017). last accsessed: Retrieved from http://www.novocraft.com

Ohba, C., Okamoto, N., Murakami, Y., Suzuki, Y., Tsurusaki, Y., Nakashima, M., … Saitsu, H. (2014). PIGN mutations cause congenital anomalies, developmental delay, hypotonia, epilepsy, and progressive cerebellar atrophy. *Neurogenetics*, *15*(2), 85–92. https://doi.org/10.1007/s10048-013-0384-7

Ohno, K., Takeda, J., & Masuda, A. (2017). Rules and tools to predict the splicing effects of exonic and intronic mutations. *Wiley Interdisciplinary Reviews: RNA*, e1451. https://doi.org/10.1002/wrna.1451

Orlean, P., & Menon, A. K. (2007). Thematic review series: Lipid Posttranslational Modifications. GPI anchoring of protein in yeast and mammalian cells, or: how we learned to stop worrying and love glycophospholipids. *The Journal of Lipid Research*, *48*(5), 993–1011. https://doi.org/10.1194/jlr.R700002-JLR200

Pagnamenta, A. T., Murakami, Y., Anzilotti, C., Titheradge, H., Oates, A. J., Morton, J., … Taylor, J. C. (2018). A homozygous variant disrupting the PIGH start-codon is associated with developmental delay, epilepsy, and microcephaly. *Human Mutation*, *39*(6), 822–826. https://doi.org/10.1002/humu.23420

Pagnamenta, A. T., Murakami, Y., Taylor, J. M. J. C., Anzilotti, C., Howard, M. F., Miller, V., … Kini, U. (2017). Analysis of exome data for 4293 trios suggests GPI-

anchor biogenesis defects are a rare cause of developmental disorders. *European Journal of Human Genetics Available Online Publication*, *22*(June 2016), 1–11. https://doi.org/10.1038/ejhg.2017.32

Pangburn, M. K., & Müller-Eberhard, H. J. (1983). Initiation of the alternative complement pathway due to spontaneous hydrolysis of the thioester of C3. *Annals of the New York Academy of Sciences*, *421*, 291–298.

Pantel, Jean T., Zhao, M., Mensah, M. A., Hajjir, N., Hsieh, T. C., Hanani, Y., … Krawitz, P. M. (2018). Advances in computer-assisted syndrome recognition by the example of inborn errors of metabolism. *Journal of Inherited Metabolic Disease*, *41*(3), 533–539. https://doi.org/10.1007/s10545-018-0174-3

Pantel, Jean Tori, Zhao, M., Mensah, M. A., Hajjir, N., Hsieh, T.-C., Hanani, Y., … Krawitz, P. M. (2017). Advances in computer-assisted syndrome recognition and differentiation in a set of metabolic disorders. *BioRxiv*. https://doi.org/https://doi.org/10.1101/219394

Paulick, M. G., & Bertozzi, C. R. (2008). The glycosylphosphatidylinositol anchor: A complex membrane-anchoring structure for proteins. *Biochemistry*, *47*(27), 6991–7000.

Perez, Y., Wormser, O., Sadaka, Y., Birk, R., Narkis, G., & Birk, O. S. (2017). A Rare Variant in PGAP2 Causes Autosomal Recessive Hyperphosphatasia with Mental Retardation Syndrome , with a Mild Phenotype in Heterozygous Carriers. *BioMed Research International*, *2017*(Article ID 3470234), 7. https://doi.org/doi:10.1155/2017/3470234

Pierleoni, A., Martelli, P. L., & Casadio, R. (2008). PredGPI: a GPI-anchor predictor. *BMC Bioinformatics (BMCBI) 9*, *9*, 392.

Posey, J. E., O'Donnell-Luria, A. H., Chong, J. X., Harel, T., Jhangiani, S. N., Coban Akdemir, Z. H., … Centers for Mendelian Genomics. (2019). Insights into genetics, human biology and disease gleaned from family based genomic studies. *Genetics in Medicine*. https://doi.org/10.1038/s41436-018-0408-7

Pruitt, K. D., Katz, K. S., Sicotte, H., & Maglott, D. R. (2017). Introducing RefSeq and LocusLink: curated human genome resources at the NCBI. *Trends in Genetics*, *16*(1), 44–47. https://doi.org/10.1016/S0168-9525(99)01882-X

Quang, D., Chen, Y., & Xie, X. (2015). DANN: a deep learning approach for annotating

the pathogenicity of genetic variants. *Bioinformatics*, *31*(5), 761–763. https://doi.org/10.1093/bioinformatics/btu703

Rabe, P., Haverkamp, F., Emons, D., Rosskamp, R., Zerres, K., & Passarge, E. (1991). Syndrome of developmental retardation, facial and skeletal anomalies, and hyperphosphatasia in two sisters: Nosology and genetics of the Coffin-Siris syndrome. *American Journal of Medical Genetics*, *41*(3), 350–354. https://doi.org/10.1002/ajmg.1320410317

Reid, M. E., Mallinson, G., Sim, R. B., Poole, J., Pausch, V., Merry, A. H., … Tanner, M. J. (1991). Biochemical studies on red blood cells from a patient with the Inab phenotype (decay-accelerating factor deficiency). *Blood*, *78*(12), 3291–3297.

Reynolds, K. K., Juusola, J., Rice, G. M., & Giampietro, P. F. (2017). Prenatal presentation of Mabry syndrome with congenital diaphragmatic hernia and phenotypic overlap with Fryns syndrome. *American Journal of Medical Genetics, Part A*, *173*(10), 2776–2781. https://doi.org/10.1002/ajmg.a.38379

Risitano, A. M. (2013). Paroxysmal nocturnal hemoglobinuria and the complement system: recent insights and novel anticomplement strategies. *Advances in Experimental Medicine and Biology*, *735*, 155–172.

Risitano, A. M., Notaro, R., Marando, L., Serio, B., Ranaldi, D., Seneca, E., … Rotoli, B. (2009). Complement fraction 3 binding on erythrocytes as additional mechanism of disease in paroxysmal nocturnal hemoglobinuria patients treated by eculizumab. *Blood*, *113*(17), 4094–4100. https://doi.org/10.1182/blood-2008-11-189944

Ritchie, G. R. S., Dunham, I., Zeggini, E., & Flicek, P. (2014). Functional annotation of non-coding sequence variants. *Nature Methods*, *11*(3), 294–296. https://doi.org/10.1038/nmeth.2832

Robinson, P. N., Köhler, S., Bauer, S., Seelow, D., Horn, D., & Mundlos, S. (2008). The Human Phenotype Ontology: A Tool for Annotating and Analyzing Human Hereditary Disease. *The American Journal of Human Genetics*, *83*(5), 610–615. https://doi.org/10.1016/j.ajhg.2008.09.017

Robinson, P. N., Köhler, S., Oellrich, A., Project, S. M. G., Wang, K., Mungall, C. J., … Smedley, D. (2014). Improved exome prioritization of disease genes through cross-species phenotype comparison. *Genome Research*, *24*(2), 340–348.

https://doi.org/10.1101/gr.160325.113

Romee, R., Foley, B., Lenvik, T., Wang, Y., Zhang, B., Ankarlo, D., … Miller, J. (2013). NK cell CD16 surface expression and function is regulated by a disintegrin and metalloprotease-17 (ADAM17). *Blood*, *121*(18).

Rother, R. P., Rollins, S. A., Mojcik, C. F., Brodsky, R. A., & Bell, L. (2007). Discovery and development of the complement inhibitor eculizumab for the treatment of paroxysmal nocturnal hemoglobinuria. *Nature Biotechnology*, *25*(11), 1256–1264. https://doi.org/10.1038/nbt1344

Rotoli, B., Bessler, M., Alfinito, F., & del Vecchio, L. (1993). Membrane proteins in paroxysmal nocturnal haemoglobinuria. *Blood Reviews*, *7*(2), 75–86. https://doi.org/http://dx.doi.org/10.1016/S0268-960X(05)80017-7

Sakaguchi, T., Žigman, T., Petković Ramadža, D., Omerza, L., Pušeljić, S., Ereš Hrvaćanin, Z., … Barić, I. (2018). A novel PGAP3 mutation in a Croatian boy with brachytelephalangy and a thin corpus callosum. *Human Genome Variation*, *5*, 18005. https://doi.org/10.1038/hgv.2018.5

Scacheri, C. A., & Scacheri, P. C. (2015). Mutations in the non-coding genome. *Current Opinion in Pediatrics*, *27*(6), 659–664. https://doi.org/10.1097/MOP.0000000000000283

Schubach, M., Re, M., Robinson, P. N., & Valentini, G. (2017). Imbalance-Aware Machine Learning for Predicting Rare and Common Disease-Associated Non-Coding Variants. *Scientific Reports*, *7*, 2959. https://doi.org/10.1038/s41598-017-03011-5

Schwarz, J. M., Cooper, D. N., Schuelke, M., & Seelow, D. (2014). MutationTaster2: mutation prediction for the deep-sequencing age. *Nature Methods*, *11*(4), 361–362. https://doi.org/10.1038/nmeth.2890

Schwarz, J. M., Rödelsperger, C., Schuelke, M., & Seelow, D. (2010). MutationTaster evaluates disease-causing potential of sequence alterations. *Nature Methods*, *7*, 575.

Shen, W., Clemente, M. J., Hosono, N., Yoshida, K., Przychodzen, B., Yoshizato, T., … Makishima, H. (2014). Deep sequencing reveals stepwise mutation acquisition in paroxysmal nocturnal hemoglobinuria. *Journal of Clinical Investigation*, *124*(10), 4529–4538. https://doi.org/10.1172/JCI74747

Sherry, S. T., Ward, M.-H., Kholodov, M., Baker, J., Phan, L., Smigielski, E. M., & Sirotkin, K. (2001). dbSNP: the NCBI database of genetic variation. *Nucleic Acids Research*, *29*(1), 308–311. https://doi.org/10.1093/nar/29.1.308

Shihab, H. A., Rogers, M. F., Gough, J., Mort, M., Cooper, D. N., Day, I. N. M., … Campbell, C. (2015). An integrative approach to predicting the functional effects of non-coding and coding sequence variation. *Bioinformatics*, *31*(10), 1536–1543. https://doi.org/10.1093/bioinformatics/btv009

Shishioh, N., Hong, Y., Ohishi, K., Ashida, H., Maeda, Y., & Kinoshita, T. (2005). GPI7 is the second partner of PIG-F and involved in modification of glycosylphosphatidylinositol. *Journal of Biological Chemistry*, *280*(10), 9728–9734. https://doi.org/10.1074/jbc.M413755200

Skauli, N., Wallace, S., Chiang, S., Barøy, T., Holmgren, A., Stray-Pedersen, A., … Misceo, D. (2016). Novel PIGT Variant in Two Brothers: Expansion of the Multiple Congenital Anomalies-Hypotonia Seizures Syndrome 3 Phenotype. *Genes*, *7*(12), 108. https://doi.org/10.3390/genes7120108

Smedley, D., Jacobsen, J. O. B., Jäger, M., Köhler, S., Holtgrewe, M., Schubach, M., … Robinson, P. N. (2015). Next-generation diagnostics and disease-gene discovery with the Exomiser. *Nature Protocols*, *10*(12). https://doi.org/10.1038/nprot.2015.124

Smedley, D., Schubach, M., Jacobsen, J. O. O., Köhler, S., Zemojtel, T., Spielmann, M., … Robinson, P. N. N. (2016). A Whole-Genome Analysis Framework for Effective Identification of Pathogenic Regulatory Variants in Mendelian Disease. *American Journal of Human Genetics*, *99*(3), 595–606. https://doi.org/10.1016/j.ajhg.2016.07.005

Smith, E. D., Blanco, K., Sajan, S. A., Hunter, J. M., Shinde, D. N., Wayburn, B., … Radtke, K. (2019). A retrospective review of multiple findings in diagnostic exome sequencing: half are distinct and half are overlapping diagnoses. *Genetics in Medicine*, 1. https://doi.org/10.1038/s41436-019-0477-2

Sobreira, N. L. M., Arachchi, H., Buske, O. J., Chong, J. X., Hutton, B., Foreman, J., … Matchmaker Exchange Consortium. (2017). Matchmaker Exchange. In *Current Protocols in Human Genetics* (Vol. 95, pp. 9.31.1-9.31.15). Hoboken, NJ, USA: John Wiley & Sons, Inc. https://doi.org/10.1002/cphg.50

Socié, G., Caby-Tosi, M.-P., Marantz, J. L., Cole, A., Bedrosian, C. L., Gasteyger, C., … Haller, H. (2019). Eculizumab in paroxysmal nocturnal haemoglobinuria and atypical haemolytic uraemic syndrome: 10-year pharmacovigilance analysis. *British Journal of Haematology*. https://doi.org/10.1111/bjh.15790

Stenson, P. D., Ball, E. V., Mort, M., Phillips, A. D., Shaw, K., & Cooper, D. N. (2012). The human gene mutation database (HGMD) and its exploitation in the fields of personalized genomics and molecular evolution. *Current Protocols in Bioinformatics*, (SUPPL.39), 1–20. https://doi.org/10.1002/0471250953.bi0113s39

Striepen, B, Tomavo, S., Dubremetz, J. F., & Schwarz, R. T. (1992). Identification and characterisation of glycosyl-inositolphospholipids in Toxoplasma gondii. *Biochem Soc Trans*, *20*(3), 296S.

Striepen, Boris, Zinecker, C. F., Damm, J. B. L., Melgers, P. A. T., Gerwig, G. J., Koolen, M., … Schwarz, R. T. (1997). Molecular Structure of the `` Low Molecular Weight Antigen ' ' of Toxoplasma gondii : A Glucose a 1-4 N -Acetylgalactosamine Makes Free Glycosyl- Phosphatidylinositols Highly Immunogenic.

Strübing, P. (1882). Paroxysmale Haemoglobinurie. *Deutsche Medizinische Wochenschrift*, *8*(1), 1–3. https://doi.org/10.1055/s-0029-1196307

Su, M. J., Coulter, A. R., Sutherland, S. K., & Chang, C. C. (1983). The presynaptic neuromuscular blocking effect and phospholipase A2 activity of textilotoxin, a potent toxin isolated from the venom of the Australian brown snake, Pseudonaja textilis. *Toxicon*, *21*(1), 143–151. https://doi.org/10.1016/0041-0101(83)90057-0

Suzuki, K. G. N., Fujiwara, T. K., Edidin, M., & Kusumi, A. (2007). Dynamic recruitment of phospholipase C gamma at transiently immobilized GPI-anchored receptor clusters induces IP3-Ca2+ signaling: single-molecule tracking study 2. *The Journal of Cell Biology*, *177*(4), 731–742. https://doi.org/10.1083/jcb.200609175

Swoboda, K. J., Margraf, R. L., Carey, J. C., Zhou, H., Newcomb, T. M., & Coonrod, E. (2014). A novel germline PIGA mutation in Ferro-Cerebro-Cutaneous syndrome: a neurodegenerative X-linked epileptic encephalopathy with systemic iron-overload. *Am J Med Genet A*, *164A*. https://doi.org/10.1002/ajmg.a.36189

Takahashi, M., Inoue, N., Ohishi, K., Maeda, Y., Nakamura, N., Endo, Y., … Kinoshita,

T. (1996). PIG-B, a membrane protein of the endoplasmic reticulum with a large lumenal domain, is involved in transferring the third mannose of the GPI anchor. *The EMBO Journal*, *15*(16), 4254–4261.

Takeda, J., Miyata, T., Kawagoe, K., Iida, Y., Endo, Y., Fujita, T., … Kinoshita, T. (1993). Deficiency of the GPI anchor caused by a somatic mutation of the PIG-A gene in paroxysmal nocturnal hemoglobinuria. *Cell*, *73*(4), 703–711.

Tanaka, S., Maeda, Y., Tashima, Y., & Kinoshita, T. (2004). Inositol Deacylation of Glycosylphosphatidylinositol-anchored Proteins Is Mediated by Mammalian PGAP1 and Yeast Bst1p. *Journal of Biological Chemistry*, *279*(14), 14256–14263. https://doi.org/10.1074/jbc.M313755200

Tanigawa, J., Mimatsu, H., Mizuno, S., Okamoto, N., Fukushi, D., Tominaga, K., … Murakami, Y. (2017). Phenotype–genotype correlations of PIGO deficiency with variable phenotypes from infantile lethality to mild learning difficulties. *Human Mutation*, *38*(7), 805–815. https://doi.org/10.1002/humu.23219

Tarailo-Graovac, M., Sinclair, G., Stockler-Ipsiroglu, S., Van Allen, M., Rozmus, J., Shyr, C., … van Karnebeek, C. D. (2015). The genotypic and phenotypic spectrum of PIGA deficiency. *Orphanet Journal of Rare Diseases*, *10*(1), 23. https://doi.org/10.1186/s13023-015-0243-8

Taron, B. W., Colussi, P. A., Wiedman, J. M., Orlean, P., & Taron, C. H. (2004). Human Smp3p adds a fourth mannose to yeast and human glycosylphosphatidylinositol precursors in vivo. *Journal of Biological Chemistry*, *279*(34), 36083–36092. https://doi.org/10.1074/jbc.M405081200

Tashima, Y., Taguchi, R., Murata, C., Ashida, H., Kinoshita, T., & Maeda, Y. (2006). PGAP2 Is Essential for Correct Processing and Stable Expression of GPI-anchored Proteins □, *17*(March), 1410–1420. https://doi.org/10.1091/mbc.E05

Telenti, A., Pierce, L. C. T., Biggs, W. H., di Iulio, J., Wong, E. H. M., Fabani, M. M., … Venter, J. C. (2016). Deep sequencing of 10,000 human genomes. *Proceedings of the National Academy of Sciences*, *113*(42), 11901–11906. https://doi.org/10.1073/pnas.1613365113

Teye, E. K., Sido, A., Xin, P., Finnberg, N. K., Gokare, P., Kawasawa, Y. I., … Pu, J. J. (2017). PIGN gene expression aberration is associated with genomic instability and leukemic progression in acute myeloid leukemia with myelodysplastic

features. *Oncotarget*, *5*(0). https://doi.org/10.18632/oncotarget.15136

Thomas, T. C., Rollins, S. A., Rother, R. P., Giannoni, M. A., Hartman, S. L., Elliott, E. A., … Evans, M. J. (1996). Inhibition of complement activity by humanized anti-C5 antibody and single-chain Fv. *Molecular Immunology*, *33*(17–18), 1389–1401.

Thompson, M. D., Roscioli, T., Marcelis, C., Nezarati, M. M., Stolte-Dijkstra, I., Sharom, F. J., … Cole, D. E. C. (2012). Phenotypic variability in hyperphosphatasia with seizures and neurologic deficit (Mabry syndrome). *American Journal of Medical Genetics, Part A*, *158 A*(3), 553–558. https://doi.org/10.1002/ajmg.a.35202

Thompson, M., Nezarati, M., Gillessen-Kaesbach, G., Meinecke, P., Mendoza, R., Mornet, E., … Cole, D. (2010). Hyperphosphatasia with seizures, neurologic deficit, and characteristic facial features: Five new patients with Mabry syndrome. *American Journal of Medical Genetics Part A*, *152A*(7), 1661–1669.

Thorvaldsdóttir, H., Robinson, J. T., & Mesirov, J. P. (2013). Integrative Genomics Viewer (IGV): High-performance genomics data visualization and exploration. *Briefings in Bioinformatics*, *14*(2), 178–192. https://doi.org/10.1093/bib/bbs017

Timms, R. T., Menzies, S. A., Tchasovnikarova, I. A., Christensen, L. C., Williamson, J. C., Antrobus, R., … Lehner, P. J. (2016). Genetic dissection of mammalian ERAD through comparative haploid and CRISPR forward genetic screens. *Nature Communications*, *7*, 1–10. https://doi.org/10.1038/ncomms11786

van der Crabben, S. N., Harakalova, M., Brilstra, E. H., van Berkestijn, F. M. C., Hofstede, F. C., van Vught, A. J., … van Haelst, M. M. (2014). Expanding the spectrum of phenotypes associated with germline PIGA mutations: A child with developmental delay, accelerated linear growth, facial dysmorphisms, elevated alkaline phosphatase, and progressive CNS abnormalities. *American Journal of Medical Genetics, Part A*, *164*(1), 29–35. https://doi.org/10.1002/ajmg.a.36184

Van Dijk, E. L., Jaszczyszyn, Y., & Thermes, C. (2014). Library preparation methods for next-generation sequencing: Tone down the bias. *Experimental Cell Research*, *322*(1), 12–20. https://doi.org/10.1016/j.yexcr.2014.01.008

Vissers, L. E. L. M., van Nimwegen, K. J. M., Schieving, J. H., Kamsteeg, E.-J., Kleefstra, T., Yntema, H. G., … Willemsen, M. A. A. P. (2017). A clinical utility study of exome sequencing versus conventional genetic testing in pediatric neurology.

Genetics in Medicine, *19*(9), 1055–1063. https://doi.org/10.1038/gim.2017.1

Walter, E. I., Roberts, W. L., Rosenberry, T. L., Ratnoff, W. D., & Medof, M. E. (1990). Structural basis for variations in the sensitivity of human decay accelerating factor to phosphatidylinositol-specific phospholipase C cleavage. *Journal of Immunology (Baltimore, Md. : 1950)*, *144*(3), 1030–1036.

Wang, K., Li, M., & Hakonarson, H. (2010). ANNOVAR: Functional annotation of genetic variants from high-throughput sequencing data. *Nucleic Acids Research*, *38*(16), 1–7. https://doi.org/10.1093/nar/gkq603

Wang, L., Uchikawa, M., Tsuneyama, H., Tokunaga, K., Tadokoro, K., & Juji, T. (1998). Molecular cloning and characterization of decay-accelerating factor deficiency in Cromer blood group Inab phenotype. *Blood*, *91*(2), 680–684.

Wang, Y., Hirata, T., Maeda, Y., Murakami, Y., Fujita, M., & Kinoshita, T. (2019). Free, unlinked glycosylphosphatidylinositols on mammalian cell surfaces revisited. *Journal of Biological Chemistry*, jbc.RA119.007472. https://doi.org/10.1074/jbc.RA119.007472

Watanabe, R., Ohishi, K., Maeda, Y., Nakamura, N., & Kinoshita, T. (1999). Mammalian PIG-L and its yeast homologue Gpi12p are N-acetylglucosaminylphosphatidylinositol de-N-acetylases essential in glycosylphosphatidylinositol biosynthesis. *Biochemical Journal*, *339*(1), 185 LP – 192. https://doi.org/10.1042/bj3390185

Williams, C., Jiang, Y. H., Shashi, V., Crimian, R., Schoch, K., Harper, A., … Petrovski, S. (2015). Additional evidence that PGAP1 loss of function causes autosomal recessive global developmental delay and encephalopathy. *Clinical Genetics*, *88*(6), 597–599. https://doi.org/10.1111/cge.12581

Wilson, G. W., & Stein, L. D. (2015). RNASequel: Accurate and repeat tolerant realignment of RNA-seq reads. *Nucleic Acids Research*, *43*(18). https://doi.org/10.1093/nar/gkv594

Wong, Y. W., & Low, M. G. (1994). Biosynthesis of glycosylphosphatidylinositol-anchored human placental alkaline phosphatase: evidence for a phospholipase C-sensitive precursor and its post-attachment conversion into a phospholipase C-resistant form. *Biochem J*, *301 (Pt 1*, 205–209. https://doi.org/10.1042/bj3010205

Xie, L. ling, Song, X. jie, Li, T. yi, & Jiang, L. (2018). A novel germline PIGA mutation causes early-onset epileptic encephalopathies in Chinese monozygotic twins. *Brain and Development*. https://doi.org/10.1016/j.braindev.2018.02.009

Xue, J., Li, H., Zhang, Y., & Yang, Z. (2016). Clinical and genetic analysis of two Chinese infants with Mabry syndrome. *Brain and Development*. https://doi.org/10.1016/j.braindev.2016.04.008

Yamashina, M., Ueda, E., Kinoshita, T., Takami, T., Ojima, A., Ono, H., … Kitani, T. (1990). Inherited Complete Deficiency of 20-Kilodalton Homologous Restriction Factor (CD59) as a Cause of Paroxysmal Nocturnal Hemoglobinuria. *The New England Journal of Medicine*, *323*(17), 1184–1189.

Yi, L., Bozkurt, G., Li, Q., Lo, S., Menon, A. K., & Wu, H. (2017). Disulfide Bond Formation and N-Glycosylation Modulate Protein-Protein Interactions in GPI-Transamidase (GPIT). *Scientific Reports*, *8*(December 2016), 1–11. https://doi.org/10.1038/srep45912

Yuan, X., Li, Z., Baines, A. C., Gavriilaki, E., Ye, Z., Wen, Z., … Brodsky, R. A. (2017). A hypomorphic PIGA gene mutation causes severe defects in neuron development and susceptibility to complement-mediated toxicity in a human iPSC model. *PLoS ONE*, *12*(4), 1–19. https://doi.org/10.1371/journal.pone.0174074

Zehavi, Y., von Renesse, A., Daniel-Spiegel, E., Sapir, Y., Zalman, L., Chervinsky, I., … Spiegel, R. (2017). A homozygous PIGO mutation associated with severe infantile epileptic encephalopathy and corpus callosum hypoplasia, but normal alkaline phosphatase levels. *Metabolic Brain Disease*, *32*(6), 2131–2137. https://doi.org/10.1007/s11011-017-0109-y

Zerbino, D. R., Achuthan, P., Akanni, W., Amode, M. R., Barrell, D., Bhai, J., … Flicek, P. (2017). Ensembl 2018. *Nucleic Acids Research*, *46*(November 2017), 754–761. https://doi.org/10.1093/nar/gkx1098

Zhang, F., & Lupski, J. R. (2015). Non-coding genetic variants in human disease. *Human Molecular Genetics*, *24*(R1), R102–R110. https://doi.org/10.1093/hmg/ddv259

Zhao, J. J., Halvardson, J., Knaus, A., Georgii-Hemming, P., Baeck, P., Krawitz, P. M., … Feuk, L. (2017). Reduced cell surface levels of GPI-linked markers in a new case

with PIGG loss of function. *Human Mutation*, *38*(10), 1394–1401. https://doi.org/10.1002/humu.23268

Zhou, J., & Troyanskaya, O. G. (2015). Predicting effects of noncoding variants with deep learning–based sequence model. *Nature Methods*, *12*(10), 931–934. https://doi.org/10.1038/nmeth.3547

Zurzolo, C., & Simons, K. (2016). Glycosylphosphatidylinositol-anchored proteins: Membrane organization and transport. *Biochimica et Biophysica Acta - Biomembranes*. https://doi.org/10.1016/j.bbamem.2015.12.018

5.2 List of abbreviation

Abbreviation	Full term
1kGP	1000 genomes project
AIF-PNH	Autoinflammation PNH
ALP	Alkaline phosphatase
bp	Base pair
BWA	Burrows-Wheeler Aligner
CADD	Combined Annotation-Dependent Depletion
Cas	CRISPR-asociated
CD	Cluster of differentiation
CDG	Congenital disorders of glycosylation
CDR	Commonly deleted region
CHO	Chinese hamster ovary
CNS	Central nervous system
CNV	Copy number variant
CRISPR	Clustered Regularly Interspaced Short Palindromic Repeats
dbSNP	Data base of single nucleotide polymorphisms
DNA	Deoxyribonucleic acid
dsDNA	Double stranded DNA
eQTL	Expression quantitative trait loci
ER	Endoplasmatic reticulum
EtNP	Phosphoethanolamine
ExAC	Exome Aggregation Consortium
FLAER	Fluorescently labeled aerolysin
gDNA	Genomic DNA
GlcNAc	N-acetylglucosamin
GPI	Glycosylphosphatidylinositol
GPI-AP	GPI anchored protein
GPIBD	GPI biosynthesis defect
GRCh	Genome Reference Consortium Human
GTEx	Genotype-Tissue Expression

Abbreviation	Full term
HGMD	Human Mutation Data Base
HGVS	Human Genome Variation Society
HPMRS	Hyperphosphatasia with mental retardation syndrome
HPO	Human Phenotype Ontology
HSC	hematopoietic stem cell
IBD	Identity-by-descent
ID	Intellectual disability
IGD	Inherited glycosylation disorders
IGV	Integrative genomics viewer
iPSC	Induced pluripotent cell
kb	Kilobase (1000bp)
LCL	Lymphoblastoid cell line
lncRNA	Long non-coding RNA
lof	Loss of function
LOVD	Leiden Open-source Variation Database
MAC	Membrane attack complex
Mb	Megabase (1000 kb)
MCAHS	Multiple congenital anomalies-hypotonia-seizures
MDS	Myelodysplastic syndrome
MFI	Median fluorescent intensity
miRNA	Micro RNA
ML	Mucolipidosis
MPN	Myeloproliferative neoplasm
MPS	Mucopolysaccharidosis type
MRI	Magnetic resonance imaging
mRNA	Messenger RNA
NGS	Next generation sequencing
NMR	Nuclear Magnetic Resonance
PCA	Principal component analysis
PCR	Polymerase chain reaction
PI	Phosphatidylinositol

Abbreviation	Full term
PL	Phospholipase
PLP	Pyridoxal phosphate
PNH	Paroxysmal nocturnal hemoglobinuria
PNK	Polynucleotide 5’-hydroxyl-kinase
RNA	Ribonucleic acid
RT-PCR	Real-time PCR
rtPCR	Reverse transcription polymerase chain reaction
SBS	Sequencing by synthesis
SD	Standard deviation
SI	Staining index
SNV	Single nucleotide variant
ssDNA	Singe stranded DNA
TGN	Trans-Golgi-network
UTR	Untranslated region
VCF	Variant file format
VEP	Variant Effect Predictor
VOUCS	Variants of unknown clinical significance
WES	Whole exome sequencing
WGS	Whole genome sequencing

5.3 List of figures

5.4 List of tables